A PROTEO-LIPOSOME SYSTEM FOR THE ANALYSIS OF THE INTRACELLULAR INTERACTOME OF MEMBRANE PROTEINS USING AMYLOID PRECURSOR PROTEIN AS A MODEL

HEATHER CURRINN

Doctor of Philosophy

ASTON UNIVERSITY

March 2015

Aston University

A PROTEO-LIPOSOME SYSTEM FOR THE ANALYSIS OF THE INTRACELLULAR INTERACTOME OF MEMBRANE PROTEINS USING AMYLOID PRECURSOR PROTEIN AS A MODEL

Heather Currinn
Doctor of Philosophy
2015

Thesis summary

Transmembrane proteins play crucial roles in many important physiological processes. The intracellular domain of membrane proteins is key for their function by interacting with a wide variety of cytosolic proteins. It is therefore important to examine this interaction. A recently developed method to study these interactions, based on the use of liposomes as a model membrane, involves the covalent coupling of the cytoplasmic domains of membrane proteins to the liposome membrane. This allows for the analysis of interaction partners requiring both protein and membrane lipid binding.

This thesis further establishes the liposome recruitment system and utilises it to examine the intracellular interactome of the amyloid precursor protein (APP), most well-known for its proteolytic cleavage that results in the production and accumulation of amyloid beta fragments, the main constituent of amyloid plaques in Alzheimer's disease pathology. Despite this, the physiological function of APP remains largely unclear. Through the use of the proteo-liposome recruitment system two novel interactions of APP's intracellular domain (AICD) are examined with a view to gaining a greater insight into APP's physiological function.

One of these novel interactions is between AICD and the mTOR complex, a serine/threonine protein kinase that integrates signals from nutrients and growth factors. The kinase domain of mTOR directly binds to AICD and the N-terminal amino acids of AICD are crucial for this interaction.

The second novel interaction is between AICD and the endosomal PIKfyve complex, a lipid kinase involved in the production of phosphatidylinositol-3,5-bisphosphate ($PI(3,5)P_2$) from phosphatidylinositol-3-phosphate, which has a role in controlling ensdosome dynamics. The scaffold protein Vac14 of the PIKfyve complex binds directly to AICD and the C-terminus of AICD is important for its interaction with the PIKfyve complex. Using a recently developed intracellular $PI(3,5)P_2$ probe it is shown that APP controls the formation of $PI(3,5)P_2$ positive vesicular structures and that the PIKfyve complex is involved in the trafficking and degradation of APP. Both of these novel APP interactors have important implications of both APP function and Alzheimer's disease.

The proteo-liposome recruitment method is further validated through its use to examine the recruitment and assembly of the AP-2/clathrin coat from purified components to two membrane proteins containing different sorting motifs.

Taken together this thesis highlights the proteo-liposome recruitment system as a valuable tool for the study of membrane proteins intracellular interactome. It allows for the mimicking of the protein in its native configuration therefore identifying weaker interactions that are not detected by more conventional methods and also detecting interactions that are mediated by membrane phospholipids.

Key words: PIKfyve, endosomal trafficking, Clathrin, AP-2, Alzheimer's disease

Acknowledgements

I would like to take this opportunity to thank my supervisors Dr Thomas Wassmer and Dr Alice Rothnie for your continued guidance and support, your enthusiasm for the project has been infectious. Thank you for making my PhD such an enjoyable experience. I would also like to thank Dr Zita Balklava and Dr Stephane Gross for their support and guidance.

To everyone in MB523 and MB524 thank you for keeping me sane, your encouragement, support and friendship has been invaluable.

Thank you to all my friends for your encouragement. Katie, thank you for being the best friend anybody could wish for.

To my family, in particular my amazing Mom, Sister and Grandpa, thank you for your support, for celebrating with me when things worked and for putting up with my moods when they did not.

Finally, Nan, thank you for believing in me, I wish you could have been here to see this.

Table of Contents

List of Abbreviations

4EBP1 = 4 E binding protein 1

ADP = Adensoine diphosphate

AICD = amyloid precursor proteins intracellular domain

Akt = protein kinase B

ALS = Amyotrophic lateral sclerosis

AMPA = α-Amino-3-hydroxy-5-methyl-4-isoxazolepropionic acid

AP = Adaptor protein

APLP1 = APP like protein 1

APLP2 = APP like protein 2

APP = Amyloid precursor protein

ARF-1 = ADP ribosylation factor 1

ATP = Adenosine triphosphate

Aβ = Amyloid beta

BACE-1 = Beta secretase -1

C. elegans = Caenorhabditis elegans

CCV's = clathrin coated vesicles

CI-MPR = cation independent mannose-6-phosphate receptor

CME = clathrin mediated endocytosis

CMT4J = Charcot-Marie-Tooth Neuropathy Type 4J

COPI = coat protein complex 1

COPII = coat protein complex 2

Crb = Crumbs

DAG = Diacylgycerol

EEA1 = Early endosome antigen 1

EGFR = Epidermal growth factor receptor

ER = Endoplasmic reticulum

ERES = endoplasmic reticulum exit sites

ESCRT = endosomal sorting complexes required for transport

GFP = green fluorescent protein

GTP = Guanosine triphosphate

HEK-293t = Human embryonic kidney 293 cells

HPLC = high performance liquid chromatography

LAMP = Lysosomal associated membrane protein

LTP = long term potentiation

MBP = Maltose binding protein

ML1N = N-terminal polybasic domain of TRPML-1

MLST8 = mammalian lethal SEC13 protein 8

mSIN1 = mammalian stress-activated protein kinase interacting protein 1

mTOR = mechanistic target of rapamycin

mTORC1 = mTOR complex 1

mTORC2 = mTOR complex 2

MVB = multi vesicular body

PCR = polymerase chain reaction

PDZ domain = post synaptic density protein (PSD95), Drosophila disc large tumor suppressor (Dlg1), and zonula occludens-1 protein domain

PE-MCC = 1,2-dioleoyl-sn-glycero-3-phosphoethanolamine-N-[4-(p-maleimidomethyl)cyclohexane-carboxamide] (sodium salt)

PI = Phosphatidylinositol

PI(3)P = Phosphatidylinositol 3 phosphate

$PI(3,4)P_2$ = phosphatidylinositol 3,4 bisphosphate

$PI(3,4,5)P_3$ = phosphatidylinositol 3,4,5 triphosphate

$PI(3,5)P_2$ = phosphatidylinositol 3,5 bisphosphate

PI(4)P = Phosphatidylinositol 4 phosphate

PI(4,5)P2 = phosphatidylinositol 4,5 bisphosphate

PI3K = phosphoinositide 3 kinase

PIKfyve = FYVE finger containing phosphoinositide kinase

PLC = phospholipase C

PTB = phosphotyrosine binding

Raptor = regulatory associated protein of mTOR

RER = rough endoplasmic reticulum

Rictor = rapamycin-insensitive companion of mTOR

S6K1 = S6 kinase 1

SDS-PAGE = sodium dodecyl sulphate polyacrylamide gel electrophoresis

SNARE = Soluble NSF attachment protein receptor

SNX = Sorting nexin

TEV = tobacco etch virus

TGN = Trans Golgi network.

TRPML1 = transient receptor potential cation channel, mucolipin subfamily-1

TSC = Tubular sclerosis complex

VPS = Vacuolar protein sorting

YFP = yellow fluorescent protein

List of Figures

Chapter 1

Chapter 3

Chapter 4

Chapter 5

Chapter 6

Chapter 7

List of Tables

Chapter 1

Introduction

Chapter 1.0 Introduction

1.1 The importance of membrane proteins

Roughly 38% of all proteins encoded for by the mammalian genome are membrane proteins which represent one-third of biomarker candidates and two-thirds of the current drug targets (Rucevic et al., 2011). Membrane proteins are an integral part of biological membranes where they contribute up to 50% of the mass of these membranes (Tan et al., 2008). Biological membranes form an essential barrier between cells and their environment and exhibit specialist functions between cell types. In eukaryotes they also form a barrier between intracellular organelles and the cytosol of the cell. The membranes of these organelles are highly specific to that particular organelle. This is due to a difference in lipid composition of these membranes and the diverse range of proteins that are associated with them. Biological membranes act as selective barriers and are necessary for creating osmotic, electrical and chemical gradients that provide the foundation of bioenergetics and signal transduction. They also function as reaction interfaces due to the wide variety of interactions that take place both within and on the surface of the membrane. Interactions between membrane lipids and proteins are crucial for membrane homeostasis. Protein-protein interactions on or near the membrane are vital for processes such as signal transduction (Barenholz and Cevc, 2000).

1.1.1 Types of membrane protein

Membrane proteins can be categorised into peripheral and integral membrane proteins. Peripheral membrane proteins associate with either the extracellular or cytosolic side of the membrane. Integral membrane proteins transverse the membrane

and can be broadly categorised into three types. Type 1 membrane proteins are single pass and have an extracellular N-terminus and a cytoplasmic C-terminus. Type 2 membrane proteins are single pass and have an extracellular C-terminus and a cytoplasmic N-terminus (Chou and Elrod, 1999). Type 3 or multipass membrane proteins have either or both of their N and C-terminus in the cytoplasm or in the extracellular space, and they pass through the membrane multiple times (Tan et al., 2008). This thesis will focus on type 1 trans-membrane proteins.

1.1.2 Membrane protein diversity

Membrane proteins are diverse in both their structure and function, and are therefore involved in a wide variety of physiological processes. As a consequence they are also linked to several diseases with membrane proteins representing over 60% of current drug targets (Arinaminpathy et al., 2009). Some membrane proteins act as receptors which transmit external signals eliciting specific cellular responses. Others act as transport proteins, transporting small molecules such as sugars and amino acids as well as ions. Channel proteins also allow for the transport of small molecules across membranes by forming a channel in the membrane. Membrane proteins have roles in cell adhesion by linking the extracellular matrix to cytoskeletal components, therefore maintaining cell shape. It is important to understand the physiological functions of membrane proteins and the mechanisms required for these proteins to exert their function, due to their vital role in multiple biological processes.

1.2 Intracellular trafficking

The localisation of membrane proteins within the cell is of vital importance to their function. Membrane proteins exert different specialist functions depending on their intracellular localisation. In order for membrane proteins to carry out their function there are mechanisms in place that allow the correct trafficking and sorting of membrane proteins to the correct intracellular organelles. This process is known as intracellular or vesicular trafficking, and allows for the continuous movement of membrane proteins between different cellular compartments. There are two main pathways in intracellular trafficking, exocytosis and endocytosis (Figure 1). Exocytosis is the transport of newly synthesised membrane proteins to the plasma membrane, and endocytosis is the internalisation of these proteins from the plasma membrane to different organelles (Tokarev et al., 2009). Both of these pathways work alongside each other and disruption of one pathway has an effect on the other pathway, therefore both are required for correct membrane protein trafficking and homeostasis. These pathways are tightly regulated by several different protein complexes that are specific to each individual stage of the trafficking pathways. Components of membrane trafficking protein complexes are able to interact with the membrane protein being transported, and therefore are crucial regulators in membrane transport.

Figure 1. The two main pathways in intracellular trafficking
Exocytosis transports newly synthesised proteins from the endoplasmic reticulum to the plasma membrane via the Golgi complex. Endocytosis is the internalisation of proteins at the plasma membrane through the endosomal compartments to the lysosomes for degradation. These proteins can be recycled back to the plasma membrane , first by trafficking between both early and late endosomes and the Golgi, and secondly by Golgi-to-plasma membrane trafficking. This therefore links the exocytic and endocytic pathways. Figure from Tokarev et al. (2009).

1.2.1 The exocytic pathway

Exocytosis involves the transport of membrane proteins to the plasma membrane via the Golgi complex. Membrane proteins are synthesised in the endoplasmic reticulum (ER) and are then transported to the Golgi. This process is mediated by COPII coated vesicular transport (Lee and Miller, 2007). Membrane proteins are synthesised in the rough ER (RER) and are either inserted into the RER membrane or translocated to the RER lumen. Proteins can only be exported from the RER by ER exit sites (ERES). These sites are coated with COPII and give rise to COPII coated vesicles (Szul and Sztul, 2011). The COPII coat is recruited to the ER membrane allowing membrane deformation, and causing vesicle release from the ER (Lee and Miller, 2007). These COPII coated vesicles, containing membrane protein cargos, then fuse with the *cis* cisternae membrane of the Golgi complex. The fusion of transport vesicles with their target membranes is crucial for membrane trafficking, and is mediated by several

proteins including SNAREs. Once at the Golgi membrane proteins can be recycled back to the ER by COPI coated vesicular transport (Szul and Sztul, 2011). ER to Golgi transport is crucial to organelle homeostasis and in maintaining the identity between the ER and Golgi. This transport pathway is important for the correction of misfolded proteins, the retrieval of ER resident proteins, and the recycling of machinery that is involved in vesicle formation and fusion, such as SNARE proteins (Lee et al., 2004).

Those membrane proteins destined for secretion are trafficked from the *cis* cisternae of the Golgi through the medial cisternae to the *trans* cisternae. The exact mechanism for this has been extensively debated with the cisternal maturation model being most widely recognised. This model suggests that the cargo membrane proteins remain in the same cisternal structure, which undergoes several re-modelling stages through the loss of early Golgi enzymes and the gain of late Golgi proteins (Szul and Sztul, 2011). Once at the TGN (trans-Golgi network) membrane proteins are transported to the plasma membrane in secretory vesicles. This vesicular transport involves cytoskeletal components such as microtubules. These secretory vesicles then dock and fuse with the plasma membrane (Kelly, 1985). Once at the plasma membrane, membrane proteins can be internalised for degradation or recycled back to the plasma membrane. One of the primary methods of internalisation is clathrin mediated endocytosis.

This thesis will mainly focus on aspects of the endocytic pathway such as clathrin mediated endocytosis and trafficking between endosomes and the TGN.

1.2.2 Clathrin mediated endocytosis

Clathrin mediated endocytosis (CME) is the classical method for the endocytosis of membrane receptors from the plasma membrane (Mayor and Pagano, 2007) (Figure 2A). It involves the internalisation of fragments of the plasma membrane as well as all of its contents, into the cell, in vesicles coated with polymerised clathrin. Clathrin coated vesicles can also be formed from other membranes at different stages of the trafficking process, such as TGN-to-endosome transport (Crottet et al., 2002). CME is a versatile process as many different cargoes can be packaged using a wide variety of cytosolic accessory and adaptor proteins (McMahon and Boucrot, 2011). It can be triggered by ligand binding to a membrane protein as is the case with the epidermal growth factor receptor (EGFR) (Vieira et al., 1996). However some receptors such as the transferrin receptor are constitutively internalised (Ajioka and Kaplan, 1986). The mechanism of clathrin mediated endocytosis is thought to occur in five stages: initiation or nucleation, cargo selection, coat assembly, scission, and uncoating (Figure 2B). The formation of the clathrin coat requires a complex network of protein-protein interactions (Figure 2C). The initiation of coated pit formation defines plasma membrane sites for clathrin recruitment, to form clathrin coated vesicles (CCVs). Initiation involves a nucleation model composed of FCH domain (FES-CIP4 homology) only proteins (FCHO), EGFR pathway substrate 15 (EPS15) and intersectins (Henne et al., 2010, Reider et al., 2009). This module binds to plasma membrane regions rich in the inositol lipid phosphatidylinositol 4,5 bisphosphate ($PI(4,5)P_2$) causing a slight bend in the membrane. Loss of any of these components inhibits clathrin coat formation (Henne et al., 2010).

The second stage is cargo selection and involves the recruitment of the clathrin adaptor AP-2. AP-2 binds to $PI(4,5)P_2$ in the membrane, the cytoplasmic domains of membrane proteins, and proteins of the initiation module (Collins et al., 2002, Kelly et al., 2008, Henne et al., 2010). AP-2 also recruits a plethora of clathrin accessory

proteins such as AP180, which help stabilise the coat, aid in the selective cargo recruitment process and help to induce membrane curvature (Schmid et al., 2006). Due to the fact that AP-2 binds the cargo, lipids, accessory proteins and clathrin it is the core part of the clathrin coat.

The third stage is the assembly of the clathrin coat itself. Clathrin triskelia are recruited from the cytosol by AP-2. Clathrin binds to the flexible region of AP-2, and the accessory proteins AP180 and epsin (Kalthoff et al., 2002). Clathrin then polymerises to stabilise the coat and the membrane is curved further by the redistribution of curvature proteins like epsin to the edge of the clathrin coated pit (Tebar et al., 1996). Vesicle scission is the fourth stage in the process and requires the enzyme dynamin (Kosaka and Ikeda, 1983). Dynamin is recruited to the neck of the vesicle by BAR domain containing proteins such as amphiphysin, which aid in the curvature and formation of the vesicle neck (Wigge et al., 1997). Dynamin polymerises around the neck of the vesicle causing GTP hydrolysis and vesicle scission from the plasma membrane (Sundborger et al., 2011).

The final stage in the process is the uncoating of the released vesicle and the fusion of the vesicle with the endosomal compartment. The clathrin coat is disassembled by the ATPase heat shock cognate 70 (HSC70), a J domain co-factor, and either auxilin in neuronal cells or GAK (G-associated kinase) elsewhere (Schlossman et al., 1984, Chappell et al., 1986, Ungewickell et al., 1995). Auxilin is recruited to the vesicle after scission by binding to the clathrin triskelia. This then recruits Hsc70 causing uncoating (Xing et al., 2010). The phosphatase synaptojanin is also thought to function in the uncoating process by modifying the phosphoinositide composition of the vesicle due to dephosphorylation of $PI(4,5)P_2$, therefore causing the release of $PI(4,5)P_2$ binding proteins such as AP-2 and AP180 (Chang-Ileto et al., 2011). The vesicle is then able to fuse with its target membrane delivering its cargo to the endosomal compartment. From here the membrane protein can be targeted for degradation in the lysosome via the late endosomal compartment. The cargo membrane protein can also be recycled

back to the plasma membrane via recycling endosomes or the TGN (Grant and Donaldson, 2009).

Clathrin mediated endocytosis functions in the internalisation of membrane proteins involved in many physiological processes meaning that CME also plays a role in these processes. CME is key to synaptic vesicle recycling, which is highlighted by the abundance of AP-2/clathrin coated vesicles in brain samples.

Figure 2. The process of clathrin mediated endocytosis
(A)A basic overview of clathrin mediated endocytosis. The cargo protein recruits the adaptor protein AP-2 as well as other clathrin accessory proteins. Clathrin is then recruited by AP-2 forming clathrin coated pits. The coated pits are pinched off and traffic towards the early endosome where the vesicle is uncoated and then fuses with the early endosome. (figure modified from Grant and Sato (2006)). (B) The five steps of clathrin mediated endocytosis. Nucleation: FCH domain only proteins bind to PI(4,5)P_2 rich membrane regions and initiate clathrin coated pit formation by recruiting EPS15 and intersections that bind to and recruit AP-2. Cargo selection: AP-2 binds to the cytoplasmic domains of membrane proteins and recruits cargo specific adaptors that aid in the selection of membrane proteins. Coat assembly: AP-2 recruits clathrin triskelia which polymerise to form the characteristic clathrin lattice around the pit. Scission: Dynamin is recruited to the neck of the pit by BAR domain containing proteins where it polymerises and causes membrane scission via the hydrolysis of GTP. Uncoating: Auxilin in the clathrin coated vesicle recruits the ATPase heat shock cognate 70 (HSC70) which causes the disassembly of the clathrin coat. (C) The clathrin coat interaction network. The protein-protein interactions at each stage of CME. The main proteins are shown by central coloured circles. The diagram indicates the complexity of clathrin coat formation and uncoating. (Figures B and C from McMahon and Boucrot (2011)).

1.2.2.1 Clathrin

Clathrin is the protein that forms the outer coat of vesicles in clathrin mediated endocytosis. It exists as triskelia which polymerise to form the clathrin lattice. The clathrin triskelion is made up of 3 heavy chains of approximately 190 kDa and three clathrin light chains of roughly 25 kDa. The heavy chains provide the support of the clathrin lattice and the light chains help to regulate the formation and the disassembly of the clathrin lattice (Liu et al., 1995).

Figure 3. The structure of the clathrin triskelion
The clathrin triskelion is composed of three heavy chains (blue) and three light chains (yellow). The heavy chain is composed of the terminal adaptor protein binding domain, the linker, ankle, distal and knee domains. The proximal segment contains the light chain binding domain. (Figure from Fotin et al. (2004)).

The clathrin heavy chain can be separated into the N-terminal globular domain, the alpha helical linker, ankle, distal, proximal, and trimerisation domains (Knuehl et al., 2006). The N-terminal domain is a seven bladed beta propeller structure which binds to the clathrin box motifs of adaptor proteins such as AP-2 (Knuehl et al., 2006). The proximal domain of the clathrin heavy chain serves as the binding site for the light chain. Clathrin light chains contain charged amino acid residues that negatively regulate the assembly of the clathrin heavy chain by preventing the self-assembly at physiological pH caused by a conformational change in the clathrin heavy chain

(Wilbur et al., 2010). This can be overcome by adaptor molecules through the alignment of the distal domain with the proximal domain from different triskelia (Greene et al., 2000). The distal domain of the heavy chain is thought to be key in the interaction with other clathrin triskelia and therefore in clathrin lattice assembly (Schmid, 1997).

There are several different structures of the clathrin lattice. This variability is required for the function of the coats as they must be able to coat cargos of different shapes and sizes. Clathrin coats can range from the 28 triskelion mini coats and the 36 triskelion hexagonal coats to extended hexagonal arrays (Fotin et al., 2004). The clathrin triskelia are not able to form direct interactions with either cargo membrane proteins or the membrane itself (Knuehl et al., 2006). Instead clathrin is linked to the membrane and cargos by adaptor proteins.

1.2.2.2 Adaptor proteins

Adaptor proteins are a group of proteins that act as a central hub in the formation of clathrin coated vesicles by acting as a bridge between the membrane, membrane cargos and the clathrin lattice. There are five main adaptor protein complexes which all localise to different intracellular compartments and aid in the membrane trafficking in distinct pathways (Figure 4).

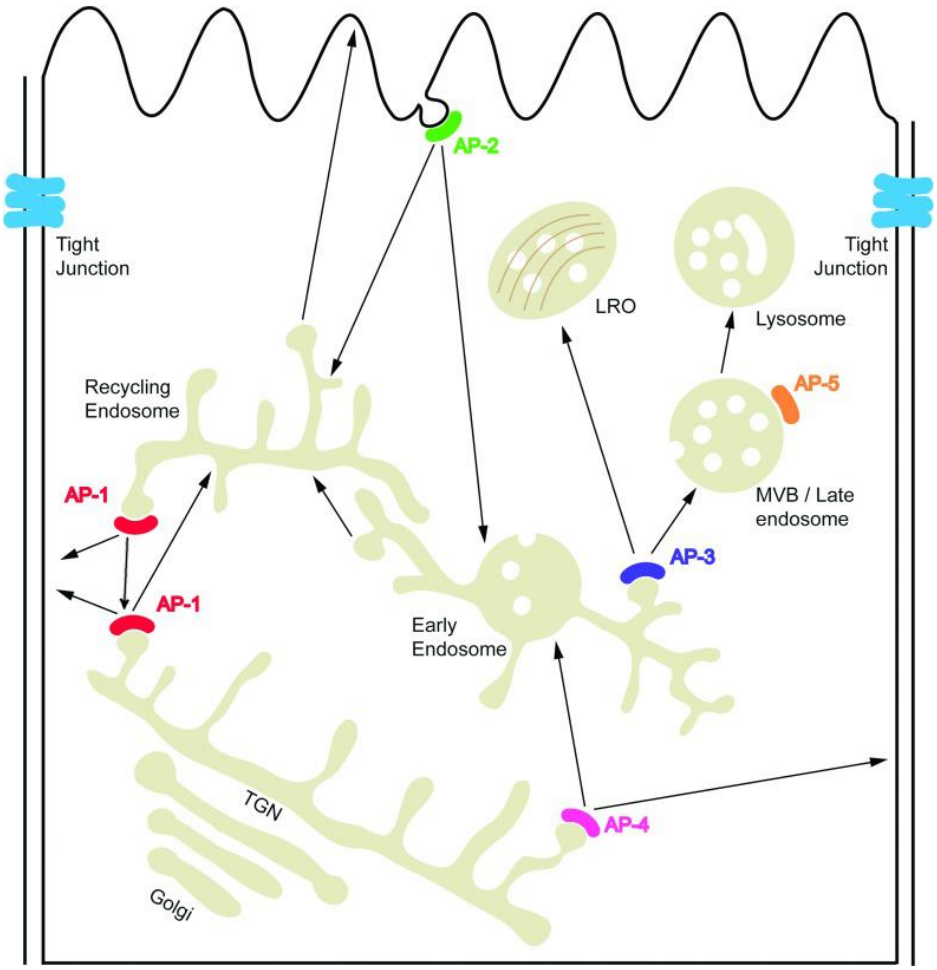

Figure 4. The role of adaptor proteins in membrane trafficking.
AP-1 localises to the TGN and recycling endosomes and is involved in the transport between them. AP-2 localises to the plasma membrane and is key to clathrin mediated endocytosis. AP-3 localises to endosomes and is involved in lysosomal- related organelle (LRO) biogenesis. AP-4 localises to the TGN and is important in TGN to endosome transport. AP-5 localises to late endosomes however its function still remains largely unclear. (Figure adapted from Park and Guo (2014)).

The first two adaptor protein complexes (AP-1 and AP-2) are clathrin associated, whereas AP-4 and AP-5 are not. AP-3 is thought to be clathrin associated however this is not fully clear. AP-1 localises to the TGN and endosomes in a ADP-ribosylation factor (Arf1) and a phosphatidylinositol 4 phosphate (PI(4)P) dependent manner (Zhu et al., 1999). AP-1 is known to mediate the bidirectional transport between the TGN and the recycling endosomes, and is thought to be involved in polarised cell sorting in epithelial cells (Bonifacino, 2014). AP-3 and AP-4 also localise to the TGN and/or endosomal membranes in an Arf1 dependent manner. AP-3 mediates the transport from tubular endosomes to late endosomes/lysosomes, and is involved in the biogenesis of lysosome-related organelles (LROs) (Baust et al., 2008, Peden et al., 2004). AP-4 is primarily localised to the TGN and mediates transport from the TGN to endosomes in a clathrin independent manner. AP-4 is also involved in polarised cell sorting, and mutations in the AP-4 gene lead to progressive spastic paraplegia (Hirst et al., 2013). AP-5 is the most recently discovered adaptor, it localises to late endosomes and also plays a role in progressive spastic paraplegia (Hirst et al., 2013, Hirst et al., 2011). The primary focus of this thesis will be on the AP-2 adaptor protein complex involved in clathrin mediated endocytosis.

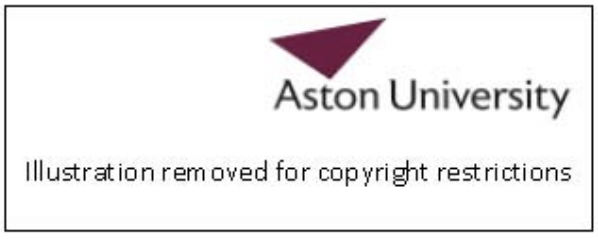

Figure 5. The structure of the adaptor protein complexes 1-5
All the adaptor protein complexes contain core, hinge and ear domains except AP-5 which lacks the hinge domain. The core domains are required for the membrane localisation and cargo binding whereas the hinge and ear domains bind accessory proteins. (Figure from Park and Guo (2014)).

1.2.2.2.1 AP-2 structure and function

AP-2 localises to the plasma membrane where it plays a key role in clathrin mediated endocytosis. AP-2's structure is similar to that of the other adaptors (Figure 5). All adaptors including AP-2 are hetrotetrameric protein complexes. AP-2 is composed of two large subunits of between 100 and 130 kDa known as the α and β subunits. AP-2 also contains a medium sized subunit of about 50 kDa known as the μ subunit, as well as a small 17 kDa σ subunit. There is a high degree of homology between the β, μ and σ subunits of AP-2 and AP-1. The α subunit of AP-2 corresponds to the γ subunit of AP-1 both of which are more diverse (Edeling et al., 2006).

AP-2 functions in CME by providing a link between the membrane, membrane proteins and clathrin. AP-2 interacts with several components of the clathrin coat complex. A comprehensive list of these coat components can be seen in McMahon and Boucrot (2011). AP-2 is recruited to the plasma membrane via three main interactions. AP-2 is able to bind to protein cargos within the membrane and to phospholipid head groups (Ohno et al., 1995). AP-2 is known to recognise the proteins of the nucleation complex such as FCH domain proteins, EPS15 and intersectins, required for the initialisation of clathrin coated pit formation (Henne et al., 2010). Both EPS15 and intersectin 1 and 2 were found to directly bind the μ subunit of AP-2 (Henne et al., 2010). This interaction is one of three main interactions that helps recruit AP-2 to the plasma membrane. The second interaction is between AP-2 and the plasma membrane lipid $PI(4,5)P_2$. AP-2 binds to $PI(4,5)P_2$ via basic residues at the N-terminus of the α subunit, and via lysine residues on the μ subunit (Collins et al., 2002). AP-2 recruitment to $PI(4,5)P_2$ is initially thought to take place via the α binding site, and also a second binding site in the β subunit (Jackson et al., 2010). The binding of $PI(4,5)P_2$ by the μ subunit is then thought to stabilise the interaction (Höning et al., 2005). This binding of $PI(4,5)P_2$ by AP-2 causes a conformational change in AP-2 from an inactive or locked form to an active or open form, allowing AP-2 to bind to the membrane protein cargo (Jackson et al., 2010,

Kelly et al., 2014). The stabilisation of this open form of AP-2 occurs through the interaction of its μ subunit with $PI(4,5)P_2$ and by the phosphorylation of Thr156 in the μ subunit by α-adaptin-associated kinase 1 (AAK1) (Höning et al., 2005). The stabilisation of the open form of AP-2 is also achieved by AP-2 binding to cargo proteins in the plasma membrane.

AP-2 is known to recognise and bind to two different sorting motifs located in the cytoplasmic domains of membrane proteins. The tyrosine based motif YXXϕ (where ϕ can be F, I, L, M or V) is recognised by hydrophobic patches in the μ2 subunit of AP-2 (Ohno et al., 1995). A second motif known as an acidic dileucine based motif [E/D]XXXL[L/I] is recognised by hydrophobic pockets in the σ subunit of AP-2 (Kelly et al., 2008). AP-2 has different binding affinities for each motif. It is thought that AP-2 has a higher affinity for the tyrosine motifs than the dileucine motifs (Höning et al., 2005). The binding of AP-2 to tyrosine motifs is enhanced and stabilised by the phosphorylation of Thr156 in the μ subunit, whereas dileucine based motifs bind to a different site (σ subunit) and binding is therefore not enhanced by this phosphorylation (Höning et al., 2005).

Once bound to $PI(4,5)P_2$ and cargo, AP-2 interacts with a number of accessory proteins via its appendage or ear domains. Cargo specific adaptor proteins bind AP-2 via its appendage domains. These cargo specific adaptor proteins aid in the recruitment of specific receptors to AP-2, and are expressed in distinct cell types to confer tissue specificity, therefore allowing for a wide range of proteins to be recruited to clathrin coated vesicles (McMahon and Boucrot, 2011). An example of a cargo specific adaptor protein is ARH (autosomal recessive hypercholesterolemia protein). It is primarily expressed in the liver where it acts as a cargo specific adaptor for low density lipoprotein receptors (LDLRs) (He et al., 2002). AP-2 also binds the accessory proteins AP180/CALM (*Drosophila*/mammalian nomenclature) and synaptojanin. AP180 is brain specific whereas CALM is ubiquitously expressed. AP180 binds to the

alpha appendage domain of AP-2 (Praefcke et al., 2004). It also binds to $PI(4,5)P_2$ and clathrin and functions in clathrin polymerisation, and is thought to regulate vesicle size (Ford et al., 2001). The lipid phosphatase synaptojanin is also recruited to the α appendage domain of AP-2 (Chang-Ileto et al., 2011). It is thought to modify the lipid composition of clathrin coated vesicles therefore aiding in the release of $PI(4,5)P_2$ binding proteins such as AP-2 and AP180 from the membrane (Haffner et al., 2000).

The appendage domains of AP-2 are crucial for the interaction between AP-2 and clathrin. The N-terminal domain of the clathrin heavy chain contains a WD40 like β propeller domain (Ter Haar et al., 2000). WD40 domains are widespread and involved in protein-protein interactions in cell signalling and sorting. This clathrin N-terminal domain binds to the hinge domain of the β subunit of AP-2 (Ter Haar et al., 2000). Clathrin also binds to the appendage domain of the β subunit (Owen et al., 2000).

AP-2 acts as a central point in the dynamic system that is the formation of clathrin coated vesicles in CME due to the number of interactions it forms with proteins of the clathrin complex. These interactions allow for the strict regulation of this crucial endocytic pathway.

1.2.2.3 Clathrin mediated endocytosis and human disease

Clathrin mediated endocytosis has been linked to several human diseases. The loss of function of any of the main components of CME results in embryonic lethality (Mitsunari et al., 2005). Many proteins of the CME machinery have been implicated in cancers. Mutations in clathrin and its adaptors EPS15 and CALM (AP180) have been linked to breast and lung cancers (Kan et al., 2010). However the link between these mutations and the development of the disease remains unclear. There have also been links between CME and neurodegenerative diseases. CME is known to be crucial for synaptic vesicle recycling, with any impairment in this process playing a role in neurodegenerative diseases such as Alzheimer's disease (Yao, 2004). CME is also

important in the endocytosis of the amyloid precursor protein (APP), and therefore its processing to form amyloid beta, a key player in Alzheimer's disease (Wu and Yao, 2009). Mutations in the LDLR specific cargo specific adaptor ARH have been seen in autosomal recessive hypercholesterolemia (He et al., 2002). The process of CME is also exploited by several toxins, viruses and bacteria (Abrami et al., 2003, Rust et al., 2004, McMahon and Boucrot, 2011).

1.3 Model membrane methods for examining the intracellular interactions of membrane proteins

The formation of protein transport machinery provides a link between the secretory and endocytic trafficking pathways through their continuous movement and recycling. Their formation requires the recruitment of various cytosolic proteins to specific membrane domains within each trafficking organelle. These complexes aid the trafficking of membrane proteins at different intracellular compartments, which helps to maintain the identity of the specific trafficking organelles (Niehage et al., 2013). These trafficking proteins and protein coat complexes recognise and bind to specialist sorting motifs in the cytoplasmic domains of membrane proteins (Kurten, 2003). Therefore, the intracellular domains of membrane proteins are key to their function. They act as mediators between the membrane protein and cytosolic proteins. Many cytosolic proteins bind to the cytoplasmic domains of membrane proteins and help to relay signals or aid in the trafficking of the protein.

1.3.1 Techniques for studying protein-protein interactions

Due to the fact that the cytosolic binding partners of membrane proteins are vital in the function and trafficking of that membrane protein it is crucial that we develop ways to examine these interactions. There are several different methods previously used for examining protein-protein interactions. A selection of these include two-hybrid based systems, affinity chromatography and co-immunoprecipitation (Phizicky and Fields, 1995). Two-hybrid systems are genetic methods that utilise transcriptional activity as a measure of protein-protein interactions (Fields and Song, 1989). It works on the principle that many site-specific transcriptional activators contain a DNA binding domain and a transcription activation domain (Keegan et al., 1986). In order to examine protein-protein interactions a DNA binding domain is fused to one protein of interest and a transcription activation domain is fused to a second protein of interest.

Both of these hybrids are generally expressed in yeast cells, with expression in mammalian cells also possible. If the two proteins interact a functional activator is created by bringing the two domains (DNA binding and transcription activation domains) together which can be detected by the expression of reporter genes (Fields and Song, 1989). As this yeast two-hybrid system only allows for the detection of interactions between proteins localised to the nucleus a split ubiquitin assay was developed to detect protein-protein interactions elsewhere within the cell (Johnsson and Varshavsky, 1994). It relies on the fusion of the C-terminal fragment of ubiquitin to one protein and the N-terminal fragment of ubiquitin to a second protein, which if in close proximity, can be cleaved by ubiquitin specific proteases (Johnsson and Varshavsky, 1994). The two-hybrid systems can be used to screen libraries of activation domain hybrids to identify multiple interactors of a specific protein. The main weakness of two-hybrid systems is that there are a high number of false positives, estimated at 70% (Deane et al., 2002). This assay also relies on fusion proteins which may inhibit protein-protein interactions.

Tandem affinity purification (TAP) coupled to mass spectrometry has also been previously used to study protein-protein interactions (Puig et al., 2001). It involves the fusion of a TAP tag to the C-terminus of the protein of interest. The TAP tag consists of a calmodulin binding peptide (CBP), a tobacco etch virus protease (TEV protease) cleavage site followed by Protein A. The fusion protein can be expressed in both yeast and mammalian cells. The cells are then lysed and the fusion complex isolated through the binding of Protein A of the TAP tag to an IgG matrix. The proteins are eluted through TEV protease cleavage of the TAP tag and analysed by mass spectrometry (Puig et al., 2001). The TEV protease can be removed by the binding of CBP to calmodulin resin. This technique allows for the detection of protein interactions without any prior knowledge of possible interactions. The use of a tag limits this technique as

the tagged protein may not bind sufficiently to the affinity resin or the tag may affect the function of the protein (Puig et al., 2001).

Co-immunoprecipitation is the most commonly used method for detecting protein-protein interactions. Essentially cell lysates are produced, antibody added, the bound antigen precipitated and washed, and the interacting proteins are eluted and can be analysed by several methods including SDS-PAGE and mass spectrometry (Moresco et al., 2010). Affinity purification can also be used for detecting protein-protein interactions. It involves the use of particular protein of interest fused to an affinity tag, such as a glutathione S-transferase (GST) tag. This can then be used to pull out interacting proteins from cytosol samples as well as from purified proteins. One advantage of using specific antibody rather than a fusion protein is that the native expression of the protein of interest is unaltered (Moresco et al., 2010). Limitations exist when using a tagged protein as the tag may interfere with protein-protein interactions. Also the use of polyclonal antibodies means that there may be non-specific binding leading to the production of false positives.

These well-established techniques for examining protein-protein interactions have several limitations when investigating interactions of membrane proteins. Firstly, the majority of these techniques require the lysis of the cell, primarily through the use of detergents. These detergents disrupt binding; therefore weak protein-protein interactions that are functionally significant may not be detected. The disruption of the membranes is also not ideal when examining membrane protein interactions. The main drawback of these methods for examining membrane protein interactions is the fact that they do not take into account any interaction between both the membrane protein and cytosolic factors with membrane lipids, and therefore fail to detect physiologically relevant interactions that require an interaction with lipids.

The formation of protein complexes on the cytoplasmic domains of membrane proteins is aided by interactions between cytosolic proteins and membrane proteins with membrane lipids at specific domains of the organelle membrane. Phosphoinositides are a group of signalling lipids that play a crucial role in this process. They are tightly regulated by sets of specific kinases and phosphatases that reside on different secretory and endocytic compartments (Mayinger, 2012). It is this tight regulation of phosphoinositides that also helps in the maintenance of trafficking organelle identity (Krauss and Haucke, 2007). Phosphoinositides are recognised by several proteins involved in trafficking and aid in the assembly of trafficking machinery.

The role played by phosphoinositides in the recruitment of cytosolic proteins to the membrane, their marking of organelle identity, and their role in membrane trafficking is vital. This needs to be taken into consideration when examining the cytosolic binding partners of membrane proteins. The inability of previous methods to take the native environment of a membrane protein into account when examining interactions, and the crucial role played by membrane lipids in these interactions, calls for the development of techniques that overcome these drawbacks. A method has recently been developed to examine these interactions based on a model membrane system. Engineered lipid vesicles known as liposomes provide a membrane environment (Kinuta and Takei, 2002). The biochemical and physical properties of liposomes can be controlled. This allows for the analysis of binding partners *in vitro* by mimicking the native environment of a membrane protein.

1.3.2 A liposome based model membrane system

Liposomes are engineered lipid vesicles and range in size from 50 nm to about 500 nm in diameter, and have previously been used to study the interaction between phospholipids and membrane proteins. They are produced by re-suspending a dry lipid film in an aqueous solution, followed by several flash freezing and thawing cycles. Liposomes of 50-200 nm in diameter are used in pharmacology as drug delivery

systems (Samad et al., 2007) and can be used for the biochemical analysis of the interaction between proteins and lipids (Walde et al., 2010).

Liposome based systems have been used previously to examine the assembly of protein coats or parts of these coats. The use of protein-free liposomes to study the assembly of the clathrin coat complex is well characterised (Höning et al., 2005, Drake et al., 2000, Ford et al., 2001, Zhu et al., 1999). Recent advances now allow for the use of so called proteo-liposomes, whereby proteins can be covalently linked to these liposomes. Crottet et al. (2002) utilised liposomes presenting peptides containing tyrosine based sorting motifs, to examine the recruitment of the clathrin adaptor AP-1. This AP-1 recruitment was dependent on several factors including ARF1, GTP and the phosphoinositide $PI(4,5)P_2$.

Bourel-Bonnet et al. (2005) developed and synthesised a hydrazine based lipid anchor allowing for the covalent attachment of peptides in a single biologically relevant orientation, to the surface of liposomes. They validated this system by coupling the cytoplasmic domain of the lysosomal associated membrane protein (LAMP) to liposomes. The adaptor protein AP-3 was recruited from brain cytosol samples onto these liposomes, and recruitment was abolished when a single tyrosine residue in the cytoplasmic domain was substituted for alanine, indicating its importance in AP-3 binding. The development of lipid anchors allowing for the covalent attachment of peptides to liposomes was a major technical advance. The intracellular domain of membrane proteins can be presented in their native configuration.

In 2006 Baust et al utilised a liposome based system to study the assembly of AP-1A protein coats required for transport between the secretory pathway, and the endosomal and lysosomal systems. The cytoplasmic tails of the gpI envelope glycoprotein of the *Varicella zoster* virus, and the lysosomal integral membrane protein Limp II were covalently coupled to the liposomes using a lipid anchor with an aldehyde-derived

head group, which reacted with a hydrazine group at the N-terminus of the peptides (Baust et al., 2006). The recruitment of the AP-1A coat from brain cytosol was analysed and approximatly 40 proteins were identified. It was found that the assembly of the coat triggered the recruitment of Rac1, the Wave/Scar complex, Rab11 and Rab14. The liposome technique was successfully used to examine the coordinated assembly of the AP-1A coat.

Jackson et al. (2010) and Kelly et al. (2014) both utilised liposomes presenting a tyrosine based sorting motif peptide amongst other techniques to examine the assembly of the AP-2/clathrin coat. A large scale conformational change in AP-2 was observed, driven by its binding to $PI(4,5)P_2$ and to cargo (tyrosine based motif peptide). This was necessary for the recruitment of clathrin and, therefore the formation of clathrin coated vesicles.

In 2011 Pocha et al designed a liposome based system to establish that the retromer complex, important for mediating endosome to TGN trafficking, is an interaction partner of the apical determinant Crumbs (Crb) (Pocha et al., 2011). Briefly the method involved the covalent coupling of the Crb2 intracellular domain to liposomes via a lipid anchor containing an activated maleimide head group. The intracellular domain of Crb2 was expressed and purified from *E. coli*. The bacterial expression plasmid contained an N-terminal tandem affinity tag followed by a TEV protease cleavage site and a single cysteine residue to allow for the covalent coupling of the intracellular domain of Crumbs 2 to liposomes. These proteo-liposomes were incubated in brain cytosol to allow for the determination of interaction partners by mass spectrometry and western blotting. Using the liposome recruitment technique, Pocha et al. (2011) showed that the intracellular domain of Crb2 interacts with the Vps35 subunit of the retromer complex. This interaction was crucial for the trafficking of Crb2 (Pocha et al, 2011).

A powerful advantage of this liposome recruitment system is that a membrane context is provided for the cytoplasmic domain of a receptor. This allows for the assembly and isolation of intricate protein complexes and coats that require both the binding of the receptor to intracellular factors, as well as the binding to membrane lipid head groups. The main advantage of this liposome system over conventional protein-protein interaction techniques such as yeast two hybrid and co-immunoprecipitation methods, is its increased sensitivity and specificity due to the membrane context provided (Pocha and Wassmer, 2011).

The primary focus of this thesis will be on the use, validation and characterisation of a liposome recruitment system based on that by (Pocha et al., 2011) to examine novel intracellular interaction partners of a model membrane protein. The major protein that will be utilised as a model is the amyloid precursor protein known as APP.

1.4 The amyloid precursor protein as a model membrane protein

The amyloid precursor protein or APP is a type 1 transmembrane protein best characterised for its role in Alzheimer's disease. APP belongs to the APP family of proteins consisting of APP itself, and the APP-like proteins APLP1 and APLP2. The APP family members exhibit functional redundancy (Caldwell et al., 2013). Homologues of APP have also been identified in *Drosophila*, *C. elegans* and *Xenopus* (De Strooper and Annaert, 2000). The gene coding for APP lies on chromosome 21 and contains 19 exons, of which exons 7, 8 and 15 can be alternatively spliced. This splicing leads to the production of 3 main isoforms of APP known as APP_{695}, APP_{751} and APP_{770}. APP is ubiquitously expressed in mammalian cells with varying levels of expression of each isoform in different tissues and cell types (Tanzi et al., 1987, Wasco et al., 1992, Caldwell et al., 2013). APP_{695} is the predominant isoform in neuronal tissue whereas non-neuronal cells mainly express the APP_{751} and APP_{770} isoforms (Kang et al., 1987) (de Silva et al., 1997).

APP is a type 1 transmembrane protein characterised by its large extracellular domain and a relatively small intracellular domain. The structure and the potential functions of each APP domain are shown in figure 6. APP's large ectodomain consists of a cysteine rich globular domain called E1, a helical domain known as E2, a transmembrane domain, and a C-terminal intracellular domain termed AICD. The longer APP isoforms also contain a Kunitz-type protease inhibitor (KPI) domain. The primary focus of previous research on APP has been on its processing by secretases, and the production of the amyloid beta (Aβ) peptide, a key contributor to amyloid plaques in the pathology of Alzheimer's disease (Robakis et al., 1987).

Figure 6. The structure and likely functions of APP.
APP has a large ectodomain comprising of the E1, E2 and the KPI domains. The KPI domain is not found in the APP695 isoform. The transmembrane domain of APP can be cleaved by a number of secretases. The C-terminal domain of APP (AICD) is physiologically the most interesting domain due to its large number of binding partners. Figure from (Dawkins and Small, 2014).

1.4.1 APP processing and Alzheimer's disease

APP is a key player in the pathology of Alzheimer's disease. Alzheimer's disease is a neurodegenerative disease characterised by progressive memory loss and reduced cognitive function (DeKosky and Scheff, 1990). It is primarily a disease that occurs during the later stages of life (Rossor et al., 1984). However, mutations in the gene encoding APP are known to lead to a familial or early onset form of Alzheimer's

disease, which can occur earlier in life (Goate et al., 1991, Murrell et al., 1991). The cleavage of APP by secretases is also known to play a major role in Alzheimer's disease. Mutations in gamma secretase have been identified which also lead to a familial form of Alzheimer's disease (Sherrington et al., 1995).

Alzheimer's disease is characterised by two main neuropathophysiological features; the presence of both amyloid plaques and neurofibrillary tangles (Lewis et al., 1987). Neurofibrillary tangles stem from the hyperphosphorylation of the microtubule associated protein Tau (Grundke-Iqbal et al., 1986). This hyperphosphorylation causes the aggregation of Tau as paired helical filaments, contributing to the neurofibrillary tangles (Augustinack et al., 2002). Amyloid beta (Aβ), formed by the aberrant cleavage of APP by secretases is the primary constituent of amyloid plaques, and plays a key role in the pathology of Alzheimer's disease (O'Brien and Wong, 2011).

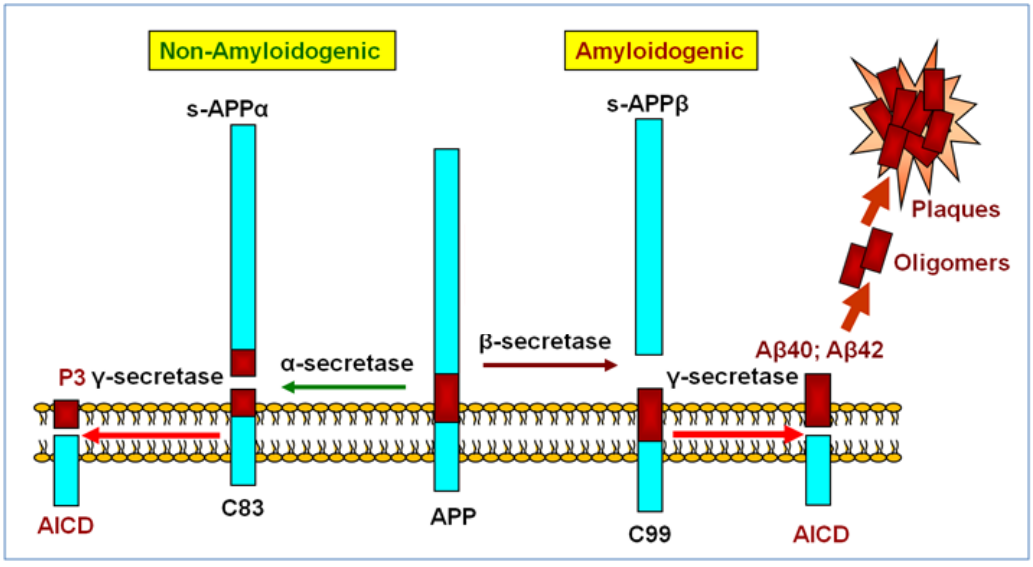

Figure 7. The secretase processing of APP.
Cleavage of APP first with α secretase and then γ secretase is thought to be non-amyloidogenic. The amyloidogenic cleavage of APP occurs with β and γ secretase cleavage releasing the amyloid beta (Aβ40, Aβ42) peptide which forms oligomers and is the main constituent of amyloid plaques. Figure adapted from Zhang (2012).

There are two different types of APP processing, which depend on two different sets of secretases. Non-amyloidogenic processing of APP occurs when it is first cleaved by α secretase between the 16th Lys and 17th Leu (residues 612 and 613 of APP). This cleaves APP in the Aβ sequence, therefore Aβ cannot be produced (hence non-amyloidogenic pathway) (De Strooper and Annaert, 2000). ADAM-10 (a disintegrin and metalloproteinase 10) is thought to be one of the major α-secretases involved in APP processing, where it resides primarily on the plasma membrane, Golgi, and exocytotic transport vesicles (Sambamurti et al., 1992). Cleavage by α-secretase releases a soluble APPα ectodomain, and subsequent cleavage by γ-secretase releases the P3 fragment and AICD. Only a small fraction of the APP pool is cleaved by α-secretase, which leaves most of APP as full length (Haass et al., 1992).

The amyloidogenic processing of APP occurs when APP is first cleaved by β-secretase and then γ-secretase. As with α-secretase, β-secretase cleavage also occurs in physiological conditions, meaning all the fragments of APP produced by secretase cleavage, including the Aβ fragment, are part of the normal cellular process (Haass et al., 1992). BACE-1 (beta-site APP cleaving enzyme) is a type 1 integral membrane protein and is the most widely studied β-secretase candidate. BACE-1 cleaves APP at the N-terminus of the Aβ peptide, releasing the soluble APPβ fragment (Haass et al., 1992). BACE-1 functions at a low pH and is thought to mainly reside in endocytic compartments such as endosomes and lysosomes, as well as the Golgi (Vassar et al., 1999, Haass et al., 1995). After BACE-1 cleavage the C99 peptide of APP can then be further processed by γ-secretases. Presenilin-1 is a subunit of γ-secretase, and contains 8 transmembrane domains. γ-secretase is localised to several intracellular compartments including; the ER, Golgi, endosomes, autophagosomes and the plasma membrane. γ-secretases cleave APP at the C-terminal end of the Aβ sequence releasing Aβ and AICD (Haass and De Strooper, 1999). The released Aβ fragment can

form toxic oligomers aggregating in amyloid fibres, the main constituent of the amyloid plaques found in the brains of patients with Alzheimer's disease.

1.4.2 The function of APP and its intracellular domain AICD

Despite the importance of APP in Alzheimer's disease the physiological role of APP still remains largely unclear. This is partly due to previous research primarily focusing on the Aβ peptide itself. APP has been implicated in several physiological processes such as cell adhesion, proliferation and differentiation, as well as neurite outgrowth, synaptogenesis and synaptic plasticity (reviewed in (Zheng and Koo, 2011). This section will briefly outline the role played by APP in these processes.

1.4.2.1 APP and neurite outgrowth, synaptic plasticity and synaptogenesis

Neurite outgrowth, synaptogenesis and synaptic plasticity are some of the physiological process APP is thought to be involved in. APP is known to promote neurite outgrowth in cell culture through its role in cell adhesion. APP binds to laminin, collagen type 1 and heparin sulphate, which all influence neurite outgrowth (Kibbey et al., 1993, Beher et al., 1996). APP is also thought to be involved in cell-cell adhesion. It is known to form homo- or hetero-dimers, with trans-dimerisation able to promote cell adhesion, as well as the binding of heparin sulphate to the E1 or E2 domains of APP (Soba et al., 2005, Dahms et al., 2010). APP is also thought to influence the activity of other cell adhesion molecules such as β1-integrin, and plays an important role in regulating adult hippocampal neurogenesis (Young-Pearse et al., 2008, Wang et al., 2014a).

APP is expressed at both pre and post synaptic sites during development, as is highly expressed during periods of synaptogenesis. Therefore it is thought to be involved in regulating synaptogenesis (Dawkins and Small, 2014). APP knock out mice show neurological defects like impaired locomotor activity, which may be explained by an effect on synaptogenesis (Zheng et al., 1995). APP knock out mice also show altered

synaptic function. Mice with double knock out of APP and APLP2 have impaired neuromuscular junction formation, observed by a reduction in synaptic vesicles and impaired synaptic transmission, which may be responsible for the lethality of the APP/APLP2 double knock out (Wang et al., 2005). APP is also thought to be involved in synaptic plasticity mainly by affecting synaptic calcium homeostasis. It is thought to alter the expression of the GluR2 subunit of the AMPA receptor, a regulator of synaptic calcium permeability (Lee et al., 2010). Aged knock out mouse models of APP show defects in long term potentiation (LTP), a persistent strengthening of synapses (Ring et al., 2007). Knock in (KI) mice of the soluble ectodomain of APP (APPsα) in an APLP2 knock out background (APPsα-KI/APLP2-KO) survive to adulthood, unlike APP/APLP2 KO mice. A reduction in LTP is also observed in APPsα-KI/APLP2-KO mice (Weyer et al., 2011). The data from these mouse models reveal that APP and APLP2 are important in the function and plasticity of central synapses (Korte et al., 2012).

1.4.2.2 APP and cell signalling

The structure of APP has led to the theory that APP acts as a receptor, and therefore has a potential role in cell signalling. Due to the similarity of the proteolytic processing of APP with that of the Notch receptor, APP has been proposed to function in cell signalling in a manner similar to Notch signalling (Nakayama et al., 2011). In Notch signalling the intracellular domain of Notch is cleaved by γ-secretases and is translocated to the nucleus where it is known to activate gene transcription. The intracellular domain of APP (AICD) is also translocated to the nucleus, where it is known to control gene expression (Cupers et al., 2001). This supports the theory that APP may function in a similar way to Notch. APP may also play a role in cell signalling via its binding to G-proteins, mediated by AICD. It is thought that binding of a ligand to the ectodomain of APP may result in signal transduction via activation of the GTP-binding protein Gαo (Okamoto et al., 1995). Recently, the interaction of the insect APP homologue APPL with Gαo has been shown to be involved in the control of neuronal

migration (Ramaker et al., 2013). In support of APP's role in cell signalling its homologue APPL in *Drosophila* was shown to be involved in wnt/planar cell polarity signalling (Soldano et al., 2013).

The intracellular domain of APP is known to be key to the function of the protein, and in its role as a cell signalling molecule. APP cleavage by secretases releases AICD which is known to translocate to the nucleus, where it has a role in gene expression. AICD is able to bind to Fe65 via the YENPTY motif at the C-terminus of AICD (Fiore et al., 1995). Fe65 contains two phosphotyrosine binding (PTB) domains, and binds to AICD via PTB2, the binding of which is thought to stabilise AICD (Beckett et al., 2012). Fe65 interacts with the histone acetyltransferase tat-interactive protein (Tip60) via PTB1, and together with AICD are delivered to the nucleus by dynamin mediated retrograde trafficking, where they affect gene expression (Beckett et al., 2012). AICD is reported to affect the expression of several different genes including APP itself, BACE-1, Aβ-degrading enzyme neprilysin (NEP) and epidermal growth factor receptor genes (von Rotz et al., 2004, Pardossi-Piquard et al., 2005, Belyaev et al., 2009, Zhang et al., 2007a). AICD, via its YENPTY motif is also known to bind to mDAB-1 which, when phosphorylated, is able to recruit kinases such as Src therefore providing a link between APP and phosphorylation dependent signalling pathways (De Strooper and Annaert, 2000).

APP has been linked to a wide variety of physiological functions and is probably one of the most well studied proteins. Despite this there is still currently no molecular model available for exactly how APP is involved in neurite outgrowth, synaptic plasticity, and synaptogenesis, and how it functions as a cell signalling molecule. This is primarily due to the lack of understanding of how APP can regulate such a wide variety of processes.

1.4.3 APP trafficking

Intracellular trafficking is known to play a key role in the pathophysiology of Alzheimer's disease. Intracellular trafficking is important in maintaining normal neuronal function. Of particular importance in neurones is the endocytic pathway, required for synapse function. In Alzheimer's disease there is thought to be a hyper activation of the endocytic pathway, as evidenced by the increased size and volume of neuronal endosomes in Alzheimer's disease brain samples (Nixon et al., 2000). The exact location of Aβ production is debated. It is thought to primarily occur in endosomal and lysosomal compartments and depends on the location of γ-secretase. The accumulation of Aβ disrupts the integrity of the lysosomal membrane (Yang et al., 1998, Tam et al., 2014). Lysosomal exocytosis of Aβ has also been shown to be important in Alzheimer's disease mouse models, with deficiency of the lysosomal sialidase NEU1 leading to an amyloidogenic type process (Annunziata et al., 2013).

As APP is a type 1 transmembrane protein, the trafficking of APP is crucial to its function. APP is produced in the ER and processed in the Golgi. It undergoes several post translational modifications such as glycosylation, and phosphorylation and ubiquitination of its intracellular domain (Watanabe et al., 2012, Acevedo et al., 2014, Oishi et al., 1997). It is then trafficked to the plasma membrane where it can be processed by α-secretase, releasing the ectodomain (Groemer et al., 2011). Figure 8 shows an overview of the trafficking of APP. APP is also known to traffic directly from the TGN to lysosomes in an AP-3 dependent manner. It is then rapidly degraded which is in line with the fact APP turnover is thought to be quite rapid (Tam et al., 2014). The trafficking of APP from the Golgi is also thought to be mediated by the adaptor Mint3 (Caster and Kahn, 2013). Mint proteins are implicated in the localisation of proteins to the plasma membrane. They are able to bind ARFs and regulate the trafficking of APP

from the Golgi (Hill et al., 2003). The adaptor protein AP-4 has also been implicated in the TGN-to-endosome transport of APP (Burgos et al., 2010).

Figure 8. APP, BACE-1 and γ-secretase trafficking pathways
APP (blue bars) is internalised by clathrin mediated endocytosis whereas BACE-1 (red bars) is endocytosed by a ARF-6 dependent pathway. Both APP and BACE-1 are sorted into early endosomes where APP can be cleaved producing the βCTF which is a substrate for γ secretase, producing AICD which can be translocated to the nucleus and Aβ. Aβ (pink bar) is sorted in multivesicular bodies and secreted via exosomes. APP retrieval from the early endosomes to the TGN is mediated by the retromer complex. γ secretase (purple lines) is produced and processed in the ER and Golgi and then transported to the plasma membrane and endosomes. The red membrane areas represent lipid raft domains. Figure from Rajendran and Annaert (2012).

Intracellular trafficking is important in the processing of APP as it is required for the correct localisation of not only APP but the β and γ-secretases also (Figure 8). In order for Aβ generation APP and the two secretases need to be trafficked to the endosomal compartments. The trafficking of these proteins regulates their intracellular localisation, and therefore the processing of APP and the production of Aβ (Rajendran and Annaert, 2012).

The intracellular domain of APP (AICD) is crucial for the trafficking of APP. The YENPTY motif of AICD is completely conserved from *C. elegans* to humans, and contains the tyrosine based sorting motif recognised by many adaptor proteins involved in membrane trafficking (King and Turner, 2004). This domain is important for the clathrin mediated endocytosis of APP. The YENPTY motif of AICD contains a tyrosine based sorting signal, and is recognised by clathrin adaptor proteins such as AP-2 that help regulate clathrin dependent endocytosis (King and Turner, 2004). Deletion of AICD and the YENPTY motif impairs the internalisation of plasma membrane APP, and decreases Aβ secretion by stopping the processing of APP in endocytic compartments (Leblanc and Gambetti, 1994, Essalmani et al., 1996). AICD also contains the motif YxxI at its N-terminus. Deletion of this motif does not affect internalisation but does affect the sorting of APP in polarised epithelial cells (Zheng et al., 1998). Both the YENPTY and YxxI motifs are required for the rapid degradation of full length APP in the lysosome (Lai et al., 1998). Clathrin is also required for the endocytosis of the β-secretase BACE-1. Mutation of the sorting motif in BACE-1, AP-2 or clathrin decreases the endosomal localisation and increases the plasma membrane localisation of BACE-1 (Prabhu et al., 2012). The clathrin adaptor CALM/AP180 (human/*Drosophila* nomenclature) is also thought to play a role in the pathophysiology of Alzheimer's disease (Ando et al., 2013). Taken together this demonstrates the importance of clathrin mediated endocytosis in the processing of APP.

The trafficking of APP from the endosomes to the TGN is also important in APP processing. The APP binding and sorting protein SorLA is known to be decreased in Alzheimer's disease (Rogaeva et al., 2007, Dodson et al., 2006). SorLA is a part of the mammalian family of vacuolar protein sorting 10 (VPS10) containing proteins, and acts as a retromer binding receptor (Seaman, 2004, Nielsen et al., 2007). The retromer is a multi-subunit complex important for regulating the endosome to TGN transport of membrane proteins such as the mannose 6-phosphate receptor (Arighi et al., 2004, Seaman, 2004). The retromer is composed of two distinct sub complexes. The cargo selective sub complex contains the vacuolar sorting proteins (VPS) 35, 29 and 26 with VPS35 binding to the cytoplasmic domains of membrane proteins. VPS35 also interacts with the sortin nexins (SNX) 1 and 2 of the membrane binding subcomplex. SNX1 and 2 interact with SNX5 and 6 and bind to phosphoinositides via their PX domain (Seaman, 2004, Seaman, 2005, Bonifacino and Hurley, 2008, Wassmer et al., 2007, Wassmer et al., 2009). The retromer subunit VPS35 co-localises with APP positive vesicular structures (Bhalla et al., 2012). Loss of VPS35 causes an increase of APP in endosomes and a decreased half-life of APP (Bhalla et al., 2012). The phosphorylation of APP at S655 in the YTSI (YxxI) motif of AICD enhances retromer mediated retrieval from endosomes (Vieira et al., 2010). The hemizygous deletion of VPS35 in a mouse model of Alzheimer's disease was shown to accelerate the Alzheimer's disease neuropathophysiology (Wen et al., 2011). The transport of the β-secretase BACE-1 from the endosomes to the TGN is also retromer dependent. Both SNX6 and VPS35 have been shown to interact with BACE-1 and control its retrieval from endosomes (Sullivan et al., 2011, Small et al., 2005). Loss of VPS35 reduces the retrieval of both APP and BACE-1 back to the TGN, meaning there is an increase of both in endosomes, leading to an increase in Aβ levels and the enlargement of endosomes (Bhalla et al., 2012).

This highlights the importance of trafficking pathways in Alzheimer's disease, in particular in the transport of APP. It suggests that the pathogenesis of Alzheimer's disease may at least, in part, be caused by the impaired transport of proteins from the endosomes to the TGN. Clathrin mediated endocytosis also plays a crucial role in Alzheimer's disease. Both of these transport pathways have the potential to be future therapeutic targets. The pathophysiology of Alzheimer's disease is highly complex. The main focus of previous research has been on disease causing mutations and Aβ, rather than understanding the physiological roles of proteins such as full length APP.

1.5 The PIKfyve complex

The retromer dependent trafficking of APP from the endosomes to the TGN is important for APP function, processing and the production of Aβ. The PIKfyve complex is another protein complex, and like the retromer it is implicated in endosome to TGN transport amongst other functions. The PIKfyve complex is a multimeric protein complex that catalyses the conversion of the endosomal signalling lipid PI(3)P to $PI(3,5)P_2$.

1.5.1 Phosphoinositides

PI(3)P and $PI(3,5)P_2$ belong to a group of signalling lipids known as phosphoinositides, minor constituents of phospholipid bilayers. Phosphoinositides derive from phosphatidylinositol (PI) and differ only in the phosphorylation of the inositol ring. PI is produced in the ER, and its phosphorylation is known to occur at many intracellular organelles, giving rise to distinct intracellular phosphoinositide pools, specific to different intracellular compartments (Cockcroft and De Matteis, 2001). Levels of phosphoinositides at these compartments are tightly regulated by specific sets of phosphoinositide kinases and phosphatases.

$PI(4,5)P_2$ is probably the most well characterised phosphoinositide. It is primarily localised to the plasma membrane where it acts as a precursor for soluble and membrane bound secondary messengers in signal transduction, and lipid signalling pathways. $PI(4,5)P_2$ can be hydrolysed to produce the secondary metabolites diacyl-glycerol (DAG) and inositol 1,4,5-trisphosphate (IP_3), by phospholipase C (PLC) enzymes, which are activated through ligand binding to G protein-coupled receptors (GPCRs) (Taylor et al., 1991). DAG remains bound to the plasma membrane where it activates protein kinase C (PKC), stimulating its translocation from the cytosol to the plasma membrane (Berridge, 1984). DAG can be phosphorylated to form phosphatidic acid (PA), which interacts with CTP (cytidine triphosphate) to form the cytidine

diphosphate diacylglycerol that replenishes PI, along with inositol (Berridge, 1984). IP_3 is soluble, and diffuses through the cytoplasm to the ER, where it binds to the IP_3 receptor on ligand gated calcium channels, triggering the release of calcium into the cytoplasm (Ferris and Snyder, 1992). It is also recycled back to inositol, required for the re-synthesis of PI, through an inositol phosphatase cycle (Berridge, 1984). The production of second messengers is described as the canonical function of PIs (Payrastre et al., 2001). Phosphatidylinositol-3,4-bisphosphate ($PI(3,4)P_2$) and phosphatidylinositol-3,4,5-tiphosphate ($PI(3,4,5)P_3$) are signalling molecules produced in response to extracellular stimuli. They activate Akt, and are involved in cell survival and proliferation (Alessi et al., 1997).

Phosphoinositides are important in membrane trafficking events. Different phosphoinositides are localised to distinct intracellular compartments, and are described as markers for organelle identity, due to their ability to recruit proteins to specific intracellular compartments (Munro, 2002). These proteins contain protein modules that bind specific phosphoinositides (PIBMs), including the pleckstrin homology (PH) domain, the Fab1, YPTB, Vac1 and EEA1 (FYVE) domain, the phox homology (PX) domain, the epsin amino-terminal homology (ENTH) domain and the band 4.1, ezrin, radixin and moesin (FERM) domain (Cullen et al., 2001). Some phosphoinositide binding proteins are able to interact with small GTPases from the Ras protein superfamily, such as Arf and Rab GTPases (Behnia and Munro, 2005). Together, phosphoinositides, phosphoinositide binding proteins, and these GTPases help control the recruitment of proteins to membranes that are involved in membrane trafficking (Mayinger, 2012) PLCδ1 contains a PH domain that binds to $PI(4,5)P_2$, causing its translocation to the plasma membrane (Stauffer et al., 1998). $PI(4,5)P_2$ can be produced from PI(4)P, $PI(3,4,5)P_3$ and PI(5)P by PI(4)P 5-kinases, PTEN and PI(5)P 4-kinases respectively (Rameh et al., 1997). $PI(4,5)P_2$ plays a crucial role in clathrin mediated endocytosis, described earlier in this chapter. As well as serving as a precursor for $PI(4,5)P_2$, PI(4)P is localised to the Golgi where it is important in

controlling exit from the Golgi to both the plasma membrane and the yeast vacuole (De Matteis et al., 2002).

Yeast VPS34 and its mammalian orthologue are phosphoinositide 3-kinases and phosphorylate PI to produce PI(3)P (Schu et al., 1993). PI(3)P is localised to the early endosome membrane where it is crucial for endocytic trafficking. The FYVE domain of EEA1 binds to PI(3)P. EEA1 interacts with the active GTPase Rab5, and helps to stimulate endosome fusion (Simonsen et al., 1998). The yeast protein Vam7p contains a PX domain that binds to PI(3)P, which is important for vacuolar sorting (Cheever et al., 2001). PI(3)P is also bound by the PX domain of the sorting nexin SNX3. This interaction is important for the targeting or proteins, including the transferrin receptor, to endosomal compartments, and in doing so enables SNX3 to regulate the structure and function of endosomes (Xu et al., 2001).

PI(3)P serves as the precursor to $PI(3,5)P_2$, a crucial regulator of late endosome dynamics, in a reaction catalysed by the PI(3)P 5-kinase PIKfyve/fab1 (mammalian/yeast nomenclature) (Dove et al., 1997, Whiteford et al., 1997, Gary et al., 1998).

1.5.2 PIKfyve structure

The PIKfyve complex was first discovered in yeast and is made up of three main proteins; the Fab1/PIKfyve kinase, a scaffold protein known as Vac14/ArPIKfyve and the phosphatase Fig4/Sac3 (yeast/mammal nomenclature).

The PIKfyve complex is found in all eukaryotic cells studied to date. It was first discovered in hyperosmotically stressed yeast, that increased Fab1 (yeast PIKfyve homologue) activity, and lead to an increase in the levels of $PI(3,5)P_2$ (Dove et al., 1997). Vac14 was also discovered to be important in this increase of $PI(3,5)P_2$. This increase showed that $PI(3,5)P_2$ plays an important role in osmotic stress by regulating the vacuolar volume (Bonangelino et al., 2002, Cooke et al., 1998).

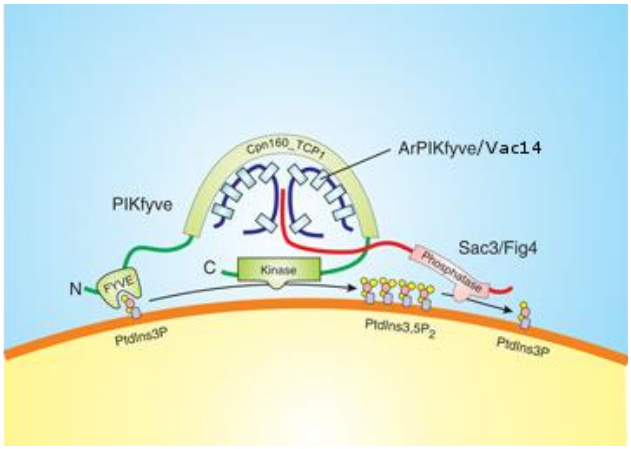

Figure 9. The structure and formation of the PIKfyve complex.
The phosphatase of Fig4 binds to a homodimer of Vac14, which in turn binds to the Cpn160_TCP1 domain of PIKfyve via HEAT repeats at the N-terminus of Vac14. The N-terminal FYVE domain of PIKfyve binds to PI(3)P on endosomal membranes. The PIKfyve complex then catalyses the conversion of PI(3)P to PI(3,5)P_2. Figure adapted from (Ikonomov et al., 2009a).

The first stage in the assembly of the PIKfyve complex is the multimerisation of the scaffolding adaptor protein Vac14 (Alghamdi et al., 2013). Vac14 and PIKfyve have been shown to physically associate in mammalian cells giving rise to the name ArPIKfyve (associated regulator of PIKfyve), with Vac14 required for the PIKfyve dependent production of PI(3,5)P_2 (Sbrissa et al., 2004, Bonangelino et al., 2002, Jin et al., 2008). Vac14 is composed almost entirely of HEAT repeats (17 in human Vac14) that help mediate protein-protein interactions (Dove et al., 2002, Jin et al., 2008). HEAT repeat containing proteins primarily function as scaffolds with several binding partners. Vac14 is the scaffold for Fig4 and PIKfyve of the PIKfyve complex (Jin et al., 2008). Vac14 is known to form a homodimer through its conserved C-terminal domain (Sbrissa et al., 2008, Alghamdi et al., 2013). The Vac14 homodimer then binds to the C-terminus of the phosphatase Fig4 via the same C-terminal fragment required for Vac14 homodimerisation. This sub-complex is independent of PIKfyve, and likely catalyses the Fig4 dependent dephosphorylation of PI(3,5)P_2 to PI(3)P (Sbrissa et al., 2008, Rudge et al., 2004).This sub-complex then binds to PIKfyve and is required for PIKfyve's kinase activity (Ikonomov et al., 2009a).

PIKfyve contains an N-terminal FYVE domain that binds to PI(3)P, followed by a DEP (Dishevelled, EG110 and Pleckstrin) domain, only found in the molecules of higher eukaryotes, and is absent from yeast and plant PIKfyve, with its function largely unknown (Shisheva, 2008). Following this is the Cpn60_TCP1 (HSP chaperonin_T-complex protein 1) domain that is thought to mediate several interactions, and is important for PIKfyve's kinase activity (Shisheva, 2008). PIKfyve contains a C-terminal kinase domain responsible for its catalytic activity. The Vac14/Fig4 subcomplex binds to the CPn60_TCP1 domain of PIKfyve, which is bound to PI(3)P via the FYVE domain. This binding induces a conformational change in PIKfyve, stabilising the complex interaction. The C-terminus of PIKfyve also aids in stabilising the complex (Ikonomov et al., 2009a). The formation of this PAS (PIKfyve, ArPIKfyve, Sac3) complex is required for the kinase activity of PIKfyve and, therefore the production of $PI(3,5)P_2$. Interestingly Fig4 is required for PIKfyve activation and is also catalytically active within the PAS complex (Ikonomov et al., 2009a). This demonstrates that the PAS complex contains proteins with antagonistic effects, which are both required for $PI(3,5)P_2$ production, indicating that the complex is able to tightly regulate $PI(3,5)P_2$ production and turnover.

1.5.3 PIKfyve function

The PIKfyve complex is expressed in all tissues which implies that it is vital in normal physiology (Zhang et al., 2007b). PIKfyve is both cytosolic and membrane bound, however, the membrane association of PIKfyve is key to its function (Ikonomov et al., 2009a). Membrane associated PIKfyve is found in compartments of the endocytic pathway. It is associated with the endosomal system, and localises to early and late endosomes/lysosomes, and multivesicular bodies (MVB), depending on cell type, protein expression level, and the rate of PI(3)P to $PI(3,5)P_2$ conversion (Shisheva, 2008). The primary role of PIKfyve is as a lipid kinase, catalysing the 5' phosphorylation of PI(3)P to $PI(3,5)P_2$, aided by Vac14 and Fig4. $PI(3,5)P_2$ produced

by PIKfyve can be dephosphorylated by myotubularin related protein 3 (MTMR3) to produce PI(5)P, therefore implicating PIKfyve in the production of PI(5)P as well as $PI(3,5)P_2$ (Zolov et al., 2012) (Oppelt et al., 2013). Although PIKfyve's primary function is as a lipid kinase it is also known to have protein kinase activity (Ikonomov et al., 2003).

1.5.2.1 PIKfyve's primary function in membrane trafficking

The PIKfyve complex is involved in the transport of membrane proteins in and out of the endosomal system (Figure 10). PIKfyve's role in the endosomal system was first indicated by an enlarged yeast vacuole, and vacuolation in mammalian cells upon deletion of any of the three components of the PIKfyve complex (Dove et al., 2009, Shisheva, 2008). This vacuolation is thought to be due to a drop in $PI(3,5)P_2$ levels caused by decreased synthesis (Ikonomov et al., 2002a). These vacuoles are derived from late endosomal pathway compartments in lower organisms, such as yeast. The identity of these vacuoles in mammalian cells is still up for debate. However, the common consensus is that these vacuoles co-localise with late endosomal/lysosomal markers, as well as a degree of co-localisation with early endosomal markers (Rutherford et al., 2006, Ikonomov et al., 2006). This points towards the fact that they are likely derived from endosomal structures and the preference for which endosomal compartment depends on the cell type (Shisheva, 2008).

In yeast, a molecular defect that contributes to the swollen vacuole phenotype observed in *fab1*Δ cells, is that the retrieval of membrane proteins from the vacuole is $PI(3,5)P_2$ dependent. In cells lacking $PI(3,5)P_2$ failure in recycling out of the vacuole might contribute to the enlargement of the vacuolar membrane (Dove et al., 2004).

In mammalian cells the mechanism contributing to vacuole formation is less clear. Endosome-to-TGN transport was found to be impaired upon the depletion of PIKfyve (Rutherford et al., 2006). This suggests that the PIKfyve catalysed conversion of PI(3)P

to $PI(3,5)P_2$ is required for the exit of membrane proteins from the endosomes (see figure 10). The trafficking from endosomes to the TGN occurs through endosomal transport intermediates, which are either carrier vesicles or maturing endosomes with distinct characteristics. PIKfyve has been shown to stimulate the formation of transport intermediates from early endosomes, and that this function of PIKfyve in endosome fusion and fission may play a role in the increase in endosome size observed upon PIKfyve inhibition (Sbrissa et al., 2007, Ikonomov et al., 2006).

Evidence for the role of PIKfyve in endosome-TGN transport also stems from the fact PIKfyve was found to phosphorylate the transport factor protein p40 (Ikonomov et al., 2003). p40 interacts with Rab9 and stimulates the late-endosome to TGN transport of the cation-independent mannose 6 phosphate receptor (CI-MPR) (Díaz et al., 1997). PIKfyve is linked to the retromer dependent endosome-TGN transport. The SNX1 and SNX2 subunits of the retromer complex bind *in vitro* to both PI(3)P and $PI(3,5)P_2$ (Carlton et al., 2004). Rutherford et al. (2006) found that PIKfyve regulates the endosome-to-TGN transport of the CI-MPR, whereas the internalisation and recycling of the EGF and transferrin receptors was unaffected by PIKfyve suppression. These results all support a role for PIKfyve in endosome to TGN trafficking.

Figure 10. The trafficking processes of the PIKfyve complex
The PIKfyve complex is required for transport out of endosomes. It effects the exit from endosomes via several different routes (purple arrows). PIKfyve binds to PI(3)P in the early endosomal membrane catalysing its conversion to $PI(3,5)P_2$ causing the formation/detachment of endosomal transport vesicles. Sac3 is then though to dephosphorylate $PI(3,5)P_2$ allowing for endosomal fusion. This process is likely to occur on other PI(3)P containing compartments such as the MVB. Figure from (Shisheva, 2008).

PIKfyve is thought to be implicated in endosomal processes other than endosome-to-TGN transport. PIKfyve is also linked to the sorting of membrane proteins into the intraluminal vesicles of the MVB, required for the degradation of these proteins in the lysosome (Shisheva, 2008, Dove et al., 2002). This process is controlled by the ESCRT protein complexes 0, I, II and III which act sequentially on the inclusion of cargo into the MVB (Wollert and Hurley, 2010). In yeast impaired Fab1 causes an increase in vacuole size, and a decrease the hydrolytic activity of the vacuole, partly caused by defects in the acidification of the vacuole lumen (Odorizzi et al., 2000). Impaired Fab1 function also inhibits the degradation of some proteins, including the type 2 transmembrane protein carboxypeptidase S (CPS), a vacuolar hydrolase (Odorizzi et al., 1998). Fewer intraluminal vacuolar vesicles are observed in yeast with impaired Fab1 activity, which may contribute to the enlargement of the vacuole, through the delivery of additional membrane to the vacuole surface (Downes et al., 2005, Odorizzi et al., 2000). PIKfyve is known to interact with the mammalian VPS4 orthologue SKD1 which catalyses the dissociation of the ESCRT complexes from the endosomes. The expression of a catalytically inactive dominant negative form of SKD1 also causes the formation of cytoplasmic vacuoles as observed with PIKfyve inhibition (Ikonomov et al., 2002b). The fact that $PI(3,5)P_2$ and therefore PIKfyve may be involved in degradative sorting downstream of ESCRT is also supported by the binding of the VPS24 ESCRT III subunit to $PI(3,5)P_2$ (Whitley et al., 2003). This provides another mechanism by which PIKfyve may influence endosome dynamics.

These findings support the role of PIKfyve and therefore $PI(3,5)P_2$ in endosomal system where PIKfyve catalyses $PI(3,5)P_2$ production. This production of $PI(3,5)P_2$ regulates endosomal processing and membrane protein transport, in both endosome to TGN transport, and trafficking through late endocytic compartments.

1.5.4 PI(3,5)P_2 and its effectors

In order to further investigate the function of PIKfyve and PI(3,5)P_2, particularly in endosomal homeostasis, PI(3,5)P_2 effectors need to be identified. PI(3,5)P_2 is of low abundance in both yeast and mammalian cells, in mammalian cells; it represents between 0.04-0.08% of total phosphoinositides (Whiteford et al., 1997). This low abundance has not only led to difficulties in detecting intracellular PI(3,5)P_2, but also in the establishment of PI(3,5)P_2 effectors. Despite this, several PI(3,5)P_2 effectors have recently been identified. One of the first established effectors was the yeast protein ATG18 (also known as SVP1), isolated from a screen of swollen vacuole phenotypes (Dove et al., 2004). ATG18 is a member of PROPPIN (β-propellers that bind phosphoinositides and epsins) and its deletion leads to a swollen vacuole in yeast. ATG18 binds to PI(3,5)P_2 in the vacuole membrane of yeast, where it exerts inhibitory control of Fab1 (Dove et al., 2009, Dove et al., 2004). ATG18 and its mammalian orthologues (WIPI's) also function in autophagy. Autophagy in yeast does not require Fab1 and PI(3,5)P_2 (Dove et al., 2009). However, in *Drosophila* Fab1 is required for autophagy (Rusten et al., 2007). It appears to be required for the fusion of autolysosomes with the late endosome (Dove et al., 2009). There is now also evidence that PI(3,5)P_2 plays an important role in autophagy in the mammalian nervous system, where mutations in Fig4 and Vac14 cause the accumulation of autophagy intermediates in the brain and spinal cord of mice (Ferguson et al., 2009).

Another recently established PI(3,5)P_2 effector is the mucolipin transient receptor potential channel (TRPML-1). TRPML-1 belongs to a family of calcium permeable cation channels that are localised to both the plasma membrane, and the membranes of intracellular organelles. TRPML-1 is localised to endosomes where it binds to PI(3,5)P_2 causing channel activation, and the release of calcium from the lumen of the endosomes into the cytosol (Dong et al., 2010, Bach et al., 2010). Interestingly deficiency of TRPML-1 causes an enlargement of the endosomes/lysosomes similar to

those observed upon $PI(3,5)P_2$ deficiency (Dong et al., 2010). This enlargement is due to impaired calcium release from the endosomal lumen. This finding suggests that TRPML-1 is involved in the regulation of membrane trafficking in the late endocytic pathway by linking the level of $PI(3,5)P_2$ with the release of calcium, which controls membrane fusion and fission (Dong et al., 2010).

$PI(3,5)P_2$ provides a link between the PIKfyve complex and the mammalian target of rapamycin complex 1 (mTORC1). mTORC1 is a protein kinase that is controlled by insulin, amino acids and growth factors. Insulin, amino acids and growth factors also increase $PI(3,5)P_2$ levels in 3T3-LI adipocytes (Bridges et al., 2012). Knock out of components of the PIKfyve complex, prevented the stimulation of the ribosomal protein S6 kinase, which requires mTORC1, and reduced mTORC1 localisation to the plasma membrane. It was found that the Raptor subunit of mTORC1 is a $PI(3,5)P_2$ effector and binds to $PI(3,5)P_2$ via its β-propeller domain (Bridges et al., 2012). The localisation of mTORC1 to lysosomes is required for mTORC1 activation in response to amino acids. Jin et al. (2014) showed that $PI(3,5)P_2$ is required for TORC1 activity in yeast, and for its localisation to the yeast vacuole, the equivalent of the mammalian lysosome. The yeast homologue of S6 kinase (Sch9) is recruited to the vacuole by $PI(3,5)P_2$, where it can be phosphorylated by TORC1. $PI(3,5)P_2$ is required for several downstream pathways by TORC1 dependent phosphorylation. Taken together these results assign another role to $PI(3,5)P_2$ in that it is required for the mTORC1 dependent input of nutrient signals.

1.5.5 PIKfyve and $PI(3,5)P_2$ in neurodegeneration

$PI(3,5)P_2$ and the PIKfyve complexes are thought to play crucial roles in neurons and at synapses, although the mechanisms remain elusive. Vac14 is concentrated at excitatory synapses, which suggest a possible role for $PI(3,5)P_2$ in synapse formation and plasticity (Zhang et al., 2012). $PI(3,5)P_2$ levels are known to increase during synaptic depression (McCartney et al., 2014b). PIKfyve is known to be involved in the

trafficking, in particular, the endocytosis and recycling of the GluA1 and GluA2 subunits of the AMPA receptor, which mediates fast neurotransmission in the brain, with $PI(3,5)P_2$ synthesis inhibition causing defects in AMPA receptor trafficking (McCartney et al., 2014b).

Loss of the PIKfyve complex and $PI(3,5)P_2$ are associated with profound neurodegeneration (Zhang et al., 2007b, Zolov et al., 2012). Mutations in the Fig4 gene are linked to Charcot-Marie-Tooth syndrome type 4J (CMT4J) (Chow et al., 2007, Nicholson et al., 2011). Charcot-Marie-Tooth syndrome is disease of the peripheral nervous system, characterised by the progressive deterioration of nerves which results in reduced nerve conduction, leading to loss of touch sensation and muscle tissue. These defects are observed in $Fig4^{-/-}$ mice which show spongiform degeneration of the brain and loss of neurons from the dorsal root ganglia, which results in lethality between the ages of 1-2 months (Chow et al., 2007). Patients with CMT4J are compound heterozygotes and carry the missense allele FIG4-I41T in combination with a null allele. This I41T mutation disrupts the interaction of Fig4 with Vac14 (Lenk et al., 2011).

Mutations in the Fig4 gene are also found in patients with amyotrophic lateral sclerosis (ALS) (Chow et al., 2009). ALS is a severe neurological disorder characterised by the neurodegeneration of lower and upper motor neurones in the spinal cord, brain stem and cortex. Fig4 is also linked to several other neurodegenerative diseases. It is present in the Lewy bodies of Parkinson's disease and in inclusion bodies in other diseases (Kon et al., 2014).

Mutations in PIKfyve and Vac14 have not been linked with neurological disorders to date however, heterozygous null mutations in PIKfye are associated with Francois-Mouchetee Felck Corneal Dystropgy (CFD) (Li et al., 2005a). This leads to white flecks in the corneal stroma of the eye which are thought to be enlarged vacuoles in enlarged keratocytes. Also Vac14 is down-regulated in patients with chronic fatigue syndrome (McCartney et al., 2014a).

One of the most interesting observations of the role of the PIKfyve complex and $PI(3,5)P_2$ in neurodegeneration is in Vac14 null mice, which show profound neurodegeneration. Vac14 null mice die 1-2 days after birth and show a significant reduction in $PI(3,5)P_2$ levels (Zhang et al., 2007b). Several neuronal defects were observed including lesions in various regions of the brain, including the preoptic area, thalamus, hypothalamus, which were filled with enlarged vacuole structures, consistent with the loss of $PI(3,5)P_2$. Fibroblasts from Vac14 null mice also showed defects in retrograde trafficking from the endosomes to the TGN.

Zolov et al. (2012) created a PIKfyve gentrap mouse ($PIKfyve^{\beta\text{-}geo/\beta\text{-}geo}$), a hypomorph with a 90% reduction in PIKfyve protein level). $PIKfyve^{\beta\text{-}geo}$ fails to interact with Vac14, and a decrease in $PI(3,5)P_2$ levels is observed, with an increase in PI(3)P. The majority of $PIKfyve^{\beta\text{-}geo/\beta\text{-}geo}$ mice exhibit perinatal lethality. A small number survived for up to 19 days. These mice showed impaired mobility, with extensive vacuolation observed in cerebellar nuclei, the brain stem, and the spinal cord, leading to profound neurodegeneration. This vacuolation was also observed in other tissues causing defects to the heart, lungs, kidneys, thymus and spleen (Zolov et al., 2012).

Taken together the mutations in Fig4 associated with neurodegenerative diseases and the profound neurodegeneration seen in both Vac14 and Fig4 knock out mice, as well as the $PIKfyve^{\beta\text{-}geo/\beta\text{-}geo}$ mice, demonstrates the importance of the PIKfyve complex, and its tight regulation of the signalling lipid $PI(3,5)P_2$ in normal neuronal function.

1.6 mTOR

$PI(3,5)P_2$ has recently been identified as a crucial component of the mTORC1 dependent input of nutrient signals, via its binding to the Raptor regulatory subunit of mTORC1 (Bridges et al., 2012, Jin et al., 2014).

1.6.1 mTOR, structure, function and signalling

The mammalian target of rapamycin known as mTOR is a serine/threonine protein kinase, a key integrator of various signalling inputs, and is involved in a wide variety of physiological processes. It is involved in complex processes such as the control of development, regulation of fat, sugar and amino acid metabolism, as well as playing an important role in the control of an organism's life span. It integrates cellular stimuli of growth factor receptors such as the insulin-like growth factor receptor, the availability of amino acids, the ATP/ADP ratio and cellular stress (Laplante and Sabatini, 2012).

mTOR mediates these various physiological processes via two mTOR complexes; mTOR complex 1 (mTORC1) and mTOR complex 2 (mTORC2) (Figure 11). The main component of both complexes is the mTOR kinase itself. mTOR belongs to the phosphoinositide-3-kinase (PI3K) related protein kinase family. The N-terminus of mTOR is highly conserved and is composed of HEAT repeats that mediate protein-protein interactions. The C-terminus of mTOR contains the kinase domain required for its activity (Baretić and Williams, 2014). mTORC1 is composed of the mTOR kinase itself, regulatory associated protein of mTOR (Raptor), mammalian lethal SEC13 protein 8 (MLST8), as well as other mTORC1 specific proteins. mTORC2 is composed of the following subunits, mTOR, rapamycin-insensitive companion of mTOR (Rictor), mammalian stress-activated protein kinase interacting protein 1 (mSIN1), mammalian lethal SEC13 protein 8 (MLST8), as well as other mTORC2 specific proteins (Laplante and Sabatini, 2012).

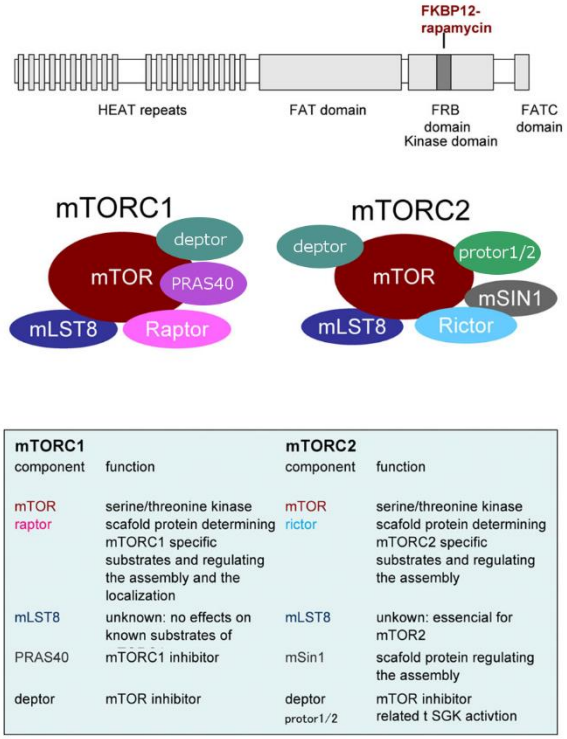

mTORC1 component	function	mTORC2 component	function
mTOR raptor	serine/threonine kinase scafold protein determining mTORC1 specific substrates and regulating the assembly and the localization	mTOR rictor	serine/threonine kinase scafold protein determining mTORC2 specific substrates and regulating the assembly
mLST8	unknown: no effects on known substrates of	mLST8	unkown: essencial for mTOR2
PRAS40	mTORC1 inhibitor	mSin1	scafold protein regulating the assembly
deptor	mTOR inhibitor	deptor protor1/2	mTOR inhibitor related t SGK activtion

Figure 11. The components of the mTOR complexes.
mTORC1 is mainly composed of mTOR itself, the scaffold protein Raptor which helps to regulate mTORC1 assembly and localisation, and the MTORC1 inhibitor PRAS40. mTORC2 is primarily composed of mTOR, the scaffold protein Rictor , mSIN1 which helps to regulate complex assembly, and protor 1/2. The mLST8 subunit is common to both mTORC1 and mTORC2, as is the mTOR inhibitor deptor. Figure adapted from Takei and Nawa (2014).

mTOR complex 1 (mTORC1) is the better characterised of the two complexes and is known to control protein translation initiation, ribosome biogenesis and cell cycle progression, mainly through its downstream effectors (Figure 12). It is activated by a set of diverse upstream signals. It integrates inputs from growth factors, stress, energy status, oxygen and amino acids, and in doing so controls several major physiological process like protein synthesis and autophagy (Laplante and Sabatini, 2012) (Figure 12). The growth factor activated mTOR pathway has been extensively studied. Growth factors bind to receptor tyrosine kinases, which activate the PI3K-Akt and/or the Ras-MAPK pathways, which stimulates mTORC1, by phosphorylation of the tuberous sclerosis complex 2 (TSC2) (Inoki et al., 2003a, Tee et al., 2003). TSC2 in complex with TSC1 functions as a GTPase activating protein (GAP) for the GTPase Rheb (Inoki et al., 2003a) (Kim et al., 2013). Rheb is present on the membranes of the endosomal

system and is negatively regulated by the TSC1/2 complex (Saito et al., 2005). Rheb, in its active form (Rheb-GTP) increases mTOR signalling. The TSC complex is responsible for converting active GTP bound Rheb to its inactive GDP bound form. The phosphorylation of the TSC complex by growth factor stimulation, inactivates TSC, thereby increases active Rheb and mTORC1 signalling. The TSC is also involved in the activation of mTORC1 upon stress signals, such as low oxygen and energy levels. Adenosine monophosphate-activated protein kinase (AMPK) phosphorylates TSC2 in response to these stresses increasing Rheb, and consequently mTORC1 activity (Inoki et al., 2003c).

mTORC1 also mediates the input of amino acids particularly leucine and arginine in a process that requires the Rag GTPases (Sancak et al., 2008). There are four Rag proteins in mammals which form heterodimers consisting of RagA or RagB with RagC or RagD. The two sets of heterodimers have different GTP loading states, when RagA/RagB is GTP bound RagC/RagD is GDP bound (Sancak et al., 2008). Amino acids stimulate GTP binding to RagA and RagB causing the Rag GTPases dock to a multi subunit complex known as the Ragulator, located on the lysosomal membrane (Bar-Peled et al., 2012). The Rag heterodimer then interacts with the Raptor subunit of mTORC1 causing the translocation of mTORC1 from the cytoplasm to the lysosomal membrane allowing for the activation of mTORC1 (Sancak et al., 2010) (Figure 12). Therefore the Rag GTPases and the Ragulator tightly control mTORC1 activation in the presence of amino acids, regardless of the presence of any other positive signals.

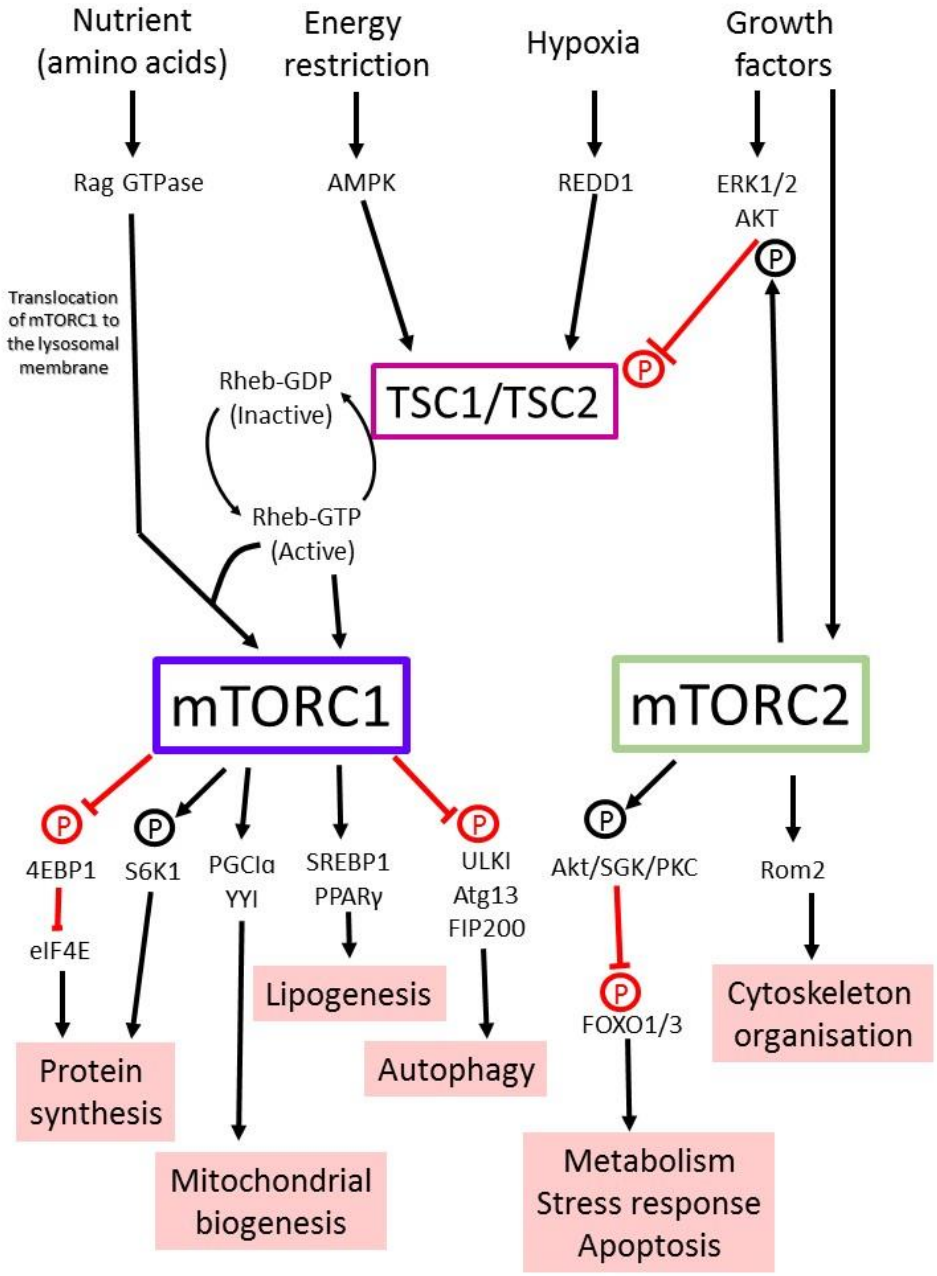

Figure 12. The mTOR signalling pathway

mTORC1 integrates signals from growth factors and amino acids, whereas the integration of growth factor signals by mTORC2 is not as well characterised. In the presence of growth factors Akt inhibits TSC1/2 via phosphorylation causing an increase in active GTP bound Rheb, which directly activates mTORC1. Amino acids activate the Rag GTPase which causes the translocation of mTORC1 to the lysosomal membrane, subsequently activating mTORC1. mTORC1 phosphorylates several downstream effectors which stimulates protein synthesis and decreases autophagy. mTORC1 is also involved in mitochondrial biogenesis and lipogenesis. mTORC2 has roles in the organisation of the cytoskeleton and in metabolism and stress response. Red arrows represent inhibition and black arrows represent activation, with (P) indicating phosphorylation of the downstream target.

mTORC1 regulates many physiological processes due to its importance in the cells energy and nutritional status. The most well characterised downstream process of mTORC1 is the control of protein synthesis (figure 12). mTORC1 phosphorylates the translational regulators the eukaryotic translation initiation factor 4E (eIF4E)-binding protein 1 (4EBP1), and the S6 kinase 1 (S6K1), which both promote protein synthesis (Laplante and Sabatini, 2012). 4EBP1 phosphorylation by mTORC1 prevents its binding to the eIF4E, allowing it to participate in the complex that initiates cap-dependent translation. S6K1 increases mRNA biogenesis, translation initiation and elongation through a number of different effectors (Magnuson et al., 2012). mTORC1 also controls lipid synthesis through the sterol regulatory element-binding protein 1 SREBP1, controlling the expression of several genes involved in fatty acid and cholesterol synthesis (Wang et al., 2011). mTORC1 promotes the activity and expression of the peroxisome proliferator activated receptor – γ (PPARγ) which regulates adipogenesis (Zhang et al., 2009). mTORC1 regulates metabolism and ATP production by activating glycolytic genes through the translation of the hypoxia inducible factor 1α, and by mediating the interaction between PPAR-γ co-activator 1α (PGC1α) and Ying-Yang 1 (YY1), which regulate mitochondrial biogenesis (Cunningham et al., 2007). mTORC1 negatively regulates autophagy which promotes cell growth (Hosokawa et al., 2009). mTORC1 inhibition causes an increase in autophagy. It directly phosphorylates the kinase complex ULK1/Atg13/FIP200 which is required to initiate autophagy. This phosphorylation renders the complex inactive, and therefore supresses autophagy (Ganley et al., 2009). The mammalian orthologue of yeast autophagy protein ATG18, WIPI2, is an mTOR effector (Hsu et al., 2011). mTORC1 is also known to regulate the biogenesis of lysosomes (Puertollano, 2014).

The mTORC2 pathway is much less understood than that of mTORC1. mTORC2 responds to growth factors such as insulin, through an ill-defined mechanism. mTORC2 is known to directly phosphorylate the kinase Akt causing its activation

(Hresko and Mueckler, 2005). Akt itself phosphorylates several proteins and in doing so regulates metabolism, apoptosis, growth and proliferation. mTORC2 also activates serum and glucocorticoid-induced protein kinase 1 (SGK1) which controls growth and ion transport, and protein kinase Cα (PKCα) which functions in many physiological processes such as cell adhesion and cell volume by controlling the actin cytoskeleton (Sarbassov et al., 2005).

1.6.2 The roles of mTOR in human diseases and ageing

Due to mTOR's role in a wide variety of physiological processes it is to be expected that defects in the mTOR signalling pathways are implicated in several diseases. The mTOR pathway is known to be important in the pathogenesis of many cancers. In many human cancers several components of the PI3K signalling pathway which inputs into the mTOR pathway are mutated (LoPiccolo et al., 2008, Morgensztern and McLeod, 2005). Loss of the tumour protein p53, key in regulating cell cycle and functioning as a tumour suppressor, increases mTORC1 activation. This results in cancer cell proliferation, growth and survival (Feng et al., 2005). The dysregulation of protein synthesis is a major player in tumour formation. Increased mTORC1 activation increases 4EBP1 phosphorylation, leading to increased protein translation. 4EBP1 and eIF4E affect tumour formation by promoting the translation of mRNAs encoding oncogenic proteins that increase cell cycle, cell proliferation and energy metabolism, amongst others (Dowling et al., 2010). An increase in mTOR controlled lipid synthesis is found in proliferating cancer cells. Taken together these results indicate that the inhibition of mTOR could play a role in cancer therapy. Indeed there are several analogues of rapamycin currently being tested and one of these has been approved for the treatment of renal cell carcinoma (Laplante and Sabatini, 2012). Due to its role in regulating nutrient input, it is not surprising that the mTOR pathway is implicated in metabolic disorders such as type 2 diabetes, with both loss and hyperactivation of mTORC1 affecting insulin sensitivity (Um et al., 2004).

The mTOR pathway has been implicated in the aging process (Johnson et al., 2013). This link was first discovered in the RNAi suppression of the *C. elegans* orthologue of mTOR, let363 which significantly increased the lifetime of the worm (Vellai et al., 2003). The inhibition of mTORC1 with rapamycin also increases the life span of mice, most likely by slowing age related pathologies (Miller et al., 2010). The mechanisms for the extension of life span upon mTORC1 inhibition are not fully known, however they

seem to include changes in mRNA translation, increasing stress resistance, changes in mitochondrial activity, and protecting stem cell function (Parkhitko et al., 2014). Nutrient restriction also extends life span (Walker et al., 2005). It is therefore interesting that mTORC1 plays such a crucial role in integrating nutritional signals.

Given the link between mTOR and ageing it is therefore not surprising that mTOR has also been implicated in age-related neurological disorders. In neurodegenerative diseases that stem from the accumulation of protein aggregates, protein degradation pathways such as autophagy are deregulated (Martinez-Vicente and Cuervo, 2007). Due to the control of autophagy by mTORC1, its role in neurodegeneration has been increasingly investigated. The inhibition of mTORC1 by rapamycin stimulates autophagy and the degradation of proteins that form aggregates in neurodegeneration. This mTORC1 inhibition reduces the severity of neurodegeneration in animal models of neurodegenerative disorders (Sarkar, 2013). The inhibition of mTORC1 by rapamycin has been shown to reduce protein aggregation by decreasing protein synthesis (King et al., 2008).

mTOR signalling is increased in the brains of Alzheimer's disease patients, and mTOR deregulation is visible before the development of the disease pathology (Li et al., 2005c). This defect in mTOR signalling in Alzheimer's disease is systemic and not only restricted to the brain (Yates et al., 2013). mTOR regulates the protein tau, phosphorylation and degradation in animal models of tauopathies (Wang et al., 2014b). Genetically increasing mTOR causes an increase in the protein level and the phosphorylation of tau (Caccamo et al., 2013). This hyperphosphorylation of tau is observed in tauopathies such as Alzheimer's disease. The inhibition of mTORC1 with rapamycin reduces tau pathology, and the associated behavioural deficits observed in a mouse model overexpressing human mutant tau (Caccamo et al., 2013). mTOR and tau are thought to be linked through the glycogen synthase kinase β (GSK3β), also

known to contribute to tau hyperphosphorylation and autophagy (Caccamo et al., 2013).

Taken together the defects of mTOR signalling in human disease add increasing evidence to its importance in a wide variety of physiological functions. In fact it is often thought that mTOR is involved in most physiological processes either directly or indirectly.

1.7 Project aims

Membrane proteins play key roles in a wide variety of physiological processes. This project aims to aid in the development of techniques to examine the interaction of the intracellular domains of membrane proteins with cytosolic proteins, and with phospholipids.

This project will focus on the continued development of a model membrane liposome recruitment system (based on that used by (Pocha et al., 2011)) to examine the intracellular interactome of membrane proteins using the amyloid precursor protein as a model, with a view to gaining new insight into APP's physiological function.

Recent unpublished studies (Balklava et al., under review A; Balklava et al., under review B) utilised a liposome based technique coupled to label free quantitative mass spectrometry to identify the intracellular interactome of APP. They identified 327 potential interacting proteins with roles in cell signalling, gene expression, trafficking and metabolism. Amongst APP's well known binding partners, such as Fe65, several novel interaction partners were detected. This thesis will focus on two of these novel interaction partners; the mTOR complex, and the PIKfyve complex. When identified by mass spectrometry these complexes were found to be significantly enriched in AICD liposome samples compared to controls. The interaction between AICD and these complexes were selected for further characterisation in this thesis primarily due to this significant enrichment as well as to gain a greater insight into the functions of APP. The link between the PIKfyve complex and neurodegeneration (Zhang et al., 2012) and APPs role in Alzheimers disease made it a good candidate for further study. mTOR signalling controls a wide range of physiological processes and is also found to be increased in Alzheimers disease (Li et al., 2005c), therefore the interaction between APP and the mTOR complex was selected for further investigation.

In this thesis the novel interaction between APP and the mTOR complex will be characterised using the proteo-liposome recruitment system, as well as the interaction of APP with the PIKfyve complex. The interaction of APP with the PIKfyve complex will be further investigated in terms of APP function and trafficking.

The liposome recruitment system will also be further developed to allow for the assessment of the recruitment protein coats from their purified components using the AP-2/clathrin coat as a model.

This thesis hypothesises that the proteo-liposome recruitment system will be able to analyse the interaction partners of the intracellular domains of membrane proteins, and that the mTOR and PIKfyve complexes will interact with AICD as detected using this technique.

These assessments will demonstrate and solidify the effectiveness of a liposome based model membrane system for the analysis of the cytosolic binding partners of membrane proteins.

Chapter 2

Materials and Methods

Chapter 2- Materials and Methods

2.1 Materials

2.1.1 Buffers and solutions

All the buffers and solutions used for the methods are given in the table below.

1 x 1 M Tris buffer	0.05 M Tris Base 0.95 M Tris HCl 1 mM EDTA (Ethylenediaminetetraacetic acid) 0.1% (v/v) ß-mercaptoethanol 0.02% (v/v) Sodium azide pH 8.0
1 x Blotting buffer	50 mM Glycine 400 mM Tris Base 20% (v/v) Methanol pH 8.3
1 x Phosphate buffered saline (PBS) solution	137 mM Sodium chloride 10 mM Disodium phosphate 1.8 mM Potassium dihydrogen phosphate 2.7 mM Potassium chloride pH 7.4
10 mM PEI solution	0.95 mg/ml polyethylenimine (PEI) (25 kD, Sigma Aldrich) pH 7.5 (adjust with HCl)
10 x Blotting buffer	0.25 M Tris Base 1.9 M Glycine pH 8.3
10 x PCR buffer	100 mM Tris Cl pH 8.8 500 mM Potassium chloride 25 mM Magnesium chloride 1% (v/v) Triton X 100
10 x TBS	0.2 M Tris Base 1.5 M Sodium chloride pH 7.5
2 x 1 M Tris buffer	0.1 M Tris base 1.9 M Tris HCl 2mM EDTA 0.2% (v/v) ß -mercaptoethanol 0.04% (v/v) sodium azide pH 8.0

4 x Laemmli buffer	200 mM Tris, pH 6.8 40% (v/v) Glycerol 4% (w/v) SDS (Sodium dodecyl sulphate) 0.04% (w/v) Bromophenol blue 4% (v/v) ß-mercaptoethanol
4 x Separation gel buffer	1.5 M Tris pH 8.8
4 x Stacking gel buffer	0.5 M Tris pH 6.5
ATG18 Dialysis Buffer	1 x Phosphate buffered saline (PBS) 10% (v/v) Glycerol
ATG18 Elution buffer	1 x Phosphate buffered saline (PBS) 10 mM Reduced glutathione
ATG18 Lysis buffer	1 x Phosphate buffered saline (PBS)
Blocking solution	5% (w/v) Bovine serum albumin (BSA) in TBSt 0.1% (v/v) Sodium azide
Buffer C (10x)	200 mM HEPES pH 7.0 250 mM Potassium chloride
Buffer C (1x)	100 ml of Buffer C (10x) 1.5 ml 2 M Magnesium chloride
Cell culture medium	Dulbecco's Modified Eagle Medium (DMEM) (Gibco –Life Technologies) 10% (v/v)Foetal Calf Serum (Gibco –Life Technologies) 1% (v/v) Pen/Strep (Gibco –Life Technologies)
Cell fixing solution	4% (v/v) Paraformaldehyde dissolved in 1 x PBS
Clearance buffer	50 mM TrisCl pH 8.0 500 mM Sodium chloride 10 mM EDTA
Coomassie destain	10% (v/v) Acetic acid 20% (v/v) Methanol 70% (v/v) Distilled water
Coomassie stain	50% (v/v) Ethanol 10% (v/v) Acetic acid 40% (v/v) Distilled water 0.25% (w/v) Coomassie Brilliant Blue-R250
Depolymerisation buffer	20 mM TEA (Triethanolamine) 1 mM EDTA 0.1% (v/v) ß-mercaptoethanol 0.02% (v/v) Sodium azide pH 8.0

Developer solution	Carestream® Kodak® autoradiography GBX developer/replenisher (Sigma Aldrich)
Dialysis Buffer	20 mM HEPES 125 mM Potassium acetate 1 mM EDTA pH 7.2 (with KOH)
Elution Buffer	50 mM Tris 150 mM Sodium chloride 250 mM Imidazole pH 7.2
Enzyme substrate solution	100 mM Tris pH 8.5 0.18 mM Coumaric acid 1.25 mM Luminol 0.01% (v/v) Hydrogen peroxide
Ficoll/sucrose buffer	6.25% (w/v)Sucrose 6.25% (w/v)Ficoll PM 70 In HKM buffer
Fixer solution	Carestream® Kodak® autoradiography RP X-Omat LO fixer/replenisher (Sigma Aldrich)
Freezing medium	30% (v/v) FCS 10% (v/v) DMSO (dimethyl sulfoxide) 70% (v/v) cell culture medium
G418 cell culture medium	750 µg/ml Geneticin (G418) in cell culture media
HKM Buffer	25 mM HEPES (4-(2-hydroxyethyl)-1-piperazineethanesulfonic acid)), pH 7.2 125 mM Potassium acetate 5 mM Magnesium acetate 0.002% (v/v) Sodium azide
LB agar	37.5 g LB agar (Fisher) dissolved in 1 L distilled water and autoclaved. For selective media one or a combination of kanamycin, ampicillin and chloramphenicol was added at a final concentration of 50 µg/µl, 100 µg/µl and 34 µg/µl respectively.
LB broth	20 g LB (Melford Bioscience) dissolved in 1 L distilled water and autoclaved. For selective media one or a combination of kanamycin, ampicillin and chloramphenicol was added at a final concentration of 50 µg/µl, 100 µg/µl and 34 µg/µl respectively.

Lysis Buffer	50 mM Tris 150 mM Sodium chloride 10 mM Imidazole pH 7.2
Mammalian cell lysis buffer	150 mM Sodium Chloride 50 mM Tris pH 8.0 1% (v/v)Triton-X100 2.5 mM βglycerophosphate 1 mM NH_4Fl 1mM Vanadate 10 mM Pyro-phosphate 3.3 µg/ml Aprotinin 4 µg/ml E-64 1 mM PMSF 1 µg/ml Pepstatin 1 mM EDTA
M^{c}Kay's Buffer	40 mM HEPES pH 7.0 75 mM potassium chloride 4.5 mM magnesium acetate
Mowiol mounting media	2.4g Mowiol 6.0g glycerol 6.0ml H_2O 12.0ml 0.2M Tris·Cl, pH 8.5 2.5% 1,4-diazobicyclo-[2.2.2]-octane (DABCO)
Polymerisation buffer	0.1 M MES (2-(*N*-morpholino)ethanesulfonic acid) 1.5 mM Magnesium chloride 0.2 mM EGTA (ethylene glycol tetraacetic acid) 0.02% (v/v) Sodium azide pH 6.5
Recruitment buffer (RB)	20 mM HEPES 125 mM Potassium acetate 2.5 mM Magnesium acetate pH 7.2 (adjusted with KOH)
Saturated ammonium sulphate solution	5.8 M Ammonium sulphate 1L 10 mM Tris pH 7 0.1 mM EDTA
SDS running buffer	25 mM Tris 190 mM Glycine 3.5 mM SDS
Solution 1	50 mM TrisCl pH 8.0 10 mM EDTA 100 µg/ml RNaseA
Solution 2	200 mM Sodium hydroxide 1% (w/v) SDS
Solution 3	3 M Potassium acetate pH 5.5

TAE buffer	40 mM Tris 20 mM Acetic acid 1 mM EDTA pH 8.0
TBSt	10% (v/v) 10 x TBS 1% (v/v)Tween 20
TE buffer	10 mM TrisCl pH 8.0 1 mM EDTA
TEV Dialysis buffer	50 mM Sodium phosphate 200 mM Sodium chloride 40% (v/v) Glycerol pH 8.0
TEV elution buffer	50 mM Sodium phosphate 200 mM Sodium chloride 10% (v/v) Glycerol 250 mM Imidazole pH 8.0
TEV lysis buffer	50 mM Sodium phosphate 200 mM Sodium chloride 10% (v/v) Glycerol 10 mM Imidazole pH 8.0
Tissue culture medium	1x 500 ml bottle of Dulbecco's Modified Eagle Medium (DMEM) (Gibco-Life Technologies) 10% (v/v) Foetal Bovine Serum (Gibco-Life Technologies) 1% (v/v) Penicillin-Streptomycin (Gibco-Life Technologies)
Wash buffer	25 mM HEPES pH 7.0 50 mM Potassium chloride 1 mM Magnesium chloride

Table 1. Buffer list.
All the buffers used in the methods described in chapter 2.

2.1.2 Lipids

Lipid	Abbreviation	Stock Concentration µg/µl	Solvent	Company	Catalogue number
1,2-dioleoyl-s*n*-glycero-3-phosphoethanolamine-N-[4-(p-maleimidomethyl)cyclohexane-carboxamide] (sodium salt)	PE MCC	10	Chloroform: Methanol (2:1)	Avanti Polar Lipids	780201
Cholesterol	C	10	Chloroform: Methanol (2:1)	Sigma Aldrich	C8667
Phosphatidylcholine	PC	25	Chloroform: Methanol (2:1)	Sigma Aldrich	P3556
Phosphatidylethanolamine	PE	10	Chloroform: Methanol (2:1)	Sigma Aldrich	P7943
Phosphatidylinositol	PI	1	Chloroform: Methanol (2:1)	Avanti Polar Lipids	850091
Phosphatidylinositol 3 phosphate	PI(3)P	1	Chloroform: Methanol (2:1)	Avanti Polar Lipids	850150
Phosphatidylinositol 3,5 bisphosphate	PI(3,5)P2	1	Chloroform: Methanol (2:1)	Avanti Polar Lipids	850154
Phosphatidylinositol 4,5-bisphosphate	PI(4,5)P2	1	Chloroform: Methanol (2:1)	Avanti Polar Lipids	850155
Phosphatidylserine	PS	10	Chloroform: Methanol (2:1)	Sigma Aldrich	P7769
1,1′-Dioctadecyl-3,3,3′,3′-tetramethylindocarbocyanine perchlorate	DiI	1	Methanol	Sigma Aldrich	42364

Table 2. Lipids.
The lipids used to produce liposomes as outlined in this chapter.

2.1.3 Antibodies

Antibody	Dilution	Company	Catalogue number
α-adaptin	1:1500	Santa Cruz Biotechnology	sc-398024
Anti-mouse HRP conjugate	1:4000	Cell Signalling Technology	7076
Anti-mouse IgG Fab2 Alexa Four 555	1:1000	Cell Signalling Technology	4409
Anti-rabbit HRP conjugate	1:4000	Cell Signalling Technology	7074
Anti-rabbit IgG Fab2 Alexa Four 555	1:1000	Cell Signalling Technology	4413
AP-180	1:5000	Santa Cruz Biotechnology	sc-135834
APLP2	1:1000	Abcam	ab140624
APP	1:1000	Santa Cruz Biotechnology	sc-53822
Clathrin heavy chain	1:1500	Santa Cruz Biotechnology	sc-271178
EEA1	1:200	BD Biosciences	610457
GST	1: 2000	Santa Cruz Biotechnology	sc-374171
LampI	1:200	Santa Cruz Biotechnology	sc-20011
MBP	1:2000	Cell Signalling Technology	2396
mTOR	1:2000	Cell Signalling Technology	2972
PIKfyve (PIP5KIII)	1:2000	Santa Cruz Biotechnology	sc-100408
Raptor	1:1000	Santa Cruz Biotechnology	sc-81537
Rictor	1:1000	Cell Signalling Technology	9476
Tubulin	1:2000	Abcam	ab125267
Vac14	1:2000	Santa Cruz Biotechnology	sc-271831
γ- adaptin	1:500	Santa Cruz Biotechnology	sc-10763

Table 3. Antibody list.
A list of all the antibodies used in western blot and immunofluorescence analysis.

2.2 Methods

2.2.1 General Methods

2.2.1.1 Sodium dodecyl sulphate-polyacrylamide gel electrophoresis (SDS-PAGE)

SDS-PAGE gels were assembled using Bio-Rad's Mini-Protean system. 5 ml of separation gel was overlaid by 100% isopropanol and allowed to set. The isopropanol was removed by several washes with distilled water. 2 ml of the stacking gel was poured on top of the set separation gel and the desired comb inserted. Samples were run on either an 8, 10 or 15% acrylamide gel. The composition of the separation and stacking gels is given in the table below.

8% Separation gel	**10% Separation gel**	**15% Separation gel**	**5% Stacking gel**
1.25 ml of 1.5 M Tris pH 8.8	1.25 ml of 1.5 M Tris pH 8.8	1.25 ml of 1.5 M Tris pH 8.8	0.5 ml of 0.5 M Tris pH 6.5
1 ml of 50% Glycerol	1 ml of 50% Glycerol	1 ml of 50% Glycerol	0.4 ml of 50% Glycerol
1 ml of 40% Bisacrylamide solution (Fisher Scientific)	1.25 ml of 40% Bisacrylamide solution (Fisher Scientific)	1.875 ml of 40% Bisacrylamide solution (Fisher Scientific)	0.25 ml of 40% Bisacrylamide solution (Fisher Scientific)
100 µl of 10% SDS	100 µl of 10% SDS	100 µl of 10% SDS	20 µl of 10% SDS
50 µl of 10% Ammonium persulphate (APS)	50 µl of 10% Ammonium persulphate (APS)	50 µl of 10% Ammonium persulphate (APS)	10 µl of 10% Ammonium persulphate (APS)
1.6 ml of distilled water	1.35 ml of distilled water	0.725 ml of distilled water	0.82 ml of distilled water
2.5 µl of Tetramethylethylene diamine (TEMED)	2.5 µl of Tetramethylethylen ediamine (TEMED)	2.5 µl of Tetramethylethylene diamine (TEMED)	1 µl of Tetramethylethylene diamine (TEMED)

Table 4. SDS-PAGE gel components.
The components needed to make 8%, 10% and 15% separation/resolving gels and 5% stacking gel.

4x or 2x Laemmli buffer was added to samples and a stated volume of the sample/Laemmli buffer mix was loaded into the wells of the gel. Gels were run at 150 V for approximately 1 hour. When required gels were either stained with coommasie stain for 1 hour followed by de-stain with Coomassie de-stain overnight, stained using InstantBlue (Expedeon), or subjected to Western blotting.

2.2.1.2 Western blotting

Western blot sandwiches were assembled as follows; 1st layer- 1 piece of Whatman filter paper, 2nd layer-SDS-PAGE gel, 3rd layer PVDF membrane (activated in 100% methanol), 4th layer- 1 piece of Whatman filter paper. The sandwich was placed into a cassette in the western blot tank and filled with 1x blotting buffer. Cooling pads were placed into the tank and the transfer ran at 200 mA for 120 minutes with 200rpm stirring. The PVDF membrane was placed in 5 ml of blocking solution for 1 hour at room temperature or overnight at 4ºC. The membrane was then incubated in 5 ml of blocking solution containing the desired diluted primary antibody for 1 hour at room temperature or at 4°C overnight. The primary antibody was removed by washing the membrane with 10 ml of TBSt for 30 minutes with 3 changes of buffer. The membrane was then incubated for 1 hour at room temperature in TBSt containing the desired diluted HRP conjugated secondary antibody. The secondary antibody was removed by washing the membrane with 10 ml of TBSt for 30 minutes with 3 changes of buffer. The membrane was incubated in either 2.5 ml of incubated of enzyme substrate for 1 minute at room temperature or Pierce ECL 2 western blotting substrate (Thermo Scientific), which was used following the manufacturer's instructions. The membrane was placed onto cling film and into the development cassette and the membrane exposed to X-ray films (X-ray film RX NIF sheets 130mm x 180mm Fujifilm, Fisher Scientific) in a dark room for various lengths of time depending on the antibodies used and the abundance of protein. The film was then placed in developer solution for up to

5 minutes, washed with water and placed in fixer solution for up to 5 minutes, washed with water and left to dry at room temperature.

2.2.1.3 Protein quantification

Bovine serum albumin (BSA) was dissolved in distilled water to yield protein solutions with concentrations of 0, 0.2, 0.4, 0.6, 0.8, 1.0, 1.2 and 1.4 mg/ml. 5 µl of each solution was added in triplicate to a 96 well plate along with 5 µl of the desired protein with an unknown concentration (in triplicate) and 5 µl of a 1:5 dilution of the desired protein with an unknown concentration. 25 µl of Bio-Rad DC protein assay reagent A was added to wells containing protein followed by 200 µl of Bio-Rad DC protein assay reagent B, mixed well, incubated at room temperature for 5 minutes and the absorbance read at 595 nm (A_{595}). The absorbance readings were plotted against the concentrations of the BSA standards and the equation of the line was used to determine the concentration of desired proteins.

2.2.1.4 Protein dialysis

Pooled protein elution fractions were dialysed against 2 x 1 L of the appropriate dialysis buffer for the purified protein in order to remove imidazole or glutathione used to elute the proteins from an affinity column. 20 cm of dialysis tubing (14000, or 8000 MWCO) was washed in 250 ml of distilled water followed by incubation in the dialysis buffer for 30 seconds. The pooled elution fractions were added and the protein was dialysed in 1 L of dialysis buffer for 24 hours at 4 °C with gentle stirring and a change of buffer.

2.2.1.5 Agarose gels

1% molecular biology grade agarose was dissolved in 50 ml of TAE buffer in a microwave for 50 seconds. Ethidium bromide was added to a final concentration of 0.01%. The solution was poured into a gel caster and was allowed to set at room temperature. 5 µl of DNA marker (PeqLab 0.1-10kb) was loaded in the 1st well (unless

stated otherwise) and 6 x loading dye (PeqLab) was added to the desired samples to make 1 x loading dye. The gel was run at 100 V for approximately 40 minutes.

2.2.1.6 Polymerase chain reaction (PCR)

For a normal PCR reaction the concentration of the template DNA was adjusted to between 1 and 10 ng/µl for plasmid DNA. The desired primers were diluted to a working concentration of 10 µM. The PCR reactions were prepared differently depending on whether the PCR product would be used for cloning or for analytical purposes. The table below shows the components of the PCR reaction mixtures for each purpose.

For Cloning- Total volume 50 µl	For analytical purposes –Total volume 20 µl
5 µl of 10 x PCR buffer	2 µl of 10 x PCR buffer
1 µl of primer 1 (10 µM)	0.4 µl of primer 1 (10 µM)
1 µl of primer 2 (10 µM)	0.4 µl of primer 2 (10 µM)
1 µl of dNTP's (10 mM)	0.4 µl of dNTP's (10 mM)
40 µl distilled autoclaved water	16 µl distilled autoclaved water
1 µl of DreamTaq DNA polymerase (Thermo Scientific) (5 units)	0.4 µl of PFU/Taq DNA polymerase mix (50x)
1-2 µl of DNA template	0.5- 1 ul of DNA template

Table 5. PCR reactions.
The constituents of PCR reactions for both cloning and analytical purposes. For analytical purposes both the PFU and Taq DNA polymerases used were expressed and purified from E. coli.

The PCR cycle was as follows:

Step 1: 94˚C - 1:30 minutes
Step 2: 94˚C – 30 seconds
Step 3: 60˚C – 30 seconds (Annealing temperature depending on primer length and composition).
Step 4: 72˚C – xxx minutes depending on the length of the PCR product (1 minute per kilobase)
Step 5: repeat steps 2-4 35 times
Step 6: 72˚C – 10 minutes
Step 7: 4˚C - ∞

For PCR reactions that involved the production of a PCR product longer than 3 Kbp a LongAmp Taq DNA polymerase (New England Biolabs) was used according to the manufacturer's protocol.

2.2.1.7 Production of electro-competent *E. coli*

500 ml of LB broth was inoculated with an overnight culture of *E. coli* (TOP10 or BL21DE3) at a dilution of 1:100. The cells were grown at 37ºC shaking at 200 rpm to an OD_{600} of 0.6. Cells were chilled on ice for 20 minutes and then harvested by centrifugation at 4000 x g for 15 minutes at 4ºC. The supernatant was removed and the pellet re-suspended in 500 ml of ice cold 10% glycerol (sterilised by autoclaving). The solution was centrifuged at 4000 x g for 15 minutes at 4ºC and the supernatant discarded. The pellet was re-suspended in 250 ml of ice cold 10% glycerol and centrifuged as previous. The supernatant was removed and the pellet re-suspended in 20 ml of ice cold 10% glycerol and centrifuged as above. The supernatant was discarded and the pellet re-suspended in a final volume of 1-2 ml of ice cold 10% glycerol. The cells were snap frozen in liquid nitrogen and stored at -80ºC.

2.2.1.8 *E. coli* transformations

5 µl of desired plasmid and 100 µl of electro-competent *E. coli* (BL21DE3 or TOP10) were added to an electroporation cuvette. Electroporation was carried out at 1.8 kV followed by the immediate addition of 1 ml of LB broth to the bacteria and incubation for 1 hour at 37°C with 200 rpm shaking. 100 µl of the LB-bacteria mix was then spread out onto selective LB agar plates and incubated at 37°C for 24 hours.

2.2.1.9 Plasmid isolation from *E. coli* –small scale

2 ml of an overnight culture of TOP10 *E. coli* containing the desired plasmid was subjected to centrifugation at 14000 rpm in a microfuge for 30 seconds. The pellet was then re-suspended in 200 µl of solution 1 (Table 1). 200 µl of solution 2 was added to the tubes and mixed, followed by the addition of 200 µl of solution 3. The solutions

were mixed by vortexing and then incubated for 10 minutes at room temperature followed by centrifugation at 14000 rpm in a microfuge for 10 minutes at room temperature. The supernatant was added to a new 1.5 ml Eppendorf tube along with 700 µl of 100% 2-propanol, vortexed and incubated at room temperature for 10 minutes. The samples were centrifuged at 14000 rpm in a microfuge for 10 minutes at room temperature. The supernatant was removed and 500 µl of 70% ethanol added to the pellet. The samples were centrifuged at 14000 rpm in a microfuge for 10 minutes at room temperature and the supernatant discarded. The tubes were placed in a 37°C incubator with the lids off until the ethanol had evaporated. The pellet was re-suspended in 50 µl of 10 mM TrisCl pH 8.0 or distilled autoclaved water. The concentration of DNA was quantified using agarose gel electrophoresis and a nanodrop.

A PeqGold plasmid mini prep kit (PeqLab) was also used, according to the manufacturer's instructions.

2.2.1.10 Plasmid isolation from *E. coli* – large scale

200 ml LB broth was inoculated with *E. coli* (TOP10) containing the desired plasmid and grown 24 hours at 37°C in a shaking incubator set to 200 rpm. The bacteria were harvested by centrifugation at 2500 xg for 20 minutes at 4°C. The supernatant was discarded and the pellet re-suspended in 5 ml of solution 1 (Table 1) by vortexing. 5 ml of solution 2 was added mixed and incubated for 5 minutes at room temperature followed by 5 ml of solution 3. The solutions were mixed by vortexing and then incubated at 4°C for 30 minutes. The suspension was then spun in a Beckman table top centrifuge at 4000 rpm for 20 minutes at 4°C. The lipid layer was removed and the supernatant was passed through a 0.45 µm syringe filter followed by the addition of 15 ml of 100% propan-2-ol, mixed and incubated on ice for 15 minutes. The solution was spun in a Beckman table top centrifuge at 4000 rpm for 20 minutes at 4°C, the supernatant discarded and the pellet washed with 10 ml 70% ethanol and centrifuged

at 4000 rpm for 10 minutes at 4°C. The pellet was dried at 37°C to remove the ethanol and was then re-suspended in 1 ml of TE buffer.

2.2.1.11 Restriction digests

Restriction digests were performed differently depending on the application of the digested DNA and the DNA to be digested. For digesting plasmid DNA for cloning 10 µg of the desired plasmid was diluted in 40 µl of distilled autoclaved water containing the appropriate concentration of restriction enzyme buffer (Roche or New England BioLabs). The plasmid was digested with a total volume of 4 µl of the appropriate restriction enzymes (Roche or New England BioLabs) (20000 units/ml) for 3 hours at the appropriate temperature. For digesting a PCR product for cloning the appropriate volume of restriction enzyme buffer was added along with a total volume of 4 µl of the desired restriction enzymes (Roche or New England BioLabs) (20000 units/ml) and incubated at the desired temperature for 3 hours. The digestion products were then loaded onto an agarose gel for analysis.

For the screening of colonies by digestion 5 µl of a plasmid (isolated by mini prep) was added to 15 µl of distilled autoclaved water and the desired concentration of restriction enzyme buffer added. A total volume of 1 µl of the chosen restriction enzymes (Roche or New England BioLabs) (20000 units/ml) were added and the mixture incubated at the appropriate temperature for 3 hours. The digestion products were then loaded onto an agarose gel for analysis.

2.2.2 Protein Expression and Purification

2.2.2.1 Expression and purification of recombinant 6xHis-MBP tagged receptor tails

1 L of LB broth (containing kanamycin or ampicillin at final concentrations of 50 µg/µl and 100 µg/µl respectively) was inoculated with 10 ml of an overnight culture of *E. coli* (BL21DE3) containing the expression plasmid for the desired protein. The cultures were grown to an optical density (OD) (600 nm) of 0.6 at 37°C in a shaking incubator at 200 rpm. IPTG was added at a final concentration of 100 µM and the culture was incubated at 37°C for 3 hours shaking at 200 rpm to induce protein expression. The cells were harvested by centrifugation at 2500 xg for 20 minutes at 4°C and the pellets stored at -20°C overnight. The bacterial pellet was re-suspended in 10 ml of lysis buffer containing the protease inhibitors aprotinin, E-64, PMSF and pepstatin at final concentrations of 3.2 µg/ml, 4 µg/ml, 1 mM and 1 µg/ml respectively. The suspension was subjected to sonication for 1 minute followed by incubation on ice for 3 minutes. This process was repeated 3 times. The lysate was cleared by centrifugation at 10000 rpm for 30 minutes at 4°C. The resulting supernatant was passed through a 0.45 µm syringe filter and loaded on to a Ni-NTA agarose column (Thermo Scientific, Pierce) equilibrated in lysis buffer. The flow through was collected and the column washed 6 times with 10 ml of lysis buffer. The bound protein was eluted from the column with 5 x 1 ml of elution buffer. 10 µl of each elution fraction were mixed with 4 x Laemmli buffer and loaded onto 10% SDS-PAGE gels and stained with either Coomassie stain or Instant Blue stain to determine which elution fractions contained the desired protein. The column was stripped with 10 ml of clearance buffer to remove any remaining bound protein. The stripped column was washed with 10 ml distilled water and stored at 4°C in 20% ethanol. The columns could be re-used by washing out the 20% ethanol and then washing the column with 5 ml of 100 mM nickel sulphate. The fractions

determined by SDS-PAGE to contain the desired protein were pooled and dialysed against dialysis buffer overnight at 4ºC with at least one buffer exchange.

2.2.2.2 Expression and purification of recombinant tobacco etch virus protease (TEV)

TEV protease was purified as described above (2.2.2.1) with the following modifications. *E. coli* (BL21DE3) containing pMalE-TEV (Addgene) was grown as described previously (2.2.2.1) and protein expression was inducted at 25°C with 100 µM. TEV protease was purified using TEV lysis buffer and TEV elution buffer (Table 1). The eluted TEV was dialysed immediately into TEV dialysis buffer to remove the imidazole, which was found to effect TEV activity. The purity of TEV protease was then assessed by Coomassie stained SDS-PAGE.

2.2.2.3 Expression and purification of recombinant His-Vac14

His-Vac14 was expressed and purified from of *E. coli* (BL21DE3) containing the expression plasmid for HIS-Vac14 (a kind gift from Lois Weisman). Protein expression was induced using 100 µM IPTG for 18 hours (200 rpm) at 25°C.

2.2.2.4 Expression and purification of recombinant GST-ATG18

GST-ATG18 was purified as above (2.2.2.1) with the following modifications. 1 L of LB broth (containing ampicillin at a final concentration of 100 µg/µl was inoculated with 10 ml of an overnight culture of *E. coli* (BL21DE3) containing pGEX 6P1- ATG18 (a kind gift from Scott Emr, Cornell University). The bacterial pellet was re-suspended in 10 ml of ATG18 lysis buffer containing the protease inhibitors aprotinin, E-64, PMSF and pepstatin at final concentrations of 3.2 µg/ml, 4 µg/ml, 1 mM and 1 µg/ml respectively. The supernatant resulting from the centrifugation steps was passed through a 0.45 µm syringe filter and loaded on to a glutathione agarose column (Thermo Scientific, Pierce) equilibrated in ATG18 lysis buffer. The flow through was collected and the column washed 6 times with 10 ml of ATG18 lysis buffer. The bound protein was

eluted from the column with 5 x 1 ml of ATG18 elution buffer. The fractions determined by SDS-PAGE to contain GST-ATG18 were pooled and dialysed against ATG18 dialysis buffer at 4ºC overnight with at least one buffer change.

2.2.2.5 Isolation and Purification of Clathrin

Clathrin was purified from pig brains (Keen, 1987) essentially as described by (Wang et al., 2014b). Approximately 8 pig brains (frozen at – 80˚C) were divided between two 1 L beakers and topped up with 1 x HKM buffer to an approximate volume of 600 ml. The protease inhibitors aprotinin, E-64, PMSF and pepstatin were added at final concentrations of 3.2 µg/ml, 4 µg/ml 1 mM and 1 µg/ml respectively. The brains were blended a beaker at a time until completely homogenised, using an electric blender. The blended pig brains were centrifuged at 7000 rpm for 30 minutes at 4˚C in a JA-14 rotor using a Beckman Coulter Avanti J-E centrifuge. The supernatant was collected and then centrifuged in a 70-Ti rotor at 36000 rpm for 45 minutes at 4˚C using a Beckman Coulter Optima L-100K Ultracentrifuge, to extract coated vesicles. The pellets were scraped into a large glass Dounce homogeniser and homogenised with 1 x HKM buffer to a final volume of approximately 40 ml. The volume of the homogenate was measured and an equal volume of ficoll/sucrose buffer added and mixed well. The mixture was centrifuged in a JA-20 rotor at 19000 rpm for 25 minutes at 4˚C using a Beckman Coulter Avanti J-E centrifuge. The supernatant was isolated and four times as much 1 x HKM buffer was added. The mixture was stored overnight at 4˚C. A sephacryl S500 column (diameter 2.6 cm, height 1 m) connected to an Akta Purifier (GE Healthcare, Life Sciences) was equilibrated in 1 M Tris buffer. The overnight sample was spun at 36000 rpm in a 70-Ti rotor (Beckman Coulter Optima L-100K Ultracentrifuge) for 1 hour at 4ºC. The pellets containing coated vesicles were re-suspended in a minimal volume of 1 x HKM buffer and then homogenised using a Dounce homogeniser. The sample was centrifuged at 13000 rpm for 10 minutes at 4ºC in a microfuge to remove cytoskeletal contaminants. The supernatant was collected

and the same volume of 2 x 1 M Tris buffer was added, mixed and incubated on ice for 1 hour to strip the protein coat off the lipid vesicles. The sample was spun a 50000 rpm (Beckman Coulter Optima TLX Ultracentrifuge) for 30 minutes at 4ºC to remove most of the lipid. The supernatant was retained and loaded onto the equilibrated sepharcryl S500 column, which was run at a flow rate of 2 ml/minute. 10 ml fractions were collected. The fractions were stored at 4ºC overnight. Sample of the fractions were run on 10% SDS-PAGE gels and stained with Instant Blue stain to determine which fractions contained clathrin. The clathrin containing fractions were pooled and an equal volume of saturated ammonium sulphate solution was added and stored at 4˚C. A superdex 200 column (diameter 1.6 cm, height 55 cm) was equilibrated in 1 M Tris buffer. The clathrin/ammonium sulphate samples were centrifuged at 20000 rpm for 30 minutes in a JA-20 rotor at 4˚C (Beckman Coulter Avanti J-E centrifuge), the pellets re-suspended in 3-5ml of 1 x 1 M Tris buffer and dialysed against 1 L of depolymerisation buffer at 4˚C for at least 2 hours with one buffer change. The sample was centrifuged at 65000 rpm for 30 minutes at 4˚C (Beckman Coulter Optima TLX Ultracentrifuge) to remove insoluble aggregates. The supernatant was loaded on the equilibrated superdex 200 column. The sample was run at a flow rate of 2 ml/minute and 2.5 ml fractions were collected using the Akta purifier (GE Healthcare, Life Sciences). A sample of the fractions were analysed by SDS-PAGE to determine the clathrin containing fractions. These were pooled together and an equal volume of saturated ammonium sulphate solution was added and stored at 4˚C overnight. The clathrin/ammonium sulphate sample was centrifuged at 20000 rpm for 30 minutes at 4ºC in a JA-20 rotor (Beckman Coulter Avanti J-E centrifuge). The pellets were re-suspended in 1 ml or 2 ml of 1 x 1 M Tris buffer and dialysed against 1 L of depolymerisation buffer at 4˚C for at least 2 hours with one buffer change. The dialysis buffer was changed to polymerisation buffer and dialysis continued for at least 4 hours with a minimum of one buffer change. The clathrin cages were harvested by centrifugation at 50000 rpm for 20 minutes at 4˚C (Beckman Coulter Optima TLX

Ultracentrifuge). The supernatant was stored at 4˚C as clathrin could be harvested from it at a later date. The pellet was re-suspended in 200 µl of polymerisation buffer and stored at 4˚C.

2.2.2.6 Purification of Clathrin Adaptor Protein 2 (AP-2)

The purification of AP-2 was carried out as with the purification of clathrin up until the Sephacryl S-500 column. The adaptor protein containing fractions from the separation of Tris extracted clathrin cages, were pooled and dialysed against Buffer C (1x) containing 10 mM potassium phosphate and 0.2 mM PMSF overnight with at least one buffer change. The dialysed adaptor proteins were loaded onto a Hydroxyapatite Bio-gel column (bed volume 5 ml) connected to an Akta Purifier (GE Healthcare, Life Sciences) which had been equilibrated in Buffer C (1x) containing 10 mM potassium phosphate pH 7.2 and 0.2 mM PMSF. AP-2 was eluted from the column using an increasing phosphate gradient from 10 mM potassium phosphate pH 7.2 to 500 mM potassium phosphate in Buffer C (1x) for a duration of 100 minutes with a flow rate of 1 ml/min. 5 ml fractions were collected and samples subjected to SDS-PAGE and instant blue staining. The fractions containing AP-2 were pooled and an equal amount saturated ammonium sulphate solution added. The AP-2/ ammonium sulphate mixture was centrifuged at 19000 rpm for 30 minutes at 4ºC in a JA-20 rotor (Beckman Coulter Avanti J-E centrifuge). The pellet was re-suspended in 0.5 ml of Buffer C (1x) containing 10 mM potassium phosphate and 0.2 mM PMSF and dialysed against 1 x 1 M Tris buffer containing 0.2 mM PMSF overnight with at least one buffer change. The concentration of AP-2 was determined (2.2.1.3) and aliquots stored at -80ºC.

2.2.3 Proteo-liposome Recruitment

2.2.3.1 Preparation of pig brain cytosol for proteo-liposome recruitment

Pig brains were washed with recruitment buffer and then homogenised in an electric blender with an equal volume of recruitment buffer (w/v) containing the protease inhibitors aprotinin, E-64, PMSF and pepstatin at final concentrations of 3.2 µg/ml, 4 µg/ml 1 mM and 1 µg/ml respectively. The suspension was centrifuged at 2500 xg for 30 minutes at 4˚C. The supernatant was harvested and centrifuged at 100000 xg for 1 hour at 4˚C to remove endogenous membranes. The resulting supernatant was aliquoted and the samples were flash frozen in liquid nitrogen and stored at -80˚C.

2.2.3.2 Production of liposomes with coupled cytoplasmic receptor tails

Recombinant 6xHis MBP tagged cytoplasmic receptor tails were expressed in *E.*coli (Bl21DE3) and were purified as explained in 2.2.2.1. 500 µg of each receptor tail was digested with 5 µg of purified recombinant tobacco etch virus protease (TEV) (2.2.2.2) and 1 mM tris(2-carboxyethyl)phosphine (TCEP) overnight at 25˚C to remove the 6xHis MBP tag.

Liposomes were prepared from a mixture of the following lipids; PC, PE, PS, C, PE MCC and one of the phosphatidylinositol containing lipids (either PI, PI(3)P, PI(3,5)P_2 or PI(4,5)P_2) unless stated otherwise (2.1.2). The final amounts of each lipid were 200 nmol, 150 nmol, 50 nmol, 50 nmol, 50 nmol and 5 nmol respectively. The lipid mixture was dried under nitrogen gas and re-suspended in 0.65 ml of recruitment buffer. The re-suspended lipid film was subjected to 5 freeze/thaw cycles in liquid nitrogen and warm water. 100 µl of the liposome suspension was incubated with one TEV digested protein sample for 60 minutes in the dark at room temperature. The coupling of the cytoplasmic receptor tails to the liposomes is due to the formation of a sulphydryl bond between an extra cysteine residue at the N terminus of the receptor tail and the activated maleimide head group on the anchor lipid (PE-MCC) (Pocha et al., 2011).

The liposomes containing the coupled receptor tail will be referred to as proteo-liposomes. The proteo-liposomes were pelleted by centrifugation at 100000 xg for 20 minutes at 4˚C, re-suspended in 1 ml of 10 mM L-cysteine (in RB) and incubated for 15 minutes in the dark at room temperature. This step was important for quenching unreactive maleimide head groups, and for the creation of cysteine control samples. The sample was subjected to centrifugation (as above) the supernatant discarded and the pellet re-suspended in 100 µl of recruitment buffer.

2.2.3.3 Proteo-liposome recruitment experiments

Pig brain cytosol was centrifuged for 1 hour at 100000 xg and at 4˚C to remove any remaining endogenous membranes. The GTP analogue GTPγS (or GMPNP) was added to the cleared pig brain cytosol (unless stated otherwise) at a final concentration of 0.15 mM. 900 µl of cleared pig brain cytosol was added to 100 µl of proteo-liposomes and incubated for 30 minutes at 37˚C. Here the pig brain cytosol acts as a protein reservoir. Recruitment was also carried out using purified protein instead of the pig brain cytosol. Here GTPγS (or GMPpnp) was not added to the recruitment mixture. The proteo-liposomes were separated from the cytosol or purified recombinant protein using a sucrose cushion (2 ml 60% sucrose in RB and 8 ml 5% sucrose in RB) in a Beckman Coulter Optima L-100k ultracentrifuge (SW40 rotor) at 38000 rpm for 90 minutes at 4˚C. The interface between the two sucrose layers containing the proteo-liposomes was removed and re-suspended in 11 ml of RB and centrifuged in a Beckman Coulter Optima L-100k ultracentrifuge (SW40 rotor) at 38000 rpm for 1 hour at 4˚C. The supernatant was removed and the pellet re-suspended in 100 µl of 2x Laemmli buffer (unless stated otherwise). The samples were analysed by SDS-PAGE and western blotting for interacting proteins.

2.2.3.4 Flow cytometry analysis of liposomes

Liposomes were produced as explained in 2.2.3.2 except they also contained 2 mol% of the fluorescent lipophilic dye DiI, and the liposomes were re-suspended in 1 ml instead of 100 µl. Six sets of liposomes were prepared containing 66 µg, 164 µg, 329 µg, 657 µg, 1350 µg and 2694 µg of coupled GFP. These liposomes were analysed using flow cytometry in a Beckman Coulter Cell Lab Quanta SC flow cytometer. GFP was excited at 498 nm and DiI at 549 nm and 10000 events were counted.

2.2.3.5 Pull downs with purified His-Vac14

20 µg of purified recombinant, MBP-AICD, MBP-Tr1, MBP-Tr2, MBP-Tr3, MBP-Tr4 and MBP (negative control) were incubated with 10 µg of purified HIS-Vac14 for 1 hour rocking on ice. The volumes were adjusted to 200 µl with wash buffer. The samples were centrifuged in a bench top centrifuge at maximum speed for 5 minutes to remove any aggregates. The supernatant was transferred to a tube containing 20 µl of amylose resin beads (New England BioLabs) which had been washed 3 x in wash buffer. The samples were incubated rocking on ice for 1 hour and the amylose beads washed 5 times with wash buffer. The proteins were eluted by incubating the beads with 50 µl of PD elution buffer for 10 minutes on ice. The samples were centrifuged at 2000 rpm in a bench top centrifuge for 1 minute at 4˚C. The supernatant was transferred to a new tube containing 12.5 µl of 4 x Laemmli buffer. The sample was heated at 95˚C for 5 minutes before being subjected to SDS-PAGE and western blotting. 25 µl of each pull down sample was loaded on an 8% acrylamide gel.

2.2.3.6 Clathrin recruitment assay

Clathrin recruitment assays were based on those used in Kelly et al. (2014). Liposomes were created comprising 10% cholesterol, 5% PE-MCC, 5% $PI(4,5)P_2$ (unless stated otherwise) 80% PC:PE in a ratio of 3:2. The liposomes were incubated

in 182 µg of TEV digested purified receptor tail (AICD and Crbs2) or cysteine (negative control). The liposomes were centrifuged at 50000 rpm for 10 minutes at 4ºC in a (Beckman Coulter Optima TLX Ultracentrifuge) and the pellet re-suspended in 1 ml of 10 mM cysteine in 1 x HKM buffer to saturate any free anchor lipid. The liposomes were centrifuged again and re-suspended in 1 ml of 1 x HKM buffer to obtain a final lipid concentration of 0.4 mg/ml. Purified AP-2 (2.2.2.6) was added at a final concentration of 0.8 µM to 50 µl of the liposomes and incubated for 30 minutes on ice. The liposomes were centrifuged at 50000 rpm for 10 minutes at 4ºC in a (Beckman Coulter Optima TLX Ultracentrifuge) the supernatant removed and the pellet re-suspended in 50 µl of 1 x HKM buffer. Purified clathrin (2.2.2.5) previously dialysed against de-polymerisation buffer to disassembly the clathrin cages was added to the liposomes at a final concentration of 0.2 µM and incubated for 30 minutes on ice and then 15 minutes at 37ºC. The sample was centrifuged at 50000 rpm for 10 minutes at 4ºC in a (Beckman Coulter Optima TLX Ultracentrifuge) and the pellet and supernatant adjusted with 2 x Laemmli buffer. The samples were subjected to analysis by western blotting and SDS-PAGE stained with Coomassie.

2.2.4 Mammalian Tissue Culture Experiments

2.2.4.1 Transfections

HeLa cells were seeded into 24 well plates at a density of 100000 cells per well for transfection using Lipofectamine 2000 (Invitrogen Life Technologies). The following day 1 µg of plasmid DNA was diluted in 50 µl of OptiMEM medium and added to 2 µl of Lipofectamine 2000 diluted in 50 µl of OptiMEM medium. This transfection mix was for one well in a 24 well plate. The transfection mixture was incubated for 15 minutes at room temperature and added to the 24 well plate. A list of the plasmids used for transfections can be seen in the appendix (A1). The cells were incubated with the transfection mixture for approximately 18 hours at 37ºC, 5% CO_2, washed several times with tissue culture medium to completely remove the transfection reagent and incubated overnight at 37ºC, 5% CO_2.

For analysis by live cell imaging the transfected cells were then transferred to a glass bottom dish for imaging and incubated overnight at 37ºC, 5% CO_2. Before imaging the tissue culture medium was removed and replaced by OptiMEM medium.

For analysis of fixed cells the cells were fixed using cell fixing solution for 30 minutes at room temperature, and were washed with 1 X PBS and then distilled water. The excess liquid was removed, and the cells mounted on a glass slide using 20 µl of Mowiol mounting media. The slides were left to dry overnight.

2.2.4.2 PIKfyve inhibition

To inhibit PIKfyve activity HeLa cells were treated with 4 µM of the PIKfyve inhibitor YM201636 (dissolved in DMSO) (Santa Cruz Biotechnology) for 4 hours at 37˚C 5% CO_2 (unless stated otherwise). The medium was removed, the cells washed with 1 x PBS, fixed and mounted onto glass slides.

2.2.4.3 Lysis of HeLa cells for Western blotting

HeLa cells were seeded into 6 well plates at a density of 400000 cells per well and incubated at 37˚C with 5% CO_2 overnight. The medium was removed and the cells washed with 1 x PBS (ice cold). 200 µl of mammalian cell lysis buffer was added to each well and the cells scraped off the bottom of the well. The cell suspension was centrifuged for 15 minutes at max speed in a benchtop centrifuge at 4˚C. 4 x Laemmli buffer was then added to the supernatant to make a 1 x solution. The samples were analysed by SDS-PAGE and western blotting using APP, APLP2 and tubulin antibodies.

2.2.4.4 Microscopy

Live cell imaging was carried out using a Leica Microsystems DM14000B inverted microscope in a temperature control chamber set to 37ºC.

Fixed cell imaging was conducted using a Leica Microsystems SP5 TCS II MP DM16000B up-right confocal microscope. The GFP and YFP constructs were excited using the 488 nm and 514 nm lasers set to 22% and 33% respectively. The mCherry construct was imaged using the 594 laser set at 33% with a constant gain of 821 HV. Z-stacks were taken of the cells with a 0.5 µm distance between slices.

2.2.4.5 Quantification of ML1Nx2 positive vesicles

For the quantification of mCherry- ML1Nx2 positive structures in cells co-expressing mCherry-ML1Nx2 and a GFP or YFP tagged APP/ACID constructs Z-stacked images were obtained using a Lecia SP5 TCS II MP confocal microscope. The images were imported into ImageJ and maximum projections created from the Z-stacks. Each cell to be quantified was individually selected and all background removed. The mCherry ML1Nx2 positive structures were analysed using the MOSAIC plugin for ImageJ (Rizk et al., 2014). The image was segmented with a background subtraction was of 10

pixels. The background subtraction reduces the background fluorescence using the rolling ball algorithm. For the segmentation parameters the regularisation was set to 0.1 and the minimum object intensity was set to 0.3. The regularisation parameter determines what to class as noise and what to class as an object. Any structure with an intensity lower than the minimum object intensity is not classed as an object. The average number of mCherry-ML1Nx2 structures per cell was calculated for each condition along with the average intensity of these structures. The data was analysed using a one way ANOVA (alpha = 0.05) with a Tukey's post hoc test in GraphPad Prism 6.

Chapter 3

The establishment of the proteo-liposome recruitment technique and it use in the analysis of the AICD-mTOR interaction

Chapter 3- The establishment of the proteo-liposome recruitment technique and its use in the analysis of the AICD-mTOR interaction

3.1 Introduction

Membrane proteins are a diverse group of proteins, important in a wide variety of biological processes. They are involved in cell signalling, transport across the cell membrane and cell adhesion. The intracellular domains of membrane proteins are key for linking the extracellular domain with the cytoplasm. They bind to a wide variety of cytoplasmic proteins which allows them to exert their physiological function. It is therefore important that we develop ways for examining the intracellular interactome of membrane proteins with a view to gaining a greater insight into their function.

Membrane protein interactions can be studied through the use of an in vitro model membrane system involving the use of synthetic membranes or liposomes. The use of a model membrane system allows for the mimicking of the intracellular domain attached to its natural membrane environment, and therefore takes into account any phospholipid based interaction. Liposome based systems have previously been used to examine the interactions of certain membrane proteins with cytosolic factors, with particular emphasis on the interactions of coat protein complexes. An overview of the use of liposome based model membrane systems can be seen in chapter 1 (1.3).

This chapter will focus on the establishment of a liposome model membrane recruitment system based on that of Pocha et al. (2011), using amyloid precursor protein as a model membrane protein.

Previous work conducted by colleagues (Balklava et al., under revision A) utilised a proteo-liposome recruitment system similar to that used by Pocha et al. (2011), coupled with label free quantitative mass spectrometry to establish an intracellular interactome of APP, through the coupling of its intracellular domain (AICD) to liposomes, and the isolation of its binding partners from mouse brain cytosol samples. As well as identifying established APP interacting proteins such as Fe65 several novel APP interactors were identified (Balklava et al., under revision A). Among these was the mTOR complex involved in the integration of nutrient and energy signals (see chapter 1.6). It was found that mTOR and its accessory subunits raptor and mLST8 were significantly enriched in AICD proteo-liposome samples, raising the possibility of an interaction between APP and mTOR. This chapter will focus on the characterisation of this observed putative interaction between APP and mTOR in order further develop and validate the proteo-liposome recruitment system.

3.1.1 The interaction between APP and mTOR?

The main reason for the investigation of the interaction between APP and mTOR is to gain insight into the physiological function of APP. The primary focus of APP research has been on is proteolytic processing, and the contribution of one if its proteolytic products, known as Aβ, in the pathology of Alzheimer's disease. Despite this vast amount of research, the physiological role of full length APP remains largely unknown (Caldwell et al., 2013). The potential interaction between APP and the mTOR complex observed by Balklava et al. (under revision A) has exciting implications for APP function due to the wide variety of crucial physiological processes the mTOR complex is involved in.

There is also an increasing amount of evidence that suggests that aberrant mTOR signalling plays a role in Alzheimer's disease (Yates et al., 2013). mTOR signalling is enhanced in the brains of Alzheimer's disease patients (Yates et al., 2013) . An increase in mTOR signalling has also been shown to potentiate Tau toxicity in a *Drosophila* tauopathy model (Khurana et al., 2006). Genetically increasing the levels of mTOR in mice increases both the levels and the phosphorylation of tau. Reducing mTOR signalling in a mouse model overexpressing mutant human reduces tau pathology (Caccamo et al., 2013). The overexpression of APP mutant proteins in mammalian cells is known to increase mTOR signalling, however the mechanism that leads to this increase in mTOR signalling remains unidentified (Caccamo et al., 2010). It has also been shown that insulin is able to influence the phosphorylation of APP, and that impaired insulin signalling can promote the formation and accumulation of Aβ (Pandini et al., 2013). Insulin is known to activate mTORC1 and stimulate protein synthesis through the phosphorylation of 4EBP1 (Wang et al., 2006). Taken together these findings also support the role of mTOR in Alzheimer's disease. For these and the fact that the native function APP still remains largely unclear we chose to examine the interaction between APP and mTOR using a proteo-liposome approach whereby the intracellular domain of AICD was covalently coupled to liposomes.

3.2 Results

3.2.1 Optimisation of the proteo-liposome recruitment technique.

Understanding the interactions between the cytoplasmic domain of membrane proteins and cytosolic proteins is crucial for elucidating the function of a particular membrane protein. It is therefore important that we have ways of examining these interactions. Using the Type I transmembrane protein APP as a model protein a model membrane system for examining APP's intracellular interactome was designed. A liposome recruitment assay based on that used by Pocha et al. (2011) was utilised as the model membrane system. The method involves coupling the intracellular domain of a membrane protein to liposomes to mimic its native configuration. For the purpose of this chapter the intracellular domain of APP (AICD) was coupled to these liposomes. AICD was expressed in *E. coli* using the pET-28-MBP-AICD plasmid, which is of the same construct as the expression plasmid used by (Pocha et al., 2011). A representation of the purified protein construct can be seen in figure 13A. The purified MBP tagged protein was digested with TEV protease overnight, which cleaved off a 6xHis-MBP tag exposing an extra N-terminal cysteine residue. This cysteine residue allows for the covalent coupling of the protein to a lipid anchor (PE-MCC) in the liposomes. The lipid anchor PE-MCC contains an activated maleimide head group which covalently couples to the sufhydryl group of the N-terminal cysteine residue. Once the TEV protease cleave protein is attached to the liposomes cysteine is used to quench any unreacted maleimide head groups. These proteo-liposomes are incubated in brain cytosol, which acts as a protein reservoir. The proteo-liposomes and their interaction partners are isolated by ultracentrifugation (Figure 13C). Samples can be analysed by SDS-PAGE, Western blotting and mass spectrometry.

The liposome recruitment method used by Pocha et al. (2011) was subjected to several modifications. The first of these was a change in the sucrose gradient used to

isolate the proteo-liposomes and their interaction partners. Instead of the proteo-liposomes being loaded at the bottom of the gradient and floated, as used by Pocha et al. (2011), they were loaded at the top of the gradient and harvested at the interface between a sucrose cushion composed of 60% and 5% sucrose dissolved in recruitment buffer (RB). An example of the sucrose cushion used can be seen in figure 13C. This method allows for the separation of the proteo-liposomes from the cytosolic protein they were incubated in. Proteo-liposome were harvested at the interface between the 5 and 60% sucrose whilst the cytosolic protein (0% sucrose) was removed from the tube before the removal of the proteo-liposomes. This method allows for any insoluble aggregates to be pelleted, which separates them from the proteo-liposomes, preventing the contamination of samples. Another important advantage of changing the sucrose cushion is that it allows for the isolation of proteo-liposomes with a large density range, compared to the flotation method used by Pocha et al. (2011) where the heaviest proteo-liposomes may not make it to the top of the gradient for isolation. This modification resulted in a change in the centrifugation time from approximately 18 hours to 2 hours therefore saving time and energy.

As the recruitment process is quite complex and involves several steps there was a need to ensure the individual steps were functioning correctly. To achieve this, samples were taken at different stages of the recruitment process and analysed by Coomassie blue stained SDS-PAGE (Figure 13B). A 2% sample (v/v) of MBP-AICD (pre), and a 2% sample of the TEV protease digested AICD (post) were taken to check for the complete digest of the protein and the consequent removal of the 6 x His-MBP tag. This could be viewed by Coomassie stained SDS-PAGE by the appearance of a band at about 5 kDa corresponding to AICD, and the presence of a band corresponding to the cleaved MBP tag, characterised by a lower molecular weight than full length MBP-AICD (Figure 13B). A sample of 2% of the volume of the supernatant resulting from the 1st centrifugation (see 2.2.3.3) was collected (supernatant). This

allowed for analysis of the coupling efficiency of AICD to PE-MCC in the liposomes evident by the absence of the low molecular weight AICD band, and the presence of a band corresponding to the cleaved MBP tag. If the lower molecular weight AICD was present in the supernatant sample this could indicate liposome saturation with AICD, or the faulty coupling of AICD to the liposomes. A 2% sample (v/v) of the re-suspended pellet was taken before the addition of pig brain cytosol to ensure AICD was coupled to the liposomes (pellet). This was detected by the presence the 5 kDa AICD band. This band was slightly higher in molecular weight than the AICD in the post digestion sample, due to the presence of lipid from the coupling of AICD to liposomes.

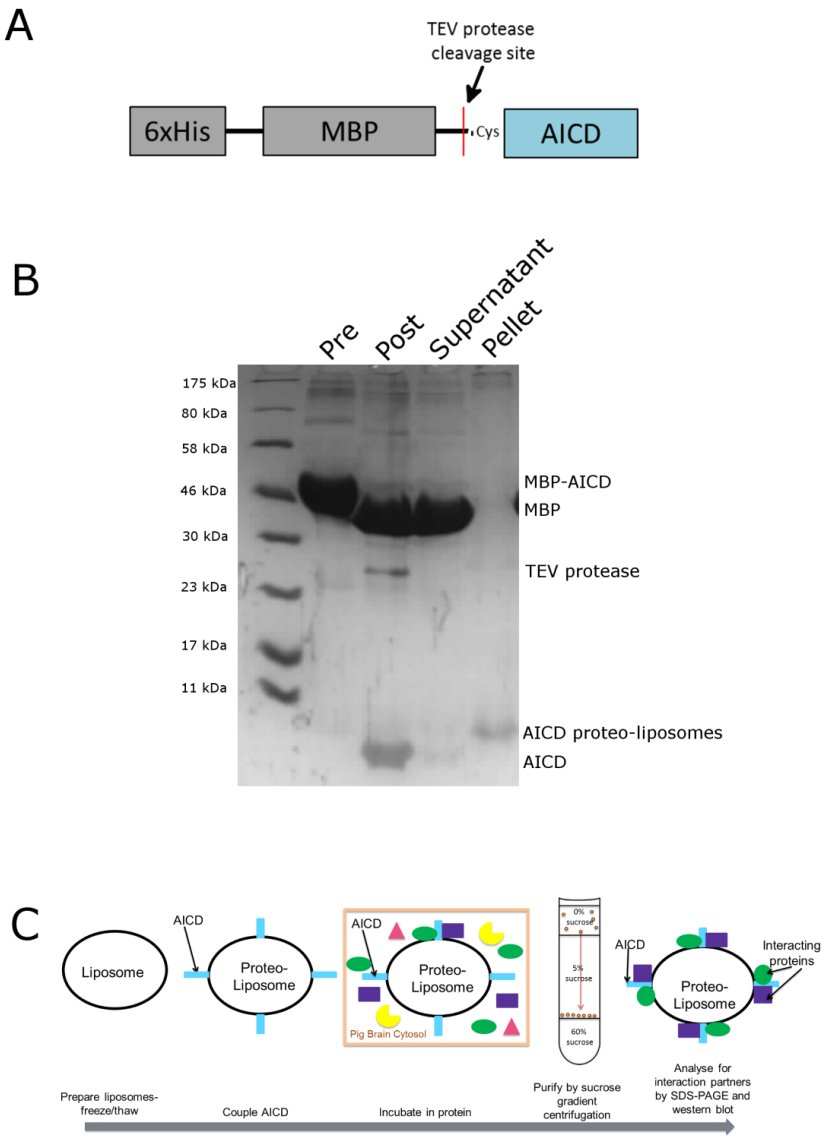

Figure 13. An overview of the proteo-liposome recruitment method. *(A) The construct of the cytoplasmic receptor tail (AICD) used to allow coupling of the protein to PE-MCC in the liposomes. (B) A Coomassie stained SDS-PAGE gel of different stages in the recruitment process to check for complete digestion of the protein tail and its coupling to liposomes. Samples (2% v/v) taken at different points during the recruitment process. Pre = MBP –AICD protein, Post = TEV protease digested MBP-AICD, Supernatant = after 1st centrifugation of proteo-liposomes, Pellet = pelleted proteo-liposomes containing coupled AICD. (C) A basic overview of the recruitment process; AICD is coupled to liposomes (now called proteo-liposomes) and incubated in pig brain cytosol which acts as a protein reservoir. The proteo-liposomes and the interaction partners are purified by density centrifugation and analysed by SDS-PAGE and western blotting.*

The next stage in the refinement of the recruitment process was to determine the most effective amount of total lipid used to create the liposomes, in terms of the yield of protein recruitment. A recruitment experiment was conducted using liposomes containing different amounts of total lipid (500, 100 and 50 nmol). The liposomes comprised of 40 mol% PC, 29 mol% PE, 10 mol% PS, 10 mol% C, 10 mol% PE-MCC and 1 mol% $PI(4,5)P_2$ (see table 2). The TEV protease digested AICD was coupled to liposomes and maltose binding protein (MBP) was coupled to liposomes as a control. MBP contains no internal cysteine residues so couples to liposomes via the introduced N-terminal cysteine residue. Therefore, it is coupled in the same orientation as AICD, mimicking protein coated liposomes. The liposomes were incubated in 300 µg of protein as established by Pocha et al. (2011). This is equivalent to 6 nmol MBP-AICD and 6.7 nmol MBP (control), as calculated using the full length undigested construct. The ratio MBP-AICD protein to the anchor lipid PE-MCC was therefore 1 nmol: 8.33 nmol, 1 nmol: 1.67 nmol and 1 nmol: 0.833 nmol for liposomes comprising 500 nmol, 100 nmol and 50 nmol total lipid respectively. The ratio of the MBP control protein to the anchor lipid PE-MCC was 1 nmol: 7.465 nmol, 1 nmol: 1.5 nmol and 1 nmol: 0.75 nmol for liposomes comprising 500 nmol, 100 nmol and 50 nmol total lipid respectively.

These proteo-liposomes were incubated in 900 µl of pig brain cytosol (16 mg/ml) (prepared as in 2.2.3.1). The proteo-liposomes and interaction partners were isolated by sucrose gradient density centrifugation (2.2.3.3), and samples of the final recruitment were subjected to SDS-PAGE stained with Coomassie blue. Figure 14A shows a Coomassie blue stained SDS gel of the final recruitment products.

AICD proteo-liposomes comprised of 100 nmol and 500 nmol total lipid significantly recruited more protein than MBP control proteo-liposomes comprised of 100 nmol and 400 nmol total lipid (Figure 14 B). Overall liposomes comprising of 500 nmol total lipid significantly recruited more protein than those comprising 50 nmol and 100 nmol total lipid (blue bars on figure 14B).

A saturation point for the maximum amount of protein that could be recruited was not reached, demonstrating that the method is not at the limits of detection. Of note is the difference in the band pattern between the AICD proteo-liposomes and the control liposomes (MBP) indicating that AICD recruits different proteins to the control, as well as bands common to both samples. The arrows on figure 14A represent bands that are present in only AICD proteo-liposome samples. For future recruitment experiments liposomes comprising 500 nmol of total lipid were used as this produced a good yield of recruited protein. These results suggest that using more than 500 nmol of lipid per recruitment would lead to a greater yield of recruited protein; however, this would be costly due to an increase in the amount of lipids used.

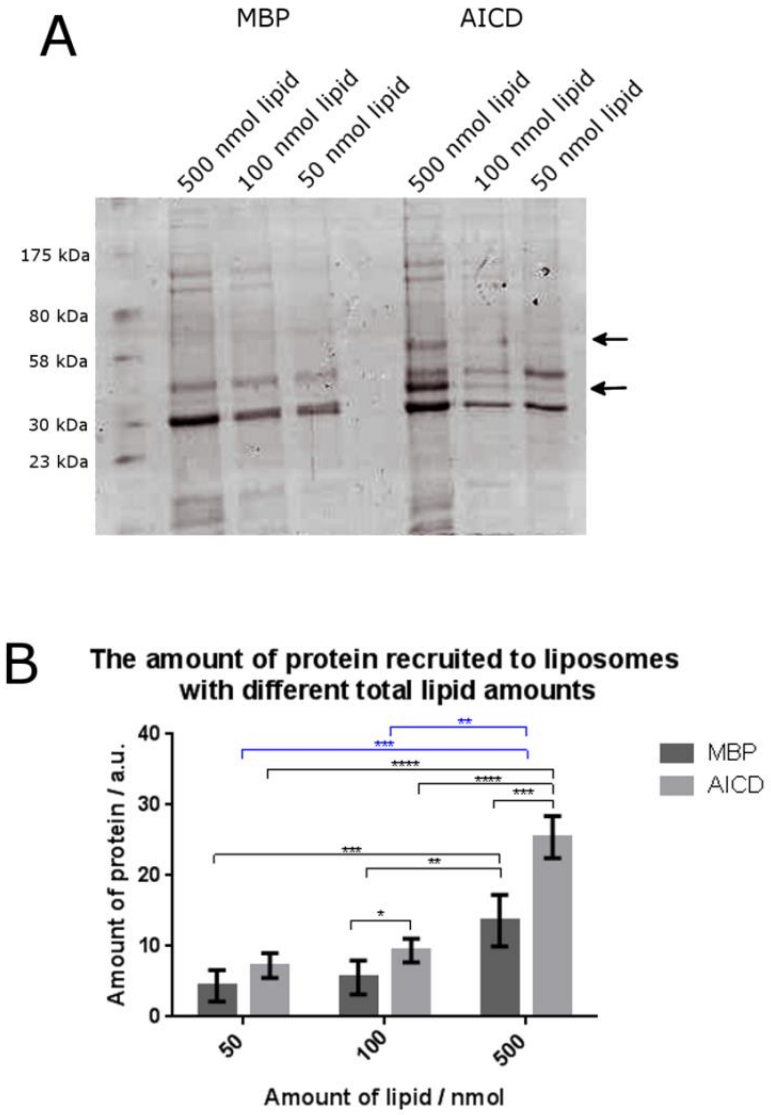

Figure 14. The effect of lipid amount on protein recruitment.
Three sets of liposomes were produced with different total lipid amounts (500, 100 and 50 nmol). These liposomes contained coupled AICD or MBP (control) at ratios of 1:8.33 nmol, 1:1.67 nmol and 1:0.833 nmol (protein:anchor lipid) for AICD and 1: 7.465 nmol, 1: 1.5 nmol and 1:0.75 nmol (protein:anchor lipid) for MBP control, for liposomes comprising 500 nmol, 100 nmol and 50 nmol total lipid respectively. The proteo-liposomes were incubated in the same volume of pig brain cytosol, isolated by ultracentrifugation and analysed by SDS-PAGE. (A) A Coomassie stained SDS-PAGE gel of the recruitment samples of liposomes comprising 50 nmol, 100 nmol and 500 nmol of total lipid. (B) Densitometry analysis of the amount of protein recruited was conducted in ImageJ (error bars = sem). Statistical analysis was conducted in GraphPad Prism 6.0 (n=3). A two- way ANOVA using a repeated measures design. Both a Tukey's (black bars) and Sidak's (blue bars) post hoc test was carried out ($p \leq 0.05$, ** $p \leq 0.01$, *** $p \leq 0.001$, **** $p \leq 0.0001$).*

In the method developed by Pocha et al. (2011), 300 µg of protein was coupled to liposomes. Due to the alteration of the lipid amount in figure 14 compared to that used by Pocha et al. (2011), the amount of protein coupled to these liposomes was also modified. The optimum amount of protein to couple to liposomes consisting of 500 nmol of total lipid was determined using liposomes coupled to different amounts of the fluorescent protein GFP. GFP contains internal cysteine residues, which when reduced using TCEP, are available to couple GFP to the anchor lipid PE-MCC in the liposomes. The amount of GFP coupled to liposomes was determined by the intensity of the GFP fluorescence present on liposomes as analysed by flow cytometry. Liposomes were produced containing 50 nmol of the anchor lipid PE-MCC, which is 10% of the total lipid amount of 500 nmol. These liposomes also contained 2 mol% of the fluorescent lipophilic dye DiI. Only liposomes exhibiting both DiI and GFP fluorescence were included in the analysis. Figures 15A and 15B show the presence of both GFP and DiI fluorescence respectively on the liposomes, indicated by a shift in the peak to the right when compared to control liposomes, without any coupled GFP or the fluorescent lipophilic dye DiI. Figure 15C shows the saturation curve obtained from the mean fluorescence intensities of the liposomes containing different amounts of coupled GFP. Figure 15 C shows that saturation of the anchor lipid with GFP, as determined by fluorescence intensity, appears to occur at approximately 1400 µg of GFP.

When examining the interaction partners of the intracellular domains of membrane proteins using the proteo-liposome recruitment technique, the complete saturation of the anchor lipid with these intracellular domains may affect the recruitment of cytosolic proteins. This is due to the steric hindrance that may arise from saturating the liposomes with these peptides, meaning the recruitment of cytosolic proteins would be affected, especially interacting proteins of a high molecular weight. Therefore, the amount of protein coupled to the liposomes needs to take this into account. 500 µg of protein was selected as the optimum amount to couple to liposomes, as according to

figure 15C this amount of protein should only saturate just below half of the anchor lipid present, allowing for a high yield of recruited protein whilst not selectively affecting protein recruitment.

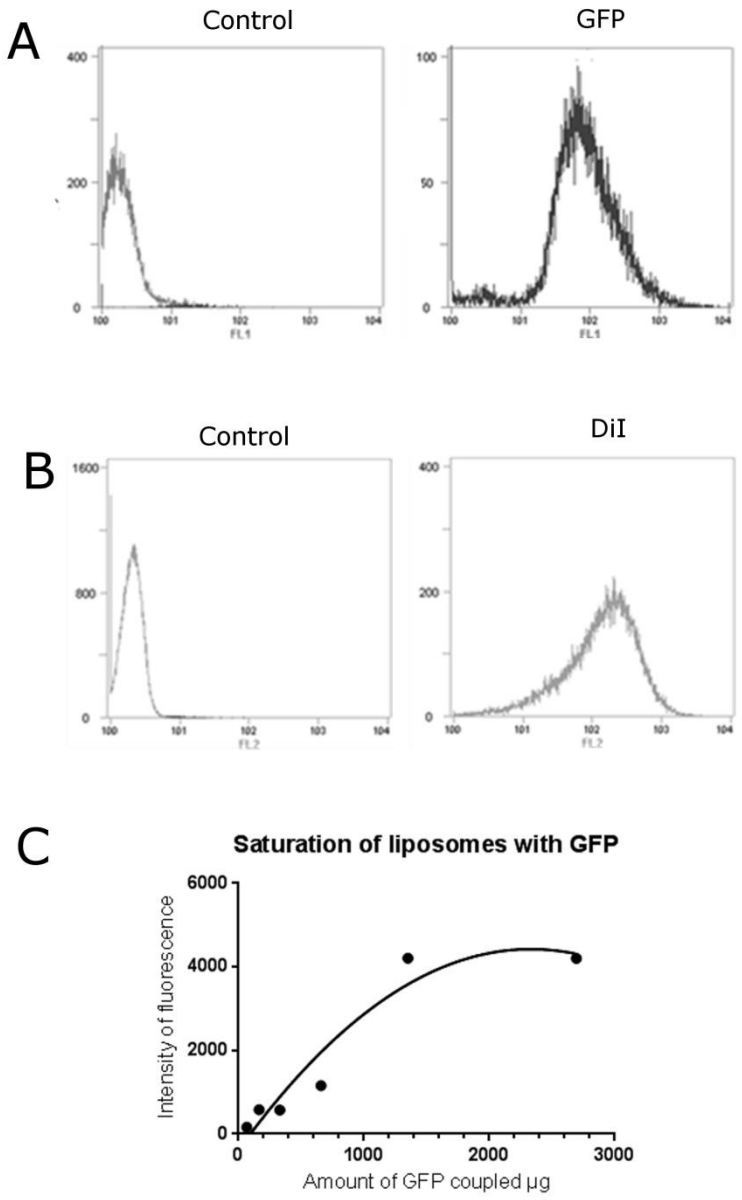

Figure 15. The saturation of liposomes with GFP
Different amounts (66 µg, 164 µg, 329 µg, 657 µg, 1350 µg, and 2694 µg) of the fluorescent protein GFP were coupled to liposomes containing 50 nmol of the anchor lipid PE-MCC and 2 mol% of the fluorescent lipophilic dye *DiI. The fluorescence intensity of these liposomes were analysed using flow cytometry. GFP was excited at 498 nm (A) and DiI was excited at 549 nm (B) and 10000 events were analysed. The intensity of GFP on the liposomes with different coupled amounts was used to determine the saturation of the anchor lipid PE-MCC with GFP (C). A saturation curve was fitted to these data points in Graphpad Prism 6.0 using non-linear regression with the least squares fit and the saturation one site, total and nonspecific binding model.*

3.2.2 AICD containing proteo-liposomes selectively recruit mTOR, raptor and rictor.

Once the proteo-liposome recruitment method was fully established this technique was then used to examine the interaction of AICD with the mTOR complex. Using mass spectrometry Balklava et al. (under revision A) established the intracellular interactome of AICD, and using a similar liposome recruitment method they identified several novel interaction partners of AICD, as well as the known interactors. One of these novel interactors was the kinase mammalian target of rapamycin (mTOR). Using this as a basis, the potential interaction between AICD and mTOR was examined. This allowed for the development of the liposome recruitment method, to enable the identification of interactions from the recruitments using western blotting.

Proteo-liposome recruitments were conducted where AICD was coupled to liposomes and incubated in brain cytosol. For the recruitment process cysteine and MBP liposomes were used as controls. Cysteine was used to quench unreactive maleimide groups. These control liposomes ensured that any selective recruitment observed was due to the presence of a specific tail (AICD). The liposomes were produced from 500 nmol total lipid. The final recruitment products were analysed by SDS-PAGE and western blotting for mTOR, and the subunits raptor and rictor (Figure 16A). The recruitments showed that AICD containing proteo-liposome samples were significantly enriched in mTOR, raptor and rictor (Figure 16B), demonstrating an interaction between the intracellular domain of AICD and the mTOR complex.

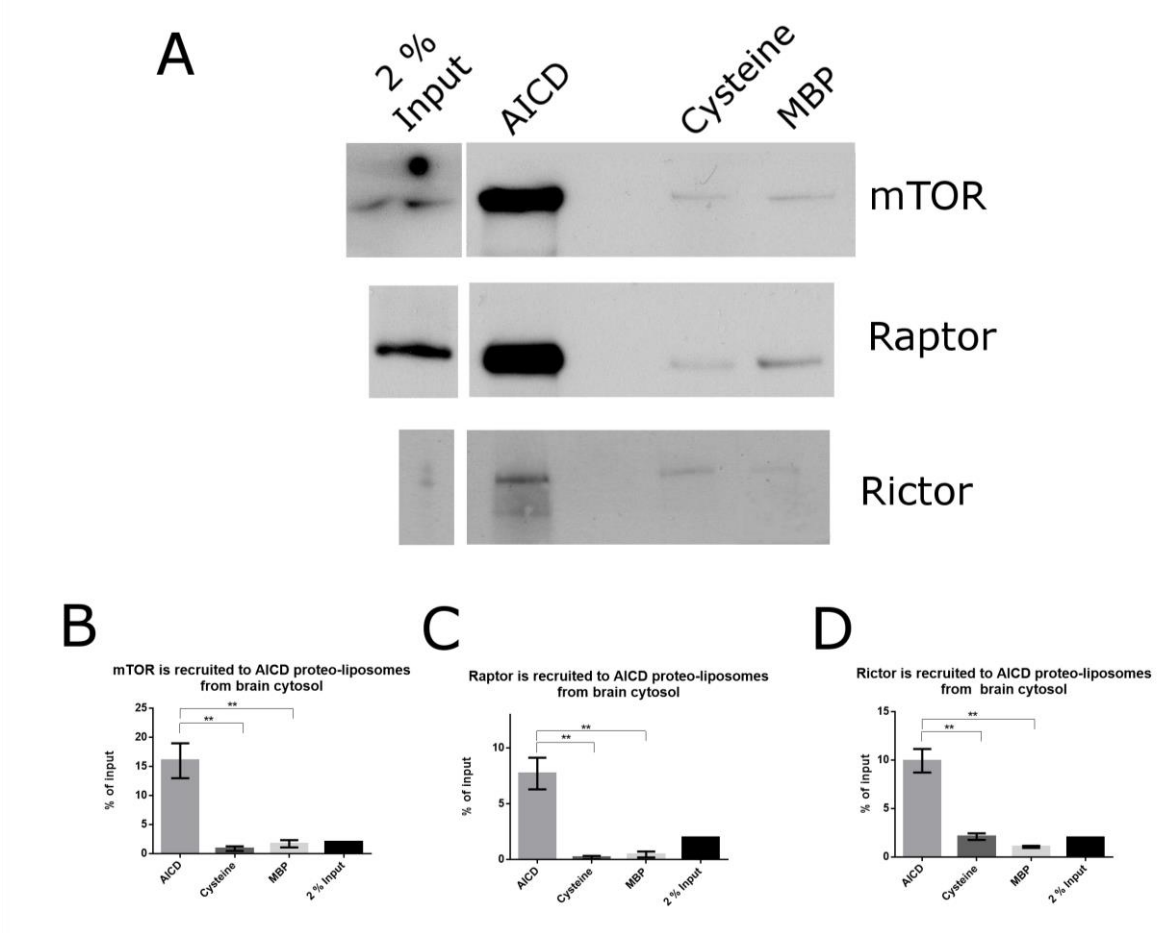

Figure 16. The mTOR kinase and the mTOR complex subunits Raptor and Rictor interact with the intracellular domain of APP (AICD). *(A) Proteo-liposome recruitments were analysed by SDS-PAGE and western blotting for mTOR and the subunits Raptor and Rictor (see 2.1.3 for the antibodies used). (B, C, D) mTOR, Raptor and Rictor were significantly recruited from brain cytosol onto proteo-liposomes containing coupled AICD compared to control liposomes (Cysteine and MBP). Densitometry analysis was conducted in ImageJ. The area obtained was expressed as a percentage of the area corresponding to the input. Statistical analysis was carried out in Graphpad Prism 6.0 using a one way ANOVA with a Tukey's post hoc test. (** $p \leq 0.01$) (n = 5).*

3.2.3 mTOR directly binds to AICD via its C-terminal kinase domain.

The mTOR complex is selectively recruited onto AICD presenting proteo-liposomes, demonstrating an interaction between the two proteins (3.2.2).The next stage was to determine if this observed interaction between AICD and mTOR was due to the direct binding to each other or was it mediated via other proteins? In order to conclude whether this interaction is direct, the recruitment method was modified. In previous recruitments pig brain cytosol acted as a protein reservoir for the recruitment. However, it does not allow for the determination of whether any interaction observed is direct, as the pig brain cytosol contains other proteins that could help mediate the interaction observed in figure 16. To overcome this, a pure source of protein was used instead of pig brain cytosol. Balklava et al. (under review A) created truncation mutants of mTOR and showed that the C-terminal mutant containing the kinase domain of mTOR was able to bind to AICD using affinity pull downs. To test this interaction using the proteo-liposome recruitment system the C-terminal kinase domain of mTOR (R1955-W2549) was expressed and purified in *E. coli* using the pET28 vector with an N-terminal MBP tag. Proteo-liposome recruitments were carried out, where AICD and control (cysteine) liposomes were incubated with two different amounts of the purified mTOR kinase domain (12 µg and 36 µg). The final recruitment samples were subjected to analysis by SDS-PAGE and western blotting using an antibody against mTOR (table 3). As shown in figure 17 the kinase domain of mTOR was selectively recruited onto AICD presenting proteo-liposomes, showing that the mTOR kinase domain is able to directly bind to AICD.

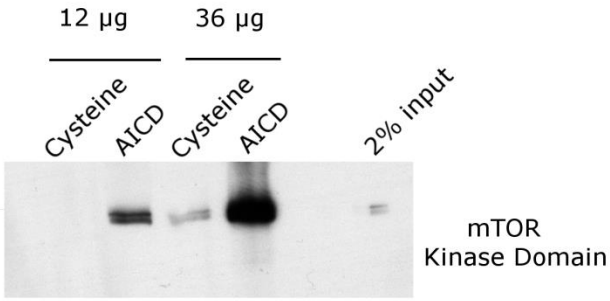

Figure 17. The Kinase domain of mTOR shows specific binding to the intracellular domain of APP (AICD). *AICD proteo-liposomes and control liposomes (cysteine) were incubated in 12 and 36 µg of purified recombinant mTOR Kinase domain (R1955-W2549). The recruitment samples were analysed by SDS-PAGE and western blotting for mTOR. The specificity of the kinase domain binding to AICD proteo-liposomes suggests that the interaction between AICD and the mTOR kinase domain is direct. (n=3)*

3.2.4 The 1st 10 N-terminal amino acids of AICD are crucial for mediating its interaction with mTOR.

Proteo-liposome recruitments have shown that mTOR is able to directly bind to AICD via its C-terminal kinase domain. The proteo-liposome recruitment method was modified further to allow for the determination of important interaction motifs on the intracellular domain of receptors. The interaction between AICD and mTOR was used as a model, whereby AICD was investigated for motifs that mediate its interaction with mTOR. This was achieved by using proteo-liposome recruitments and two different truncation mutants of AICD (Figure 18A). The mutant AICD truncation 1 (Tr1) contains the first 10 N-terminal amino acids of AICD only. In the AICD truncation 4 (Tr4) mutant the 1st 10 N-terminal amino acids of AICD are deleted. These truncation mutants were designed to split AICD into motifs that are most likely to mediate the interaction with mTOR. Figure 18D shows the potential AICD interaction motifs. Truncation 1 was created to single out the YTSI motif of AICD and truncation 4 was created as it has truncation 1 deleted.These AICD truncations were expressed and purified in *E.coli* (methods 2.2.2.1). Proteo-liposome recruitment experiments were undertaken, in

which AICD and the truncations 1 and 4 were coupled to liposomes along with MBP and cysteine (negative controls). These liposomes were incubated in pig brain cytosol and then isolated by sucrose density centrifugation. The final liposome pellet was subjected to SDS-PAGE and western blotting using an antibody against mTOR (Figure 18B). The western blots obtained showed that mTOR was significantly recruited to AICD liposomes and not to control liposomes (MBP or cysteine) (Figure 18C). mTOR was also significantly recruited onto liposomes containing Tr1, but not liposomes containing Tr4 (Figures 18B and C). This indicates that mTOR is recruited to the first 10 N-terminal amino acids of AICD. These results show that it is possible to use the proteo-liposome recruitment system to analyse interaction interfaces between proteins, through the use of truncated intracellular domains of membrane proteins.

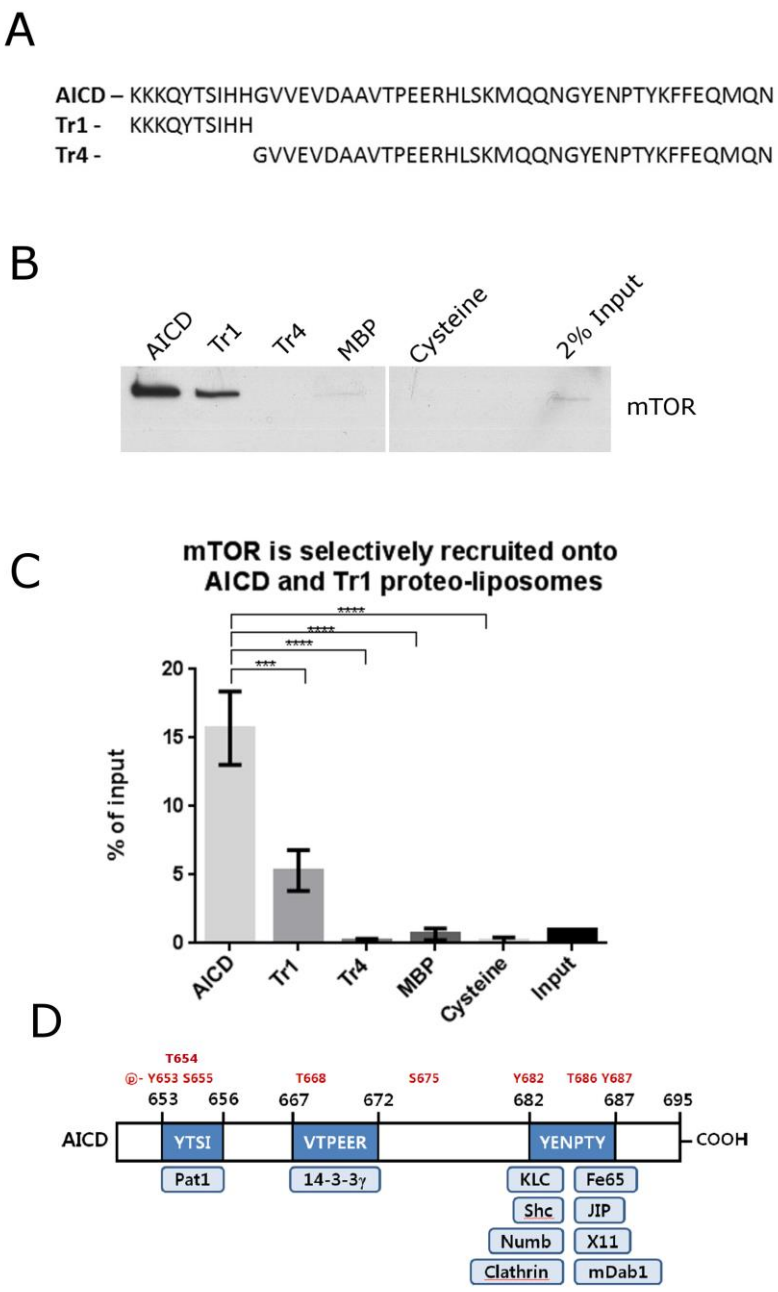

Figure 18. The 1st N-terminal 10 amino acid residues of AICD are able to mediate mTOR recruitment. *(A) The amino acid sequence of full length AICD, the truncation mutant Tr1 and the deletion mutant Tr4 used in the recruitment. (B) A representative western blot of a proteo-liposome recruitment in which AICD, Tr1, Tr4 and controls (MBP and cysteine) were coupled to liposomes and incubated in pig brain cytosol. The first 10 amino acids of AICD (Tr1) are needed to mediate the interaction between AICD and mTOR. (C) Densitometry analysis of B. Analysis was conducted using ImageJ. The area was expressed as a percentage of the area corresponding to the input band. Statistical analysis was carried out using a one-way analysis of variance (ANOVA) with a Tukey's post hoc test in Graphpad Prism 6.0 (*** $p \leq 0.001$, ** $p \leq 0.01$).(n=3). (D) Important known binding motifs and phosphorylation sites of AICD. The phosphorylation sites are shown in red and the binding motifs in blue, with the interacting proteins below (adapted from Chang (2010)).*

3.3 Discussion

3.3.1 The proteo-liposome recruitment system

This chapter focuses on the establishment and development of the proteo-liposome recruitment method for examining the interaction partners of the intracellular domains of membrane proteins. A similar liposome recruitment system has previously been used to examine the assembly of AP-1A protein coats onto liposomes containing the covalently coupled cytoplasmic tails of the gpI envelope glycoprotein of the *Varicella zoster* virus and the lysosomal integral membrane protein Limp II (Baust et al., 2006). In 2011 Pocha et al also used a liposome recruitment system to examine the trafficking of the apical determinant Crb2. They show that the intracellular domain of Crb2 interacts with the Vps35 subunit of the retromer complex required for mediating retrograde trafficking (Pocha et al., 2011). There were several major changes made to the proteo-liposome recruitment system in this chapter which have considerably advanced the method. The manipulation of the sucrose cushion used to isolate and purify the proteo-liposomes allowed for the detection of heavy, protein dense liposomes, which may have otherwise not been detected using the floatation gradient described by Pocha et al. (2011). This means that proteo-liposomes that have recruited a large number of interaction partners, and interaction partners consisting of large protein complexes, are not excluded from analysis due their inability to float to the top of the sucrose gradient.

The proteo-liposome recruitment method was modified to allow for the detection of direct binding. Previously the proteo-liposome recruitment method has been used to isolate binding partners from cytosol samples (Baust et al., 2006, Pocha et al., 2011). This technique allows for the detection of both direct interaction partners and interaction partners mediated via other proteins, known as indirect interaction partners, however it does not discriminate between direct and indirect interactions. This is

advantageous when examining the complete interaction profile of the intracellular domain of a membrane protein, as an overall view of the interaction partners is generated. Through the use of purified recombinant protein, the proteo-liposome method was improved to allow for the detection of direct interaction partners. Therefore the proteo-liposome method can be used to gain an overall insight into the intracellular interactome of a membrane protein, and to directly target and examine specific interactions.

The proteo-liposome recruitment method was further developed to examine these specific interactions in more detail, in particular the discovery of binding motifs required for the interaction. The generation of truncated forms of AICD allowed for the identification of the mTOR binding site on AICD. The use of truncation mutants of a membrane proteins intracellular domain, allows for the detection of domains important for binding. To further develop the proteo-liposome recruitment method the resolving power of the system needs to be determined. For example, can the method detect differences in binding upon the manipulation of a single amino acid residue in the intracellular domain, and can it discriminate between several mutants each with a different single amino acid change?

3.3.2 The APP-mTOR interaction

Using the proteo-liposome recruitment system it has been established that AICD is able to interact with mTOR, with the N-terminal 10 amino acids of AICD, crucial for mediating this interaction. The use of the proteo-liposome recruitment method, modified in order to detect direct binding, showed that the C-terminal kinase containing domain of mTOR is able to directly bind to AICD. This work demonstrates an interaction between APP and mTOR through the N-terminus of AICD and mTOR's kinase domain. This raises interesting questions about the functional significance of this interaction. In work conducted by other members of the group (Balklava et al., under review A) it was shown that overexpressed mTOR and APP co-localise on late

endosomes and lysosomes in HeLa cells, with APP also co-localising with endogenous mTOR. This co-localisation was greatly decreased when cells were amino acid starved, consistent with the fact mTOR is known to dissociate from endosomes when cells are amino acid deprived (Sancak et al., 2008).

Balklava et al. (under review A) used the model organism *C. elegans* to determine that several mTOR dependent developmental processes, including germ line expansion, fat metabolism and autophagy are APL-1 sensitive. APL-1 is the *C. elegans* homologue, of APP and was required for mediating Rag-GTPase input into mTORC1 (Balklava et al., under review A). The findings of this chapter and work by Balklava et al. (under review A) raise a number of interesting questions. Firstly, how does the binding of mTOR to APP mediate the input by the Rag-GTPases? The mTOR activator Rheb is known to bind to the kinase domain of mTOR (Long et al., 2005). Therefore, could APP serve as an activator of mTOR through its interaction with mTOR's kinase domain, raising the possibility that a complex could exist between APP/APL-1, mTORC1 and the Rag-GTPases?

The binding of mTOR to APP could enhance the recruitment of mTOR to membranes. The membrane attachment of mTOR is crucial for the amino acid dependant activation of mTORC1 (Sancak et al., 2010). The activity of the Rag-GTPases and the Ragulator are required for the localisation of mTORC1 on late endosomes / lysosomes (Sancak et al., 2008, Sancak et al., 2010). If APP was involved in membrane attachment of mTOR, the loss of APP or its intracellular domain would limit membrane attachment, and consequently mTOR activation.

The findings of this chapter establish mTOR as a novel interaction partner of APP. This interaction of APP with mTOR has significant implications for Alzheimer's disease which will be discussed in chapter 7.

Chapter 4

The analysis of the AICD-PIKfyve complex interaction through the use of proteo-liposome recruitment

Chapter 4 – The analysis of the AICD-PIKfyve complex interaction through the use of proteo-liposome recruitment

4.1 Introduction

In chapter 3 the proteo-liposome recruitment method was established and utilised to examine the interaction between APP and the mTOR complex. In this chapter the same proteo-liposome recruitment method is used to examine the interaction of APP with the PIKfyve complex, identified from a screen of APP's interactome (Balklava et al., under review B). This not only examines the interaction between APP and the PIKfyve complex in more detail but also validates the proteo-liposome recruitment method for examining interactions of the intracellular domain of membrane proteins.

4.1.1 The interaction between the PIKfyve complex and APP

It is widely known that the intracellular trafficking of APP is important for its processing by secretases. APP traffics through the Golgi complex en route to the plasma membrane, where it is either rapidly released or internalised (Koo et al., 1996). A portion of internalised APP is recycled, however the majority is targeted to the lysosomes for degradation (Koo et al., 1996, Caporaso et al., 1994). APP is known to traffic between the plasma membrane, endosomes and the TGN (Burgos et al., 2010). APP traffics between sorting endosomes and the TGN, a process mediated by a trafficking complex known as the Retromer (Vieira et al., 2010).

The endosomal system is a key organelle in APP trafficking and processing. The amyloidogenic cleavage of APP mainly occurs in endosomes (Bhalla et al., 2012, Nixon et al., 2000). Endosomes are the ideal environment for BACE-1 activity which occurs at mildly acidic pH, and APP interacts with BACE-1 in the endocytic pathway (De Strooper et al., 2010, Kinoshita et al., 2003, Sannerud et al., 2011). The C-terminal fragments of APP, resulting from β-secretase cleavage, are produced in endosomes where they are further processed by γ-secretases (Rajendran et al., 2006, Kaether et al., 2006).

Endosomal dysfunction is thought to be key to the pathogenesis of Alzheimer's disease. It has been documented that abnormal endosomal morphology, and increased endosomal Aβ production are found in the brains of Alzheimer disease patients (Cataldo et al., 2000, Nixon et al., 2000). Deficiencies in several retromer components and retromer receptors such as SorL1, implicated in APP trafficking, have been identified in late onset Alzheimer's disease (Small et al., 2005, Muhammad et al., 2008, Lane et al., 2012). Neurones derived from the fibroblasts of patients with Alzheimer's disease, including those with presenilin mutations, have enlarged endosomes (Israel et al., 2012). The importance of endosomes to APP trafficking and Alzheimer's disease is also evident by the fact that the crucial endosomal lipid PI(3)P is deficient in brain samples from Alzheimer's disease patients, and also mouse models of Alzheimer's disease. Decreasing PI(3)P levels by targeting the class 3 PI 3-kinase VPS34 causes endosome enlargement and enhances APP processing (Morel et al., 2013). Given the role of the endosomal system in APP trafficking and Alzheimer's disease, it is therefore interesting that the PIKfyve complex, crucial for endosomal homeostasis, was identified in the interactome of APP's intracellular domain (AICD) (Balklava et al., under review B).

The PIKfyve complex is a trimeric protein complex consisting of the kinase PIKfyve, the scaffold protein Vac14 and the phosphatase Fig4, which together form a unique complex that tightly regulates the levels of the endosomal lipid $PI(3,5)P_2$ (Bonangelino et al., 2002, de Lartigue et al., 2009). $PI(3,5)P_2$ and the PIKfyve complex are required for the retromer dependant transport of cargo from the endosomes to the trans Golgi network (TGN), and are important for endosomal morphology and function (Zolov et al., 2012, Rutherford et al., 2006). $PI(3,5)P_2$ regulates the calcium permeability of late endosomes and lysosomes by binding to TRPML-1 (Sopjani et al., 2010). The levels of $PI(3,5)P_2$ are greatly reduced in loss of function mutations of the Fig4 and both Vac14 and PIKfyve knockout mutants in in mice. Loss of the PIKfyve complex, and therefore a reduction of $PI(3,5)P_2$ levels causes the accumulation of vacuoles within the cell, which are through to derive from the endosomal system (Jefferies et al., 2008, Zhang et al., 2007b, Zolov et al., 2012). These mice also show profound neurodegeneration which results in the perinatal death of the animals (Chow et al., 2007, Zhang et al., 2007b). Furthermore $PI(3,5)P_2$ regulates the late endosomal and lysosomal TRPML-1 calcium channel, defects in which lead to mucolipidosis type IV which is a form of lysosomal storage disease that causes profound neurodegeneration (Bach et al., 2010). In humans, mutations in the gene encoding the Fig4 phosphatase leads to the neurodegenerative diseases Charcot-Marie-Tooth syndrome and Amyotrophic Lateral Sclerosis (Chow et al., 2007, Chow et al., 2009).

The link between APP and the PIKfyve complex was selected from the AICD interactome data of Balklava et al. (under review B) for further investigation due to a number of factors. The crucial role played by the endosomal system in APP trafficking and Alzheimer's disease, and PIKfyve's importance in regulating endosomal homeostasis provide a basis for further study. APP's role in the neurodegenerative disorder Alzheimer's disease, and the neurodegeneration observed upon loss of the PIKfyve complex and $PI(3,5)P_2$, provide a second reason to further characterise the putative interaction between APP and the PIKfyve complex.

4.2 Results

4.2.1 The PIKfyve complex is selectively recruited to AICD presenting proteo-liposomes

The aim of this chapter is to investigate the interaction between APP and the PIKfyve complex observed by Balklava et al, (under review B) using the proteo-liposome recruitment system characterised and established in chapter 3.

To study the interaction between APP and the PIKfyve complex in more detail, proteo-liposome recruitments were conducted where the intracellular domain of APP (AICD) was coupled to liposomes along with the amino acid cysteine and MBP as negative controls. Cysteine and MBP were chosen as controls to show that any observed difference in the recruitment would be due to the presence of the AICD tail. These proteo-liposomes contained 1 mol% phosphatidylinositol-3-phosphate (PI(3)P), mimicking the natural membrane environment of PIKfyve, due to the fact that PI(3)P is located on the membranes of endosomes, and is recognised by the FYVE domain of PIKfyve. The proteo-liposomes were incubated in 900 µl of pig brain cytosol (16 mg/ml), and the final recruitment products were analysed by SDS-PAGE and Western, blotting using antibodies against Vac14 and PIKfyve (Figure 19A). The experiments showed that both Vac14 and PIKfyve were significantly recruited to AICD presenting proteo-liposomes compared to control liposomes (cysteine and MBP) (Figures 19B and 19C), demonstrating an interaction between APP and the PIKfyve complex.

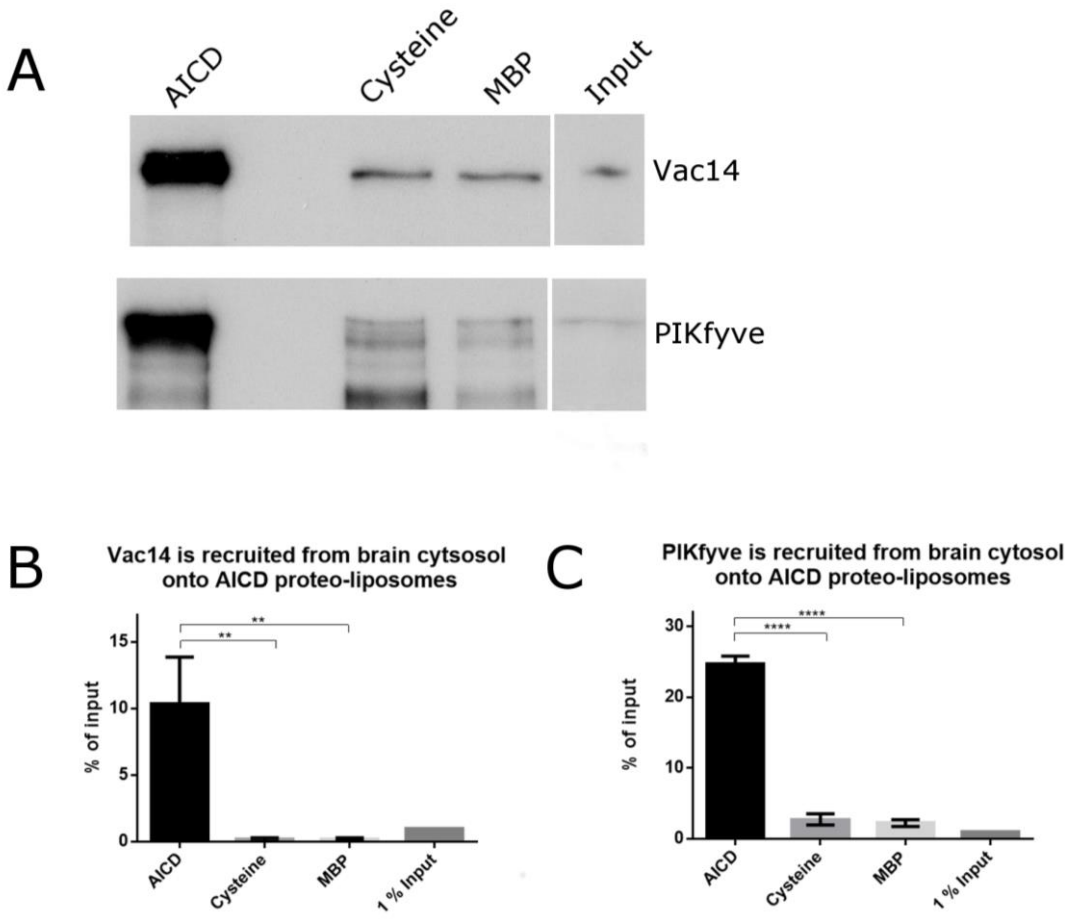

Figure 19. AICD presenting proteo-liposomes are able to recruit the kinase PIKfyve and the scaffold protein Vac14 of the PIKfyve complex.

*(A) A representative western blot of a proteo-liposome recruitment in which AICD , MBP (negative control) and cysteine (negative control) presenting liposomes were incubated in pig brain cytosol and probed for Vac14 and PIKfyve. (B and C) Densitometry analysis of the Vac14 and PIKfyve western blots. Analysis was conducted using ImageJ. The area was expressed as a percentage of the area corresponding to the input band. Statistical analysis was carried out using a one way ANOVA with a Tukey's post hoc test in Graphpad Prism 6.0 (**** $p \leq 0.001$, ** $p \leq 0.01$) (input = 1%) (n=4).*

4.2.2 Purified recombinant 6 x HIS tagged Vac14 binds directly to AICD proteo-liposomes

As shown in 4.2.1 AICD selectively recruits Vac14 and the kinase PIKfyve. The next stage in the investigation into this interaction was to determine whether the interaction between AICD and the PIKfyve complex is direct. To achieve this, the proteo-liposome system was modified through the use of purified protein rather than brain cytosol, allowing for the detection of direct binding partners. Proteo-liposome recruitments were conducted using recombinant Vac14, purified from and expressed in *E. coli* (Figure 20C). Vac14 was selected over the other components of the PIKfyve complex for several reasons. First Vac14 is able to be recombinantly expressed and purified, whereas producing recombinant, intact PIKfyve is much more of a challenge, due to its large molecular weight. Secondly Vac14 is the scaffold protein of the PIKfyve complex, and is primarily composed of HEAT repeats that provide docking sites for other proteins, therefore mediating protein-protein interactions (Jin et al., 2008). Therefore it is reasonable to think that Vac14 may provide the link between APP and the PIKfyve complex.

Proteo-liposome recruitments were conducted where AICD or control proteo-liposomes (cysteine) were incubated in 4 µg of 6 x HIS-Vac14. The amount of HIS-Vac14 to use was determined from pilot proteo-liposome recruitment experiments where AICD liposomes and controls were incubated in several different amounts of purified HIS-Vac14. 4 µg of HIS-Vac14 was selected as it gave a good signal in western blotting, without saturation, and the liposomes were in excess of HIS-Vac14. The proteo-liposomes contained 1 mol% PI(3)P to mimic the composition of the membranes PIKfyve is recruited to. The recruitments were analysed by SDS-PAGE and Western blotting for Vac14. Vac14 was significantly enriched on AICD containing liposomes compared to control liposomes (cysteine) (Figures 20A and 20B), demonstrating that

Vac14 directly binds to AICD. This establishes that Vac14 mediates the interaction between APP and the PIKfyve complex, via AICD.

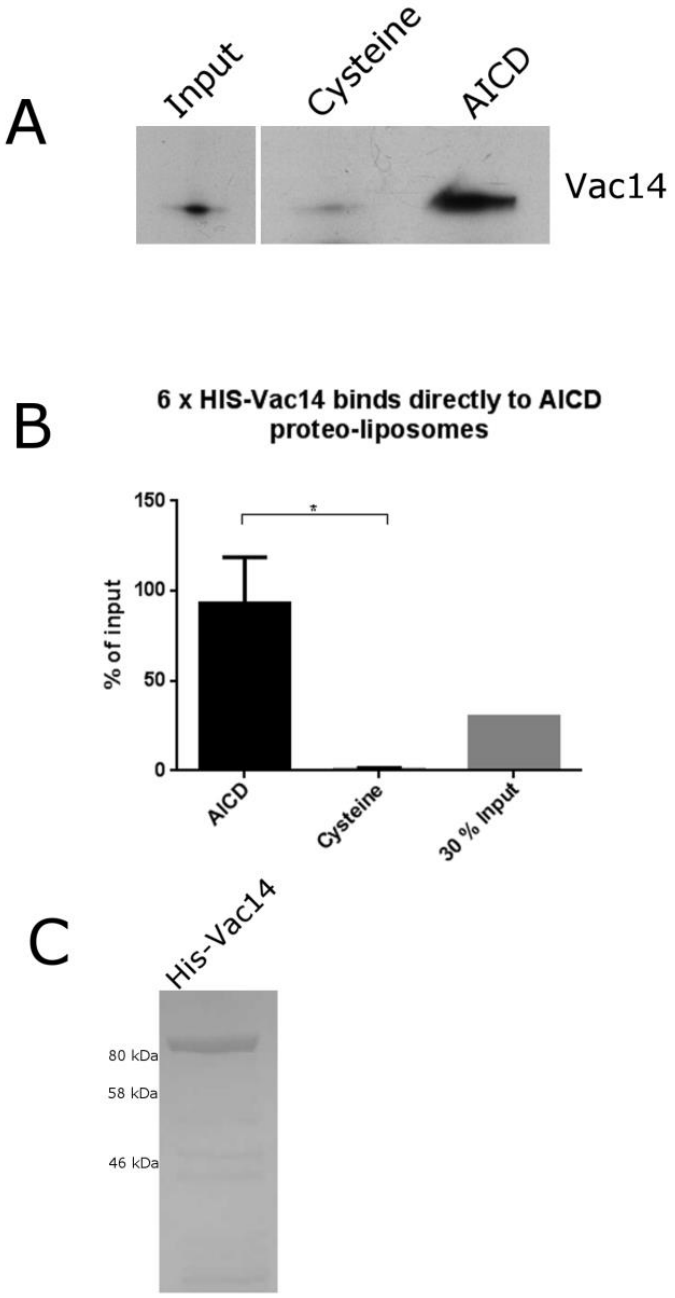

Figure 20. Purified recombinant Vac14 is able to directly bind to AICD presenting proteo-liposomes.

(A) A western blot of a proteo-liposome recruitment where AICD and control (cysteine) liposomes were incubated in 4 µg of purified recombinant 6 x HIS-Vac14. The western blot was probed with an antibody against Vac14 (2.1.3). (B) Densitometry analysis of (A). Analysis was conducted using ImageJ. The area was expressed as a percentage of the area corresponding to the input band. Statistical analysis was carried out using a two-tailed unpaired T-test with a 95 % confidence interval in Graphpad Prism 6.0 ($p \leq 0.05$) (input = 30%)(n=3).(C) Coomassie stained SDS-PAGE of purified His-Vac14.*

4.2.3 The C-terminus of AICD is crucial for the recruitment of the PIKfyve complex

The next stage in the analysis of the interaction between APP and the PIKfyve complex was to examine AICD for domains important for the recruitment of the PIKfyve complex. This was achieved through the use of four truncation mutants of AICD. A representation of these truncations can be seen in figure 21A. AICD and its truncations were expressed in and purified from *E. coli*. Proteo-liposome recruitments were conducted where AICD and its truncations 1-4 were coupled to liposomes and incubated in 900 µl of pig brain cytosol (16 mg/ml). For these experiments PI(3)P was excluded from the liposomes to make sure that the choice of receptor tail (AICD or truncations 1-4) was the limiting factor in the recruitment, rather than PI(3)P binding by PIKfyve. The final recruitment products were analysed by SDS-PAGE and Western blotting for Vac14 and PIKfyve. Figure 21B shows a representative western blot of the final recruitment products. Consistent with previous data both Vac14 and PIKfyve were significantly enriched on AICD liposomes compared to controls (Figures 21B, 21C and 21D). Vac14 and PIKfyve were also significantly recruited to AICD truncation 4 (Tr4) compared to controls and truncations 1-3 (Figures 21B, 21C and 21D). This indicated that the C-terminal 7 amino acids may be important for this interaction, therefore demonstrating that the C-terminus of AICD is required for the recruitment of the PIKfyve complex from brain cytosol.

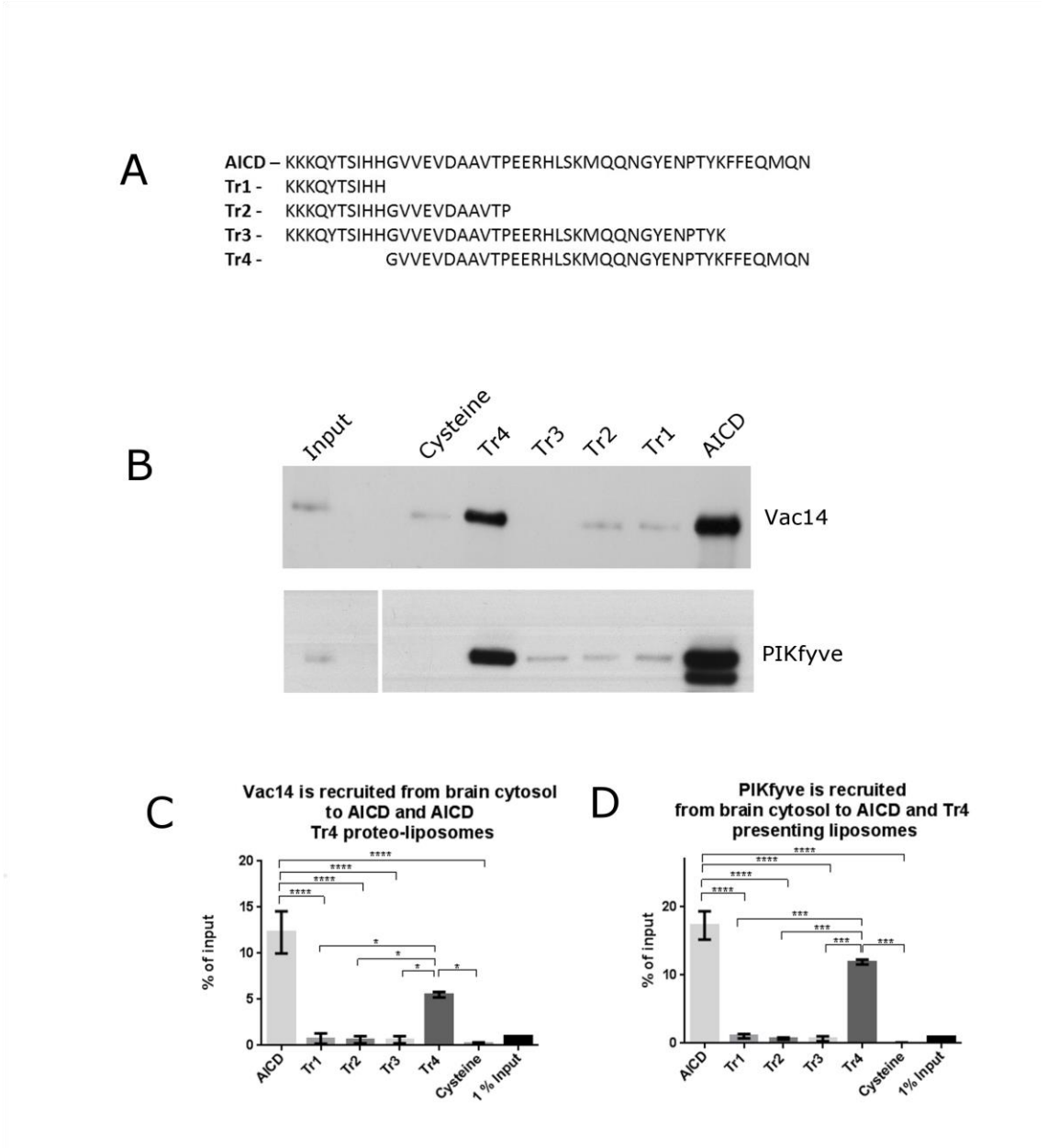

Figure 21. The C-terminus of AICD is important in the interaction between AICD and the PIKfyve complex.

(A) A representation of the amino acid sequence of the AICD truncation mutants used in (B). (B) Western blot analysis of a proteo-liposome recruitment in pig brain cytosol where AICD, truncations 1-4 (Tr) and cysteine (control) were coupled to liposomes. AICD truncation 4 (tr4) is required for the recruitment of both Vac14 and PIKfyve. (C and D) Densitometry analysis of (B). Analysis was conducted using ImageJ. The area was expressed as a percentage of the area corresponding to the input band. Statistical analysis was carried out using a one way ANOVA with a Tukey's post hoc test with a 95% confidence interval in Graphpad Prism 6.0 ($p \leq 0.05$, *** $p \leq 0.001$. **** $p \leq 0.0001$) (input = 1%) (n=4).*

4.2.4 The C-terminus of AICD is needed for the direct binding of recombinant 6 x HIS-Vac14

As shown in figure 21 the C-terminus of AICD was important in the recruitment of Vac14 and PIKfyve from brain cytosol. As Vac14 is able to directly bind to AICD (Figure 20), the interaction of 6 x HIS-Vac14 with AICD and its truncations (1-4) (Figure 22C) was examined. Proteo-liposomes containing coupled AICD and the AICD truncations 1-4 were incubated in 4 µg of 6 x HIS-Vac14. PI(3)P was excluded from the liposomes so that the cytoplasmic tails were the limiting factor in the binding, and not PIKfyve binding to PI(3)P. The recruitment samples were subjected to SDS-PAGE and Western blot analysis, using an antibody against Vac14. Vac14 is significantly and directly recruited to AICD proteo-liposomes (as seen previously) (Figures 22A and 22B). Vac14 directly interacted with the truncations 2, 3 and 4, with its recruitment to Tr3 and Tr4 deemed significant from densitometry analysis. This result differs when compared to recruitments conducted using brain cytosol, where Vac14 was only recruited to Tr4, and not Tr3 liposomes.

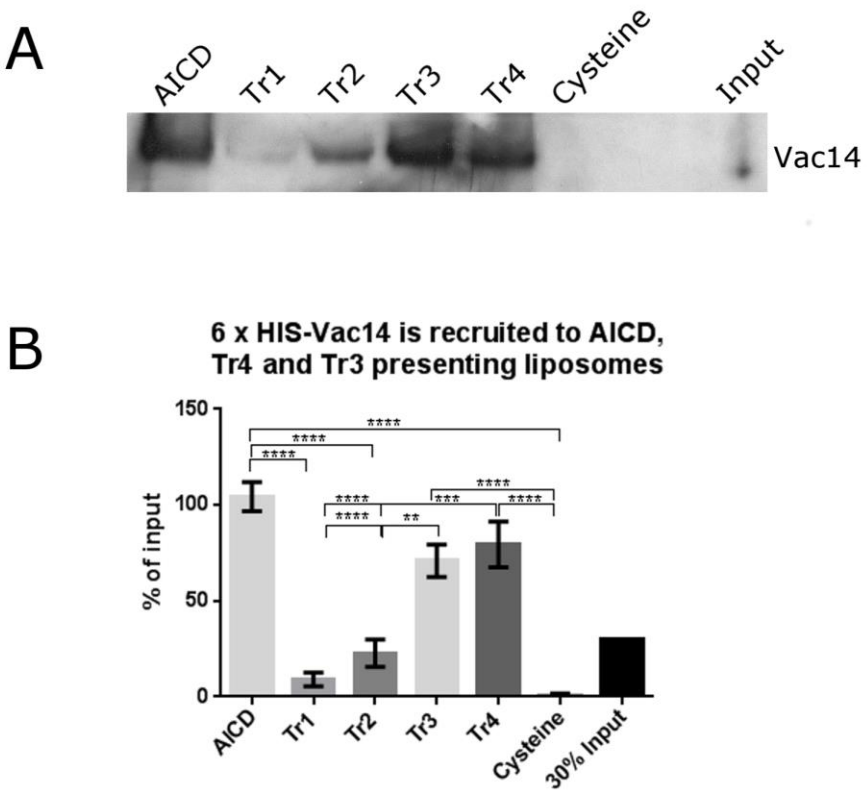

Figure 22. The C-terminus of AICD is required for the direct binding of purified recombinant Vac14.

*(A) A representative western blot of a proteo-liposome recruitment in which AICD, AICD truncation presenting and control (cysteine) liposomes were incubated in 4 µg of purified recombinant 6 x HIS-Vac14 (input = 1%). (B) Densitometry analysis of (A). Analysis was conducted using ImageJ. The area was expressed as a percentage of the area corresponding to the input band. Statistical analysis was carried out using a one way ANOVA with a Tukey's post hoc test with a 95% confidence interval in Graphpad Prism 6.0 (** $p \leq 0.01$, *** $p \leq 0.001$, **** $p \leq 0.0001$)(n=4). (C) A representation of the amino acid sequence of the AICD truncation mutants used in (A).*

4.3 Discussion

This chapter further establishes the use of the proteo-liposome recruitment system for examining the interaction partners of the intracellular domains of membrane proteins, by studying the interaction of AICD with a second protein complex PIKfyve. Therefore the proteo-liposome recruitment method has been used successfully to examine the interaction of AICD with two different protein complexes, mTOR and PIKfyve. The PIKfyve complex was recruited to AICD proteo-liposomes demonstrating and interaction between the two. Using the proteo-liposome system with purified protein it was shown that the Vac14 subunit of the PIKfyve complex binds directly to AICD, likely mediating the interaction between APP and the PIKfyve complex.

Using proteo-liposome recruitments in brain cytosol it was established that the AICD-Tr4 mutant, which lacks the first 10 N-terminal amino acids, was able to recruit both Vac14 and PIKfyve whereas the other three AICD mutants (Tr1-3) did not recruit Vac14 or PIKfyve (Figure 21). When purified recombinant Vac14 was used in the recruitments, it bound directly to both the AICD-Tr4 mutant and the AICD-Tr3 mutant, which lacks the last 7 C-terminal amino acids. This difference in recruitment between the different proteo-liposome recruitment methods (brain cytosol and purified recombinant Vac14) may be due to a number of factors. One explanation for this is that Vac14 is most likely in complex with Fig4 and/or PIKfyve in brain cytosol. The assembly of the PIKfyve complex is known to cause a conformational change in its components (Ikonomov et al., 2009a). The Fig4 and PIKfyve subunits of the PIKfyve complex are not present in purified recombinant Vac14 samples; therefore the binding site on AICD for Vac14 may differ depending on whether it is in complex with Fig4 and PIKfyve, as in brain cytosol samples, or in purified recombinant Vac14, which should not contain other components of the PIKfyve complex.

APP contains several phosphorylation sites in its intracellular domain, and the phosphorylation state of AICD is known to affect its binding to other proteins such as Fe65 (Borg et al., 1996, Oishi et al., 1997, Schettini et al., 2010). The brain cytosol used for the proteo-liposome recruitments is likely to contain kinases and some ATP, which could alter the phosphorylation state of the AICD coupled to liposomes. Purified recombinant Vac14 should not contain any kinases or ATP, therefore AICD should not be phosphorylated. This potential phosphorylation of AICD may account for the differing recruitment results between the use of brain cytosol and purified recombinant Vac14. Another factor that may be involved is the enrichment of Vac14. Brain cytosol would not be as enriched in Vac14 when compared to purified recombinant Vac14. This needs to be taken into consideration when interpreting the results of the proteo-liposome recruitments. The recruitments in brain cytosol and purified Vac14 demonstrate that the C-terminal half of AICD is required for its interaction with the PIKfyve complex.

The biochemical analysis of the APP-PIKfyve complex interaction demonstrates that the two proteins interact via the scaffold protein Vac14. This poses the question; what is the functional relevance of this interaction? Balklava et al. (under review B) used the model organism *C. elegans* to examine the functional significance of the interaction between APL-1 (APP), PPK-3 (PIKfyve) and vacl-14 (Vac14). APL-1 yn5 mutants, lacking the intracellular domain, show hypodermal vacuolation. Hypodermal vacuolation is also observed in both PPK-3 partial loss of function mutant animals and vacl-14 deletion mutant animals. APL-1 (yn5) mutant combined with a PPK-3 partial loss of function mutant increases the amount of vacuolation observed, and the combination of both mutations is synthetically lethal (Balklava et al., under review B). This demonstrates that APL-1 acts upstream of PPK-3 and controls both endosomal and lysosomal homeostasis, and neuronal function in *C. elegans.*

The results of this chapter and the work of Balklava et al. (under review B) allows for the construction of a model whereby APP, up on arrival at endosomes, interacts with and activates the PIKfyve complex by binding to Vac14 causing the stimulation of endosome to TGN trafficking and endosome/lysosome fusion. This model leads to a number of questions. Firstly, what is the significance of the APP-PIKfyve interaction in terms of the levels of $PI(3,5)P_2$? Is the relationship between APP and the PIKfyve complex the same in mammals and humans as observed in *C. elegans?* What is the importance of this interaction as regards the trafficking of APP?

Chapter 5

Functional analysis of the interaction between APP and the PIKfyve complex

Chapter 5- Functional analysis of the interaction between APP and the PIKfyve complex

5.1 Introduction

The results of chapter 4 demonstrate that the PIKfyve complex interacts with the intracellular domain of APP (AICD) biochemically, via the Vac14 subunit of the PIKfyve complex. This chapter investigates the functional significance of this interaction. In order to determine what effect APP has on the PIKfyve complex it is necessary to examine the activity of the complex in response to APP. Examining the product of the reaction catalysed by the PIKfyve complex is one way to determine the effect of APP on PIKfyve. In this case the product would be the production of the endosomal lipid $PI(3,5)P_2$.

5.1.1 Measuring $PI(3,5)P_2$ levels

Up until recently there have been two main ways of measuring the levels of $PI(3,5)P_2$, both involving the use of radioactive isotopes with a combination of thin layer chromatography (TLC) and high-performance liquid chromatography (HPLC), or both. The first way is to examine the incorporation of tritium [^{3}H] labelled inositol into cells grown in myo-inositol depleted media (Dove et al., 1997). The second way is to measure the incorporation of radioactive phosphate [^{32}P] into cells grown in phosphate free media. The lipids then need to be extracted and de-acetylated, and the level of phosphoinositides can then be measured by HPLC and scintillation counting, by comparison with standards. $PI(3,5)P_2$ levels have been measured using both tritium (Dove et al., 1997, Rudge et al., 2004, McCartney et al., 2014b, Bonangelino et al., 2002, Cai et al., 2013, Jin et al., 2014) and ^{32}P (Zhang et al., 2007b, Nicot et al., 2006,

Jefferies et al., 2008). While this method has several advantages it also has some disadvantages. The first being the low abundance of $PI(3,5)P_2$ can make it difficult to detect (Zhang et al., 2007b). The second disadvantage is that it requires the use of radiolabeling and access to a HPLC. The number of laboratories that have access to a HPLC machine available for use with radionuclides is in decline. The use of radionuclides severely limits the measurement of phosphoinositides in difficult samples, such as animal and human tissue. More recently techniques that do not require the use of radionuclides have been used, such as mass spectrometry (Wakelam and Clark, 2011, Kielkowska et al., 2014). Whilst overcoming the use of radionuclides it can be difficult to analyse different phosphoinositide species using mass spectrometry as it does not take into account the phosphorylation position on the inositol ring even though the phosphorylation is detected. The low cellular concentrations of phosphoinositides compared to other phosphor lipids and their highly charged head groups that affect their solubility all complicate the analysis of phosphoinositides by mass spectrometry (Wakelam and Clark, 2011). Recent advances into the use of phosphoinositide specific probes could overcome some of the disadvantages of using radionuclides.

5.1.2 Phosphoinositide specific probes

Recent advances in the analysis of phosphoinositide binding proteins have led to the characterisation of phosphoinositide binding domains with distinct affinities and specificities (Cullen et al., 2001). These binding domains have been utilised to study the dynamics of phosphoinositides in cells by fusing GFP or a GFP variant to the relevant binding domain and analysis by microscopy. There are now a number of florescent probes for specific phosphoinositides. Examples of these probes include the pleckstrin homology (PH) domain of phospholipase C, and more recently the Tubby domain as $PI(4,5)P_2$ probes (Szentpetery et al., 2009). The PH domain of FAPP1 (four phosphate adaptor protein) has been used as a probe for PI(4)P. The PH domains of

Akt are probes for PI(3,4)P_2 and PI(3,4,5)P_3, and the FYVE domain of the early endosome antigen 1 (EEA1) is a probe for PI(3)P (Halet, 2005, Balla, 2007). Until recently a protein probe did not exist for PI(3,5)P_2, mainly due to the lack of well characterised PI(3,5)P_2 effectors, and PI(3,5)P_2's low abundance (Li et al., 2013).

5.1.3 A PI(3,5)P_2 probe?

One of the most well characterised PI(3,5)P_2 effectors is the yeast protein ATG18 (also called Svp1). It was identified as a PI(3,5)P_2 effector by Dove et al. (2004) in a screen of *Saccharomyces cerevisiae* mutants that displayed a swollen vacuole phenotype, like that associated with the Fab1 (yeast homologue of PIKfyve) mutant. They also showed that ATG18p is able to bind specifically to PI(3,5)P_2. ATG18p is a component of the autophagic and the cytosol to vacuole transport pathways (Cvt) in yeast (Efe et al., 2007) and is related to the WIPI proteins in mammals (Proikas-Cezanne et al., 2007). It is a multi WD domain containing protein that is predicted to fold into a beta barrel. It does not display a specific PI(3,5)P_2 binding motif, instead it is thought that the whole beta barrel plays a role in PI(3,5)P_2 binding with the FRRG^{287} motif to be the most likely candidate for a specific motif (Dove et al., 2004, Krick et al., 2006).

This chapter utilises the work of Dove et al. (2004) to examine the use of ATG18p as a probe for PI(3,5)P_2, with a view to investigating the functional significance of the interaction between APP and the PIKfyve complex, by the analysis of PIKfyve activity in response to APP.

5.2 Results

5.2.1 ATG18 binds preferentially to PI(3,5)P2 containing liposomes

In order to examine whether ATG18p would be a suitable probe for $PI(3,5)P_2$ a liposome binding assay was carried out. GST tagged ATG18p (a kind gift from Scott Emr) was expressed and purified from *E. coli* as described in chapter 2 (2.2.2.4). Liposomes were prepared as described in chapter 2 (2.2.3.2) with a final lipid amount of 252.5 nmol, which is half the amount of lipid used for previous recruitments (505 nmol). Seven sets of liposomes were prepared containing either 3 mol% PI, 3 mol% PI(3)P, 3 mol% $PI(3,5)P_2$ or 3 mol% $PI(4,5)P_2$. Control liposomes either did not contain any phosphoinositide (No PIs) or were composed entirely of PC (PC only). The different sets of liposomes were incubated with GST-ATG18 at a final concentration of 4.5 µM for 30 minutes at 25ºC. The liposomes were pelleted and the samples analysed by SDS-PAGE and Western blotting using an antibody against the GST tag of ATG18p. GST-ATG18 bound significantly ($p \leq 0.01$) to $PI(3,5)P_2$ containing liposomes compared to those containing other phosphoinositides and control liposomes, which did not bind significant amounts of GST-ATG18 (Figure 23A and 23B). This indicates that ATG18p could be used as a $PI(3,5)P_2$ specific probe.

The next stage was to determine if ATG18 could be used as an intracellular probe for $PI(3,5)P_2$. ATG18p was PCR cloned into pEYFP-c1. HeLa cells were transfected with pEYFP-ATG18-c1 using multiple transfection methods including lipofectamine 2000 and PEI. The transfected cells were analysed by confocal microscopy. However, it appeared that YFP-ATG18 was not expressed in HeLa cells. This was repeated multiple times using both HeLa and HEK-293t cells and no YFP-AGT18 fluorescence was visible, indicating that the construct does not express in these cell lines.

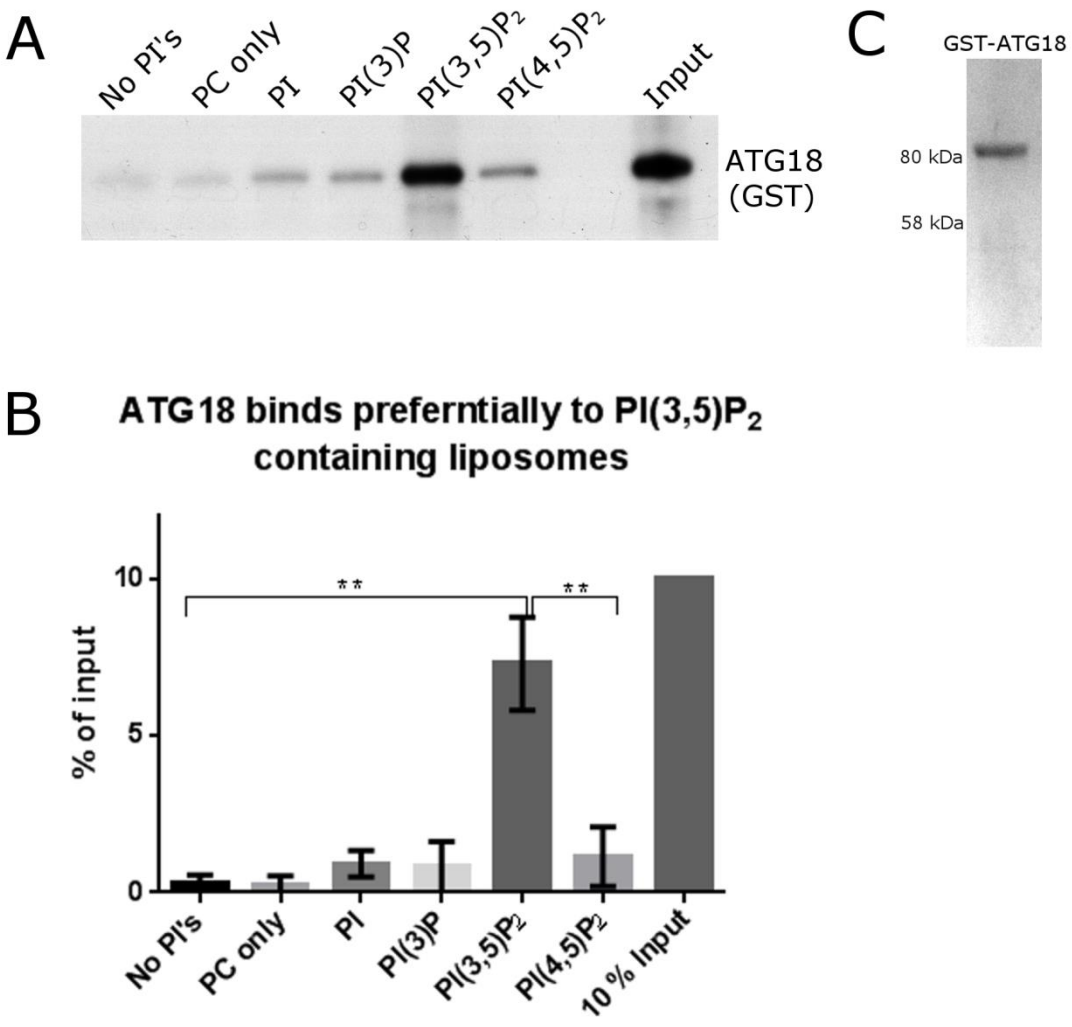

Figure 23. ATG18 binds to PI(3,5)P_2 containing liposomes.
*(A) Liposomes were prepared containing either 3 mol% PI(3)P, 3 mol% PI(3,5)P_2, 3 mol% PI(4,5)P_2 or without any inositol containing lipid (No PI's and PC only) and incubated with GST tagged ATG18 at a final concentration of 4.5 µM. The samples were analysed by SDS-PAGE and western blotting using an antibody against the GST tag on ATG18. (B) Densitometry analysis of (A) was conducted using ImageJ. The area was expressed as a percentage of the area corresponding to the input band. Statistical analysis was carried out using a one –way ANOVA in Graphpad Prism 6.0 (** $p \leq 0.01$) (input = 10%) (n=3). (C) Commassie stained SDS-PAGE of purified recombinant GST-ATG18.*

Whilst attempting to express YFP-ATG18 in both HeLa and HEK-293t cells a paper was published that described the development of a $PI(3,5)P_2$ probe. Li et al. (2013) produced a $PI(3,5)P_2$ specific probe from the $PI(3,5)P_2$ binding domain of the late endosome/lysosome calcium channel TRPML-1. The probe involved the fusion of a fluorescent tag to tandem repeats of the $PI(3,5)P_2$ binding domain of TRPML-1, which is known as ML1N. The probe primarily localised to LAMP-1 positive structures and this localisation was disrupted by mutating the probe and by the genetic and pharmacological inhibition of the PIKfyve complex, thereby reducing cellular $PI(3,5)P_2$ levels. This probe allows the detection of $PI(3,5)P_2$ in a spatially defined way that has not previously been possible. Due to the fact this ML1Nx2 probe was well characterised by Li et al. (2013) and that YFP-ATG18 would not express successfully in HeLa or HEK-293t cells, the ML1Nx2 probe was used to investigate the functional significance of the interaction between APP and the PIKfyve complex.

5.2.2 Pharmacological inhibition of PIKfyve abolishes the vesicular localisation of the $PI(3,5)P_2$ probe GFP-ML1Nx2

In order to use the ML1Nx2 probe to investigate the functional relevance of the APP-PIKfyve complex interaction the dynamics of the ML1Nx2 probe were examined by the pharmacological inhibition of PIKfyve. HeLa cells were transfected with pEGFP-c3-ML1Nx2 (kindly provided by Dr. H. Xu (University of Michigan)) using Lipofectamine 2000. The transfected cells were then treated with 4 µM of the PIKfyve inhibitor YM-201636 for 4 hours or DMSO (control), and fixed on glass coverslips with 4% PFA. Upon image analysis by confocal microscopy it was found that in control cells the probe GFP-ML1Nx2 localises to vesicular structures. The inhibition of the PIKfyve complex by YM-201636, and therefore the decrease in the levels of $PI(3,5)P_2$, caused this vesicular localisation to be abolished (Figure 24), as observed previously (Li et al., 2013). The remaining vesicular structures observed upon PIKfyve inhibition are likely

due to the incomplete inhibition of the PIKfyve complex and therefore the presence of low levels of $PI(3,5)P_2$ (Jefferies et al., 2008).

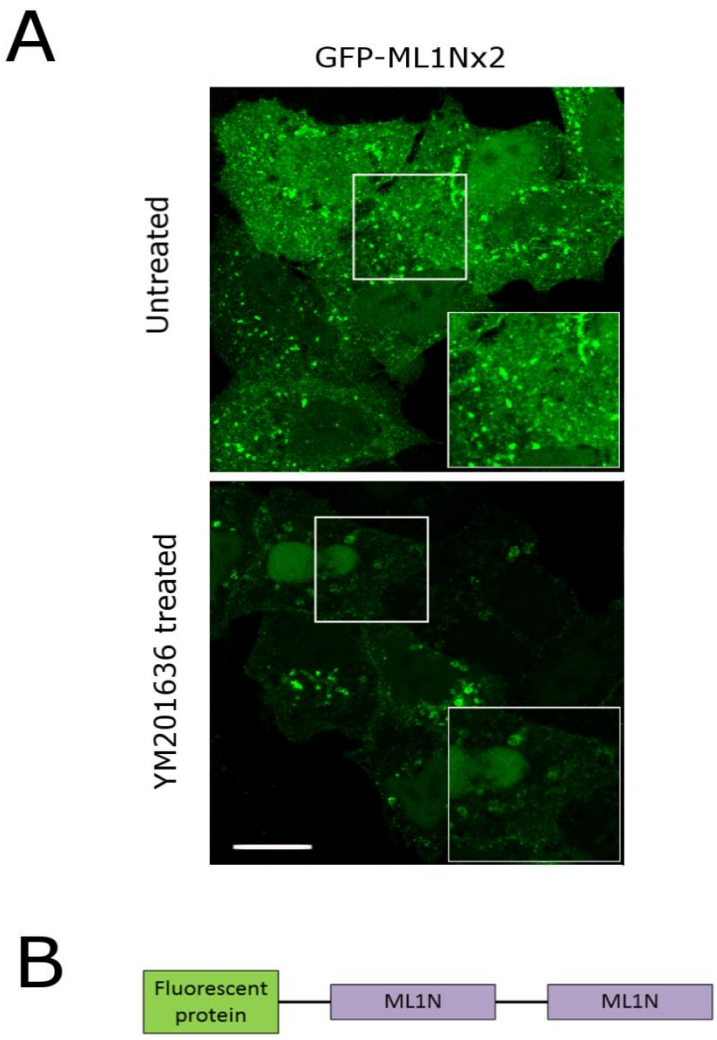

Figure 24. Treatment of HeLa cells with the PIKfyve inhibitor YM201636 abolishes the vesicular localisation of the $PI(3,5)P_2$ probe GFP-ML1Nx2.
(A) HeLa cells were transiently transfected with the $PI(3,5)P_2$ probe GFP-ML1Nx2 and then treated with 4 µM YM201636 for 4 hours. The vesicular localisation of GFP-ML1Nx2 is greatly decreased upon treatment with YM201636 (scale bar = 25 µm).The displayed image is the maximum projection of z-stacks taken at 0.5 µm increments. (B)The construct of the $PI(3,5)P_2$ probe GFP-ML1Nx2 (n=3).

5.2.3 The PI(3,5)P_2 probe shows co-localisation with Vac14 in fixed HeLa cells.

After establishing that the vesicular localisation of the probe GFP-ML1Nx2 is abolished upon PIKfyve inhibition the localisation of the probe and the PIKfyve complex were characterised. ML1Nx2 was PCR cloned from pEGFP-c3 into pMcherry-c1. HeLa cells were co-transfected with both mCherry-ML1Nx2 and mCitrine-Vac14 (kindly provided by Dr L. Weisman) or mCherry-ML1Nx2 and mCitrine (control) using lipofectamine 2000. The cells were fixed on glass coverslips with 4% PFA and imaged using confocal microscopy. Overexpressed mCherry-ML1Nx2 and mCitrine-Vac14 co-localise in HeLa cells (Figure 25A), indicating that Vac14 is present of PI(3,5)P_2 positive vesicular structures as detected using the probe mCherry-ML1Nx2. This was compared to the control transfected cells, where no co-localisation is observed (Figure 25B). This indicates that the PI(3,5)P_2 probe mCherry ML1Nx2 is localised to a similar location as that of the PIKfyve complex.

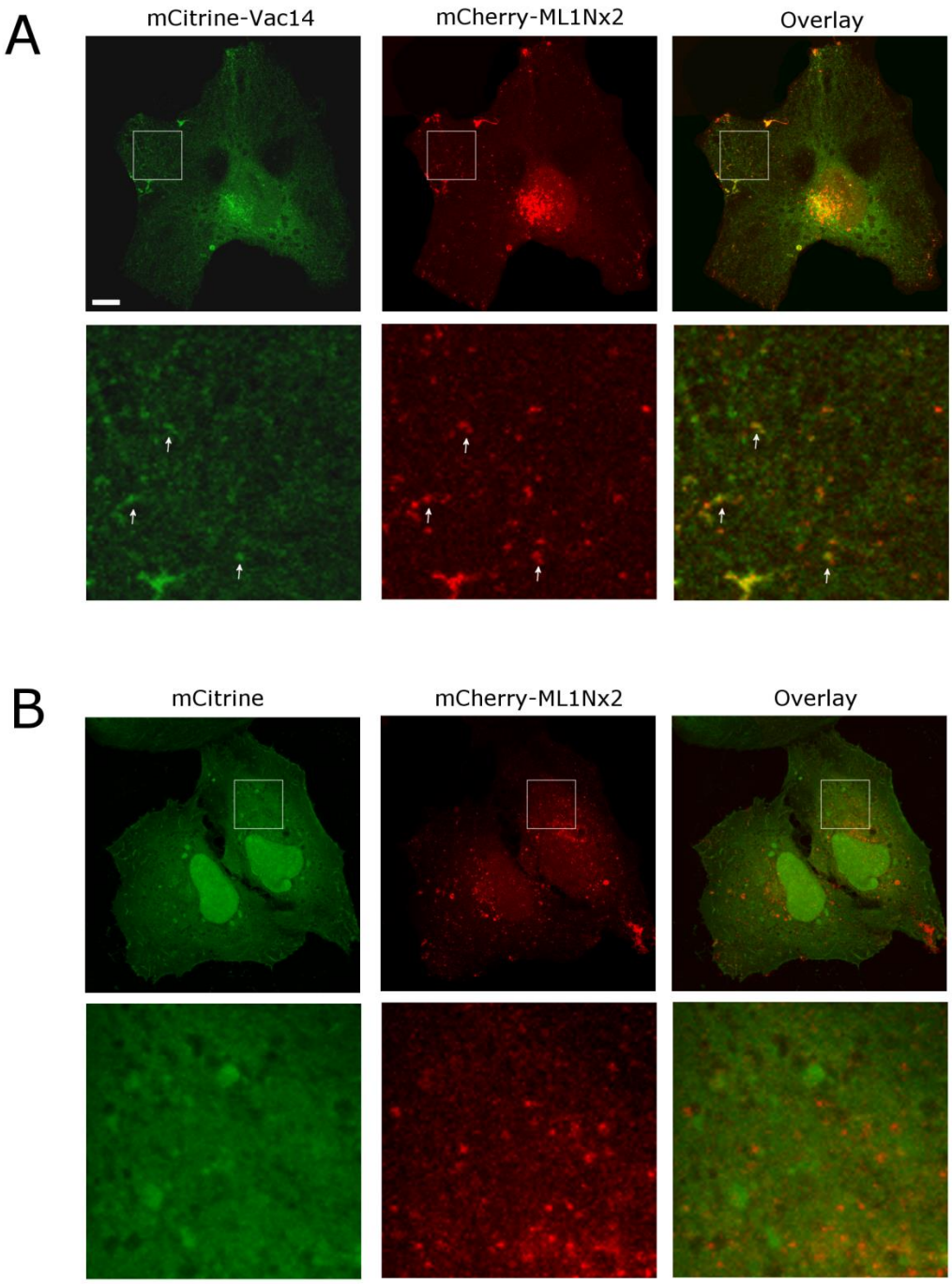

Figure 25. The PI(3,5)P_2 probe mCherry-ML1Nx2 and Vac14 co-localise in HeLa cells.

HeLa cells were co-transfected with mCherry-ML1Nx2 and mCitrine-Vac14 (A) or mCherry-ML1Nx2 and mCitrine (control) (B). There appears to be co-localisation of mCherry-ML1Nx2 and mCitrine-Vac14 as indiated by arrows in A. (scale bar = 10 µm) (n=3). The displayed image is the maximum projection of z-stacks, enlarged images are 5x.

5.2.4 APP and Vac14 co-localise and display co-movement in live HeLa cells

In chapter 4 the use of the proteo-liposome recruitment system demonstrated that the intracellular domain of APP (AICD) was directly bound by the Vac14 subunit of the PIKfyve complex. This led to the question; do Vac14 and APP co-localise in cells given their biochemical interaction? To investigate this Vac14 was cloned from pmCitrine into pmCherry. Live HeLa cells co-overexpressing a combination of mCherry-Vac14 with APP-GFP or GFP (control) were analysed by fluorescence microscopy for 30 seconds with 0.15 s between frames. APP-GFP and mCherry-Vac14 co-localise on vesicular strictures in HeLa (Figure 26A) compared to control cells overexpressing GFP (Figure 26B). APP-GFP and mCherry-Vac14 display co-movement on vesicular structures (Figure 26C). This demonstrates that APP-GFP resides on the same vesicular structures as mCherry-Vac14, which display co-movement, therefore suggesting that APP resides on the same vesicular structures as the PIKfyve complex. This further supports the recruitment results in chapter 4 by demonstrating that the biochemical interaction between APP and the PIKfyve complex in chapter 4 is likely physiologically relevant.

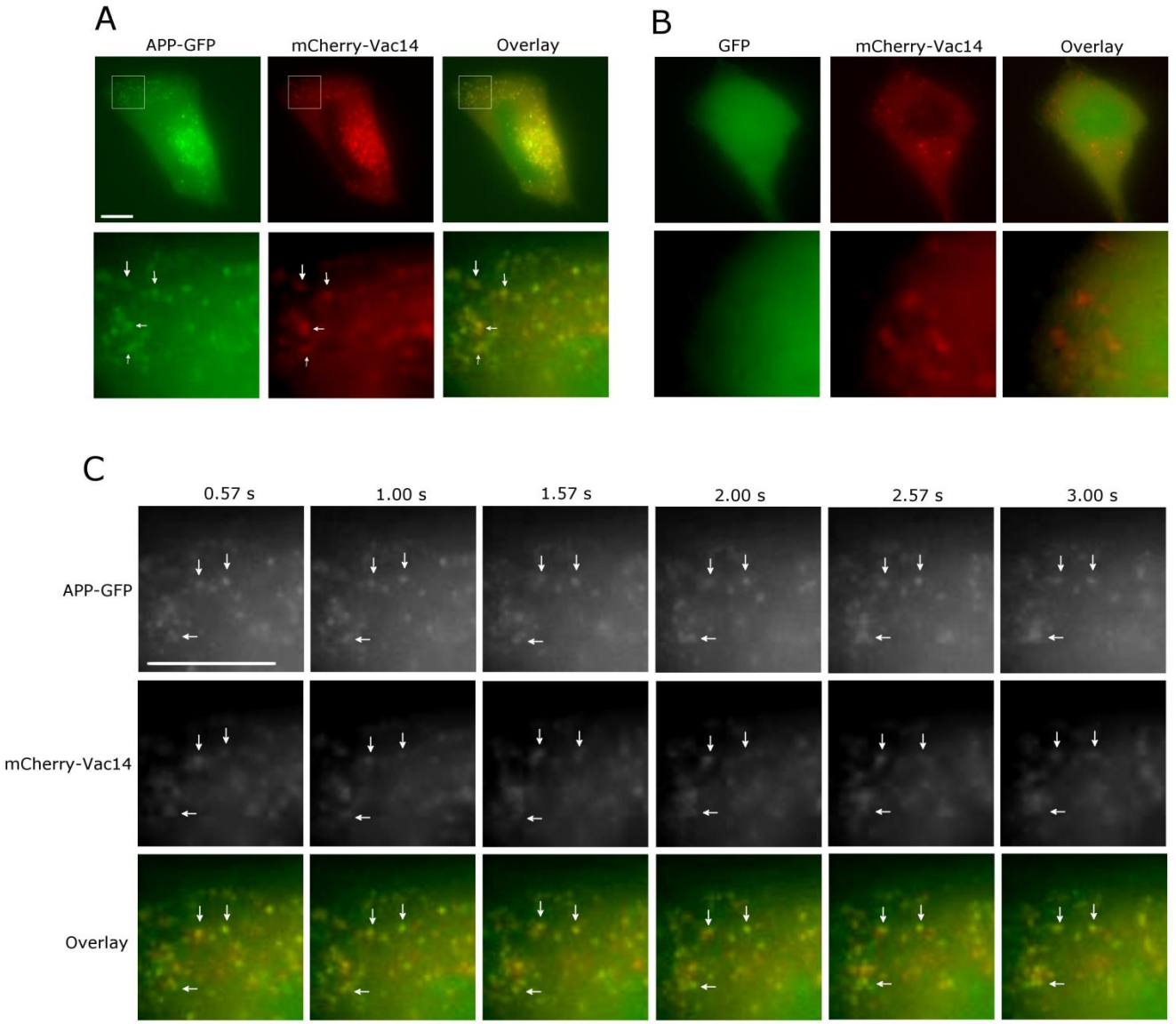
A
APP-GFP
mCherry-Vac14
Overlay
B
GFP
mCherry-Vac14
Overlay
C
0.57 s
1.00 s
1.57 s
2.00 s
2.57 s
3.00 s
APP-GFP
mCherry-Vac14
Overlay

Figure 26. Vac14 and APP co-localise and display co-movement in HeLa cells using live cell imaging.

(A and C) HeLa cells co-expressing mCherry-Vac14 and APP-GFP there is co-localisation and co-movement of vesicular structures positive for both APP and Vac14. No co-localisation was observed in HeLa cells co-expressing mCherry-Vac14 and GFP (B). (C) Stills taken from 0.57, 1.00, 1.57, 2.00, 2.57 and 3.00 seconds time points. Arrows represent vesicular structures displaying co-localisation and co-movement. (Scale bar = 10 µm) (n=3). Enlarged images are magnified 4x. The video files for each condition can be viewed on the CD attached to the thesis (Appendix 2).

5.2.5 APP and the PI(3,5)P_2 probe mCherry-ML1Nx2 show co-localisation and co-migration of vesicular structures in live cells

APP and Vac14 co-localised in fixed cells (5.2.4) suggesting APP and the PIKfyve complex are present on the same vesicular structure. Therefore the co-localisation between APP and the ML1Nx2, PI(3,5)P_2 probe was examined in live cells as PI(3,5)P_2 is produced by the PIKfyve complex. HeLa cells overexpressing mCherry-ML1Nx2 and either APP-GFP or GFP (control) were subjected to live cell imaging as described in chapter 2. APP-GFP was found to co-localise with the probe mCherry-ML1Nx2 (Figure 27A). The probe mCherry-ML1Nx2 did not co-localise with GFP (control) (Figure 27B). Figure 27C shows still frames of a 4 x zoomed in section of still frames taken at 3.57, 4.00, 4.57, 5.00, 5.57 and 6.00 seconds of imaging. APP-GFP and mCherry-ML1Nx2 displayed co-movement on vesicular structures (Figure 27C) (see video on attached disk). These results demonstrate that APP is localised on PI(3,5)P_2 positive vesicular structures.

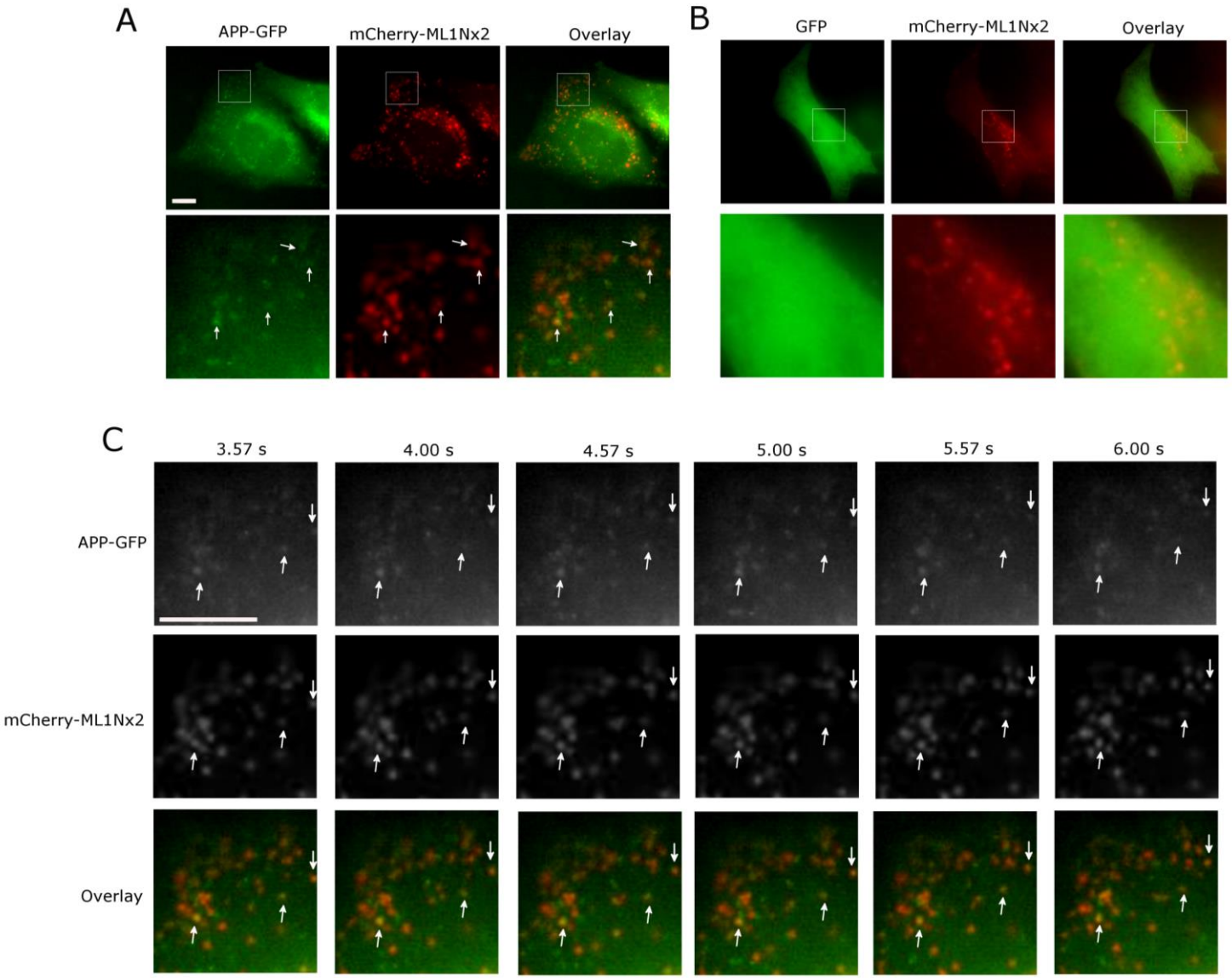
A
APP-GFP
mCherry-ML1Nx2
Overlay
B
GFP
mCherry-ML1Nx2
Overlay
C
3.57 s
4.00 s
4.57 s
5.00 s
5.57 s
6.00 s
APP-GFP
mCherry-ML1Nx2
Overlay

Figure 27. The PI(3,5)P_2 probe mCherry-ML1Nx2 and APP-GFP display co-localisation and co-movement in live HeLa cells.

In HeLa cells co-expressing mCherry-ML1Nx2 and APP-GFP there is co-localisation and co-movement of vesicular structures positive for both APP and ML1Nx2 (A and C). (C) The cells were imaged for 30 seconds in total. Displayed are frames of the images taken at 3.57, 4.00, 4.57, 5.00, 5.57 and 6.00 seconds of imaging. (Scale bar = 3 µm) (n=3) (enlarged images are 4x).. The video files for each condition can be viewed on the CD attached to the thesis (Appendix 2).

5.2.6 APP-GFP and the PI(3,5)P_2 probe mCherry-ML1Nx2 display co-localisation on vesicular structures in fixed HeLa cells

This chapter has so far shown that the PI(3,5)P_2 probe mCherry-ML1Nx2 displays co-localisation with mCitrine-Vac14 and that APP-GFP and Vac14-mCherry co-localise on vesicular structures that show co-movement. Next the effect of overexpression of APP on the dynamics of the PI(3,5)P_2 probe mCherry-ML1Nx2 were examined. mCherry-ML1Nx2 was expressed in HeLa cells along with either APP-GFP or GFP (control). The cells were fixed on glass coverslips and images were taken using a confocal microscope. Figure 28A shows that APP-GFP and the PI(3,5)P_2 probe mCherry-ML1Nx2 co-localise on vesicular structures, indicating that APP may play a role in PI(3,5)P_2 production. Interestingly it was noted when imaging the cells that those overexpressing APP-GFP seemed to have a higher number of mCherry-ML1Nx2 positive structures than control cells (GFP).

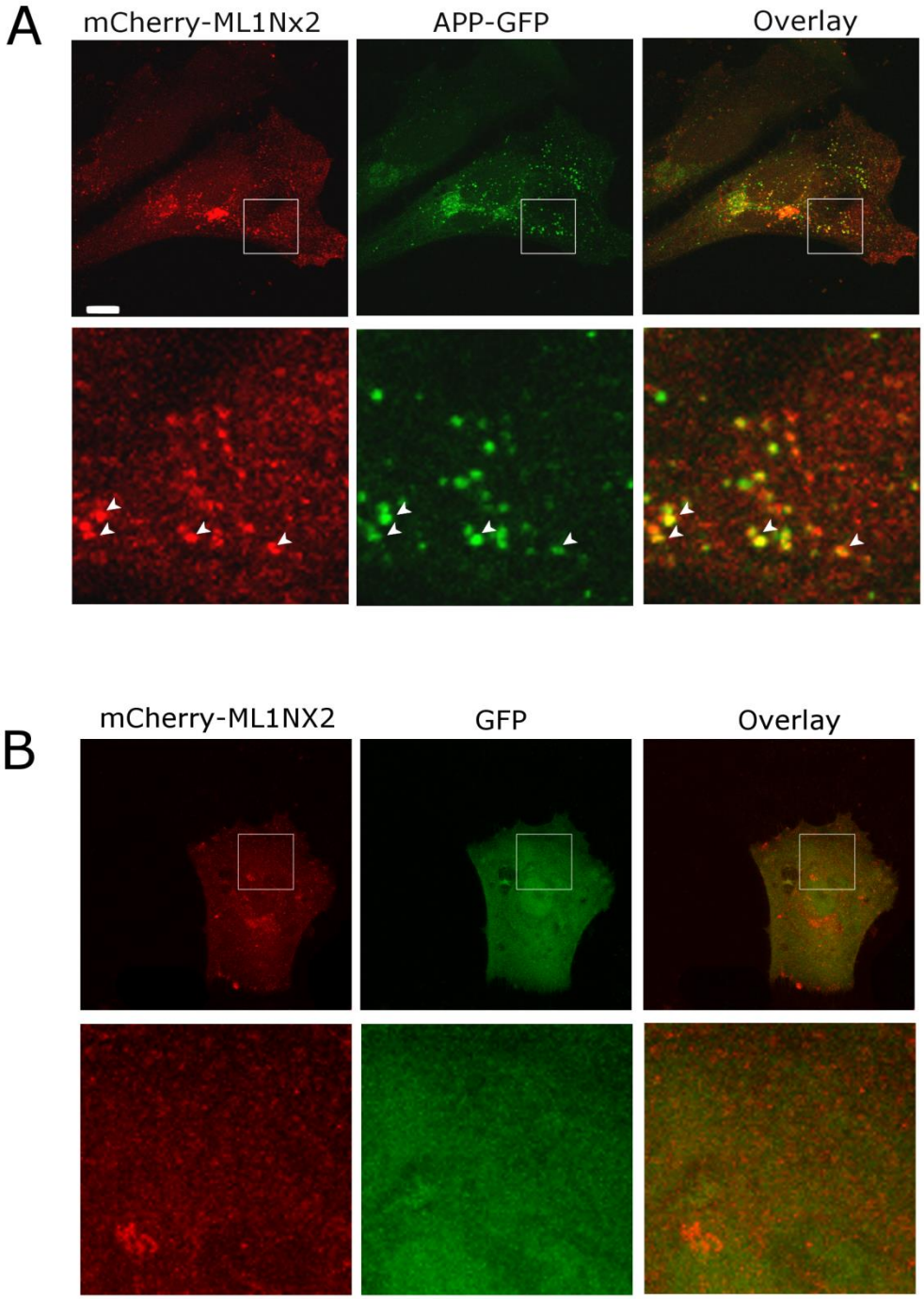

Figure 28. APP-GFP and the PI(3,5)P_2 probe mCherry-ML1Nx2 co-localise in HeLa cells.

In HeLa cells co-expressing APP-GFP and mCherry-ML1Nx2 there is co-localisation on vesicular structures in fixed cells (A). GFP shows no co-localisation with the mCherry-ML1Nx2 probe. This demonstrates that APP is found on mCherry-ML1Nx2 structures. (Scale bar = 10 µm) (n=3). The displayed image is the maximum projection of z-stacks. Enlarged image = 5 x

5.2.7 The overexpression of APP increases the number of PI(3,5)P_2 positive vesicular structures

The previous observation that the overexpression of APP-GFP seemed to increase the number of mCherry-ML1Nx2 positive vesicular structures was examined in more detail. The number of PI(3,5)P_2 positive structures, as determined by the probe mCherry-ML1Nx2, were analysed in HeLa cells overexpressing either APP-GFP, AICD-GFP, APP and AICD truncation mutants or GFP (control). 25 cells were analysed using the MOSAIC plug in for ImageJ, as described in chapter 2. The MOSAIC plugin has previously been used to quantify intracellular vesicular structures (Rizk et al., 2014). It connects image segmentation with biological reality by accounting for the microscopes point spread function, therefore correcting for microscope blur and noise, producing deconvolved segmentations. It provides data on the number of objects and the mean intensity of each object.

The overexpression of APP-GFP led to a significant increase in the average number of PI(3,5)P_2 positive vesicles per cell when compared to the overexpression of GFP (negative control) (Figures 29A and 29C). In contrast, the overexpression of a mutant of APP lacking the intracellular domain (APPΔAICD) did not significantly alter the number of PI(3,5)P_2 positive structures, which suggests that APP's intracellular domain is needed to stimulate the formation of PI(3,5)P_2 positive vesicles.

In order to confirm that the increase in the number of PI(3,5)P_2 positive vesicles upon the overexpression of APP was PIKfyve dependant, the overexpression of APP was combined with the inhibition of PIKfyve by treatment with 4 µM YM-201636 for 4 hours. The average number of PI(3,5)P_2 positive structures in cells overexpressing APP-GFP and treated with the PIKfyve inhibitor was significantly reduced (Figures 29B and 29C). This demonstrates that the increase in the number of PI(3,5)P_2 positive structures upon overexpression of APP is dependent on the activity of PIKfyve. This is consistent with the recent finding that the only source for PI(3,5)P_2 production in mammals is the

phosphorylation of PI(3)P, which is PIKfyve dependent (Zolov et al., 2012). One interesting observation of note was that in cells overexpressing APP-GFP the intracellular location of APP-GFP was altered upon treatment with the PIKfyve inhibitor YM-201636. This observation is examined in more detail later on in this chapter.

The intensity of each PI(3,5)P_2 positive vesicle was also recorded. The average intensity per vesicle did not differ significantly between APP, APP∆AICD and GFP (Figure 29D). The treatment with the PIKfyve inhibitor YM-201636 also did not alter the intensity of any remaining vesicles (Figure 29D). This indicates that APP drives the production of PI(3,5)P_2 positive vesicles and not the levels of PI(3,5)P_2 in individual vesicles.

The fact that the APP∆AICD mutant failed to stimulate the production of PI(3,5)P_2 positive structures suggests that AICD plays an important role in the APP dependent production of PI(3,5)P_2 positive vesicles. This led to the question: can the intracellular domain of APP (AICD) alone stimulate PI(3,5)P_2 vesicle formation? The overexpression of AICD-GFP significantly increased the number of PI(3,5)P_2 positive structures to a similar level of that observed with the overexpression of APP-GFP (Figures 29A and 29B). In chapter 4 it was found that the AICD truncation 4 mutant (AICD-Tr4) still bound to purified Vac14 and recruited both Vac14 and PIKfyve from brain cytosol. Therefore, the effect of AICD-Tr4 on the production of PI(3,5)P_2 positive vesicles was examined. The overexpression of AICD-Tr4 significantly increased the number of PI(3,5)P_2 positive structures when compared to control GFP expression. This increase was similar to that observed by APP and AICD overexpression (Figures 29A and 29C). This data and that of chapter 4 suggests that APP needs to bind to Vac14, via AICD, to stimulate the PIKfyve dependent formation of PI(3,5)P_2 positive vesicles.

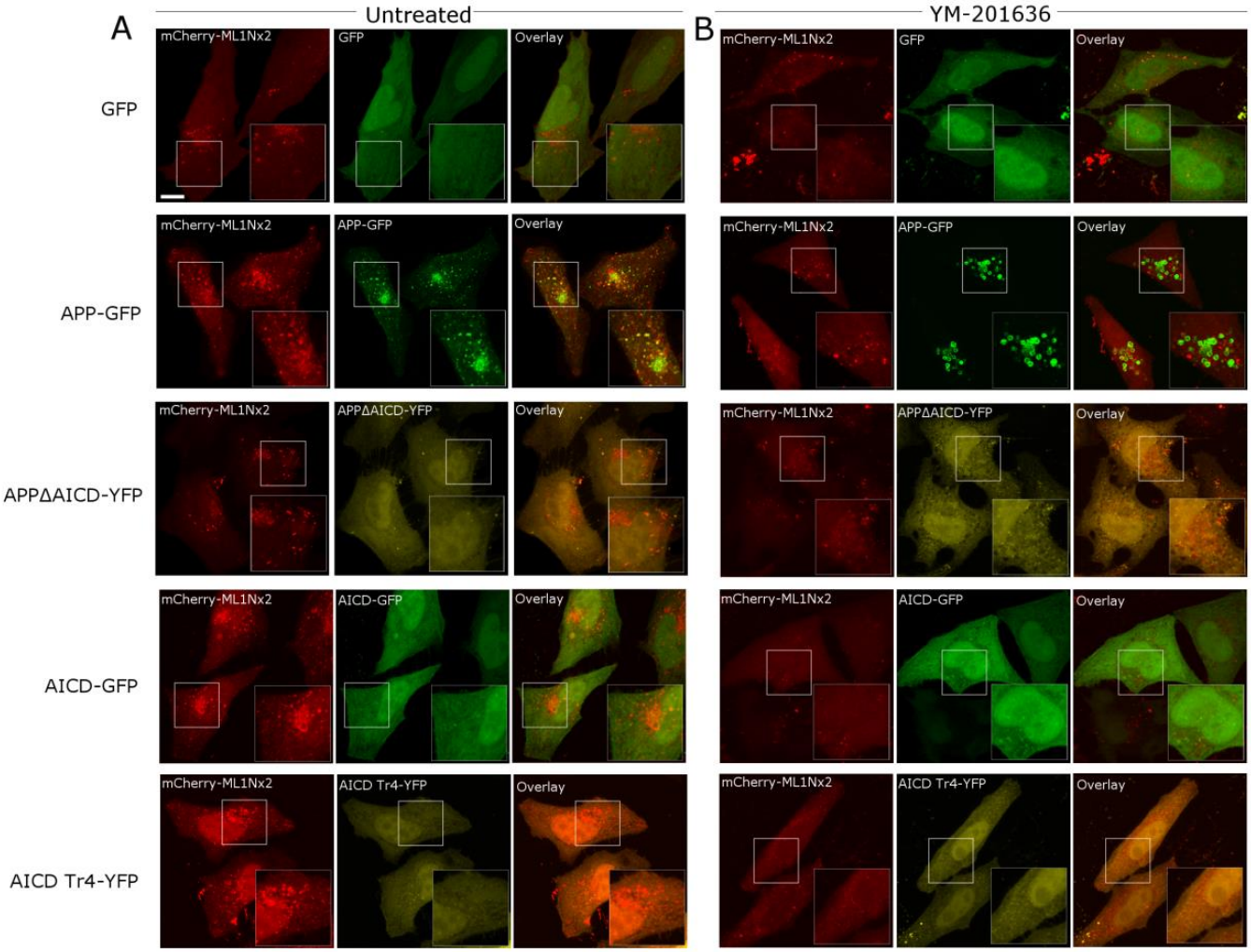
A
Untreated
B
YM-201636
GFP
APP-GFP
APPΔAICD-YFP
AICD-GFP
AICD Tr4-YFP
mCherry-ML1Nx2
GFP
APP-GFP
APPΔAICD-YFP
AICD-GFP
AICD Tr4-YFP
Overlay

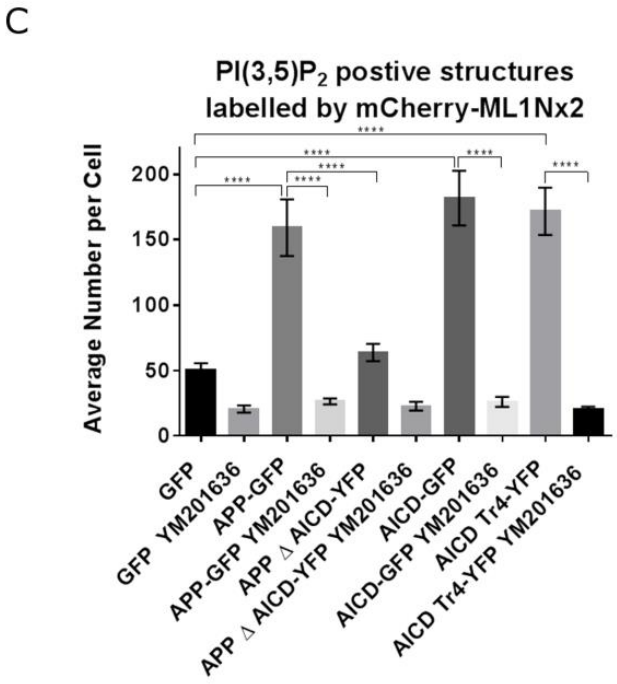
C
PI(3,5)P2 postive structures labelled by mCherry-ML1Nx2
Average Number per Cell
0
50
100
150
200
****
GFP
GFP YM201636
APP-GFP
APP-GFP YM201636
APP Δ AICD-YFP
APP Δ AICD-YFP YM201636
AICD-GFP
AICD-GFP YM201636
AICD Tr4-YFP
AICD Tr4-YFP YM201636

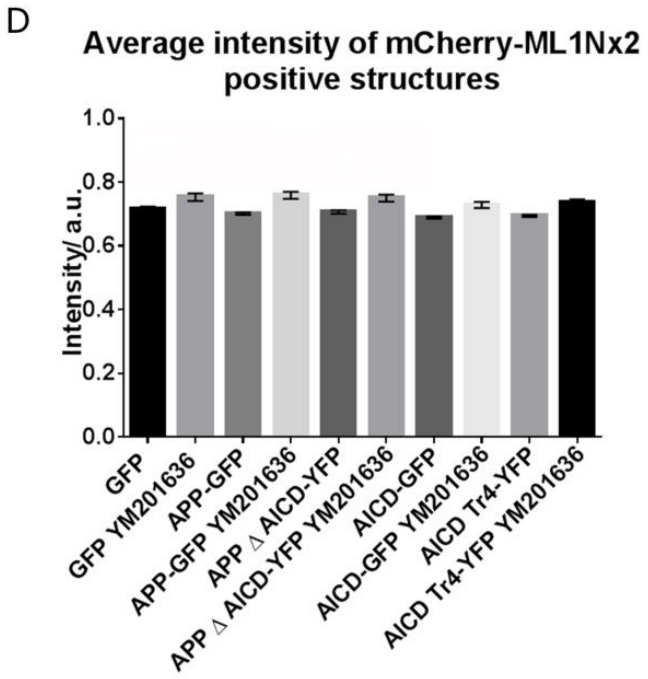
D
Average intensity of mCherry-ML1Nx2 positive structures
Intensity/ a.u.
0.0
0.2
0.4
0.6
0.8
1.0
GFP
GFP YM201636
APP-GFP
APP-GFP YM201636
APP Δ AICD-YFP
APP Δ AICD-YFP YM201636
AICD-GFP
AICD-GFP YM201636
AICD Tr4-YFP
AICD Tr4-YFP YM201636

Figure 27. Overexpression of APP and AICD controls PIKfyve function in HeLa cells.

*(A, B and C) Co-expression of GFP-tagged proteins and the mCherry-labelled PI(3,5)P_2 probe ML1Nx2 was used to analyse the impact of APP-derived constructs on PI(3,5)P2 positive structures. YM201636 was used to inhibit PIKfyve function (4 µM). APP expression strongly increased the average number of PI(3,5)P_2 positive vesicles (A and C). The increase could be abolished by PIKfyve inhibition, demonstrating the dependency on PIKfyve (B and C). APP lacking its intracellular domain (APPΔAICD) was unable to stimulate formation of PI(3,5)P_2 positive vesicles. AICD and AICD-Tr.4 both stimulated formation of PI(3,5)P_2 positive vesicles. The displayed image is the maximum projection of z-stacks. (C) Quantification of mCherry-ML1Nx2 structures of 25 cells for each condition. Statistical analysis was conducted in Graphpad Prism 6.0. A one- way ANOVA test followed by Tukey's post-hoc analysis was used (**** $p \leq 0.0001$) (n=3). Error bars are s.e.m. (D) APP, AICD and AICD-Tr.4 expression did not majorly affect the average intensity of mCherry-ML1Nx2 vesicles, suggesting that APP controls number of PI(3,5)P_2 positive vesicles rather than PI(3,5)P_2 content within a vesicle. Error bars are s.e.m.*

(Scale bar = 10 µm)

5.2.8 The YENPTY motif of AICD plays an important role in the relationship between APP and the PIKfyve complex

The results of the proteo-liposome recruitments in chapter 4 showed that AICD-Tr4 was able to bind to purified recombinant Vac14, and recruit both Vac14 and PIKfyve from brain cytosol. In this chapter it has so far been shown that AICD-Tr4 was able to stimulate the production of $PI(3,5)P_2$ positive vesicles to a similar extent of that observed by APP and AICD overexpression. Therefore the question, what domain of AICD, present in its C-terminus, could be interacting with Vac14, was asked. The YENPTY motif of AICD is a known endocytosis signal, and a binding site for many cytosolic and adaptor proteins (Nhan and Koo, 2013). Therefore, could the YENPTY motif of AICD be the interaction site for Vac14? To test this theory a mutant of AICD was created, in which the YENPTY motif was deleted (AICD∆YENPTY). The ability of this mutant to stimulate the production of $PI(3,5)P_2$ positive vesicles was examined. HeLa cells overexpressing AICD∆YENPTY-GFP failed to significantly stimulate the production of $PI(3,5)P_2$ positive vesicles as determined by the probe mCherry-ML1Nx2, when compared to cells overexpressing full length AICD (Figures 30A and 30B). The average intensity of the $PI(3,5)P_2$ vesicles was the same in all three overexpression conditions (AICD-GFP, AICD∆YENPTY-GFP and GFP), consistent with the data in figure 29 (Figure 30C).

These results indicate that the YENPTY domain, at the C-terminus of AICD, is required for the PIKfyve dependent stimulation of $PI(3,5)P_2$ positive vesicles production. This is in line with the proteo-liposome recruitment data from chapter 4, which showed that the C-terminus of AICD was crucial for Vac14 binding. It was not possible to conduct proteo-liposome recruitments with 6 x HIS-MBP-AICD∆YENPTY as the protein was strongly degraded when expressed and purified from *E.coli*, thereby preventing protein interaction studies.

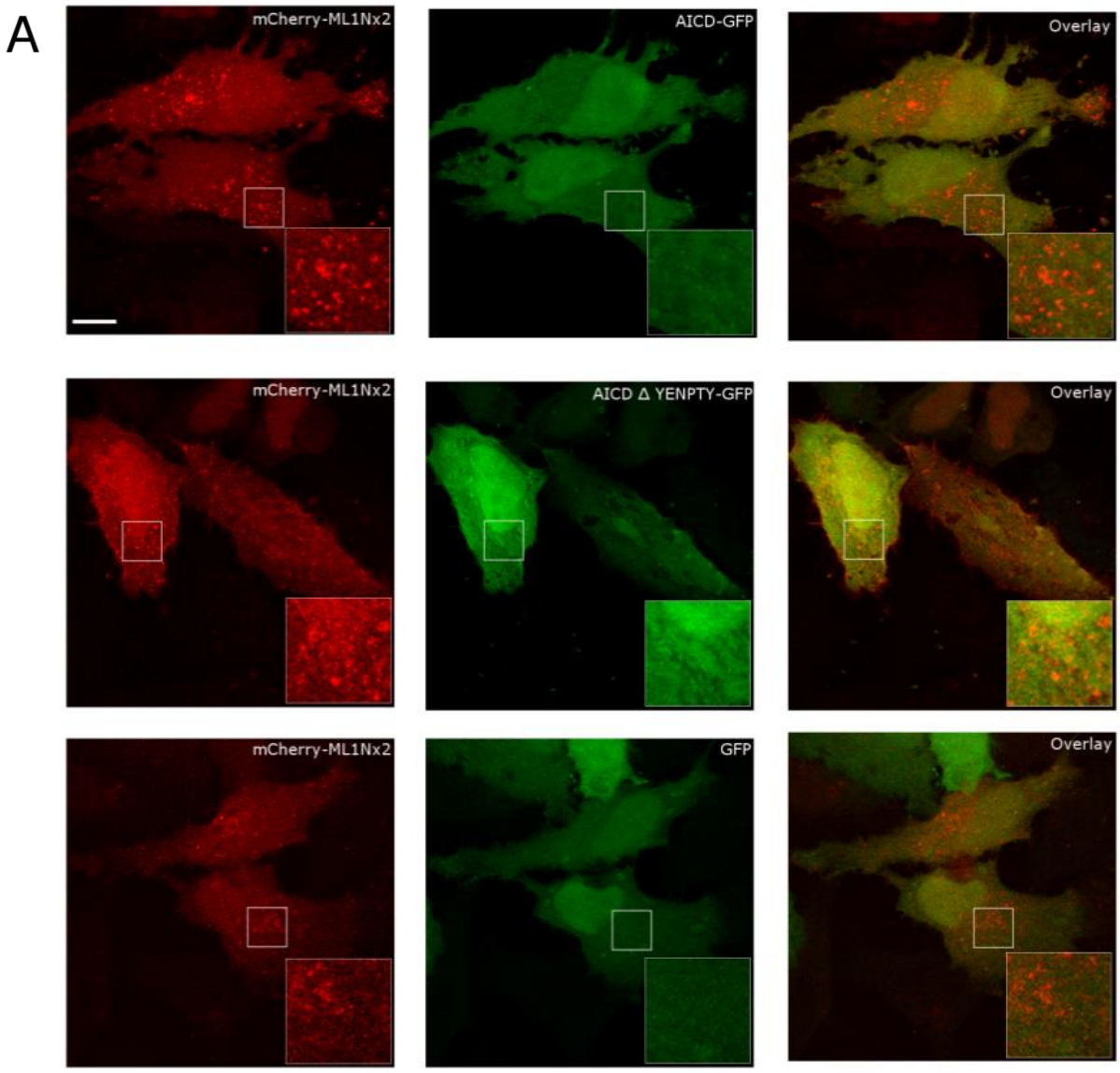
A
mCherry-ML1Nx2
AICD-GFP
Overlay
mCherry-ML1Nx2
AICD Δ YENPTY-GFP
Overlay
mCherry-ML1Nx2
GFP
Overlay

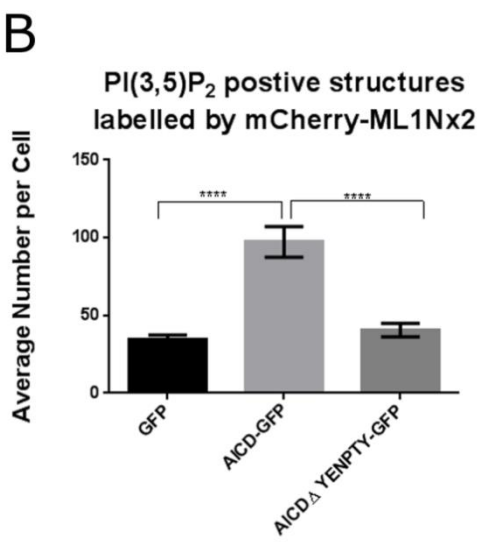
B
PI(3,5)P2 postive structures labelled by mCherry-ML1Nx2
Average Number per Cell
150
100
50
0
****
****
GFP
AICD-GFP
AICDΔ YENPTY-GFP

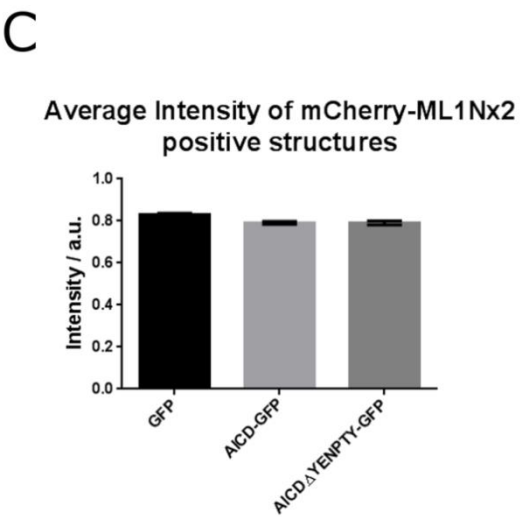
C
Average Intensity of mCherry-ML1Nx2 positive structures
Intensity / a.u.
1.0
0.8
0.6
0.4
0.2
0.0
GFP
AICD-GFP
AICDΔYENPTY-GFP

Figure 28. The YENPTY motif of AICD is crucial for controlling PIKfyve function in HeLa cells.

*(A,B) Co-expression of AICD-GFP, AICD ∆ YENPTY-GFP and GFP with the PI(3,5)P_2 probe mCherry-ML1Nx2. The AICD ∆ YENPTY-GFP mutant fails to stimulate the production of mcherry-ML1Nx2 positive vesicles significantly above control (GFP) indicating the YENPTY motif of AICD is important in the production of PI(3,5)P_2 positive vesicles. The displayed image is the maximum projection of z-stacks. (B) Quantification of mCherry-ML1Nx2 structures of 25 cells for each condition. Statistical analysis was conducted in Graphpad Prism 6.0. A one- way ANOVA test followed by Tukey's post-hoc analysis was used (**** $p \leq 0.0001$) (n=3). Error bars are s.e.m. (C) The expression of AICD and AICD ∆ YENPTY did not affect the intensity of the mCherry-ML1Nx2 positive vesicles consistent with the idea that APP and therefore AICD controls the number of PI(3,5)P_2 positive structures rather than PI(3,5)P_2* levels in each structure.(Scale bar = 10 µm)

5.2.9 Inhibiting PIKfyve activity causes a re-distribution of APP

When examining the number of $PI(3,5)P_2$ positive structures upon APP-GFP overexpression it was noted that in cells treated with the PIKfyve inhibitor YM-201636 the localisation of APP-GFP changed from small vesicular structures to what appeard to be vacuolar-like structures (Figure 29). To examine this phenomenon in more detail APP-GFP was overexpressed in HeLa cells which were treated with 4 µM YM-201636 for six different time points. HeLa cells overexpressing APP-GFP were exposed to YM-201636 for 15 minutes, 30 minutes, 1 hour, 2 hours and 4 hours. After treatment with YM-201636 for between 30 minutes and 1 hour, vacuoles became visible in the cells. This is consistent with PIKfyve inhibition, both pharmacological (PIKfyve inhibitors) and genetic (RNAi knock-down) (Jefferies et al., 2008, Zolov et al., 2012, Zhang et al., 2007b).

After treatment with YM-201636 for 30 minutes, small APP-GFP positive vacuole-like structures were observed. After 1 hours treatment with YM-201636 it becomes apparent that APP-GFP accumulates in vacuole-like structures, which are highlighted by white arrows in figure 31. At longer time points (2 hours and 4 hours) APP becomes increasingly trapped in vacole like structures, reducing the the localisation of APP to small vesicular structures. These results indicate that APP trafficking is disrupted by PIKfyve inhibition.

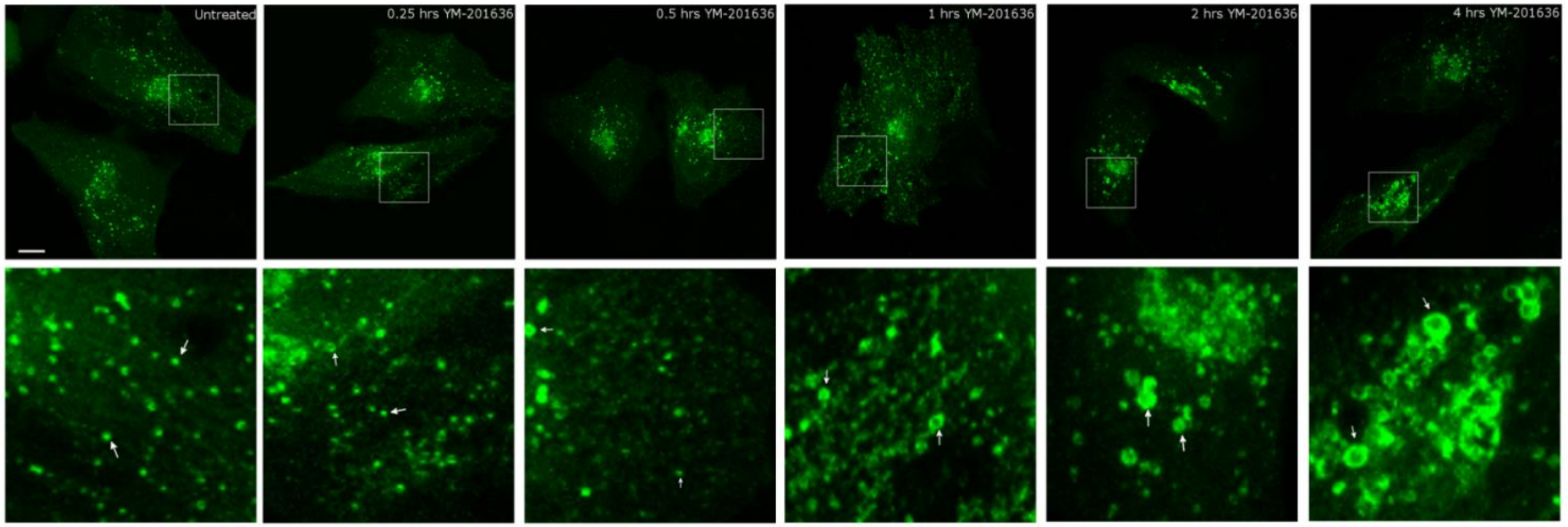

Figure 29. Inhibition of PIKfyve with YM-201636 causes a re-distribution of APP-GFP
HeLa cells overexpressing APP-GFP were treated with 4 µM of the PIKfyve inhibitor YM-201636 for between 15 minutes and 4 hours. Over time APP-GFP gets re-distributed from small vesicular structures to vaculoar like structures indicating PIKfyve could potentially be required for correct APP trafficking. (Scale bar = 10 µm) (n=3). The displayed image is the maximum projection of z-stacks.

5.2.10 Inhibition of the PIKfyve complex causes accumulation of APP

The observation that APP-GFP becomes trapped in vacuole structures upon PIKfyve inhibition, and the implications of this in terms of APP trafficking led to the analysis of this observation in more detail. APP endosome-to-TGN trafficking is known to be regulated by the retromer complex (Vieira et al., 2010). PIKfyve complex activity is also known to be important in the retrograde trafficking of the cation-independent mannose-6 phosphate receptor (MPR), amongst other cargos (Rutherford et al., 2006, de Lartigue et al., 2009, Zhang et al., 2007b). HeLa cells overexpressing APP-GFP were treated for 4 hours the PIKfyve inhibitors YM-201636 Apilimod at several different concentrations (Figures 32A, 32B, 32C and 32D) (Cai et al., 2013). YM-201636 was used at concentrations of 0.1 µM, 0.33 µM, 1 µM, 3 µM and 10 µM, whilst Apilimod was used at concentrations of 3 nM, 10 nM, 30 nM, 100 nM and 300 nM. The inhibitor Apilimod was used as well as YM-201636 due to the fact that YM-201636 has been shown to posess some activity towards phosphoinositide 3-kinase (PI3K) family members (Jefferies et al., 2008, Ikonomov et al., 2009g). The cells were stained for the early endosome marker EEA1 (Figures 32A and 32C), and the late endosomal/lysosomal marker LAMP-1 (Figures 32B and 32D), and were analysed by confocal microscopy. It was apparent that the inhibition of PIKfyve with both YM-201636 and Apilimod caused APP-GFP to accumulate in vacuole structures (Figures 32A and 32B), with no difference observed between the two inhibitors. This accumulation of APP-GFP in vacuole like structures occurred at all concentrations of inhbitors used.

APP-GFP in untreated cells exhibits a degree of colocalisation with the early endosome marker EEA1 (Figures 32A and 32C). The enlarged APP-GFP vacuoles co-localise with EEA1 upon the inhibition of PIKfyve with both inibitors, and at the range of concentrations used. In untreated cells APP-GFP shows little co-localisation with the late endosomal/lysosomal marker LAMP1 (Figures 32B and 32D). The enlarged APP-

GFP positive vacuoles upon PIKfyve inhibition do not show co-localisation with LAMP1. Taken together these results indicate that upon PIKfyve inhibition APP-GFP becomes trapped in enlarged early endosomes positive for EEA1.

The protein levels of endogenous APP and its homologure APLP2 were examined. APLP2 is a homologue of APP and like APP is ubiqutiously expressed. APP and APLP2 are known to exhibit functional redundancy, therefore the effect of PIKfyve inhibition on the protein levels of both APP and APLP2 were examined. HeLa cells were treated with 4 µM of the PIKfyve inhibitor YM-201636 overnight to determine if endogenous APP and APLP2 protein levels are affected by PIKfyve function. The relative protein levels were analysed by SDS-PAGE and Western blotting of HeLa cell lysates, using antibodies against APP and APLP2. There was no significant difference in the levels of APLP2 between treated and untreated cells (Figures 32F and 32G). In contrast, the overall levels of APP were significantly increased upon treatment with the PIKfyve inhibitor YM-201636 (Figures 32E and 32G). The multiple bands observed on the APP Western blot (Figure 32E) represent different isoforms of APP. It was difficult to distinguish between these isoforms, therefore, all bands were taken into consideration when quantifying the level of APP. The re-distrubution of APP-GFP and the increase in the level of endogenous APP upon YM-201636 treatment suggests that APP trafficking and APP levels are dependent on the activity of PIKfyve.

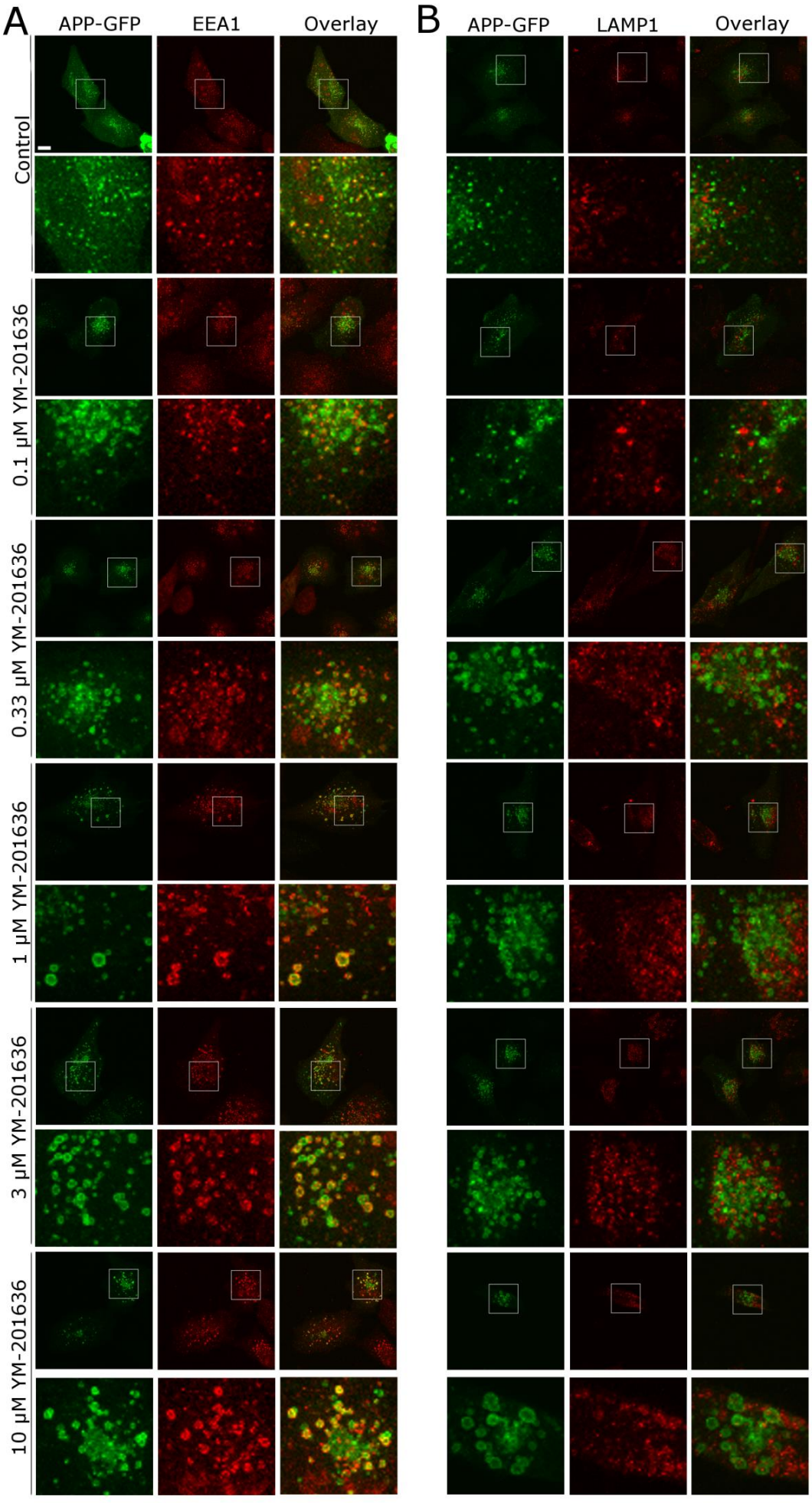
A
APP-GFP
EEA1
Overlay
B
APP-GFP
LAMP1
Overlay
Control
0.1 µM YM-201636
0.33 µM YM-201636
1 µM YM-201636
3 µM YM-201636
10 µM YM-201636

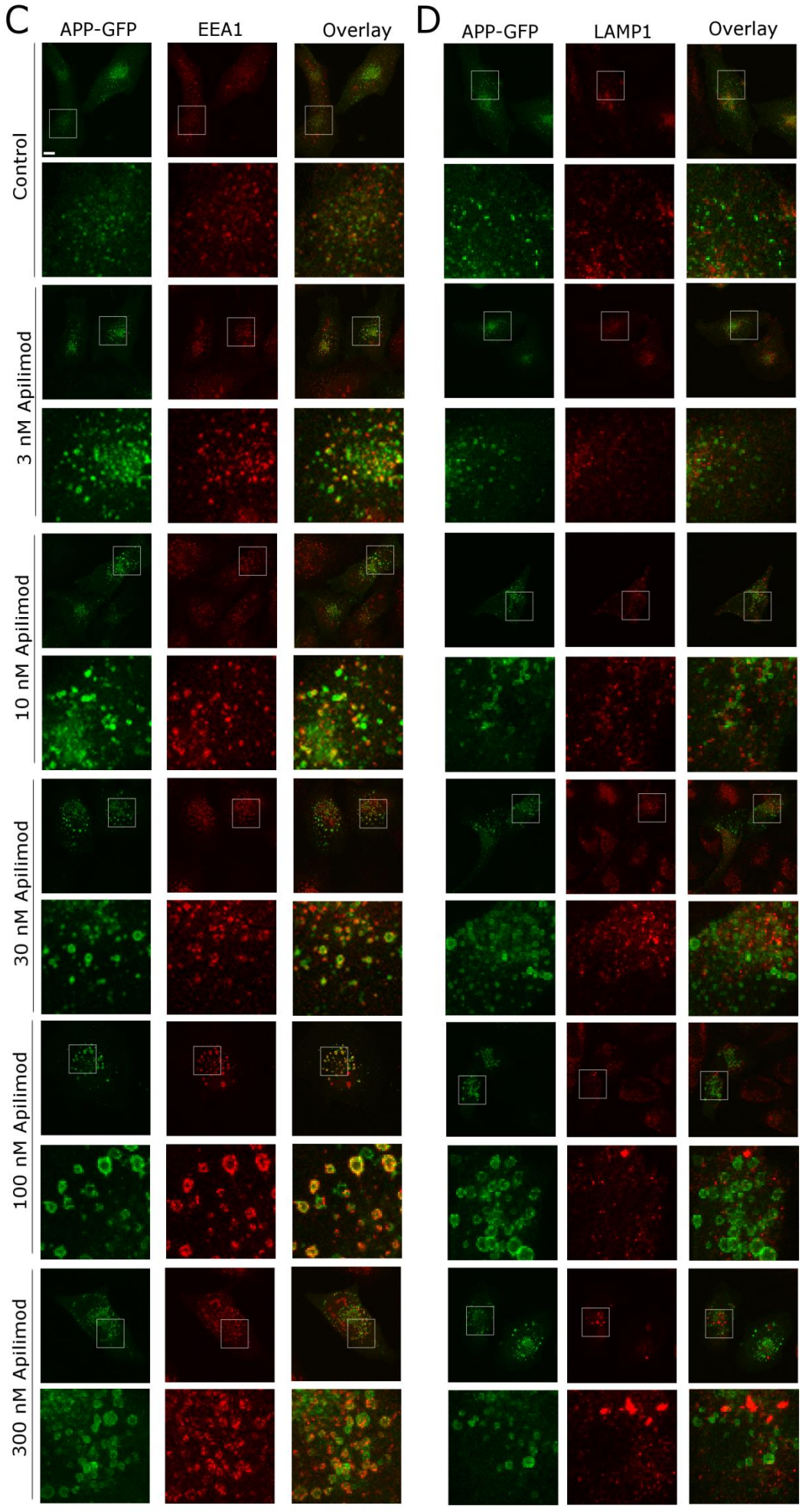
C
APP-GFP
EEA1
Overlay
D
APP-GFP
LAMP1
Overlay
Control
3 nM Apilimod
10 nM Apilimod
30 nM Apilimod
100 nM Apilimod
300 nM Apilimod

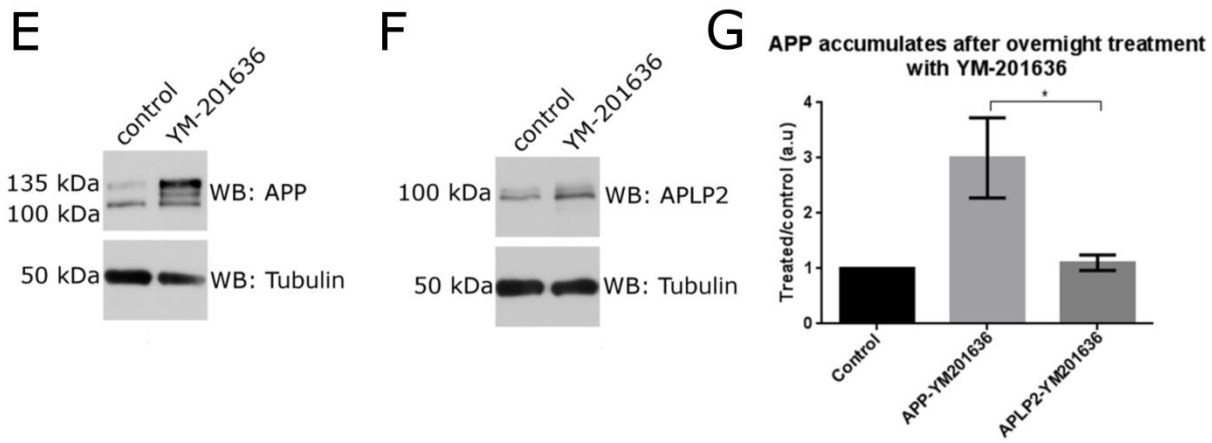

Figure 30. PIKfyve is required for the correct trafficking and distribution of APP-GFP

(A) HeLa cells overexpressing APP-GFP, treated with 0.1 µM, 0.33 µM, 1 µM, 3 µM and 10 µM of YM-201636 (4hrs), stained for the early endosome marker EEA1 using Alexa Flour 555 secondary antibody. (B) HeLa cells overexpressing APP-GFP, treated with 0.1 µM, 0.33 µM, 1 µM, 3 µM and 10 µM of YM-201636 (4hrs), stained for the late endosomal/lysosomal marker LAMP-I using an Alexa Flour 555 secondary antibody. (C) HeLa cells overexpressing APP-GFP, treated with 3 nM, 10 nM, 30 nM, 100 nM and 300 nM of Apilimod (4hrs), stained for the early endosome marker EEA1 using Alexa Flour 555 secondary antibody. (D) HeLa cells overexpressing APP-GFP, treated with 3 nM, 10 nM, 30 nM, 100 nM and 300 nM of Apilimod (4hrs), stained for the late endosomal/lysosomal marker LAMP-I using an Alexa Flour 555 secondary antibody.Treatment with YM-201636 and Apilimod caused the accumulation of APP-GFP in vacuole like structures. These vacuole like structures were EEA1 but not LAMP-1 positive. The displayed images are the maximum projection of z-stacks. (E) The treatment of HeLa cells overnight with YM-201636 caused and accumulation of all APP species detected by western blotting. It was not possible to determine if specific isoforms were affected. (F)Treatment with YM-201636 did not significantly affect the levels of APLP2 as determined by western blotting. (G) Quantification of the increase in APP was conducted in ImageJ. Displayed is the area corresponding to the bands in the treated condition compared to controls. Statistical analysis was conducted in Graphpad Prism 6.0 using a two-tailed unpaired t-test ($p \leq 0.05$) (n=6).*
(Scale bar =10 µm).

5.3 Discussion

This chapter demonstrates that the interaction between APP and the PIKfyve complex is functionally relevant. Using the $PI(3,5)P_2$ probe ML1Nx2 it was established that Vac14 and APP co-localise to $PI(3,5)P_2$ positive vesicles in both fixed and live cells. APP overexpression stimulates the production of $PI(3,5)P_2$ positive vesicles in a PIKfyve dependent process. The overexpression of a mutant protein in which the intracellular domain is removed, fails to stimulate $PI(3,5)P_2$ positive vesicle production, demonstrating the importance of AICD. AICD alone, and the Tr4 mutant of AICD (lacks the 10 N-terminal amino acids) are able to stimulate $PI(3,5)P_2$ vesicle production, again demonstrating the importance of AICD. An AICD mutant lacking the YENPTY motif fails to stimulate $PI(3,5)P_2$ positive vesicle production, indicating that this motif is important for the interaction with the PIKfyve complex. The catalytic inhibition of PIKfyve results in the accumulation of APP-GFP in early endosome derived, positive vacuole like structures, and an increase in endogenous APP levels. Taken together these results establish a functional link between APP and the PIKfyve complex, and implicate PIKfyve in the trafficking and therefore the degradation of APP.

5.3.1 The effect of APP on the $PI(3,5)P_2$ probe mCherry-ML1Nx2

In order to investigate the functional significance of the interplay between APP and the PIKfyve complex the $PI(3,5)P_2$ probe GFP/mCherry-ML1Nx2 was of key importance. The probe developed by Li et al. (2014) allowed for the detection of $PI(3,5)P_2$ in a spatial and temporal way, which has not previously been possible. Here the $PI(3,5)P_2$ probe mCherry-ML1Nx2 was used to show that the number of $PI(3,5)P_2$ positive vesicles was significantly increased upon the overexpression of APP, AICD and AICD-Tr4. The probe ML1Nx2 has been extensively validated by Li et al. (2013). It has also been used by McCartney et al. (2014b) to demonstrate that dynamic changes in the synthesis of $PI(3,5)P_2$ influences synaptic strength by regulating the trafficking of the

AMPA-type glutamate receptor, and therefore that $PI(3,5)P_2$ signalling plays an important role in synapse regulation. The use of mCherry-ML1Nx2 by McCartney et al. (2014b) further validates its use as a $PI(3,5)P_2$ specific probe and therefore supports its use in this chapter to study changes in $PI(3,5)P_2$ in response to APP.

The significant increase in the number of $PI(3,5)P_2$ positive structures in HeLa cells overexpressing APP is supported by work from Currinn et al. (under review) (Appndix 3) who showed that the RNAi mediated suppression of APP reduced the number of $PI(3,5)P_2$ positive structures, detected using the $PI(3,5)P_2$ probe ML1Nx2. Knock down experiments of APP in mammalian cells are complicated by the fact that APP has two homologues, APLP1 and APLP2. The APP family members exhibit functional redundancy, therefore the effect of knocking down one member may be alleviated by the function of the other two members. The suppression of the APP homologue APLP2 also reduced the amount of $PI(3,5)P_2$ positive vesicles (Currinn et al., under review) (Appendix 3). The double knock down of APP and APLP2 enhanced the decrease in the number of $PI(3,5)P_2$ positive vesicles, suggesting functional redundancy between APP and APLP2 in terms of PIKfyve dependent $PI(3,5)P_2$ positive vesicle production (Currinn et al., under review) (Appendix 3). The opposite effects of APP overexpression and knock down demonstrate that APP activates a pathway which leads to the production of $PI(3,5)P_2$ positive vesicles in a PIKfyve dependent manner.

In this chapter it is shown that AICD is crucial for the stimulation of $PI(3,5)P_2$ positive vesicles. The APP mutant APPΔAICD failed to stimulate $PI(3,5)P_2$ vesicle production, whilst the overexpression of AICD increased the amount of $PI(3,5)P_2$ positive vesicles to similar levels as APP overexpression. The truncation 4 mutant of AICD (AICD-Tr4), which lacks the 10 N-terminal amino acids, was able to stimulate the production of $PI(3,5)P_2$ positive vesicles. These results are consistent with the biochemical interaction data from chapter 4, which showed that the C-terminal half of AICD is important for mediating the interaction between AICD and the PIKfyve complex. This indicates that the Vac14 binding motif is located within the last 20 amino acids of AICD.

The inability of a mutant of AICD, in which the YENPTY motif was deleted (AICDΔYENPTY), to stimulate $PI(3,5)P_2$ vesicle production, indicates that the YENPTY domain of AICD plays a crucial role in the interaction of APP with the PIKfyve complex. Unfortunately it was not possible to validate the result biochemically using proteo-liposome recruitments due to the strong degradation of the bacterially expressed AICDΔYENPTY. The YENPTY motif of AICD is known for mediating a number of APP interactions. It is 100% conserved from *C.elegans* to humans, demonstrating its importance (King and Turner, 2004), and it contains a tyrosine based motif, which is an internalisation signal for clathrin mediated endocytosis (Buoso et al., 2010, Kurten, 2003, Ohno et al., 1995, Owen and Evans, 1998). The YENPTY motif of AICD also contains a consensus sequence for phosphotyrosine binding (PTB) domain interaction (Pardossi-Piquard and Checler, 2012). Known interactors of APP's YENPTY motif include the PTB domain containing protein families X11 (mint), FE65, JIP (Borg et al., 1996, King and Turner, 2004). This demonstrates that the YENPTY motif is important for the interaction of APP with proteins that are crucial to its function, therefore lending support to the role of the YENPTY domain in the APP-PIKfyve complex interaction.

5.3.2 A role of the PIKfyve complex in the trafficking of APP

The catalytic inhibition of PIKfyve by the inhibitors YM-201636 and Apilimod caused the accumulation of APP-GFP in vacuole like structures, and an increase in the protein level of endogenous APP. These APP-GFP positive vacuoles displayed some co-localisation with the early endosome marker EEA1, however there was no detectable overlap of these APP-GFP positive vacuoles with the late endosomal/lysosomal marker LAMP-1. This suggests that APP becomes trapped in vesicles derived from the early endosome upon the inhibition of PIKfyve. These results support the idea that APP trafficking is dependent of the activity of PIKfyve. The PIKfyve complex is known to be important in normal endosomal function, and it is crucial in mediating endosome

to TGN transport, and endosome/lysosome fusion (Rutherford et al., 2006, Dong et al., 2010). Another protein complex known to play a crucial role in regulating endosome to TGN trafficking is the retromer complex (Arighi et al., 2004). APP is known to traffic between the endosomes and the TGN in a process mediated by the retromer complex (Vieira et al., 2010). The results of this chapter show that PIKfyve is required to prevent APP becoming trapped in early endosome derived vacuoles. This is supported by the crucial role PIKfyve plays in the sorting of several receptors in endosomes, and the importance of the endosomal location of APP and its transport from endosomes.

5.3.3 A model of APP's interaction with the PIKfyve complex

The results described in this chapter and those in chapter 4 allows for the proposition of a model for the functional significance of the interaction between APP and the PIKfyve complex. Upon arrival at early endosomes during APP trafficking, APP is able to interact with the Vac14 subunit of the PIKfyve complex, probably via the YENPTY motif of AICD. This interaction stimulates the production of PI(3,5)P_2 positive vesicles therefore allowing APP to be sorted away from the endosomal system. The inhibition of PIKfyve would stop this sorting of APP, causing APP to accumulate in vacuole like structures. This model suggests a relationship between APP and PIKfyve were APP can regulate its own trafficking by binding to the PIKfyve complex, and triggering the production of PI(3,5)P_2 positive vesicles. This interplay between APP and the PIKfyve complex also has important implications for Alzheimer's disease. These implications will be discussed in chapter 7.

Chapter 6

The use of proteo-liposomes to examine the interactions of the clathrin coat complex

Chapter 6- The use of proteo-liposomes to examine interactions of the clathrin coat complex

6.1 Introduction

The proteo-liposome recruitment method established in chapter 3 was utilised in chapters 3 and 4 to examine the novel interactions of the intracellular domain of the membrane protein APP with the signalling modules mTOR and PIKfyve.

A model membrane system based on liposomes has previously been utilised to examine the recruitment of protein coats involved in intracellular trafficking events. Protein-free liposomes have been used to study the assembly of parts of the clathrin coat complex from cytosol samples (Zhu et al., 1999, Drake et al., 2000). Baust et al. (2006) utilised a liposome based system to study the assembly of AP-1A protein coats, required for transport between the secretory pathway, and the endosomal and lysosomal systems. The recruitment of the AP-1A coat from brain cytosol onto liposomes containing the cytoplasmic tails of the gpI envelope glycoprotein of the *Varicella zoster* virus, and the lysosomal integral membrane protein Limp II, was examined. The liposome technique was successfully used to examine the coordinated assembly of the AP-1A coat from brain cytosol. A liposome based recruitment system has also been utilised in a proteomic screen of AP-3 coats recruited from cytosol samples, to identify new proteins supporting the role of AP-3 in the targeting of certain transmembrane proteins to lysosomes (Baust et al., 2008).

There is a need for the proteo-liposome technique to be advanced to allow for the in-depth analysis of the recruitment of specific proteins involved in coat assembly, allowing the examination of coat assembly in more detail. This chapter focuses on the development of the proteo-liposome recruitment system to examine the assembly of coat complexes from their purified components, which should enable greater analysis of coat protein assembly. The recruitment of the established coat complex, the AP-2/clathrin coat from its purified components was utilised to further develop the proteo-liposome recruitment method. The recruitment of the AP-2/clathrin coat onto liposomes containing the intracellular domains of two model membrane proteins was examined. These membrane proteins are APP and the apical determinant Crumbs.

6.1.2 Crumbs

Crumbs (Crb), like APP is a type 1 transmembrane protein. Its extracellular domain is primarily composed of epidermal growth factor (EGF)-like repeats. Its intracellular domain is 37 amino acids long and contains two highly conserved regions, the C-terminal PDZ binding motif ERLI and a 4.1 protein, ezrin, radxin, moesin (FERM) binding domain (Bulgakova and Knust, 2009). Crumbs was first discovered in *Drosophila melanogaster* (Tepass et al., 1990), and has since been shown to play a crucial role in epithelial cell polarity. Crb is part of a protein complex, which in *Drosophila,* is primarily composed of Crb, the scaffold protein Stardust/Pals1, PatJ and Lin-7. There are 3 mammalian orthologues of the *Drosophila* Crb, Crb1, Crb2, and Crb3 (Bulgakova and Knust, 2009). This chapter will focus on the Crb2 mammalian orthologue, which is known to be crucial for embryonic development in mice (Xiao et al., 2011). The mammalian orthologue of Stardust known as Pals1 binds to the EERLI motif on Crb, where it acts as a scaffold protein for the assembly of the rest of the Crb complex (Roh et al., 2002).

6.1.2.3 The trafficking of Crumbs

Due to the fact that the cellular levels of Crb are crucial for its role in cell polarity by maintaining the apical-basal polarity, and the integrity of epithelial cells, the trafficking of Crb is key. Crb is a known cargo of the retromer complex that regulates endosome-to-TGN trafficking. Loss of the retromer complex causes Crb to be targeted to the lysosomes for degradation, thereby reducing the level of Crb. This reduction in the level of Crb causes a disruption to the apical-basal polarity of epithelial cells (Pocha and Wassmer, 2011, Pocha et al., 2011, Zhou et al., 2011). Given that the endosome-to-TGN retrograde trafficking of Crb is vital to its function it is not unlikely that Crb endocytosis is also important for its function in regulating cell polarity. There is increasing evidence to suggest that Crb undergoes AP-2 dependent clathrin mediated endocytosis. It has been shown that the clathrin adaptor AP-2 is required for the endocytosis of Crb and that the Scribble protein helps to regulate the polarity of epithelial cells by influencing the endocytosis of Crb (de Vreede et al., 2014).

The intracellular domains of membrane proteins are crucial for mediating their endocytosis as they contain endocytic motifs which are recognised by coat proteins (Kurten, 2003). Unlike APP, Crb2 does not contain the conventional tyrosine based endocytosis motif. It does however contain a potential acidic dileucine based motif (Klebes and Knust, 2000). These motifs are also important in protein trafficking. They are recognised by adaptor proteins such as the clathrin adaptor AP-2, which form part of coat protein complexes involved in trafficking events (Kelly et al., 2008).

The aims of this chapter were to determine if the proteo-liposome recruitment system could be used to examine the assembly of protein coats from their purified components, using the AP-2/clathrin coat as a model, and to test this assembly onto the intracellular domains of membrane proteins containing two different motifs; the tyrosine based motif and the acidic dileucine based motif.

6.2 Results

6.2.1 Purification of clathrin from pig brain

In order to test whether the proteo-liposome recruitment system could be used to examine the assembly of coat proteins from their purified components, using the AP-2/clathrin coat as a model, the components needed to be purified. The analysis of coat assembly from purified components would allow the examination of the recruitment of individual components in more detail than has previously been possible using earlier liposome based systems.

To examine the assembly of the AP-2/ clathrin coat, clathrin was purified from pig brains essentially as described in Pearse (1976). A detailed method for clathrin purification can be seen in chapter 2. Briefly, coated vesicles were isolated from pig brain and the protein released from the lipid using 1 M Tris. The majority of the lipid was then removed by ultracentrifugation and the supernatant loaded on a Sephacryl S500 gel filtration column to separate the clathrin from the lipid and the clathrin adaptors. Figure 33A shows the UV trace obtained from the Sephacryl S500 column. The first peak corresponds to lipid, the second to clathrin, and the third to the clathrin adaptors, demonstrating the complete removal of protein from the lipid and therefore the purity of the samples. Figure 33B shows a Coomassie stained SDS-PAGE gel of fractions from the Sephacryl S500 column. The band at approximately 180 kDa corresponds to the clathrin heavy chain. The light chain was also visible at around 25 kDa. The double band observed in the later elution fractions, at around 100 kDa is characteristic of the clathrin adaptors. To obtain a more pure clathrin preparation the clathrin containing fractions from the Sephacryl S500 column were further purified using a Superdex-200 column. Figures 33C and 33D show the UV trace and a Coomassie stained SDS-PAGE gel of the fractions obtained from the Superdex-200 column. Note the single peak in the UV trace (Figure 33C) indicating a pure clathrin

sample, and the presence of the clathrin heavy chain (180kDa) and light chain (25kDa) shown on the gel in figure 33D. Clathrin was re-assembled into empty cages for storage, by dialysis into a buffer with a pH of 6.5 (polymerisation buffer).

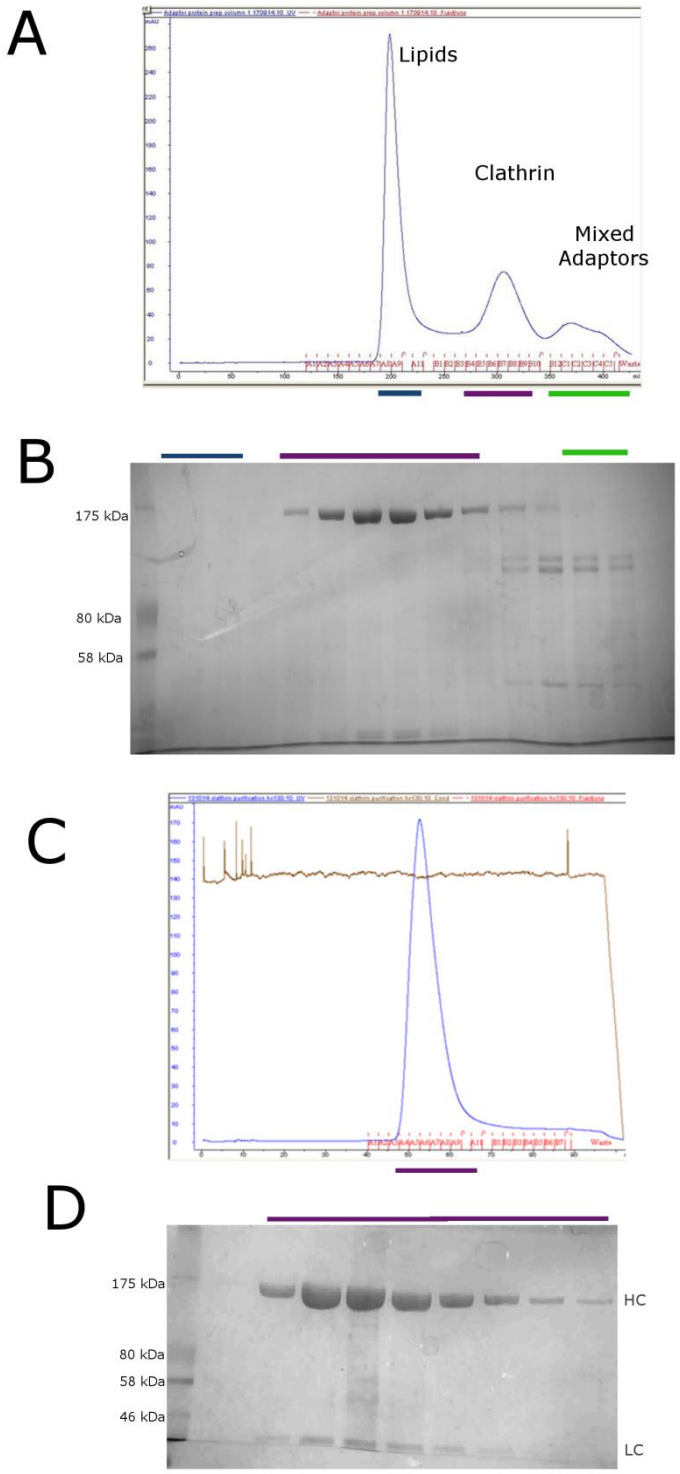

Figure 31. Purification of Clathrin from pig brain.
(A) UV trace after gel filtration using Sephacryl S500. The first peak corresponds to the lipid containing fractions, the second peak to the clathrin containing fractions and the third peak to the adaptor protein containing fractions. (B) A Coomassie stained SDS-gel of fractions from gel filtration with Sephacryl S500. The coloured bars indicate which fractions correspond to which peak shown in A. (C) The UV trace after the clathrin containing fractions from A and B were run on aSuperdex-200 gel filtration column. (D). A Coomassie stained SDS-gel of the fractions from the clathrin peak in C. HC indicates the clathrin heavy chain and LC the light chain.

6.2.2 Purification of mixed clathrin adaptors and AP-2 from pig brain

As well as the purification of clathrin, the purification of the clathrin adaptors, in particular AP-2, was also required to test the creation of artificial clathrin coated vesicles. Mixed clathrin adaptors were obtained from the final elution peak following gel filtration of the stripped coated vesicles using Sephacryl S500 as described previously (Figure 34A and 34B). These mixed adaptors were either concentrated down by precipitation with ammonium sulphate and used as a population of mixed clathrin adaptors for the proteo-liposome recruitments, or they were subjected to further purification steps to isolate the clathrin adaptor AP-2.

AP-2 was purified from these isolated mixed adaptors essentially as described by Pearse and Robinson (1984). A more detailed AP-2 purification method can be seen in chapter 2. Essentially AP-2 was purified from mixed adaptors using hydroxyapatite Bio-gel. The proteins were eluted from the column using an increasing phosphate gradient to a final concentration of 500mM potassium phosphate. Figures 34A and 34B show the UV trace obtained from the elution from the hydroxyapatite Bio-gel column and Coomassie stained SDS-PAGE gels of the fractions from the elution. AP-2 bound to the hydroxyapatite and was eluted from the column at higher phosphate concentrations. The final peak (highlighted by the purple bar) corresponds to the AP-2 containing fractions (Figure 34A). The Coomassie stained gel (Figure 34B) of the AP-2 containing fractions (again highlighted by the purple bar) showed three distinct bands which correspond the α, β and μ subunits of AP-2. The σ subunit has a molecular weight of 17 kDa and therefore is smaller than the 30 kDa cut-off of the 8% SDS-PAGE gel. Both purified AP-2 and the less pure mixed adaptors were used in the proteo-liposome recruitments for the analysis of the interaction between Crumbs and AP-2.

A

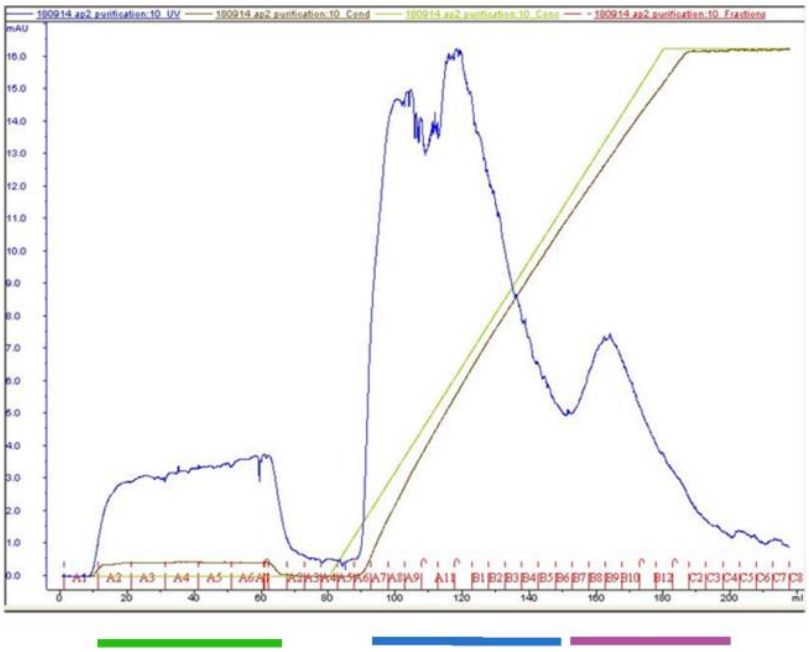

B

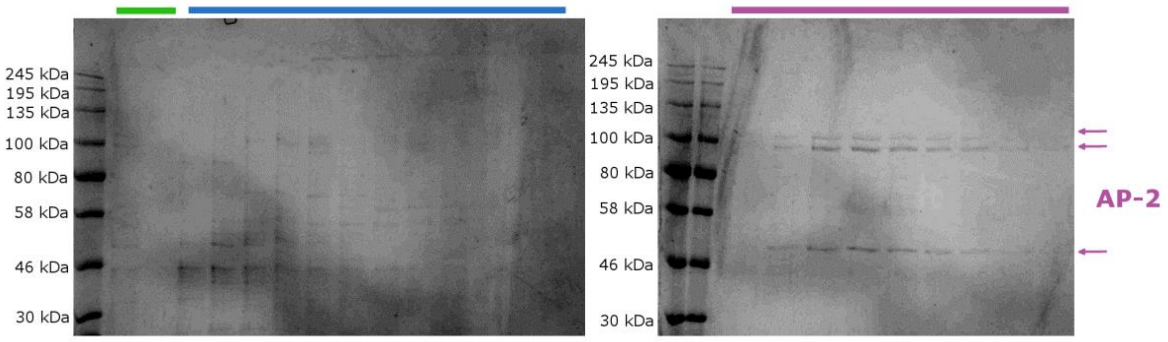

Figure 32. Purification of Adaptor protein 2 (AP-2) from pig brain.
(A) The UV trace from mixed adaptors run on hydroxyapatite biogel. AP-2 was eluted from the column with a linear phosphate gradient from 10 mM phosphate to 500 mM phosphate. The green line represents the expected increase in phosphate concentration and the brown line represents the detected salt concentration, corresponding to an increase in the amount of phosphate present. (B) Coomassie stained SDS-gels of the fractions obtained from the hydroxyapatite column. The coloured lines indicate the peaks in C that the fractions correspond to.

6.2.3 Both Crumbs and AICD recruit AP-2 from brain cytosol

Not all AP-2 is membrane bound; as well as existing on clathrin coated vesicles there is a cytosolic pool of AP-2 (Jackson et al., 2010). Therefore, the interaction of Crumbs and APP with cytosolic AP-2, using brain cytosol as with previous proteo-liposome recruitments, was examined. The intracellular domain of Crb2 was coupled to liposomes along with cysteine as a negative control (Pocha et al., 2011). The Crb2 human homologue was chosen due to the fact it is mainly expressed in the brain, as well as the retina and kidneys (van den Hurk et al., 2005), and that the recruitments were carried out in either brain cytosol or purified proteins isolated from brain. AICD was coupled to liposomes as a positive control. Full length APP is known to undergo AP-2 dependent clathrin mediated endocytosis, and AICD contains the tyrosine sorting motif (YXXϕ) which is recognised by the μ subunit of AP-2 (King and Turner, 2004, Owen and Evans, 1998, Ohno et al., 1995, Koo and Squazzo, 1994). The proteo-liposomes were incubated in brain cytosol, and contained 1 mol% $PI(4,5)P_2$ to help mimic the lipid composition of the plasma membrane. Also cytoplasmic AP-2 is thought to be in a locked form, blocking its binding to the cytoplasmic tails of membrane proteins. $PI(4,5)P_2$ in the plasma membrane causes a conformational change of AP-2 allowing the simultaneous binding of $PI(4,5)P_2$ and the cytoplasmic domains of membrane proteins (Jackson et al., 2010, Höning et al., 2005). The proteo-liposomes and their interaction partners were recovered by ultracentrifugation and samples were subjected to SDS-PAGE and Western blot analysis, using an antibody against the α subunit of AP-2 (Figure 35). Both AICD and Crb2 presenting liposomes were able to recruit AP-2 from brain cytosol. Both AICD and Crb2 were more efficient in recruiting AP-2 than control liposomes (cysteine). These control liposomes also showed some residual recruitment of AP-2 which is likely due to the $PI(4,5)P_2$ binding of AP-2.

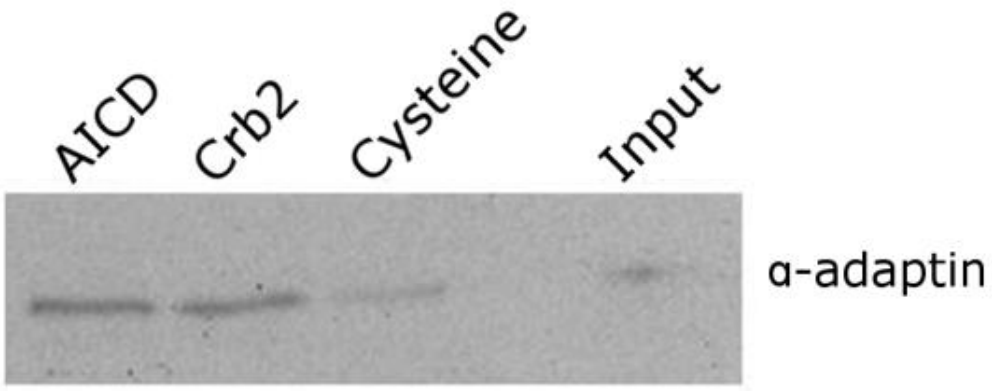

Figure 33 AP-2 is recruited from brain cytosol to AICD and Crb2 proteo-liposomes.
AICD, Crb2 and control (Cysteine) proteo-liposomes were incubated in brain cytosol. The final recruitment samples were analysed by SDS-PAGE and western blotting using an antibody against the α subunit of AP-2. (Input = 1%) (n=3).

6.2.4 AP-2 is recruited from mixed adaptors onto Crb2 proteo-liposomes

To develop the proteo-liposome recruitment system to allow for the creation and examination of artificial clathrin coated vesicles from purified components, the proteo-liposome method was modified through the use of the semi-pure mixed clathrin adaptors. These mixed adaptors were harvested from clathrin coated vesicles isolated from brain (6.2.2), and are therefore more pure than the previously used brain cytosol.

Figure 36A shows a Coomassie stained SDS-PAGE gel of the mixed adaptors used to test the effectiveness of the proteo-liposome recruitment system in the analysis of coat assembly from their purified components. Of note is the characteristic double band at around 80 to 100 kDa corresponding to the α and β subunits of AP-2. Figure 36B shows a comparison of the mixed adaptors and pig brain cytosol. Equal amounts of total protein were subjected to SDS-Page and Western blotting. AP-2 was found to be highly enriched in the mixed adaptors compared to brain cytosol, as determined using an antibody specific for the α subunit (Figure 36B). This was also the case for AP-1 as visualised using an antibody against its γ subunit. The clathrin adaptor AP180 was not enriched in the mixed adaptors compared to the brain cytosol (Figure 36B). Also of importance was that the Pals1 (Stardust) subunit of the Crumbs complex was not present in the mixed adaptors, this indicates that any interaction seen was not mediated by Pals1.

Proteo-liposome recruitments were conducted where $PI(4,5)P_2$ was excluded from the liposomes to allow for the specific analysis of the interaction partners of the cytoplasmic domains. AICD, Crb2 and control (cysteine) liposomes were incubated in two different amounts (25 µg and 125 µg) of mixed adaptors. Samples were isolated by ultracentrifugation and analysed by Western blotting using antibodies against the α-subunit of AP-2, the γ subunit of AP-1 and Pals-1. AP-2 was recruited from mixed adaptors to AICD and Crbs proteo-liposomes (Figure 36C). At lower amounts (25 µg) of mixed adaptors it becomes apparent that AP-2 has a lower affinity for Crb2 than it

does for AICD. The recruitment showed that no Pals1 was found in the samples. This and the fact that the mixed adaptors are semi-pure indicates that AP-2 is likely binding directly to the intracellular domain of Crb2 and AICD, and therefore that the interaction between AP-2 and Crb2 is not mediated by Pals1. It was also found that AP-1 was recruited to both AICD and Crb2 containing liposomes with a greater affinity for AICD than Crb2 at lower amounts of mixed adaptors (25 µg) (Figure 36C).

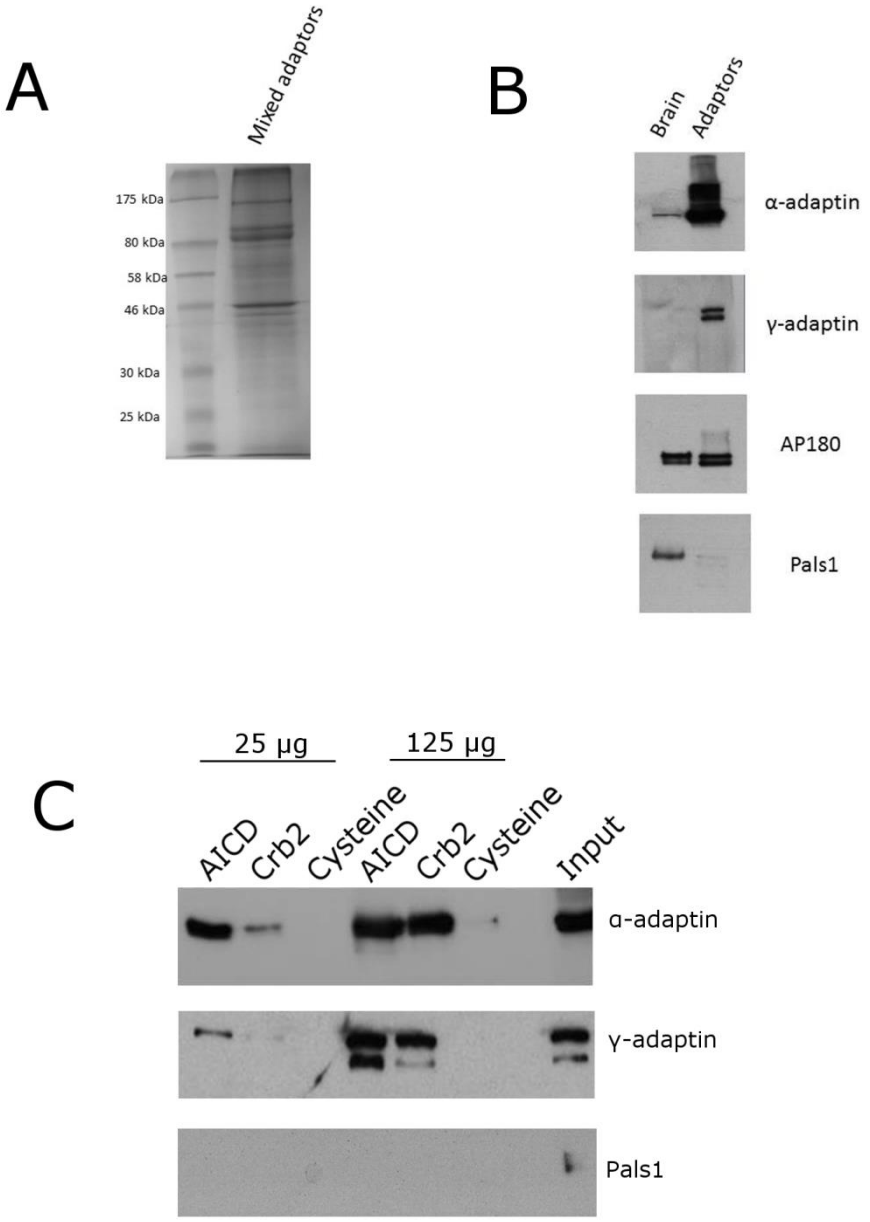

Figure 34 . AP-2 is recruited from mixed adaptors onto AICD and Crb2 proteo-liposomes.

(A) A Coomassie stained SDS-PAGE gel of the mixed adaptors used for the recruitment in C. (B) Western blot analysis of brain cytosol and mixed adaptors. Equal amounts of protein were loaded. Both AP-2 (α-adaptin) and AP-1 (γ-adaptin) are enriched in the mixed adaptors with the Pals1 subunit of the Crumbs complex is enriched in brain cytosol and not mixed adaptors. AICD, Crb2 and control (cysteine) proteo-liposomes were incubated with 25 µg and 125 µg of mixed adaptors. The samples were analysed by SDS-PAGE and western blotting using antibodies against the subunit of AP-2, the γ subunit of AP-1 and Pals-1 of the Crb complex. Brain cytosol was used as an input for Pals1 rather than mixed adaptors as B showed that Pals1 was not present in the mixed adaptors. (C) Both AP-2 and AP-1 are recruited to both AICD and Crb2 containing liposomes. (Input for α and γ adaptin = 14% of 125 µg and 71% of 25 µg) (n=3).

6.2.5 The C-terminal PEERLI motif of Crb2 is important for its interaction with AP-2 from mixed adaptors

The next stage in the development of the proteo-liposome recruitment system to analyse the assembly of protein coats from their purified components, was to determine if this modified system would allow for the examination of motifs in the intracellular domain of Crb2 that are important for AP-2 recruitment and binding.

Unlike APP, Crb2 does not contain a conventional tyrosine based sorting motif required for AP-2 binding. However, AP-2 can also recognise acidic dileucine based motifs in the cytoplasmic domains or membrane proteins. The dileucine motif [ED]xxxL[LI] is recognised by the σ subunit of AP-2 (Kelly et al., 2008, Janvier et al., 2003, Doray et al., 2007). The cytoplasmic domain of Crb2 does not contain this conventional dileucine motif. However, it does contain a PDZ (PSD-95/Discs large/ZO-1) binding, C-terminal EERLI motif. This motif is crucial for the interaction between Crb and the rest of the Crb complex (Bulgakova and Knust, 2009). The acidic dileucine like nature of the EERLI makes it a likely candidate for the AP-2 binding site of Crb2. To test this, several mutants of Crb2 C-terminal PEERLI domain were used. These mutant proteins were kindly provided by Elizabeth Knust's lab, and included a deletion of the PEERLI motif (dPEERLI), the substitution of either the C-terminal LI, the middle EE, or both, for alanine's (LI-AA, PAARLI and PAARAA respectively). The amino acid sequences of these Crb2 mutants can be seen in figure 37B. These mutants were selected to firstly determine if the PEERLI motif mediated the interaction between Crb2 and AP-2, and if so which particular amino acids in the motif could be important for this interaction.

Proteo-liposome recruitments were conducted using 25 µg of mixed adaptors, where wild type Crb2 (WT-Crb2) and the mutants described above were coupled to liposomes. Cysteine was used as a negative control to prove that any recruitment observed was due to the presence of the protein tails. Again no $PI(4,5)P_2$ was included

in the liposomes to ensure that the recruitment was specific to the tail used and not to the binding of the adaptors to $PI(4,5)P_2$ in the liposome membrane. The liposome samples were analysed by SDS-PAGE and Western blotting for AP-2 using an antibody directed against it's α subunit. All the mutant proteo-liposomes showed a reduction in the recruitment of AP-2 when compared to WT-Crb2, with all the mutants reducing the binding of AP-2 from the mixed adaptors, to a similar level (Figure 37A). This indicates that the PEERLI motif of Crb2 plays a key role in the interaction of Crb2 with AP-2.

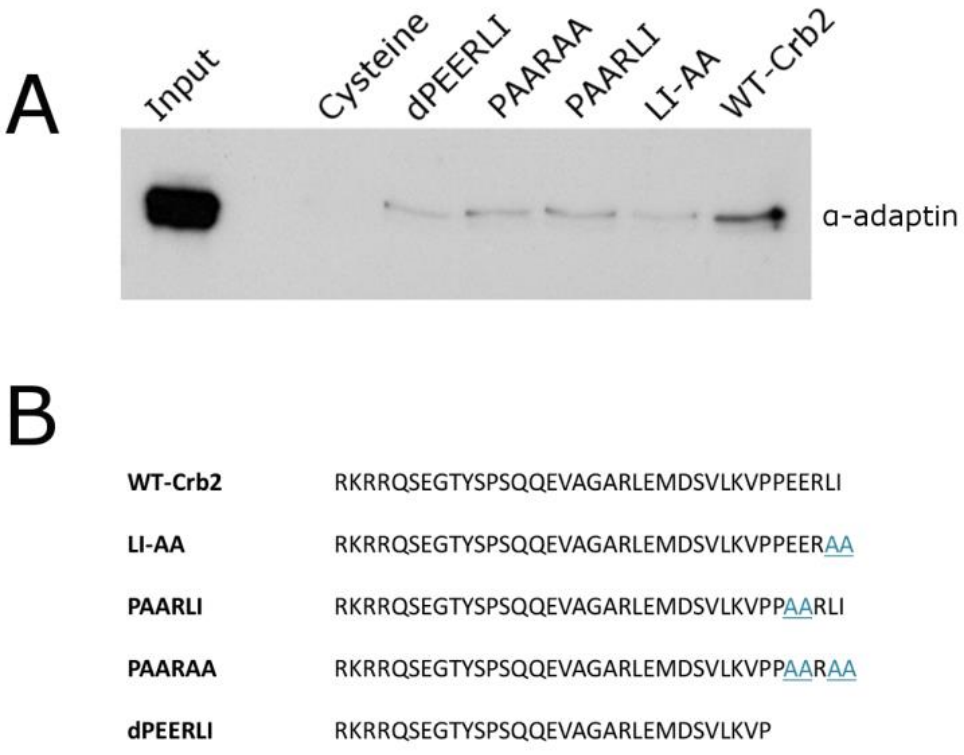

Figure 35. The PEERLI motif or Crb2 is crucial for the interaction between Crb2 and AP-2 recruited from mixed adaptors.
Crb2, mutants of Crb2 (LI-AA, PAARLI, PAARAA and dPEERLI) and control (cysteine) proteo-liposomes were incubated in 25 µg of mixed adaptors. Samples were analysed by SDS-PAGE and western blotting using an antibody against the α subunit of AP-2 (A). The mutations in the PEERLI motif of Crb2 reduce binding to AP-2. (B) The amino acid sequences of the Crb2 mutants and wild type (WT) Crb2 used for the recruitment in A. (Input = 71%) (n=3).

6.2.6 Disruption of the PEERLI motif of Crb2 reduces the binding of purifed AP-2

So far this chapter describes th modification of the proteo-liposome recruitment system to examine the recruitment of purifed protein coat components using the AP-2/ clathrin coat as a model. Using this system the PEERLI motif of Crb2 has been shown to be important for the recruitment of AP-2 from a sample of mixed adaptors. Due to the fact that the mixed adaptors used were only semi-pure, in order to further advance this system to examine the assembly of coats from purifed components, the purifed adaptor AP-2 was utilised. AP-2 was purifed from the mixed adaptors as described earlier in this chapter (6.2.2). Using purifed AP-2 also further refines the proteo-lipsome recruitment technique to allow for the analysis of native purifed proteins, rather than recombinant proteins, as seen in chapters 3 and 4.

To test whether the same effect is observed in AP-2 as well as mixed adaptors proteo-liposome recruitment experiments were conducted where AICD, WT Crb2 or the Crb2 mutants LI-AA, PAARLI and PAARAA, were coupled to liposomes. The amino acid sequence of the mutants used for this recruitment are shown in figure 38A. PI(4,5)P_2 was excluded from the liposomes to determine that any recruitment observed was due to binding to the cytoplasmic tail and not AP-2 binidng to PI(4,5)P_2. Figure 38C shows a Coomassie stained SDS-PAGE gel of the purifed AP-2 used in the recruitment. The AP-2 was also subjected to Western blot analysis using an antibody against the α subunit to ensure that the purifed protein was definetely AP-2 (Figure 38D).The proteo-liposomes containing the coupled tails were incubated in 25 µg of purifed AP-2. The recruitment samples were analysed by SDS-PAGE and Western blotting for AP-2 using an antibody directed against the α subunit (Figure 38B).

AP-2 was recruited to AICD and Crb2 proteo-liposomes (Figure 38B) demonstrating that this interaction due to the direct binding of AP-2 to the cytoplasmic tails. The mutant Crb2 proteins showed a reduction in the binding of AP-2, which supports the

results observed from the mixed adaptors. This demonstrates that the PEERLI motif of Crb2 is crucial for AP-2 binding, and adds another layer to the capabilities of the proteo-liposome recruitment system.

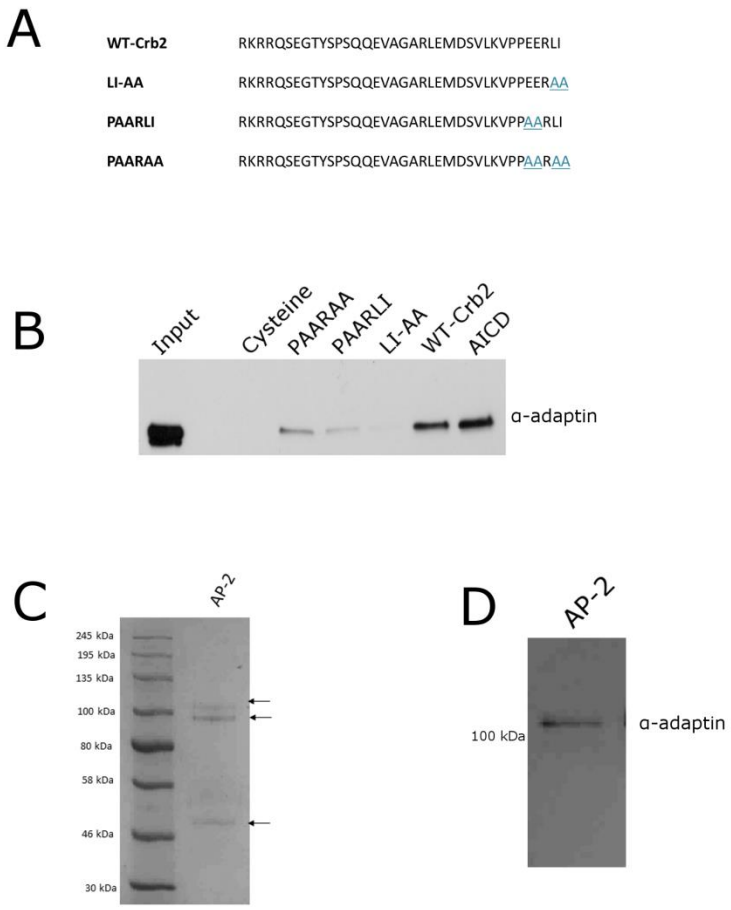

Figure 36. The PEERLI motif of Crb2 is required for its interaction with purified AP-2.
(A) The amino acid sequence of the Crb2 mutants used for the recruitment. AICD (positive control),Crb2, Crb2 mutants (LI-AA,PAARLI and PAARAA) and control (cysteine) proteo-liposomes were incubated in 25 µg of AP-2 purified from mixed adaptors. The recruitment samples were analysed by SDS-PAGE and western blotting using an antibody against the α subunit of AP-2. (B) AP-2 purifed from the mixed adaptors isolated from pig brain binds directly to Crb2 and the PEERLI motif is important in the AP-2/Crb2 binding.(Input = 20%) (n=3). (C) A Coomassie stained SDS-PAGE gel of the AP-2 purified from pig brain used in B. The arrows represent the α, β and µ subunits of AP-2 with the σ subunit being too small to appear on the gel (18 kDa). (D) Western blot of 0.5 µg of AP-2 using an antibody against the α-adaptin subunit.

6.2.7 The recruitment of clathrin to Crb2 and AICD proteo-liposomes

The use of the modified proteo-liposome recruitment system has so far shown that the clathrin adaptor AP-2 is recruited onto liposomes presenting the intracellular domains of the membrane proteins APP and Crb2. The next stage in the modification of the proteo-liposome recruitment method was to examine the recruitment of clathrin onto AICD and Crb2 presenting proteo-liposomes which contained bound AP-2. The process of clathrin mediated endocytosis is vital for the internalisation of various membrane proteins. The disruption of clathrin mediated endocytosis is known to play a role in human diseases, such as Alzheimer's disease (Wu and Yao, 2009). Therefore it is important that we have ways of examining the assembly and disassembly of the clathrin coat.

Liposome based systems have previously been utilised for examining certain stages of clathrin cage assembly. Primarily liposomes have been used in one of two ways. Protein free liposomes were used to examine certain aspects of coat assembly. This technique has been used to examine the assembly of the AP-3 coat (Drake et al., 2000), and the interaction of AP-2 with $PI(4,5)P_2$ (Höning et al., 2005). The second method involved the anchoring of a clathrin adaptor or a specific domain of a clathrin adaptor to the liposomes, and the examination of the assembly of a select part of the clathrin coat complex. This technique has been used to study the assembly of AP-1 coats (Crottet et al., 2002, Baust et al., 2006) , and the assembly of clathrin vesicles using the ENTH domain of the clathrin adaptor epsin (Dannhauser and Ungewickell, 2012). The recruitment of clathrin coats onto liposomes containing the cytoplasmic domains of receptors has not been examined until very recently. Kelly et al. (2014) have used a small Yxxϕ tyrosine based motif peptide anchored to liposomes to examine the assembly of AP-2 clathrin coats using recombinantly expressed AP-2.

The rest of this chapter examines the assembly of the AP-2/clathrin coat onto AICD and Crb2 containing proteo-liposomes. In this chapter it has been previously shown

that AP-2 was able to bind to both AICD and Crb2, but possibly with different affinities. Therefore the effect each receptor tail has on the recruitment of clathrin was examined. To do this the proteo-liposome recruitment assay was modified to resemble the liposome binding assay used by (Kelly et al., 2014). A detailed description of this method can be seen in chapter 2. Briefly AICD, Crb2 and control (cysteine) proteo-liposomes were created with a final lipid concentration of 0.4 mg/ml. Two sets of liposomes were created, one containing 5 mol% $PI(4,5)P_2$, while $PI(4,5)P_2$ was omitted from the second set. The proteo-liposomes were incubated in 0.8 µM of purified AP-2, followed by ultracentrifugation to recover the liposomes, and then the subsequent incubation in 0.2 µM clathrin. These proteo-liposomes were collected by ultracentrifugation and the supernatant and pellet analysed by SDS-PAGE on Coomassie stained gels.

Clathrin was recruited on to AICD proteo-liposomes containing $PI(4,5)P_2$ (Figure 39A). Clathrin was also recruited onto Crb2 $PI(4,5)P_2$ containing proteo-liposomes, and to a minor extent to control liposomes containing $PI(4,5)P_2$ (Figure 39A). Clathrin appeared to be recruited in similar levels onto AICD and Crb2 proteo-liposomes without $PI(4,5)P_2$, with very little clathrin recruited to control liposomes without $PI(4,5)P_2$ (Figure 39B). Of note is the fact there was no clathrin found in the pellet sample when no liposomes were added (see no lipid in figure 39B). This showed that the clathrin was definitely binding to liposomes. One observation was that the AP-2 was not detected in the pellet samples, which was likely due to the lack of sensitivity of the Coomassie stain. These results indicate that the presence of the cytoplasmic domain of membrane proteins does promote the recruitment of clathrin to synthetic liposomes.

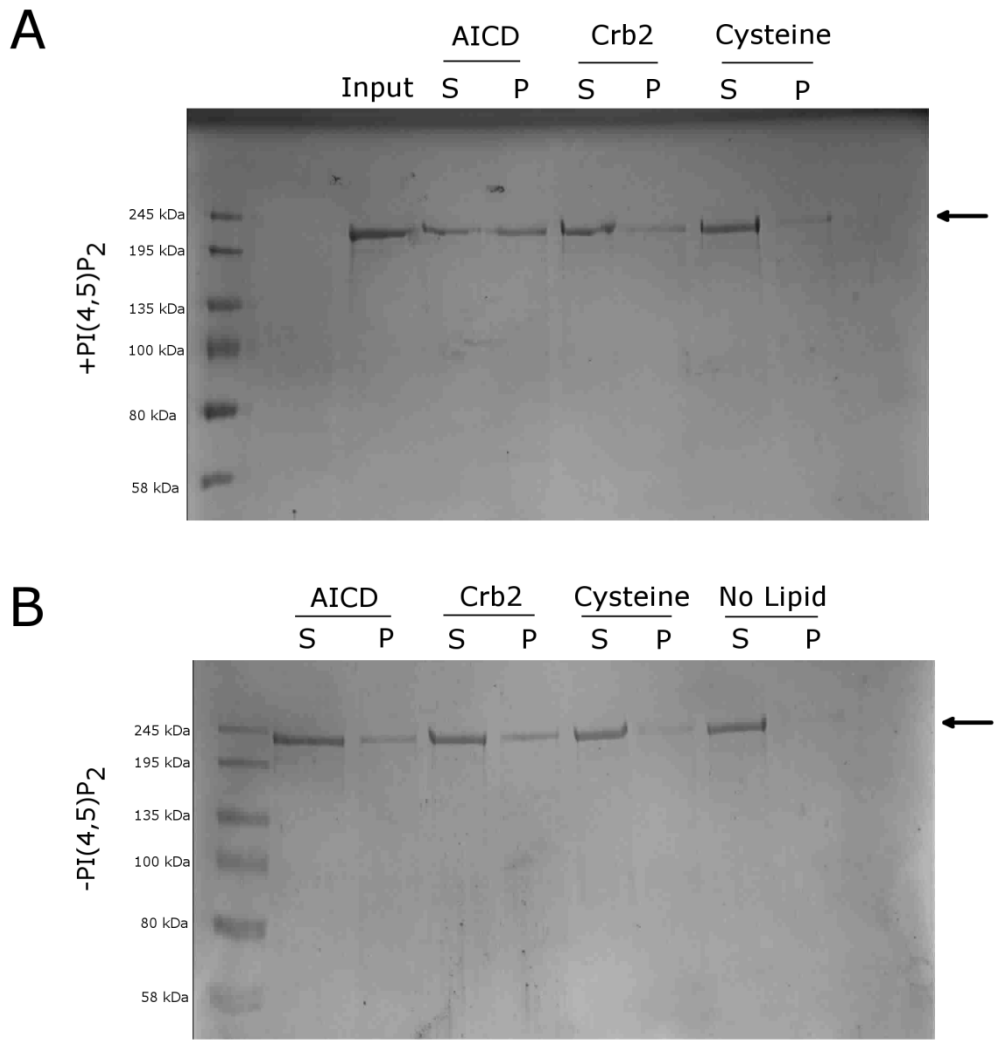

Figure 37. Clathrin is selectively recruited to AICD proteo-liposomes containing PI(4,5)P2.

AICD, Crb2 and control (cysteine) proteo-liposomes with (A) and without (B) PI(4,5)P_2 were sequentially incubated in AP-2 and clathrin. The proteo-liposomes were collected by ultracentrifugation and samples were analysed by SDS-PAGE. (A) A Coomassie stained SDS-gel of the samples obtained from the recruitment with liposomes containing PI(4,5)P_2. The arrow shows the band corresponding to the clathrin heavy chain. AICD and PI(4,5)P_2 containing liposomes recruits more clathrin than both Crb2 and cysteine (input = 100%). (B) A Coomassie stained SDS-gel of the samples obtained from the recruitment where PI(4,5)P_2 was omitted from the liposomes. Clathrin is recruited to AICD and Crb2 liposomes. The presence of both AICD PI(4,5)P_2 appears to be required for substantial clathrin recruitment.(n=3).

6.2.8 The clathrin/AP-2 complex is assembled on both Crb2 and AICD proteo-liposomes

Previously in this chapter it has been shown that Crb2 and AICD proteo-liposomes are able to recruit both AP-2 and clathrin. Therefore they could potentially be used to examine the assembly of AP-2/clathrin coats. As the AP-2 was not detectable previously by Coomassie stain, Western blot analysis was therefore used to detect both AP-2 and clathrin. AICD, Crb2 and control (cysteine) proteo-liposomes were created with a final lipid concentration of 0.4 mg/ml. Two sets of liposomes were created, one containing 5 mol% $PI(4,5)P_2$, and on in which $PI(4,5)P_2$ was omitted.

The proteo-liposomes were incubated in 0.8 µM of purified AP-2 followed by ultracentrifugation to recover the liposomes, and then the subsequent incubation in 0.2 µM clathrin. These proteo-liposomes were collected by ultracentrifugation. The supernatant (from the clathrin incubation step as the supernatant from the AP-2 incubation step was discarded before the incubation in clathrin) (Figure 40C) and the pellet were analysed by SDS-PAGE and Western blotting using antibodies against the clathrin heavy chain and the α subunit of AP-2.

AP-2 was recruited to AICD and Crb2 proteo-liposomes compared to the cysteine control liposomes (Figures 40A and 40B). AP-2 was also preferentially recruited to liposomes containing PI(4,5)P2, which is consistent with the fact that AP-2 is known to bind to $PI(4,5)P_2$ (Höning et al., 2005). Also of note is the difference in the recruitment of AP-2 observed between AICD and Crb2 proteo-liposomes, with AICD showing more efficient recruitment of AP-2. This demonstrates that AP-2 binds to AICD and Crb2 with different affinities probably due to the difference in their AP-2 binding motifs.

Clathrin was found to be enriched on AICD proteo-liposomes compared to both Crb2 liposomes and control liposomes (Figure 40B). Crb2 proteo-liposomes in the absence of $PI(4,5)P_2$ appeared to recruit slightly more clathrin than control liposomes. In the presence of however Crb2 and control liposomes were able to recruit clathrin to a

similar extent (Figure 40B). The presence of $PI(4,5)P_2$ in the liposome membrane, appeared to enhance the recruitment of clathrin (Figure 40B), indicating $PI(4,5)P_2$ is key to the assembly of the clathrin complex.

Taken together these results demonstrate that AICD proteo-liposomes are more efficient recruiters of the AP-2/clathrin complex than Crb2 proteo-liposomes which also have a slightly higher affinity for the complex than control liposomes. They also show that the AP-2 clathrin complex can be assembled on liposomes without the cytoplasmic domain of a membrane protein, likely through the binding of $PI(4,5)P_2$, and that the presence of this domain enhances the recruitment of the AP-2/clathrin complex. The type of binding motif present in the intracellular domain of membrane proteins also appears to influence the recruitment of the AP-2/clathrin complex. Crucially this work demonstrates the ability of the modified proteo-liposome recruitment system to examine the assembly of the AP-2/clathrin complex protein complexes onto liposomes containing the intracellular domains of membrane proteins. It also allows for the discrimination between cytoplasmic tails containing different binding motifs.

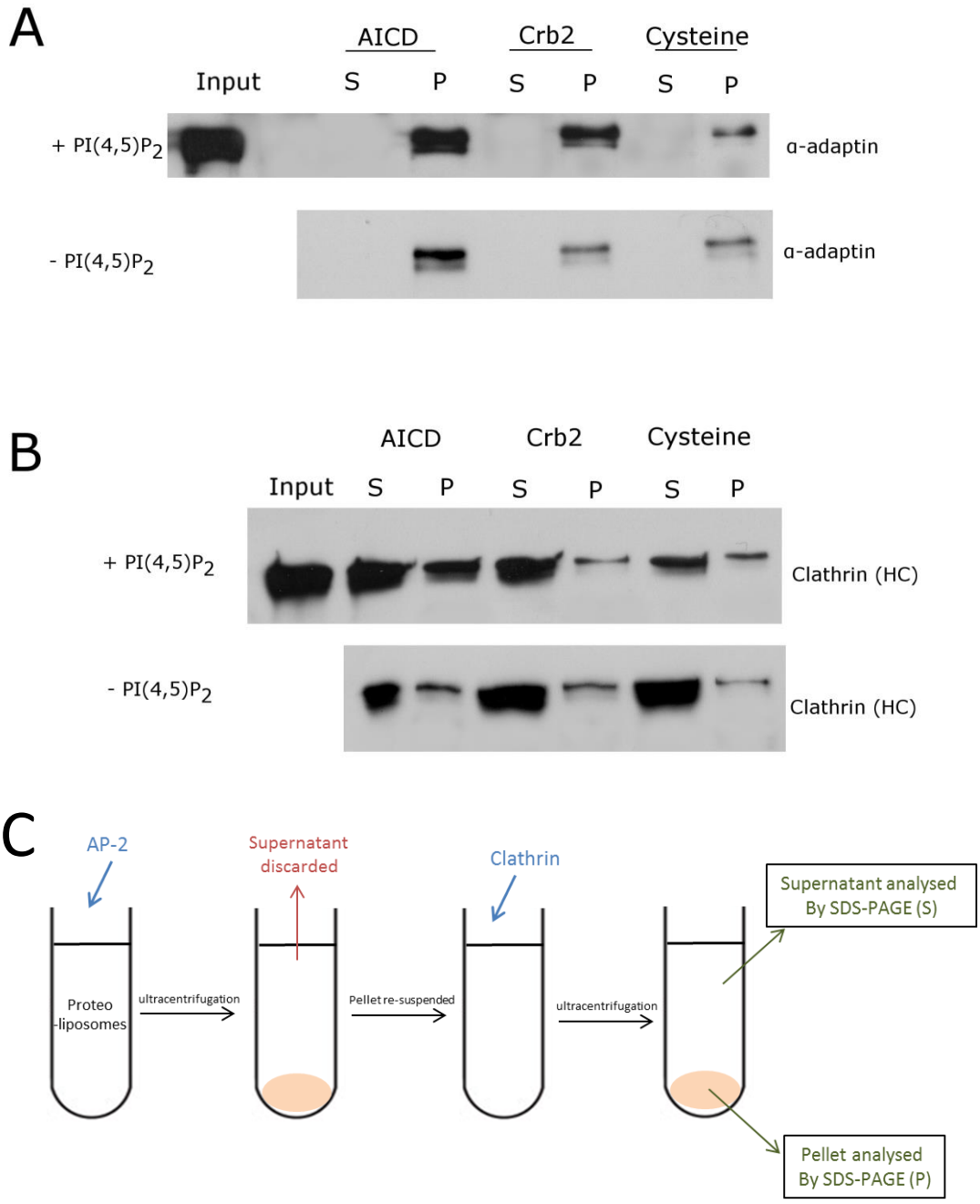

Figure 38. Both AP-2 and clathrin are recruited preferentially to AICD containing liposomes.

AICD, Crb2 and control (cysteine) proteo-liposomes with and without PI(4,5)P_2 were used to try and create in vitro clathrin coated vesicles by sequential incubation in AP-2 and clathrin. The liposomes were pelleted by ultracentrifugation and the supernatant and pellet fractions adjusted with Laemmli buffer and analysed by SDS-PAGE and western blotting using antibodies against the α subunit of AP-2 and clathrin's heavy chain. (A) AP-2 is recruited on to AICD and Crb2 liposomes compared to controls. This recruitment is enhanced when the liposomes contained PI(4,5)P_2. (B) The presence of AICD and to a lesser extent Crb2 increases the recruitment of clathrin. This recruitment is enhanced onto liposomes containing PI(4,5)P_2 . (Input = 100) (n=3) (C) An overview of the method used.

6.3 Discussion

This chapter describes the development of the proteo-liposome system to analyse the assembly of protein coats from their purified components, using the AP-2/clathrin coat as a model. It is show that AP-2 was able to directly interact with the cytoplasmic domain of both APP (AICD) and Crb2. Through the use of the proteo-liposome recruitment system and mutant proteins of Crb2 intracellular domain it was shown that the C-terminal PEERLI motif in the cytoplasmic domain of Crb2 was the likely binding site for AP-2 as mutations in this site reduced the binding of AP-2. The proteo-liposome recruitment system was also used to create artificial clathrin coated vesicles, demonstrating that purified coat analysis is possible using this system.

6.3.1 The AP-2 binds to AICD and Crb2

The results from this chapter demonstrates that AP-2 binds to the intracellular domain of AICD and Crb2, and that AP-2/clathrin complex can be assembled on both AICD and Crb2 containing liposomes to different degrees. APP is known to undergo clathrin mediated endocytosis. AICD contains a tyrosine based endocytic motif recognised by AP-2. The endocytosis of APP is important in its trafficking and processing (Thinakaran and Koo, 2008).

This interplay between Crb2 and the AP-2/clathrin links Crb2 to clathrin mediated endocytosis. This is consistent with previous studies that show that the Scribble module is able to regulate the polarity of epithelial cells by modulating the AP-2 dependent endocytosis of Crb (de Vreede et al., 2014). The Scribble module is a protein complex that also controls epithelial cell polarity. It is an important regulator of the basolateral membrane where it excludes apical protein localisation (de Vreede et al., 2014). The proteo-liposome recruitment system was able to establish that a direct interaction exists between the intracellular domain of Crb2 and the clathrin adaptor AP-2.

6.3.2 The importance of the PEERLI motif of Crb2 for its interaction with AP-2

Through the use of the proteo-liposome recruitment system and the use of mutant proteins of the cytoplasmic domain of Crb2, it was shown that the PEERLI motif, located at the C-terminus of Crb2 intracellular domain, was crucial for its interaction with AP-2. Mutant proteins were used where EE, LI, or both from the PEERLI motif, were substituted for alanine. There was also a mutant where the PEERLI motif was removed. These mutants showed a reduction in the binding of AP-2 compared to wild type Crb2. However, the method could not distinguish between AP-2 binding to the different mutants. This could have been due to a number of factors. Firstly, the proteo-liposome recruitment assay might not be sensitive enough to pinpoint the binding domain of AP-2 to one or two amino acids. On the other hand, the whole of the PEERLI domain might be required for AP-2 binding, and not just one or two amino acids in this domain. The EERLI motif in Crbs is known to be vital for the function of the protein. It is highly conserved between *Drosophila, C. elegans* and humans, and serves as the binding site for the Stardust/Pals1 protein (Klebes and Knust, 2000, Roh et al., 2002, van den Hurk et al., 2005). The EERLI motif is also required to but not sufficient to rescue the phenotype of Crb mutants, with rescue also requiring the N-terminus of the intracellular domain of Crb (Klebes and Knust, 2000).

The intracellular domain of Crb2 does not contain the conventional tyrosine based sorting motif for clathrin mediated endocytosis (Yxxϕ), unlike APP. However, its PEERLI domain does contain a C-terminal leucine and isoleucine which is characteristic of the classical dileucine based motif ([ED]XXXL[LI]) found in the cytoplasmic domains of some membrane proteins, and is recognised by the σ subunit of AP-2. Therefore the fact that mutating this domain reduces the binding of AP-2, suggests that it is this motif that is required for AP-2 binding. The binding of AP-2 to the PEERLI motif of Crb2 suggests that Crb2 may be internalised by AP-2 mediated

clathrin endocytosis. Indeed, AP-2 has been found to regulate the endocytosis of Crb2 as the mutation of AP-2 retains Crb2 on the plasma membrane (Lin et al., Unpublished).

6.3.3 The recruitment of the clathrin coat complex to proteo-liposomes

The proteo-liposome recruitment system has been successfully used in this chapter to recruit the AP-2 clathrin complex. AP-2 was able to bind both AICD and Crb2 with a stronger binding to AICD. This is in keeping with the fact APP and Crb2 have different binding motifs for AP-2. APP contains a tyrosine based sorting motif (Yxxϕ), whereas Crb2 contains a dileucine based motif (King and Turner, 2004). These two motifs are known to bind AP-2 with different affinities (Jackson et al., 2010) explaining the fact that AICD proteo-liposomes seem more efficient at recruiting AP-2.

AP-2 was recruited to liposomes both with and without $PI(4,5)P_2$, however, its recruitment was enhanced by the presence of PI(4,5)P2. Previous work has shown that AP-2 is not recruited when $PI(4,5)P_2$ is not present (Höning et al., 2005, Jackson et al., 2010, Kelly et al., 2014). AP-2 is thought to recognise $PI(4,5)P_2$ in the plasma membrane which causes it to switch to an "open" conformation allowing the further binding of $PI(4,5)P_2$ and the intracellular domains of membrane proteins via the tyrosine or dileucine based sorting motifs (Jackson et al., 2010, Kelly et al., 2014).

The modified proteo-liposome recruitment system used for the assembly of artificial clathrin coated vesicles was based on the method used by Kelly et al. (2014). However, it is worth noting that Kelly et al. (2014) utilised AP-2 that was recombinantly expressed and purified from *E.coli*, and contained a truncated α subunit. Jackson et al. (2010) also used individual subunits of AP-2. The proteo-liposome recruitments in this chapter used native full length AP-2 purified from coated vesicles, harvested from pig brain, indicating that all the subunits of AP-2 were present and functional. The AP-2 purified from brain has been previously shown to contain contaminants of other clathrin coated vesicle components which may influence the recruitment of the clathrin

complex (Lindner and Ungewickell, 1992). This was used by Kelly et al. (2014) as a reason for the use of recombinant AP-2. Although in this chapter the Coomassie stained gel of the native purified AP-2 showed that it was pure, and did not visibly contain any contaminating proteins, the presence proteins not detected by the Coomassie stain may account for the slight recruitment of both AP-2 and clathrin to cysteine control liposomes absent of $PI(4,5)P_2$.

Overall this chapter shows the proteo-liposome recruitment system is both valuable and versatile. Its use in the analysis of the recruitment of the AP-2/clathrin complex demonstrates that the analysis of protein coats from their purified components is possible using this modified proteo-liposome recruitment method.

Chapter 7

Discussion

Chapter 7-Discussion

This thesis describes the development of a proteo-liposome recruitment system based on similar methods that have been used previously. Baust et al. (2006) utilised a liposome based system to examine the ARF1, GTP and PI(4,5)P_2 mediated assembly of AP-1 coats, onto liposomes presenting the cytoplasmic tails of the gpI envelope glycoprotein of the *Varicella zoster* virus and the lysosomal integral membrane protein Limp II (Crottet et al., 2002, Baust et al., 2006). Similar liposome based methods have also been used to examine the recruitment of AP-3 onto liposomes presenting the cytoplasmic domain of LAMP (Bourel-Bonnet et al., 2005). Pocha et al. (2011) utilised a proteo-liposome recruitment system to examine the interaction of the intracellular domain of Crb2 with the retromer complex.

In this thesis the proteo-liposome recruitment system was developed and used for the analysis of the interactomes of the intracellular domains of membrane proteins, and the assembly of protein coats from their purified components. APP was used as a model membrane protein to help establish the method, and also to examine novel interactors of APP's intracellular domain (AICD), with a view to gaining a greater understanding of APP's physiological function. Two novel AICD binding partners the mTOR complex and the PIKfyve complex were investigated.

7.1 APP interacts with both the mTOR and PIKfyve complex's

Using the proteo-liposome recruitment system it was established that the mTOR complex interacts with AICD (chapter 3). This interaction was mediated by the N-terminal region of AICD. The interaction was also found to be enabled by the direct binding of mTOR to AICD, via mTOR's kinase domain. The same proteo-liposome recruitment system was utilised to examine the interaction of AICD with the PIKfyve

complex (chapter 4). AICD was shown to recruit both PIKfyve itself, and the scaffold subunit Vac14, and this interaction was mediated by the C-terminal region of AICD. AICD was found to interact with the PIKfyve complex through direct binding between the C-terminus of AICD and the Vac14 subunit of the PIKfyve complex. The proteo-liposome recruitment system was therefore able to demonstrate that the mTOR and PIKfyve complexes bind to different motifs on AICD. This led to the question: what motifs in the N-terminus and C-terminus of AICD are required for the binding to the mTOR and PIKfyve complexes respectively?

APP is known to interact with a number of cytosolic proteins through its intracellular domain (Thinakaran and Koo, 2008). This intracellular domain is also crucial for APP endocytosis and trafficking (Thinakaran and Koo, 2008, Vieira et al., 2010). AICD has been shown to be an intrinsically unstructured protein that undergoes conformational switching, allowing it to adopt different conformations depending on the binding partner present (Das et al., 2012). This is one explanation of how AICD can bind to a variety of intracellular proteins.

AICD is also known to contain several motifs important for mediating its interaction with other proteins, and the phosphorylation of a number of AICD residues is also crucial for AICD protein interactions (Oishi et al., 1997, Schettini et al., 2010) (Figure 41). The YTSI motif of AICD is located near the cell membrane, and is required for APP's basolateral sorting in polarised epithelial cells (Icking et al., 2007, Lai et al., 1995). The YENPTY motif is the most widely studied AICD motif due to its array of interaction partners. It contains the consensus sequence for clathrin mediated endocytosis, and a motif for phosphotyrosine binding domain interactions. The YTSI and YENPTY motifs are both required for the degradation of APP in lysosomes (Lai et al., 1995, Chang, 2010). AICD also contains an N-terminal helix capping box motif (VTPEER) which serves as a binding site for 14-3-3γ involved in the FE65 dependent gene transcription

by AICD (Sumioka et al., 2005). AICDs multiple motifs, and its phosphorylation sites, both contribute to its ability to bind a wide variety of adaptors, and may help explain how AICD is able to bind mTOR and PIKfyve. AICD is not likely to bind both the mTOR and PIKfyve complexes at the same time due the large size of the two complexes compared with the short AICD peptide.

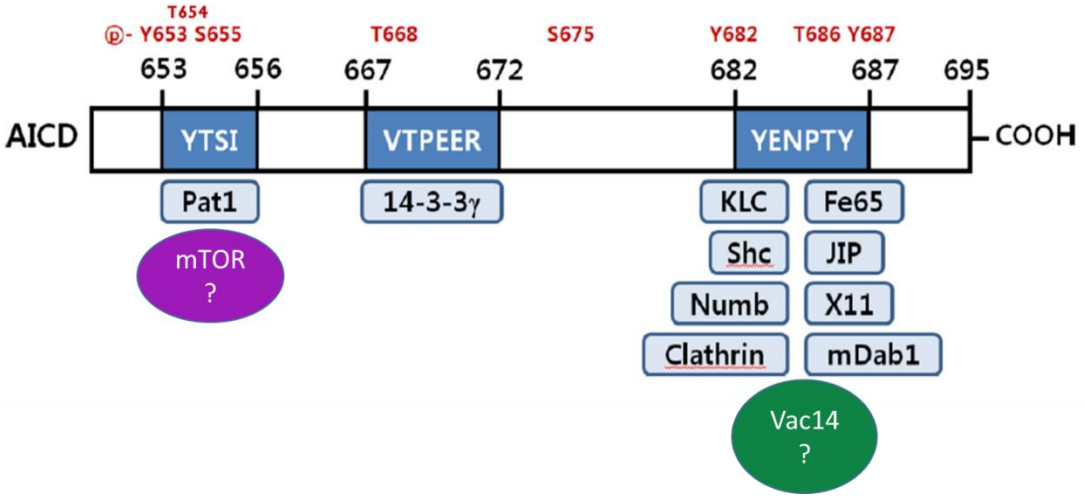

Figure 39. Binding motifs and phosphorylation sites on AICD.
AICD contains 3 major binding motifs shown in blue. The binding partners of these motifs are shown below each motif, with the potential binding sites for mTOR and Vac14 included. The eight phosphorylation sites of AICD are shown in red. Figure adapted from Chang (2010).

7.1.1 The AICD-mTOR complex interaction

In chapter 3 it was shown that mTOR was recruited to the first 10 N-terminal amino acids of AICD. The only motif shown in figure 41 that is contained in these first 10 N-terminal amino acids is the YTSI motif. This motif is required for the basolateral sorting of APP, and is bound by the microtubule binding protein Pat1 (protein interacting with APP tail 1), and this interaction mediates APP's transport through the secretory pathway (Buoso et al., 2010, Lai et al., 1998). The YTSI motif also contains 3 phosphorylation sites Y653, T654 and S655. S655 is required for the retromer

dependent endosome to TGN trafficking of APP (Vieira et al., 2010). T654 and S655 are known to be phosphorylated in vitro by protein kinase C, and by calcium and calmodulin dependent protein kinase II (CaMKII) in several cell lines (Oishi et al., 1997). Both of these enzymes are serine/threonine protein kinases, as is mTOR. Therefore, this YTSI motif of AICD is a likely candidate for mTOR phosphorylation and would explain the results of chapter 3 where mTOR is recruited to the first 10 amino acids of AICD, which contains the YTSI motif.

Work conducted by Balklava et al. (under review A) suggests that the *C. elegans* homologue of APP (APL-1) activates mTOR in concert with Rag-GTPases, and that several mTOR developmental processes including germ line expansion and fat metabolism are APL-1 sensitive. The results shown in chapter 3 and those of Balklava et al. (under review A) allow for the suggestion of a potential model, whereby mTOR binds to AICD, via its kinase domain, activating mTOR, which may lead to phosphorylation of APP's YTSI motif. The interaction between APP and mTOR has several implications for Alzheimer's disease.

mTOR signalling has previously been shown to be elevated in the brains of Alzheimer's disease patients, and this elevation in mTOR signalling correlates with the progression of the disease (Pei and Hugon, 2008). Additionally mTORC1 and mTORC2 have been shown to drive Tau toxicity in a *Drosophila* tauopathy model, with mTOR known to regulate the phosphorylation and degradation of Tau (Khurana et al., 2006, Caccamo et al., 2013). Could mTOR signalling provide a link between the processing of APP and the modification of Tau? Does the amyloidogenic processing of APP lead to increase mTOR signalling, which then causes the phosphorylation of tau and contribute to tau toxicity? (Li et al., 2005b, Tang et al., 2013). The investigation of the functional significance of the interaction between APP and mTOR, as characterised by the proteo-liposome recruitment method, would have important implications for both APP function and Alzheimer's disease.

7.1.2 The AICD-PIKfyve complex interaction

Chapters 4 and 5 examined the interaction between APP and the PIKfyve complex and what this interaction means in terms of APP function. Using the proteo-liposome recruitment method it was established that the intracellular domain of APP (AICD) recruits both Vac14 and PIKfyve. It was also established that the interaction was direct between AICD and Vac14, and was mediated by AICD's C-terminus. The role of AICD's C-terminus in mediating the interaction with the PIKfyve complex is supported by the results of chapter 5 which showed that APP co-localises with Vac14 and $PI(3,5)P_2$ (observed with the ML1Nx2 probe) in HeLa cells and that APP, AICD and AICD-Tr4 overexpression drives the production of $PI(3,5)P_2$ positive vesicles.

A candidate AICD motif for mediating the PIKfyve interaction is the YENPTY motif. This motif contains the NPXY type 1 β turn and is required for AICD binding to a number of well-established effectors including Fe65 (Borg et al., 1996). In chapter 5 the expression of a mutant of AICD, in which the YENPTY motif was deleted, failed to stimulate the production of $PI(3,5)P_2$ positive vesicles observed upon APP, AICD and AICD-Tr4 overexpression, further adding support to the YENPTY motif being important in the APP/PIKfyve complex interaction. In AICD the YENPTY motif is followed by a lysine, two phenylalanine residues and a glutamic acid residue, giving rise to the YENPTYKFFE motif, which contains two overlapping tyrosine based motifs (Lai et al., 1995, Tuli et al., 2009). This YKKFE motif mediates the interaction of APP with AP-4, which is important for mediating APP TGN-to-endosome transport (Burgos et al., 2010). The proteo-liposome recruitments from chapter 4 demonstrate that the AICD mutant Tr4 was able to recruit the PIKfyve complex from brain cytosol. However, both Tr4 and Tr3 AICD mutants were bound directly by purified recombinant Vac14. The Tr3 mutant lacked the C-terminal seven amino acids of AICD, present in Tr4, therefore deleting the two phenylalanine and the glutamic acid residues from the end of the

YENPTYKFFE motif. One explanation for this result could be that one tyrosine based motif in the YEPNTYKFFE domain might be enough to mediate the interaction with purified recombinant Vac14 alone; however, both tyrosine motifs may be required to recruit the whole PIKfyve complex.

7.1.2.1 Implications of the relationship between APP and PIKfyve in Alzheimer's disease

In chapter 5 a potential model for the role of the PIKfyve complex in APP trafficking was proposed. APP, upon arrival at endosomes interacts with the PIKfyve complex through direct binding to Vac14, stimulating the PIKfyve dependent production of $PI(3,5)P_2$ positive vesicles, leading to APP sorting away from the endosomal system. This model can be used to propose a novel mechanism for the role of APP in Alzheimer's disease. Rather than the toxic gain of the beta amyloid peptide upon APP cleavage, could it be that the cleavage of APP may prevent APP from activating the PIKfyve complex, and therefore reduce the levels of $PI(3,5)P_2$? This would interrupt the function of endosomes, resulting in vacuolation of the cell, characteristic of decreased $PI(3,5)P_2$ levels. Interestingly enlarged vesicles with the characteristics of endosomes and lysosomes have been observed in the brains of Alzheimer's disease patients (Nixon et al., 2000). The disruption of the endosomal and lysosomal systems could also account for the accumulation of beta amyloid through the defective clearance of the peptide.

The results of chapter 4 and 5 demonstrate that APP interacts with the PIKfyve complex, both biochemically and functionally. The PIKfyve complex has previously been shown to be crucial for neuronal function and integrity, with the knock-out or pharmacological inhibition of the PIKfyve complex causing endosomal dysfunction and profound neurodegeneration (Chow et al., 2007, Chow et al., 2009, Zolov et al., 2012, Zhang et al., 2007b). The results of chapter 5 support the idea that APP may act as an activator of the PIKfyve complex. Balklava et al. (under revision B) showed that in *C.*

elegans, the homologue of APP (APL-1) is linked both genetically and functionally to PIKfyve, was required for PIKfyve function, and was able to act as an upstream activator of the PIKfyve complex.

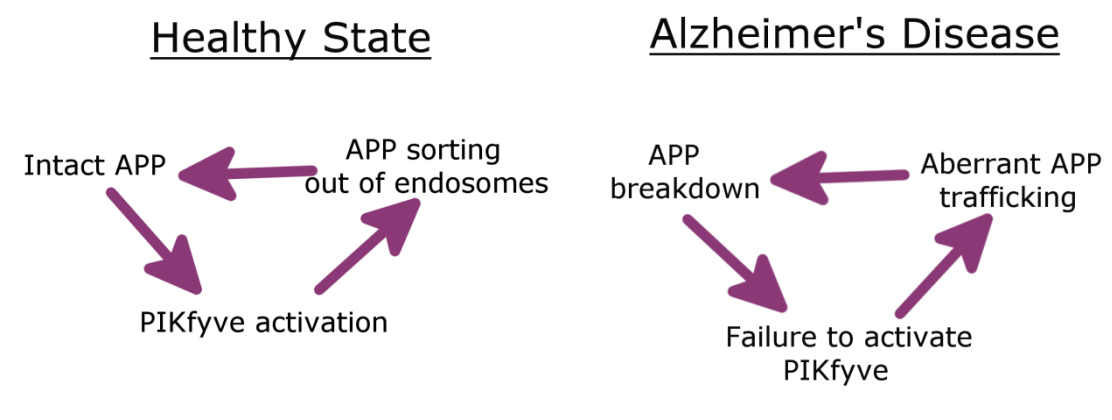

Figure 40. A potential model for the role of the APP/PIKfyve complex interaction in Alzheimer's disease
The model suggests that in the normal healthy state APP may be able to regulate its own trafficking out of the endosomal system through the activation of PIKfyve. In Alzheimer's disease APP breakdown may mean APP fails to activate PIKfyve, resulting in aberrant APP trafficking potentially leading to APP accumulation in endosomes contributing to its increased breakdown by secretases residing in endosomal compartments.

It is widely known that the aberrant processing of APP by beta and gamma secretases plays a crucial role in the pathology of Alzheimer's disease. This aberrant processing of APP both produces Aβ, the toxic peptide that aggregates and is a key component of the plaques in Alzheimer's disease brains, and also destroys full length APP. Could it be that APP is able to meditate its own trafficking away from the endosomal/lysosomal system, which is also enriched in gamma secretases (Tam et al., 2014, Pasternak et al., 2003), in a PIKfyve dependent process? If this was the case the inhibition of PIKfyve would likely cause APP to become stuck in the endo/lysosomal system, making it more susceptible to cleavage by gamma secretases. PIKfyve complex inhibition would not only effect the trafficking of APP but would also effect the trafficking of other PIKfyve cargo, therefore disrupting normal endosomal homeostasis. It could also be possible that the aberrant processing of APP would reduce its ability to

interact with and activate the PIKfyve complex, which would disrupt normal endosome function. Abnormal endosome function is known to play a role in Alzheimer's disease and it thought to be involved in neurodegeneration (Nixon et al., 2000). Figure 42 shows schematic of the potential role the APP/PIKfyve complex interaction may have in Alzheimer's disease.

7.1.2.2 The use of a PI(3,5)P_2 probe

The use of the PI(3,5)P_2 probe (ML1Nx2 fused to a fluorescent protein tag) (Li et al., 2013) was a valuable tool for examining the functional significance of the interaction between APP and the PIKfyve complex. The probe allows for the dynamic analysis of PI(3,5)P_2 which has not previously been possible. Using the probe it was established that APP-GFP co-localises with PI(3,5)P_2 vesicular structures in HeLa cells further supporting the proteo-liposome recruitment data of AICD. The number of PI(3,5)P_2 positive vesicles (as observed using the probe) was increased upon over expression of APP, AICD and ACID-Tr4. This suggests that APP increases PIKfyve dependant fission of vesicles with important implications for trafficking. Also the role of PIKfyve in APP trafficking may have important implications for Alzheimer's disease. According to our model the inhibition of PIKfyve and therefore the reduction in PI(3,5)P_2 levels cause an accumulation of APP and inhibit its degradation. Low levels of PI(3,5)P_2 have been associated with neurodegeneration (Zhang et al., 2007b). Therefore the PI(3,5)$P_{2\ probe}$ may prove a valuable tool to examine PI(3,5)P_2 dynamics in tissue from Alzheimer's disease patients to ultimately see if PI(3,5)P_2 loss may be a contributing factor in neurodegeneration.

These ideas and the findings of chapters 4 and 5 lead to a number of questions that will need to be addressed to investigate any role the APP/PIKfyve complex interaction may have in Alzheimer's disease. How does a dysfunctional endo/lysosomal system caused by PIKfyve loss of function lead to neurodegeneration? Can abnormal PIKfyve function be observed in Alzheimer's disease models and in patient samples? Could

finding a PIKfyve activator be able to reduce endosomal and lysosomal dysfunction, and ultimately reduce neurodegeneration.

7.1.3 The link between mTOR and PIKfyve

The interactions observed between APP and mTOR, and APP and the PIKfyve complex are especially interesting considering the mTOR and PIKfyve complexes are linked. The PIKfyve dependant production of $PI(3,5)P_2$ is known to play an important role in the recruitment of mTORC1 to lysosomal membranes (Bridges et al., 2012, Jin et al., 2014). The raptor subunit of mTORC1 is known to bind to $PI(3,5)P_2$ aiding in the translocation of mTORC1 from the cytosol to late endosomal/lysosomal membranes (Bridges et al., 2012). Jin et al. (2014) showed that $PI(3,5)P_2$ is required for the activation of TORC1 in yeast; the TORC1 inhibition of autophagy is defective in mutants with low levels of $PI(3,5)P_2$, and that $PI(3,5)P_2$ is required for complete autophagy in yeast. Therefore $PI(3,5)P_2$ is a negative regulator of autophagy, by positively regulating TORC1 activity (Jin et al., 2014).

The ability of APP to interact with and activate both mTOR and PIKfyve (as observed in this thesis, and by Balklava et al. (under revision A), and Balklava et al. (under revision B)) and the link between PIKfyve and mTOR undoubtedly have implications for APP function as well as that of $PI(3,5)P_2$. Examining the interplay and the functional significance of these three proteins in more detail will have important implications for the roles played by these three proteins in neurodegeneration and Alzheimer's disease.

7.2 The proteo-liposome system: a valuable tool for studying receptor interactions.

The primary aim of this thesis was to validate and extend the use of a model membrane proteo-liposome recruitment system, as a method for determining the intracellular interactome of membrane receptors, and for examining these interactions in more detail.

The main advantages of this technique for studying the intracellular interactome of membrane proteins are that the liposomes provide a membrane context where the lipid composition can be manipulated depending of the native lipid environment the membrane protein resides in. Therefore, it takes into account interactions of membrane proteins, in which the surrounding membrane lipids also play a role. This allows for the detection of interactions that would not be possible using more conventional methods such as pull downs or co-immunoprecipitations. Another advantage of the proteo-liposome recruitment method over more conventional and widely used methods, such as pull downs is that there is no need to include any form of detergent. This allows for the detection of weaker interactions as well as stronger ones. These weaker interactions would be disrupted by the detergent included in more conventional methods for examining protein-protein interactions (Otzen, 2011).

Using APP as a model transmembrane protein the proteo-liposome recruitment method was used to examine two novel interaction partners of its intracellular domain (AICD); the mTOR and PIKfyve complexes. The proteo-liposome recruitment method was used to examine the interactions from brain cytosol samples where the complete set of proteins should be available, so both indirect and direct interactions can be detected. One advantage of using the proteo-liposome recruitment method in brain cytosol samples is that an analogue of GTP (GTPγS) can be added activating GTPases, and therefore allowing for the detection of interactions dependant on GTPase activity. Baust et al. (2006) utilised this liposome recruitment method to

examine the assembly of adaptor protein 1A coats, a process which requires the activity of ARF1, a guanine nucleotide binding protein.

During the analysis of AICD's interaction with the mTOR and PIKfyve complexes the proteo-liposome recruitment method was modified so that direct binding could be detected by the use of purified recombinant proteins. This shows the versatility of the proteo-liposome recruitment method due to the fact that interaction partners can be identified from a number of different samples.

In chapter 6 the proteo-liposome recruitment method was further developed and validated due to its ability to examine the assembly of protein coats from their purified components, using the AP-2/clathrin coat as a model. This allowed for the detection of interactions from native purified proteins as well as recombinant proteins. The proteo-liposome recruitment method allowed for the analysis of the difference in this complex assembly onto proteo-liposomes containing the intracellular domains of two membrane proteins with different endocytic sorting motifs. It also allowed for the analysis of the effect the lipid $PI(4,5)P_2$ had on the assembly of the AP-2/clathrin coat complex. The binding of AP-2 to two different membrane proteins (AICD and Crb2) was scrutinised. These two proteins contain different sorting motifs in their intracellular domains (tyrosine and dileucine motifs) that are known to bind to AP-2 with different affinities, which supports the results from chapter 6 (Ohno et al., 1995, Kelly et al., 2008, Owen and Evans, 1998). This demonstrates that this system could also be utilised to examine other aspects of clathrin coat assembly, and to ultimately examine the disassembly of the coat, and what affect different cytoplasmic tails have on the disassembly of the clathrin coat. The success of this proteo-liposome recruitment system in examining the assembly of the AP-2/clathrin complex demonstrates the versatility of the method. It indicates that this system would be effective in examining the assembly of other protein coat complexes, with a view to increasing the knowledge

of the mechanisms that govern coat assembly, and therefore intracellular trafficking events.

The proteo-liposome recruitment method was further modified to try and detect specific regions/motifs on the intracellular domains of membrane proteins that are required for the binding with interaction partners. Truncation mutants of AICD were successfully used to determine that the N-terminus of AICD was required for its binding to the mTOR complex, and that AICD's C-terminus was required for its interaction with the PIKfyve complex. This further enhances the proteo-liposome method as a tool for defining regions required for interactions, therefore broadening the field to which this system is applicable. In chapter 6 mutant Crb2 proteins are used, where a small number of amino acid residues were substituted for alanine in order to determine if the PEERLI motif of Crb2 was required for its interaction with the clathrin adaptor AP-2. Here all the mutants reduced the binding of AP-2 to a similar level, but did not completely abolish binding. This observed affect could have been due to the fact that the whole of the PEERLI motif might be necessary for mediating the interactions. Therefore, suggesting that the structure and the interactions between the amino acids of this motif may be important for AP-2 binding. Another explanation is that the proteo-liposome recruitment method was not sensitive enough to detect changes in binding observed upon the mutation of one or two amino acid residues. This is due to the fact that the proteo-liposome recruitment system is a qualitative method, and to truly pinpoint the most crucial amino acid would take more quantitative methods, such as surface plasmon resonance (SPR) which gives a measure of binding affinities.

This thesis clearly demonstrates the ability and usefulness of the proteo-liposome recruitment system in examining interactions of the cytoplasmic domains of membrane proteins. This method was able to characterise the interactions of the intracellular domain of APP with both the mTOR and PIKfyve complexes, and was further developed to allow for the analysis of the AP-2/clathrin coat from purified components.

Taken together this demonstrates that the proteo-liposome recruitment system is a formidable method for examining a wide variety of both protein-protein and lipid-protein interactions. The proteo-liposome recruitment system could be utilised to analyse the interaction of any transmembrane, or membrane associated protein, to any coat, trafficking complex or other cytosolic factor, making it an extremely valuable and versatile tool.

References

ABRAMI, L., LIU, S., COSSON, P., LEPPLA, S. H. & VAN DER GOOT, F. G. 2003. Anthrax toxin triggers endocytosis of its receptor via a lipid raft–mediated clathrin-dependent process. *The Journal of cell biology,* 160**,** 321-328.

ACEVEDO, K. M., OPAZO, C. M., NORRISH, D., CHALLIS, L. M., LI, Q.-X., WHITE, A. R., BUSH, A. I. & CAMAKARIS, J. 2014. Phosphorylation of Amyloid Precursor Protein at Threonine 668 Is Essential for Its Copper-responsive Trafficking in SH-SY5Y Neuroblastoma Cells. *Journal of Biological Chemistry,* 289**,** 11007-11019.

AJIOKA, R. S. & KAPLAN, J. 1986. Intracellular pools of transferrin receptors result from constitutive internalization of unoccupied receptors. *Proceedings of the National Academy of Sciences,* 83**,** 6445-6449.

ALESSI, D. R., JAMES, S. R., DOWNES, C. P., HOLMES, A. B., GAFFNEY, P. R. J., REESE, C. B. & COHEN, P. 1997. Characterization of a 3-phosphoinositide-dependent protein kinase which phosphorylates and activates protein kinase B alpha. *Current Biology,* 7**,** 261-269.

ALGHAMDI, T. A., HO, C. Y., MRAKOVIC, A., TAYLOR, D., MAO, D. & BOTELHO, R. J. 2013. Vac14 Protein Multimerization Is a Prerequisite Step for Fab1 Protein Complex Assembly and Function. *Journal of Biological Chemistry,* 288**,** 9363-9372.

ANDO, K., BRION, J. P., STYGELBOUT, V., SUAIN, V., AUTHELET, M., DEDECKER, R., CHANUT, A., LACOR, P., LAVAUR, J., SAZDOVITCH, V., ROGAEVA, E., POTIER, M. C. & DUYCKAERTS, C. 2013. Clathrin adaptor CALM/PICALM is associated with neurofibrillary tangles and is cleaved in Alzheimer's brains. *Acta Neuropathologica,* 125**,** 861-878.

ANNUNZIATA, I., PATTERSON, A., HELTON, D., HU, H., MOSHIACH, S., GOMERO, E., NIXON, R. & D'AZZO, A. 2013. Lysosomal NEU1 deficiency affects amyloid precursor protein levels and amyloid-beta secretion via deregulated lysosomal exocytosis. *Nature Communications,* 4.

ARIGHI, C. N., HARTNELL, L. M., AGUILAR, R. C., HAFT, C. R. & BONIFACINO, J. S. 2004. Role of the mammalian retromer in sorting of the cation-independent mannose 6-phosphate receptor. *J Cell Biol,* 165**,** 123-33.

ARINAMINPATHY, Y., KHURANA, E., ENGELMAN, D. M. & GERSTEIN, M. B. 2009. Computational analysis of membrane proteins: the largest class of drug targets. *Drug Discov Today,* 14**,** 1130-5.

AUGUSTINACK, J., SCHNEIDER, A., MANDELKOW, E.-M. & HYMAN, B. 2002. Specific tau phosphorylation sites correlate with severity of neuronal cytopathology in Alzheimer's disease. *Acta Neuropathologica,* 103**,** 26-35.

BACH, G., ZEEVI, D. A., FRUMKIN, A. & KOGOT-LEVIN, A. 2010. Mucolipidosis type IV and the mucolipins. *Biochem Soc Trans,* 38**,** 1432-5.

BALLA, T. 2007. Imaging and manipulating phosphoinositides in living cells. *The Journal of Physiology,* 582**,** 927-937.

BAR-PELED, L., SCHWEITZER, L. D., ZONCU, R. & SABATINI, D. M. 2012. Ragulator Is a GEF for the Rag GTPases that Signal Amino Acid Levels tomTORC1. *Cell,* 150**,** 1196-1208.

BARENHOLZ, Y. & CEVC, G. 2000. Structure and properties of membranes. *Physical chemistry of biological surfaces***,** 171-241.

BARETIĆ, D. & WILLIAMS, R. L. 2014. The structural basis for mTOR function. *Seminars in Cell & Developmental Biology,* 36**,** 91-101.

BAUST, T., ANITEI, M., CZUPALLA, C., PARSHYNA, I., BOUREL, L., THIELE, C., KRAUSE, E. & HOFLACK, B. 2008. Protein networks supporting AP-3 function in targeting lysosomal membrane proteins. *Mol Biol Cell,* 19**,** 1942-51.

BAUST, T., CZUPALLA, C., KRAUSE, E., BOUREL-BONNET, L. & HOFLACK, B. 2006. Proteomic analysis of adaptor protein 1A coats selectively assembled on liposomes. *Proc Natl Acad Sci U S A,* 103**,** 3159-64.

BECKETT, C., NALIVAEVA, N. N., BELYAEV, N. D. & TURNER, A. J. 2012. Nuclear signalling by membrane protein intracellular domains: The AICD enigma. *Cellular Signalling,* 24**,** 402-409.

BEHER, D., HESSE, L., MASTERS, C. L. & MULTHAUP, G. 1996. Regulation of amyloid protein precursor (APP) binding to collagen and mapping of the binding sites on APP and collagen type I. *Journal of Biological Chemistry,* 271**,** 1613-1620.

BEHNIA, R. & MUNRO, S. 2005. Organelle identity and the signposts for membrane traffic. *Nature,* 438**,** 597-604.

BELYAEV, N. D., NALIVAEVA, N. N., MAKOVA, N. Z. & TURNER, A. J. 2009. Neprilysin gene expression requires binding of the amyloid precursor protein intracellular domain to its promoter: implications for Alzheimer disease. *EMBO reports,* 10**,** 94-100.

BERRIDGE, M. J. 1984. Inositol trisphosphate and diacylglycerol as second messengers. *Biochemical Journal,* 220**,** 345.

BHALLA, A., VETANOVETZ, C. P., MOREL, E., CHAMOUN, Z., DI PAOLO, G. & SMALL, S. A. 2012. The location and trafficking routes of the neuronal retromer and its role in amyloid precursor protein transport. *Neurobiology of Disease,* 47**,** 126-134.

BONANGELINO, C. J., NAU, J. J., DUEX, J. E., BRINKMAN, M., WURMSER, A. E., GARY, J. D., EMR, S. D. & WEISMAN, L. S. 2002. Osmotic stress-induced increase of phosphatidylinositol 3,5-bisphosphate requires Vac14p, an activator of the lipid kinase Fab1p. *J Cell Biol,* 156**,** 1015-28.

BONIFACINO, J. S. 2014. Adaptor proteins involved in polarized sorting. *J Cell Biol,* 204**,** 7-17.

BONIFACINO, J. S. & HURLEY, J. H. 2008. Retromer. *Curr Opin Cell Biol,* 20**,** 427-36.

BORG, J. P., OOI, J., LEVY, E. & MARGOLIS, B. 1996. The phosphotyrosine interaction domains of X11 and FE65 bind to distinct sites on the YENPTY motif of amyloid precursor protein. *Molecular and Cellular Biology,* 16**,** 6229-6241.

BOUREL-BONNET, L., PÉCHEUR, E.-I., GRANDJEAN, C., BLANPAIN, A., BAUST, T., MELNYK, O., HOFLACK, B. & GRAS-MASSE, H. 2005. Anchorage of synthetic peptides onto liposomes via hydrazone and α-oxo hydrazone bonds. Preliminary functional investigations. *Bioconjugate chemistry,* 16**,** 450-457.

BRIDGES, D., MA, J.-T., PARK, S., INOKI, K., WEISMAN, L. S. & SALTIEL, A. R. 2012. Phosphatidylinositol 3,5-bisphosphate plays a role in the activation and subcellular localization of mechanistic target of rapamycin 1. *Molecular Biology of the Cell,* 23**,** 2955-62.

BULGAKOVA, N. A. & KNUST, E. 2009. The Crumbs complex: from epithelial-cell polarity to retinal degeneration. *J Cell Sci,* 122**,** 2587-96.

BUOSO, E., LANNI, C., SCHETTINI, G., GOVONI, S. & RACCHI, M. 2010. beta-Amyloid precursor protein metabolism: focus on the functions and degradation of its intracellular domain. *Pharmacological Research,* 62**,** 308-317.

BURGOS, P. V., MARDONES, G. A., ROJAS, A. L., DASILVA, L. L. P., PRABHU, Y., HURLEY, J. H. & BONIFACINO, J. S. 2010. Sorting of the Alzheimer's Disease Amyloid Precursor Protein Mediated by the AP-4 Complex. *Developmental Cell,* 18**,** 425-436.

CACCAMO, A., MAGRI, A., MEDINA, D. X., WISELY, E. V., LOPEZ-ARANDA, M. F., SILVA, A. J. & ODDO, S. 2013. mTOR regulates tau phosphorylation and degradation: implications for Alzheimer's disease and other tauopathies. *Aging Cell,* 12**,** 370-380.

CACCAMO, A., MAJUMDER, S., RICHARDSON, A., STRONG, R. & ODDO, S. 2010. Molecular Interplay between Mammalian Target of Rapamycin (mTOR), Amyloid-beta, and Tau EFFECTS ON COGNITIVE IMPAIRMENTS. *Journal of Biological Chemistry,* 285**,** 13107-13120.

CAI, X., XU, Y., CHEUNG, A. K., TOMLINSON, R. C., ALCAZAR-ROMAN, A., MURPHY, L., BILLICH, A., ZHANG, B., FENG, Y., KLUMPP, M., RONDEAU, J.-M., FAZAL, A. N., WILSON, C. J., MYER, V., JOBERTY, G., BOUWMEESTER, T., LABOW, M. A., FINAN, P. M., PORTER, J. A., PLOEGH, H. L., BAIRD, D., DE CAMILLI, P., TALLARICO, J. A. & HUANG, Q. 2013. PIKfyve, a Class III PI Kinase, Is the Target of the Small Molecular IL-12/IL-23 Inhibitor Apilimod and a Player in Toll-like Receptor Signaling. *Chemistry & Biology,* 20**,** 912-921.

CALDWELL, J. H., KLEVANSKI, M., SAAR, M. & MUELLER, U. C. 2013. Roles of the amyloid precursor protein family in the peripheral nervous system. *Mechanisms of Development,* 130**,** 433-446.

CAPORASO, G., TAKEI, K., GANDY, S., MATTEOLI, M., MUNDIGL, O., GREENGARD, P. & DE CAMILLI, P. 1994. Morphologic and biochemical analysis of the intracellular trafficking of the Alzheimer beta/A4 amyloid precursor protein. *The Journal of neuroscience,* 14**,** 3122-3138.

CARLTON, J., BUJNY, M., PETER, B. J., OORSCHOT, V. M. J., RUTHERFORD, A., MELLOR, H., KLUMPERMAN, J., MCMAHON, H. T. & CULLEN, P. J. 2004. Sorting nexin-1 mediates tubular endosome-to-TGN transport through coincidence sensing of high-curvature membranes and 3-phosphoinositides. *Current Biology,* 14**,** 1791-1800.

CASTER, A. H. & KAHN, R. A. 2013. Recruitment of the Mint3 Adaptor Is Necessary for Export of the Amyloid Precursor Protein (APP) from the Golgi Complex. *Journal of Biological Chemistry,* 288**,** 28567-28580.

CATALDO, A. M., PETERHOFF, C. M., TRONCOSO, J. C., GOMEZ-ISLA, T., HYMAN, B. T. & NIXON, R. A. 2000. Endocytic pathway abnormalities precede amyloid β deposition in sporadic Alzheimer's disease and Down syndrome: differential effects of APOE genotype and presenilin mutations. *The American journal of pathology,* 157**,** 277-286.

CHANG-ILETO, B., FRERE, S. G., CHAN, R. B., VORONOV, S. V., ROUX, A. & DI PAOLO, G. 2011. Synaptojanin 1-mediated PI (4, 5) P 2 hydrolysis is modulated by membrane curvature and facilitates membrane fission. *Developmental cell,* 20**,** 206-218.

CHANG, K. A. 2010. Mini Review: Possible roles of amyloid intracellular domain of amyloid precursor protein. *Biochemistry and Molecular Biology Reports,* 43**,** 656-663.

CHAPPELL, T. G., WELCH, W. J., SCHLOSSMAN, D. M., PALTER, K. B., SCHLESINGER, M. J. & ROTHMAN, J. E. 1986. Uncoating ATPase is a member of the 70 kilodalton family of stress proteins. *Cell,* 45**,** 3-13.

CHEEVER, M. L., SATO, T. K., DE BEER, T., KUTATELADZE, T. G., EMR, S. D. & OVERDUIN, M. 2001. Phox domain interaction with PtdIns (3) P targets the Vam7 t-SNARE to vacuole membranes. *Nature cell biology,* 3**,** 613-618.

CHOU, K. C. & ELROD, D. W. 1999. Prediction of membrane protein types and subcellular locations. *Proteins,* 34**,** 137-53.

CHOW, C. Y., LANDERS, J. E., BERGREN, S. K., SAPP, P. C., GRANT, A. E., JONES, J. M., EVERETT, L., LENK, G. M., MCKENNA-YASEK, D. M., WEISMAN, L. S., FIGLEWICZ, D., BROWN, R. H. & MEISLER, M. H. 2009. Deleterious Variants of FIG4, a Phosphoinositide Phosphatase, in Patients with ALS. *The American Journal of Human Genetics,* 84**,** 85-88.

CHOW, C. Y., ZHANG, Y., DOWLING, J. J., JIN, N., ADAMSKA, M., SHIGA, K., SZIGETI, K., SHY, M. E., LI, J., ZHANG, X., LUPSKI, J. R., WEISMAN, L. S. & MEISLER, M. H. 2007. Mutation of FIG4 causes neurodegeneration in the pale tremor mouse and patients with CMT4J. *Nature,* 448**,** 68-72.

COCKCROFT, S. & DE MATTEIS, M. 2001. Inositol lipids as spatial regulators of membrane traffic. *Journal of Membrane Biology,* 180**,** 187-194.

COLLINS, B. M., MCCOY, A. J., KENT, H. M., EVANS, P. R. & OWEN, D. J. 2002. Molecular Architecture and Functional Model of the Endocytic AP2 Complex. *Cell,* 109**,** 523-535.

COOKE, F. T., DOVE, S. K., MCEWEN, R. K., PAINTER, G., HOLMES, A. B., HALL, M. N., MICHELL, R. H. & PARKER, P. J. 1998. The stress-activated phosphatidylinositol 3-phosphate 5-kinase Fab1p is essential for vacuole function in S. cerevisiae. *Current Biology,* 8**,** 1219-S2.

CROTTET, P., MEYER, D. M., ROHRER, J. & SPIESS, M. 2002. ARF1.GTP, tyrosine-based signals, and phosphatidylinositol 4,5-bisphosphate constitute a minimal machinery to recruit the AP-1 clathrin adaptor to membranes. *Mol Biol Cell,* 13**,** 3672-82.

CULLEN, P. J., COZIER, G. E., BANTING, G. & MELLOR, H. 2001. Modular phosphoinositide-binding domains–their role in signalling and membrane trafficking. *Current Biology,* 11**,** R882-R893.

CUNNINGHAM, J. T., RODGERS, J. T., ARLOW, D. H., VAZQUEZ, F., MOOTHA, V. K. & PUIGSERVER, P. 2007. mTOR controls mitochondrial oxidative function through a YY1–PGC-1&agr; transcriptional complex. *nature,* 450**,** 736-740.

CUPERS, P., ORLANS, I., CRAESSAERTS, K., ANNAERT, W. & DE STROOPER, B. 2001. The amyloid precursor protein (APP)-cytoplasmic fragment generated by γ-secretase is rapidly degraded but distributes partially in a nuclear fraction of neurones in culture. *Journal of neurochemistry,* 78**,** 1168-1178.

DAHMS, S. O., HOEFGEN, S., ROESER, D., SCHLOTT, B., GÜHRS, K.-H. & THAN, M. E. 2010. Structure and biochemical analysis of the heparin-induced E1 dimer of the amyloid precursor protein. *Proceedings of the National Academy of Sciences,* 107**,** 5381-5386.

DANNHAUSER, P. N. & UNGEWICKELL, E. J. 2012. Reconstitution of clathrin-coated bud and vesicle formation with minimal components. *Nat Cell Biol,* 14**,** 634-9.

DAS, S., GHOSH, S., DASGUPTA, D., SEN, U. & MUKHOPADHYAY, D. 2012. Biophysical studies with AICD-47 reveal unique binding behavior characteristic of an unfolded domain. *Biochemical and Biophysical Research Communications,* 425**,** 201-206.

DAWKINS, E. & SMALL, D. H. 2014. Insights into the physiological function of the beta-amyloid precursor protein: beyond Alzheimer's disease. *Journal of Neurochemistry,* 129**,** 756-769.

DE LARTIGUE, J., POLSON, H., FELDMAN, M., SHOKAT, K., TOOZE, S. A., URBÉ, S. & CLAGUE, M. J. 2009. PIKfyve Regulation of Endosome-Linked Pathways. *Traffic,* 10**,** 883-893.

DE MATTEIS, M. A., GODI, A. & CORDA, D. 2002. Phosphoinositides and the Golgi complex. *Curr Opin Cell Biol,* 14**,** 434-447.

DE SILVA, H. R., JEN, A., WICKENDEN, C., JEN, L.-S., WILKINSON, S. L. & PATEL, A. J. 1997. Cell-specific expression of β-amyloid precursor protein isoform mRNAs and proteins in neurons and astrocytes. *Molecular brain research,* 47**,** 147-156.

DE STROOPER, B. & ANNAERT, W. 2000. Proteolytic processing and cell biological functions of the amyloid precursor protein. *Journal of Cell Science,* 113**,** 1857-1870.

DE STROOPER, B., VASSAR, R. & GOLDE, T. 2010. The secretases: enzymes with therapeutic potential in Alzheimer disease. *Nature reviews. Neurology,* 6**,** 99-107.

DE VREEDE, G., SCHOENFELD, J. D., WINDLER, S. L., MORRISON, H., LU, H. & BILDER, D. 2014. The Scribble module regulates retromer-dependent

endocytic trafficking during epithelial polarization. *Development,* 141**,** 2796-2802.

DEANE, C. M., SALWIŃSKI, Ł., XENARIOS, I. & EISENBERG, D. 2002. Protein Interactions: Two Methods for Assessment of the Reliability of High Throughput Observations. *Molecular & Cellular Proteomics,* 1**,** 349-356.

DEKOSKY, S. T. & SCHEFF, S. W. 1990. Synapse loss in frontal cortex biopsies in Alzheimer's disease: correlation with cognitive severity. *Ann Neurol,* 27**,** 457-64.

DÍAZ, E., SCHIMMÖLLER, F. & PFEFFER, S. R. 1997. A novel Rab9 effector required for endosome-to-TGN transport. *The Journal of cell biology,* 138**,** 283-290.

DODSON, S. E., GEARING, M., LIPPA, C. F., MONTINE, T. J., LEVEY, A. I. & LAH, J. J. 2006. LR11/SorLA expression is reduced in sporadic Alzheimer disease but not in familial Alzheimer disease. *Journal of neuropathology and experimental neurology,* 65**,** 866.

DONG, X.-P., SHEN, D., WANG, X., DAWSON, T., LI, X., ZHANG, Q., CHENG, X., ZHANG, Y., WEISMAN, L. S., DELLING, M. & XU, H. 2010. PI(3,5)P(2) Controls Membrane Traffic by Direct Activation of Mucolipin Ca(2+) Release Channels in the Endolysosome. *Nature communications,* 1**,** 38.

DORAY, B., LEE, I., KNISELY, J., BU, G. & KORNFELD, S. 2007. The γ/σ1 and α/σ2 hemicomplexes of clathrin adaptors AP-1 and AP-2 harbor the dileucine recognition site. *Molecular biology of the cell,* 18**,** 1887-1896.

DOVE, S. K., COOKE, F. T., DOUGLAS, M. R., SAYERS, L. G., PARKER, P. J. & MICHELL, R. H. 1997. Osmotic stress activates phosphatidylinositol-3,5-bisphosphate synthesis. *Nature,* 390**,** 187-192.

DOVE, S. K., DONG, K., KOBAYASHI, T., WILLIAMS, F. K. & MICHELL, R. H. 2009. Phosphatidylinositol 3,5-bisphosphate and Fab1p/PlKfyve underPPIn endo-lysosome function. *Biochemical Journal,* 419**,** 1-13.

DOVE, S. K., MCEWEN, R. K., MAYES, A., HUGHES, D. C., BEGGS, J. D. & MICHELL, R. H. 2002. Vac14 controls PtdIns (3, 5) P 2 synthesis and Fab1-dependent protein trafficking to the multivesicular body. *Current biology,* 12**,** 885-893.

DOVE, S. K., PIPER, R. C., MCEWEN, R. K., YU, J. W., KING, M. C., HUGHES, D. C., THURING, J., HOLMES, A. B., COOKE, F. T., MICHELL, R. H., PARKER, P. J. & LEMMON, M. A. 2004. Svp1p defines a family of phosphatidylinositol 3,5-bisphosphate effectors. *EMBO J,* 23**,** 1922-1933.

DOWLING, R. J., TOPISIROVIC, I., ALAIN, T., BIDINOSTI, M., FONSECA, B. D., PETROULAKIS, E., WANG, X., LARSSON, O., SELVARAJ, A. & LIU, Y. 2010.

mTORC1-mediated cell proliferation, but not cell growth, controlled by the 4E-BPs. *Science,* 328**,** 1172-1176.

DOWNES, C. P., GRAY, A. & LUCOCQ, J. M. 2005. Probing phosphoinositide functions in signaling and membrane trafficking. *Trends in Cell Biology,* 15**,** 259-268.

DRAKE, M. T., ZHU, Y. & KORNFELD, S. 2000. The Assembly of AP-3 Adaptor Complex-containing Clathrin-coated Vesicles on Synthetic Liposomes. *Molecular Biology of the Cell,* 11**,** 3723-3736.

EDELING, M. A., SMITH, C. & OWEN, D. 2006. Life of a clathrin coat: insights from clathrin and AP structures. *Nat Rev Mol Cell Biol,* 7**,** 32-44.

EFE, J. A., BOTELHO, R. J. & EMR, S. D. 2007. Atg18 Regulates Organelle Morphology and Fab1 Kinase Activity Independent of Its Membrane Recruitment by Phosphatidylinositol 3,5-Bisphosphate. *Molecular Biology of the Cell,* 18**,** 4232-4244.

ESSALMANI, R., MACQ, A.-F., MERCKEN, L. & OCTAVE, J.-N. 1996. Missense mutations associated with familial Alzheimer's disease in Sweden lead to the production of the amyloid peptide without internalization of its precursor. *Biochemical and biophysical research communications,* 218**,** 89-96.

FENG, Z., ZHANG, H., LEVINE, A. J. & JIN, S. 2005. The coordinate regulation of the p53 and mTOR pathways in cells. *Proceedings of the National Academy of Sciences of the United States of America,* 102**,** 8204-8209.

FERGUSON, C. J., LENK, G. M. & MEISLER, M. H. 2009. Defective autophagy in neurons and astrocytes from mice deficient in PI(3,5)P-2. *Human Molecular Genetics,* 18**,** 4868-4878.

FERRIS, C. D. & SNYDER, S. H. 1992. Inositol 1, 4, 5-trisphosphate-activated calcium channels. *Annual Review of Physiology,* 54**,** 469-488.

FIELDS, S. & SONG, O.-K. 1989. A novel genetic system to detect protein-protein interactions. *Nature***,** 245-6.

FIORE, F., ZAMBRANO, N., MINOPOLI, G., DONINI, V., DUILIO, A. & RUSSO, T. 1995. The regions of the Fe65 protein homologous to the phosphotyrosine interaction/phosphotyrosine binding domain of Shc bind the intracellular domain of the Alzheimer's amyloid precursor protein. *Journal of Biological Chemistry,* 270**,** 30853-30856.

FORD, M. G., PEARSE, B. M., HIGGINS, M. K., VALLIS, Y., OWEN, D. J., GIBSON, A., HOPKINS, C. R., EVANS, P. R. & MCMAHON, H. T. 2001. Simultaneous binding of PtdIns (4, 5) P2 and clathrin by AP180 in the nucleation of clathrin lattices on membranes. *Science,* 291**,** 1051-1055.

FOTIN, A., CHENG, Y., SLIZ, P., GRIGORIEFF, N., HARRISON, S. C., KIRCHHAUSEN, T. & WALZ, T. 2004. Molecular model for a complete clathrin lattice from electron cryomicroscopy. *Nature,* 432**,** 573-579.

GANLEY, I. G., LAM, D. H., WANG, J., DING, X., CHEN, S. & JIANG, X. 2009. ULK1· ATG13· FIP200 complex mediates mTOR signaling and is essential for autophagy. *Journal of Biological Chemistry,* 284**,** 12297-12305.

GARY, J. D., WURMSER, A. E., BONANGELINO, C. J., WEISMAN, L. S. & EMR, S. D. 1998. Fab1p is essential for PtdIns (3) P 5-kinase activity and the maintenance of vacuolar size and membrane homeostasis. *The Journal of cell biology,* 143**,** 65-79.

GOATE, A., CHARTIERHARLIN, M. C., MULLAN, M., BROWN, J., CRAWFORD, F., FIDANI, L., GIUFFRA, L., HAYNES, A., IRVING, N., JAMES, L., MANT, R., NEWTON, P., ROOKE, K., ROQUES, P., TALBOT, C., PERICAKVANCE, M., ROSES, A., WILLIAMSON, R., ROSSOR, M., OWEN, M. & HARDY, J. 1991. Segregation of a missense mutation in the amyloid precursor protein gene with familial Alzheimer's disease. *Nature,* 349**,** 704-706.

GRANT, B. D. & DONALDSON, J. G. 2009. Pathways and mechanisms of endocytic recycling. *Nature reviews Molecular cell biology,* 10**,** 597-608.

GRANT, B. D. & SATO, M. 2006. Intracellular trafficking. *WormBook : the online review of C. elegans biology***,** 1-9.

GREENE, B., LIU, S. H., WILDE, A. & BRODSKY, F. M. 2000. Complete reconstitution of clathrin basket formation with recombinant protein fragments: adaptor control of clathrin self-assembly. *Traffic,* 1**,** 69-75.

GROEMER, T. W., THIEL, C. S., HOLT, M., RIEDEL, D., HUA, Y., HUEVE, J., WILHELM, B. G. & KLINGAUF, J. 2011. Amyloid Precursor Protein Is Trafficked and Secreted via Synaptic Vesicles. *Plos One,* 6.

GRUNDKE-IQBAL, I., IQBAL, K., TUNG, Y.-C., QUINLAN, M., WISNIEWSKI, H. M. & BINDER, L. I. 1986. Abnormal phosphorylation of the microtubule-associated protein tau (tau) in Alzheimer cytoskeletal pathology. *Proceedings of the National Academy of Sciences,* 83**,** 4913-4917.

HAASS, C. & DE STROOPER, B. 1999. The presenilins in Alzheimer's disease--proteolysis holds the key. *Science,* 286**,** 916-919.

HAASS, C., KOO, E. H., CAPELL, A., TEPLOW, D. B. & SELKOE, D. J. 1995. Polarized sorting of beta-amyloid precursor protein and its proteolytic products in MDCK cells is regulated by two independent signals. *The Journal of cell biology,* 128**,** 537-547.

HAASS, C., SCHLOSSMACHER, M. G., HUNG, A. Y., VIGO-PELFREY, C., MELLON, A., OSTASZEWSKI, B. L., LIEBERBURG, I., KOO, E. H., SCHENK, D. & TEPLOW, D. B. 1992. Amyloid β-peptide is produced by cultured cells during normal metabolism. *Nature,* 359**,** 322-325.

HAFFNER, C., DI PAOLO, G., ROSENTHAL, J. A. & DE CAMILLI, P. 2000. Direct interaction of the 170 kDa isoform of synaptojanin 1 with clathrin and with the clathrin adaptor AP-2. *Current Biology,* 10**,** 471-474.

HALET, G. 2005. Imaging phosphoinositide dynamics using GFP-tagged protein domains. *Biol Cell,* 97**,** 501-18.

HE, G., GUPTA, S., YI, M., MICHAELY, P., HOBBS, H. H. & COHEN, J. C. 2002. ARH is a modular adaptor protein that interacts with the LDL receptor, clathrin, and AP-2. *Journal of Biological Chemistry,* 277**,** 44044-44049.

HENNE, W. M., BOUCROT, E., MEINECKE, M., EVERGREN, E., VALLIS, Y., MITTAL, R. & MCMAHON, H. T. 2010. FCHo Proteins Are Nucleators of Clathrin-Mediated Endocytosis. *Science,* 328**,** 1281-1284.

HILL, K., LI, Y., BENNETT, M., MCKAY, M., ZHU, X., SHERN, J., TORRE, E., LAH, J. J., LEVEY, A. I. & KAHN, R. A. 2003. Munc18 Interacting Proteins: ADP-RIBOSYLATION FACTOR-DEPENDENT COAT PROTEINS THAT REGULATE THE TRAFFIC OF β-ALZHEIMER'S PRECURSOR PROTEIN. *Journal of Biological Chemistry,* 278**,** 36032-36040.

HIRST, J., BARLOW, L. D., FRANCISCO, G. C., SAHLENDER, D. A., SEAMAN, M. N., DACKS, J. B. & ROBINSON, M. S. 2011. The fifth adaptor protein complex. *PLoS biology,* 9**,** e1001170.

HIRST, J., IRVING, C. & BORNER, G. H. 2013. Adaptor Protein Complexes AP-4 and AP-5: New Players in Endosomal Trafficking and Progressive Spastic Paraplegia. *Traffic,* 14**,** 153-164.

HÖNING, S., RICOTTA, D., KRAUSS, M., SPÄTE, K., SPOLAORE, B., MOTLEY, A., ROBINSON, M., ROBINSON, C., HAUCKE, V. & OWEN, D. J. 2005. Phosphatidylinositol-(4,5)-Bisphosphate Regulates Sorting Signal Recognition by the Clathrin-Associated Adaptor Complex AP2. *Molecular Cell,* 18**,** 519-531.

HOSOKAWA, N., HARA, T., KAIZUKA, T., KISHI, C., TAKAMURA, A., MIURA, Y., IEMURA, S.-I., NATSUME, T., TAKEHANA, K., YAMADA, N., GUAN, J.-L., OSHIRO, N. & MIZUSHIMA, N. 2009. Nutrient-dependent mTORC1 Association with the ULK1-Atg13-FIP200 Complex Required for Autophagy. *Molecular Biology of the Cell,* 20**,** 1981-1991.

HRESKO, R. C. & MUECKLER, M. 2005. mTOR center dot RICTOR is the Ser(473) kinase for Akt/protein kinase B in 3T3-L1 adipocytes. *Journal of Biological Chemistry,* 280**,** 40406-40416.

HSU, P. P., KANG, S. A., RAMESEDER, J., ZHANG, Y., OTTINA, K. A., LIM, D., PETERSON, T. R., CHOI, Y., GRAY, N. S. & YAFFE, M. B. 2011. The mTOR-regulated phosphoproteome reveals a mechanism of mTORC1-mediated inhibition of growth factor signaling. *Science,* 332**,** 1317-1322.

ICKING, A., AMADDII, M., RUONALA, M., HÖNING, S. & TIKKANEN, R. 2007. Polarized Transport of Alzheimer Amyloid Precursor Protein Is Mediated by Adaptor Protein Complex AP1-1B. *Traffic,* 8**,** 285-296.

IKONOMOV, O. C., SBRISSA, D., FENNER, H. & SHISHEVA, A. 2009a. PIKfyve-ArPIKfyve-Sac3 Core Complex: Contact sites and their consequence for Sac3 phosphatase activity and endocytic membrane homeostasis. *Journal of Biological Chemistry,* 284**,** 35794-35806.

IKONOMOV, O. C., SBRISSA, D., MLAK, K., DEEB, R., FLIGGER, J., SOANS, A., FINLEY, R. L. & SHISHEVA, A. 2003. Active PIKfyve associates with and promotes the membrane attachment of the late endosome-to-trans-Golgi network transport factor Rab9 effector p40. *Journal of Biological Chemistry,* 278**,** 50863-50871.

IKONOMOV, O. C., SBRISSA, D., MLAK, K., KANZAKI, M., PESSIN, J. & SHISHEVA, A. 2002a. Functional dissection of lipid and protein kinase signals of PIKfyve reveals the role of PtdIns 3, 5-P2 production for endomembrane integrity. *Journal of Biological Chemistry,* 277**,** 9206-9211.

IKONOMOV, O. C., SBRISSA, D. & SHISHEVA, A. 2006. Localized PtdIns 3, 5-P2 synthesis to regulate early endosome dynamics and fusion. *American Journal of Physiology-Cell Physiology,* 291**,** C393-C404.

IKONOMOV, O. C., SBRISSA, D. & SHISHEVA, A. 2009g. YM201636, an inhibitor of retroviral budding and PIKfyve-catalyzed PtdIns (3, 5) P 2 synthesis, halts glucose entry by insulin in adipocytes. *Biochemical and biophysical research communications,* 382**,** 566-570.

IKONOMOV, O. C., SBRISSA, D., YOSHIMORI, T., COVER, T. L. & SHISHEVA, A. 2002b. PIKfyve Kinase and SKD1 AAA ATPase Define Distinct Endocytic Compartments only PIKfyve expression inhibits the cell-vacuolating activity of Helicobacter pylori VacA toxin. *Journal of Biological Chemistry,* 277**,** 46785-46790.

INOKI, K., LI, Y., XU, T. & GUAN, K. L. 2003a. Rheb GTPase is a direct target of TSC2 GAP activity and regulates mTOR signaling. *Genes & Development,* 17**,** 1829-1834.

INOKI, K., ZHU, T. & GUAN, K.-L. 2003c. TSC2 mediates cellular energy response to control cell growth and survival. *Cell,* 115**,** 577-590.

ISRAEL, M. A., YUAN, S. H., BARDY, C., REYNA, S. M., MU, Y., HERRERA, C., HEFFERAN, M. P., VAN GORP, S., NAZOR, K. L. & BOSCOLO, F. S. 2012. Probing sporadic and familial Alzheimer/'s disease using induced pluripotent stem cells. *Nature,* 482**,** 216-220.

JACKSON, L. P., KELLY, B. T., MCCOY, A. J., GAFFRY, T., JAMES, L. C., COLLINS, B. M., HÖNING, S., EVANS, P. R. & OWEN, D. J. 2010. A Large-Scale Conformational Change Couples Membrane Recruitment to Cargo Binding in the AP2 Clathrin Adaptor Complex. *Cell,* 141**,** 1220-1229.

JANVIER, K., KATO, Y., BOEHM, M., ROSE, J. R., MARTINA, J. A., KIM, B.-Y., VENKATESAN, S. & BONIFACINO, J. S. 2003. Recognition of dileucine-based sorting signals from HIV-1 Nef and LIMP-II by the AP-1 γ–σ1 and AP-3 δ–σ3 hemicomplexes. *The Journal of cell biology,* 163**,** 1281-1290.

JEFFERIES, H. B., COOKE, F. T., JAT, P., BOUCHERON, C., KOIZUMI, T., HAYAKAWA, M., KAIZAWA, H., OHISHI, T., WORKMAN, P., WATERFIELD, M. D. & PARKER, P. J. 2008. A selective PIKfyve inhibitor blocks PtdIns(3,5)P(2) production and disrupts endomembrane transport and retroviral budding. *EMBO Rep,* 9**,** 164-70.

JIN, N., CHOW, C. Y., LIU, L., ZOLOV, S. N., BRONSON, R., DAVISSON, M., PETERSEN, J. L., ZHANG, Y., PARK, S., DUEX, J. E., GOLDOWITZ, D., MEISLER, M. H. & WEISMAN, L. S. 2008. VAC14 nucleates a protein complex essential for the acute interconversion of PI3P and PI(3,5)P-2 in yeast and mouse. *Embo Journal,* 27**,** 3221-3234.

JIN, N., MAO, K., JIN, Y., TEVZADZE, G., KAUFFMAN, E. J., PARK, S., BRIDGES, D., LOEWITH, R., SALTIEL, A. R., KLIONSKY, D. J. & WEISMAN, L. S. 2014. Roles for PI(3,5)P-2 in nutrient sensing through TORC1. *Molecular Biology of the Cell,* 25**,** 1171-1185.

JOHNSON, S. C., RABINOVITCH, P. S. & KAEBERLEIN, M. 2013. mTOR is a key modulator of ageing and age-related disease. *Nature,* 493**,** 338-345.

JOHNSSON, N. & VARSHAVSKY, A. 1994. Split ubiquitin as a sensor of protein interactions in vivo. *Proceedings of the National Academy of Sciences,* 91**,** 10340-10344.

KAETHER, C., SCHMITT, S., WILLEM, M. & HAASS, C. 2006. Amyloid precursor protein and Notch intracellular domains are generated after transport of their precursors to the cell surface. *Traffic,* 7**,** 408-415.

KALTHOFF, C., ALVES, J., URBANKE, C., KNORR, R. & UNGEWICKELL, E. J. 2002. Unusual Structural Organization of the Endocytic Proteins AP180 and Epsin 1. *Journal of Biological Chemistry,* 277**,** 8209-8216.

KAN, Z., JAISWAL, B. S., STINSON, J., JANAKIRAMAN, V., BHATT, D., STERN, H. M., YUE, P., HAVERTY, P. M., BOURGON, R. & ZHENG, J. 2010. Diverse somatic mutation patterns and pathway alterations in human cancers. *Nature,* 466**,** 869-873.

KANG, J., LEMAIRE, H.-G., UNTERBECK, A., SALBAUM, J. M., MASTERS, C. L., GRZESCHIK, K.-H., MULTHAUP, G., BEYREUTHER, K. & MÜLLER-HILL, B. 1987. The precursor of Alzheimer's disease amyloid A4 protein resembles a cell-surface receptor.

KEEGAN, L., GILL, G. & PTASHNE, M. 1986. Separation of DNA binding from the transcription-activating function of a eukaryotic regulatory protein. *Science,* 231**,** 699-704.

KEEN, J. H. 1987. Clathrin assembly proteins: affinity purification and a model for coat assembly. *The Journal of cell biology,* 105**,** 1989-1998.

KELLY, B. T., GRAHAM, S. C., LISKA, N., DANNHAUSER, P. N., HONING, S., UNGEWICKELL, E. J. & OWEN, D. J. 2014. Clathrin adaptors. AP2 controls clathrin polymerization with a membrane-activated switch. *Science,* 345**,** 459-63.

KELLY, B. T., MCCOY, A. J., SPATE, K., MILLER, S. E., EVANS, P. R., HONING, S. & OWEN, D. J. 2008. A structural explanation for the binding of endocytic dileucine motifs by the AP2 complex. *Nature,* 456**,** 976-979.

KELLY, R. 1985. Pathways of protein secretion in eukaryotes. *Science,* 230**,** 25-32.

KHURANA, V., LU, Y. R., STEINHILB, M. L., OLDHAM, S., SHULMAN, J. M. & FEANY, M. B. 2006. TOR-mediated cell-cycle activation causes neurodegeneration in a Drosophila tauopathy model. *Current Biology,* 16**,** 230-241.

KIBBEY, M. C., JUCKER, M., WEEKS, B. S., NEVE, R. L., VAN NOSTRAND, W. E. & KLEINMAN, H. K. 1993. beta-Amyloid precursor protein binds to the neurite-promoting IKVAV site of laminin. *Proceedings of the National Academy of Sciences,* 90**,** 10150-10153.

KIELKOWSKA, A., NIEWCZAS, I., ANDERSON, K. E., DURRANT, T. N., CLARK, J., STEPHENS, L. R. & HAWKINS, P. T. 2014. A new approach to measuring phosphoinositides in cells by mass spectrometry. *Adv Biol Regul,* 54**,** 131-41.

KIM, S. G., BUEL, G. R. & BLENIS, J. 2013. Nutrient regulation of the mTOR Complex 1 signaling pathway. *Molecules and Cells,* 35**,** 463-473.

KING, G. D. & TURNER, R. S. 2004. Adaptor protein interactions: modulators of amyloid precursor protein metabolism and Alzheimer's disease risk? *Experimental Neurology,* 185**,** 208-219.

KING, M. A., HANDS, S., HAFIZ, F., MIZUSHIMA, N., TOLKOVSKY, A. M. & WYTTENBACH, A. 2008. Rapamycin inhibits polyglutamine aggregation independently of autophagy by reducing protein synthesis. *Molecular pharmacology,* 73**,** 1052-1063.

KINOSHITA, A., FUKUMOTO, H., SHAH, T., WHELAN, C. M., IRIZARRY, M. C. & HYMAN, B. T. 2003. Demonstration by FRET of BACE interaction with the amyloid precursor protein at the cell surface and in early endosomes. *Journal of cell science,* 116**,** 3339-3346.

KINUTA, M. & TAKEI, K. 2002. Utilization of liposomes in vesicular transport studies. *Cell Structure and Function,* 27**,** 63-69.

KLEBES, A. & KNUST, E. 2000. A conserved motif in Crumbs is required for E-cadherin localisation and zonula adherens formation in Drosophila. *Current Biology,* 10**,** 76-85.

KNUEHL, C., CHEN, C. Y., MANALO, V., HWANG, P. K., OTA, N. & BRODSKY, F. M. 2006. Novel binding sites on clathrin and adaptors regulate distinct aspects of coat assembly. *Traffic,* 7**,** 1688-700.

KON, T., MORI, F., TANJI, K., MIKI, Y., TOYOSHIMA, Y., YOSHIDA, M., SASAKI, H., KAKITA, A., TAKAHASHI, H. & WAKABAYASHI, K. 2014. ALS-associated protein FIG4 is localized in Pick and Lewy bodies, and also neuronal nuclear inclusions, in polyglutamine and intranuclear inclusion body diseases. *Neuropathology,* 34**,** 19-26.

KOO, E. H. & SQUAZZO, S. L. 1994. Evidence that production and release of amyloid beta-protein involves the endocytic pathway. *Journal of Biological Chemistry,* 269**,** 17386-17389.

KOO, E. H., SQUAZZO, S. L., SELKOE, D. J. & KOO, C. H. 1996. Trafficking of cell-surface amyloid beta-protein precursor. I. Secretion, endocytosis and recycling as detected by labeled monoclonal antibody. *Journal of cell science,* 109**,** 991-998.

KORTE, M., HERRMANN, U., ZHANG, X. & DRAGUHN, A. 2012. The role of APP and APLP for synaptic transmission, plasticity, and network function: lessons from genetic mouse models. *Experimental brain research,* 217**,** 435-440.

KOSAKA, T. & IKEDA, K. 1983. Reversible blockage of membrane retrieval and endocytosis in the garland cell of the temperature-sensitive mutant of Drosophila melanogaster, shibirets1. *The Journal of cell biology,* 97**,** 499-507.

KRAUSS, M. & HAUCKE, V. 2007. Phosphoinositides: Regulators of membrane traffic and protein function. *Febs Letters,* 581**,** 2105-2111.

KRICK, R., TOLSTRUP, J., APPELLES, A., HENKE, S. & THUMM, M. 2006. The relevance of the phosphatidylinositolphosphat-binding motif FRRGT of Atg18 and Atg21 for the Cvt pathway and autophagy. *Febs Letters,* 580**,** 4632-4638.

KURTEN, R. C. 2003. Sorting motifs in receptor trafficking. *Advanced Drug Delivery Reviews,* 55**,** 1405-1419.

LAI, A., GIBSON, A., HOPKINS, C. R. & TROWBRIDGE, I. S. 1998. Signal-dependent Trafficking of β-Amyloid Precursor Protein-Transferrin Receptor Chimeras in Madin-Darby Canine Kidney Cells. *Journal of Biological Chemistry,* 273**,** 3732-3739.

LAI, A., SISODIA, S. S. & TROWBRIDGE, I. S. 1995. Characterization of sorting signals in the β-amyloid precursor protein cytoplasmic domain. *Journal of Biological Chemistry,* 270**,** 3565-3573.

LANE, R. F., ST GEORGE-HYSLOP, P., HEMPSTEAD, B. L., SMALL, S. A., STRITTMATTER, S. M. & GANDY, S. 2012. Vps10 family proteins and the retromer complex in aging-related neurodegeneration and diabetes. *The Journal of Neuroscience,* 32**,** 14080-14086.

LAPLANTE, M. & SABATINI, DAVID M. 2012. mTOR Signaling in Growth Control and Disease. *Cell,* 149**,** 274-293.

LEBLANC, A. C. & GAMBETTI, P. 1994. Production of Alzheimer 4-kDa β-Amyloid Peptide Requires the C-Terminal Cytosolic Domain of the Amyloid Precursor Protein. *Biochemical and biophysical research communications,* 204**,** 1371-1380.

LEE, K. J., MOUSSA, C. E.-H., LEE, Y., SUNG, Y., HOWELL, B. W., TURNER, R. S., PAK, D. T. & HOE, H.-S. 2010. Beta amyloid-independent role of amyloid precursor protein in generation and maintenance of dendritic spines. *Neuroscience,* 169**,** 344-356.

LEE, M. C., MILLER, E. A., GOLDBERG, J., ORCI, L. & SCHEKMAN, R. 2004. Bi-directional protein transport between the ER and Golgi. *Annu. Rev. Cell Dev. Biol.,* 20**,** 87-123.

LEE, M. C. S. & MILLER, E. A. 2007. Molecular mechanisms of COPII vesicle formation. *Seminars in Cell & Developmental Biology,* 18**,** 424-434.

LENK, G. M., FERGUSON, C. J., CHOW, C. Y., JIN, N., JONES, J. M., GRANT, A. E., ZOLOV, S. N., WINTERS, J. J., GIGER, R. J., DOWLING, J. J., WEISMAN, L. S. & MEISLER, M. H. 2011. Pathogenic Mechanism of the FIG4 Mutation Responsible for Charcot-Marie-Tooth Disease CMT4J. *Plos Genetics,* 7.

LEWIS, D. A., CAMPBELL, M. J., TERRY, R. D. & MORRISON, J. H. 1987. LAMINAR AND REGIONAL DISTRIBUTIONS OF NEUROFIBRILLARY TANGLES AND NEURITIC PLAQUES IN ALZHEIMERS-DISEASE - A QUANTITATIVE STUDY OF VISUAL AND AUDITORY CORTICES. *Journal of Neuroscience,* 7**,** 1799-1808.

LI, S., TIAB, L., JIAO, X., MUNIER, F. L., ZOGRAFOS, L., FRUEH, B. E., SERGEEV, Y., SMITH, J., RUBIN, B. & MEALLET, M. A. 2005a. Mutations in PIP5K3 are associated with Francois-Neetens mouchetee fleck corneal dystrophy. *The American Journal of Human Genetics,* 77**,** 54-63.

LI, S. C., DIAKOV, T. T., XU, T., TARSIO, M., ZHU, W., COUOH-CARDEL, S., WEISMAN, L. S. & KANE, P. M. 2014. The signaling lipid PI(3,5)P2 stabilizes V1-Vo sector interactions and activates the V-ATPase. *Molecular Biology of the Cell,* 25**,** 1251-1262.

LI, X., ALAFUZOFF, I., SOININEN, H., WINBLAD, B. & PEI, J.-J. 2005b. Levels of mTOR and its downstream targets 4E-BP1, eEF2, and eEF2 kinase in relationships with tau in Alzheimer's disease brain. *FEBS Journal,* 272**,** 4211-4220.

LI, X., ALAFUZOFF, I., SOININEN, H., WINBLAD, B. & PEI, J. J. 2005c. Levels of mTOR and its downstream targets 4E-BP1, eEF2, and eEF2 kinase in relationships with tau in Alzheimer's disease brain. *Febs Journal,* 272**,** 4211-4220.

LI, X., WANG, X., ZHANG, X., ZHAO, M., TSANG, W. L., ZHANG, Y., YAU, R. G. W., WEISMAN, L. S. & XU, H. 2013. Genetically encoded fluorescent probe to visualize intracellular phosphatidylinositol 3,5-bisphosphate localization and dynamics. *Proceedings of the National Academy of Sciences of the United States of America,* 110**,** 21165-21170.

LIN, Y., CURRINN, H., POCHA, S. M., ROTHNIE, A., WASSMER, T. & KNUST, E. Unpublished. AP-2 complex-mediated endocytosis of Drosophila Crumbs regulates polarity via antagonizing Stardust. *Journal of Cell Science*.

LINDNER, R. & UNGEWICKELL, E. 1992. Clathrin-associated proteins of bovine brain coated vesicles. An analysis of their number and assembly-promoting activity. *Journal of Biological Chemistry,* 267**,** 16567-73.

LIU, S.-H., WONG, M. L., CRAIK, C. S. & BRODSKY, F. M. 1995. Regulation of clathrin assembly and trimerization defined using recombinant triskelion hubs. *Cell,* 83**,** 257-267.

LONG, X., LIN, Y., ORTIZ-VEGA, S., YONEZAWA, K. & AVRUCH, J. 2005. Rheb binds and regulates the mTOR kinase. *Current Biology,* 15**,** 702-713.

LOPICCOLO, J., BLUMENTHAL, G. M., BERNSTEIN, W. B. & DENNIS, P. A. 2008. Targeting the PI3K/Akt/mTOR pathway: Effective combinations and clinical considerations. *Drug Resistance Updates,* 11**,** 32-50.

MAGNUSON, B., EKIM, B. & FINGAR, D. C. 2012. Regulation and function of ribosomal protein S6 kinase (S6K) within mTOR signalling networks. *Biochemical Journal,* 441**,** 1-21.

MARTINEZ-VICENTE, M. & CUERVO, A. M. 2007. Autophagy and neurodegeneration: when the cleaning crew goes on strike. *Lancet Neurology,* 6**,** 352-361.

MAYINGER, P. 2012. Phosphoinositides and vesicular membrane traffic. *Biochimica Et Biophysica Acta-Molecular and Cell Biology of Lipids,* 1821**,** 1104-1113.

MAYOR, S. & PAGANO, R. E. 2007. Pathways of clathrin-independent endocytosis. *Nat Rev Mol Cell Biol,* 8**,** 603-612.

MCCARTNEY, A. J., ZHANG, Y. & WEISMAN, L. S. 2014a. Phosphatidylinositol 3,5-bisphosphate: Low abundance, high significance. *Bioessays,* 36**,** 52-64.

MCCARTNEY, A. J., ZOLOV, S. N., KAUFFMAN, E. J., ZHANG, Y., STRUNK, B. S., WEISMAN, L. S. & SUTTON, M. A. 2014b. Activity-dependent PI (3, 5) P2 synthesis controls AMPA receptor trafficking during synaptic depression. *Proceedings of the National Academy of Sciences***,** 201411117.

MCMAHON, H. T. & BOUCROT, E. 2011. Molecular mechanism and physiological functions of clathrin-mediated endocytosis. *Nature Reviews Molecular Cell Biology,* 12**,** 517-533.

MILLER, R. A., HARRISON, D. E., ASTLE, C., BAUR, J. A., BOYD, A. R., DE CABO, R., FERNANDEZ, E., FLURKEY, K., JAVORS, M. A. & NELSON, J. F. 2010. Rapamycin, but not resveratrol or simvastatin, extends life span of genetically heterogeneous mice. *The Journals of Gerontology Series A: Biological Sciences and Medical Sciences***,** glq178.

MITSUNARI, T., NAKATSU, F., SHIODA, N., LOVE, P. E., GRINBERG, A., BONIFACINO, J. S. & OHNO, H. 2005. Clathrin adaptor AP-2 is essential for early embryonal development. *Molecular and cellular biology,* 25**,** 9318-9323.

MOREL, E., CHAMOUN, Z., LASIECKA, Z. M., CHAN, R. B., WILLIAMSON, R. L., VETANOVETZ, C., DALL'ARMI, C., SIMOES, S., DU JOUR, K. S. P. & MCCABE, B. D. 2013. Phosphatidylinositol-3-phosphate regulates sorting and processing of amyloid precursor protein through the endosomal system. *Nature communications,* 4.

MORESCO, J. J., CARVALHO, P. C. & YATES, J. R. 2010. Identifying components of protein complexes in C. elegans using co-immunoprecipitation and mass spectrometry. *Journal of proteomics,* 73**,** 2198-2204.

MORGENSZTERN, D. & MCLEOD, H. L. 2005. PI3K/Akt/mTOR pathway as a target for cancer therapy. *Anti-Cancer Drugs,* 16**,** 797-803.

MUHAMMAD, A., FLORES, I., ZHANG, H., YU, R., STANISZEWSKI, A., PLANEL, E., HERMAN, M., HO, L., KREBER, R. & HONIG, L. S. 2008. Retromer deficiency observed in Alzheimer's disease causes hippocampal dysfunction, neurodegeneration, and Aβ accumulation. *Proceedings of the National Academy of Sciences,* 105**,** 7327-7332.

MUNRO, S. 2002. Organelle identity and the targeting of peripheral membrane proteins. *Current opinion in cell biology,* 14**,** 506-514.

MURRELL, J., FARLOW, M., GHETTI, B. & BENSON, M. D. 1991. A mutation in the amyloid precursor protein associated with hereditary Alzheimer's disease. *Science,* 254**,** 97-99.

NAKAYAMA, K., NAGASE, H., KOH, C.-S. & OHKAWARA, T. 2011. γ-Secretase-Regulated Mechanisms Similar to Notch Signaling May Play a Role in Signaling Events, Including APP Signaling, Which Leads to Alzheimer's Disease. *Cellular and Molecular Neurobiology,* 31**,** 887-900.

NHAN, H. & KOO, E. 2013. The -YENPTY- domain of the amyloid precursor protein: Much more than just endocytosis? *Bioessays,* 35**,** 844-844.

NICHOLSON, G., LENK, G. M., REDDEL, S. W., GRANT, A. E., TOWNE, C. F., FERGUSON, C. J., SIMPSON, E., SCHEUERLE, A., YASICK, M., HOFFMAN, S., BLOUIN, R., BRANDT, C., COPPOLA, G., BIESECKER, L. G., BATISH, S. D. & MEISLER, M. H. 2011. Distinctive genetic and clinical features of CMT4J: a severe neuropathy caused by mutations in the PI(3,5)P-2 phosphatase FIG4. *Brain,* 134**,** 1959-1971.

NICOT, A. S., FARES, H., PAYRASTRE, B., CHISHOLM, A. D., LABOUESSE, M. & LAPORTE, J. 2006. The phosphoinositide kinase PIKfyve/Fab1p regulates

terminal lysosome maturation in Caenorhabditis elegans. *Molecular Biology of the Cell,* 17**,** 3062-3074.

NIEHAGE, C., STANGE, C., ANITEI, M. & HOFLACK, B. 2013. Liposome-based assays to study membrane-associated protein networks. *Methods in enzymology,* 534**,** 223-243.

NIELSEN, M. S., GUSTAFSEN, C., MADSEN, P., NYENGAARD, J. R., HERMEY, G., BAKKE, O., MARI, M., SCHU, P., POHLMANN, R. & DENNES, A. 2007. Sorting by the cytoplasmic domain of the amyloid precursor protein binding receptor SorLA. *Molecular and cellular biology,* 27**,** 6842-6851.

NIXON, R. A., CATALDO, A. M. & MATHEWS, P. M. 2000. The endosomal-lysosomal system of neurons in Alzheimer's disease pathogenesis: a review. *Neurochem Res,* 25**,** 1161-72.

O'BRIEN, R. J. & WONG, P. C. 2011. Amyloid precursor protein processing and Alzheimer's disease. *Annu Rev Neurosci,* 34**,** 185-204.

ODORIZZI, G., BABST, M. & EMR, S. D. 1998. Fab1p PtdIns (3) P 5-kinase function essential for protein sorting in the multivesicular body. *Cell,* 95**,** 847-858.

ODORIZZI, G., BABST, M. & EMR, S. D. 2000. Phosphoinositide signaling and the regulation of membrane trafficking in yeast. *Trends in biochemical sciences,* 25**,** 229-235.

OHNO, H., STEWART, J., FOURNIER, M., BOSSHART, H., RHEE, I., MIYATAKE, S., SAITO, T., GALLUSSER, A., KIRCHHAUSEN, T. & BONIFACINO, J. 1995. Interaction of tyrosine-based sorting signals with clathrin-associated proteins. *Science,* 269**,** 1872-1875.

OISHI, M., NAIRN, A. C., CZERNIK, A. J., LIM, G. S., ISOHARA, T., GANDY, S. E., GREENGARD, P. & SUZUKI, T. 1997. The cytoplasmic domain of Alzheimer's amyloid precursor protein is phosphorylated at Thr654, Ser655, and Thr668 in adult rat brain and cultured cells. *Molecular Medicine,* 3**,** 111-123.

OKAMOTO, T., TAKEDA, S., MURAYAMA, Y., OGATA, E. & NISHIMOTO, I. 1995. Ligand-dependent G-protein coupling function of amyloid transmembrane precursor. *Journal of Biological Chemistry,* 270**,** 4205-4208.

OPPELT, A., LOBERT, V. H., HAGLUND, K., MACKEY, A. M., RAMEH, L. E., LIESTOL, K., SCHINK, K. O., PEDERSEN, N. M., WENZEL, E. M., HAUGSTEN, E. M., BRECH, A., RUSTEN, T. E., STENMARK, H. & WESCHE, J. 2013. Production of phosphatidylinositol 5-phosphate via PIKfyve and MTMR3 regulates cell migration. *Embo Reports,* 14**,** 57-64.

OTZEN, D. 2011. Protein–surfactant interactions: A tale of many states. *Biochimica et Biophysica Acta (BBA) - Proteins and Proteomics,* 1814**,** 562-591.

OWEN, D., VALLIS, Y., PEARSE, B., MCMAHON, H. & EVANS, P. 2000. The structure and function of the β2-adaptin appendage domain. *The EMBO journal,* 19**,** 4216-4227.

OWEN, D. J. & EVANS, P. R. 1998. A Structural Explanation for the Recognition of Tyrosine-Based Endocytotic Signals. *Science,* 282**,** 1327-1332.

PANDINI, G., PACE, V., COPANI, A., SQUATRITO, S., MILARDI, D. & VIGNERI, R. 2013. Insulin Has Multiple Antiamyloidogenic Effects on Human Neuronal Cells. *Endocrinology,* 154**,** 375-387.

PARDOSSI-PIQUARD, R. & CHECLER, F. 2012. The physiology of the beta-amyloid precursor protein intracellular domain AICD. *Journal of Neurochemistry,* 120**,** 109-124.

PARDOSSI-PIQUARD, R., PETIT, A., KAWARAI, T., SUNYACH, C., DA COSTA, C. A., VINCENT, B., RING, S., D'ADAMIO, L., SHEN, J. & MÜLLER, U. 2005. Presenilin-dependent transcriptional control of the Aβ-degrading enzyme neprilysin by intracellular domains of βAPP and APLP. *Neuron,* 46**,** 541-554.

PARK, S. Y. & GUO, X. 2014. Adaptor protein complexes and intracellular transport. *Bioscience reports,* 34**,** 381-390.

PARKHITKO, A. A., FAVOROVA, O. O., KHABIBULLIN, D. I., ANISIMOV, V. N. & HENSKE, E. P. 2014. Kinase mTOR: Regulation and role in maintenance of cellular homeostasis, tumor development, and aging. *Biochemistry-Moscow,* 79**,** 88-101.

PASTERNAK, S. H., BAGSHAW, R. D., GUIRAL, M., ZHANG, S., ACKERLEY, C. A., PAK, B. J., CALLAHAN, J. W. & MAHURAN, D. J. 2003. Presenilin-1, Nicastrin, Amyloid Precursor Protein, and γ-Secretase Activity Are Co-localized in the Lysosomal Membrane. *Journal of Biological Chemistry,* 278**,** 26687-26694.

PAYRASTRE, B., MISSY, K., GIURIATO, S., BODIN, S., PLANTAVID, M. & GRATACAP, M.-P. 2001. Phosphoinositides: key players in cell signalling, in time and space. *Cellular signalling,* 13**,** 377-387.

PEARSE, B. M. & ROBINSON, M. S. 1984. Purification and properties of 100-kd proteins from coated vesicles and their reconstitution with clathrin. *The EMBO Journal,* 3**,** 1951-1957.

PEARSE, B. M. F. 1976. Clathrin-unique protein associated with intracellular transfer of membrane by coated vesicles. *Proceedings of the National Academy of Sciences of the United States of America,* 73**,** 1255-1259.

PEDEN, A. A., OORSCHOT, V., HESSER, B. A., AUSTIN, C. D., SCHELLER, R. H. & KLUMPERMAN, J. 2004. Localization of the AP-3 adaptor complex defines a

novel endosomal exit site for lysosomal membrane proteins. *The Journal of cell biology,* 164**,** 1065-1076.

PEI, J.-J. & HUGON, J. 2008. mTOR-dependent signalling in Alzheimer's disease. *Journal of Cellular and Molecular Medicine,* 12**,** 2525-2532.

PHIZICKY, E. M. & FIELDS, S. 1995. Protein-protein interactions: methods for detection and analysis. *Microbiological Reviews,* 59**,** 94-123.

POCHA, S. M. & WASSMER, T. 2011. A novel role for retromer in the control of epithelial cell polarity. *Communicative & integrative biology,* 4**,** 749-51.

POCHA, S. M., WASSMER, T., NIEHAGE, C., HOFLACK, B. & KNUST, E. 2011. Retromer controls epithelial cell polarity by trafficking the apical determinant Crumbs. *Curr Biol,* 21**,** 1111-7.

PRABHU, Y., BURGOSA, P. V., SCHINDLER, C., FARIAS, G. G., MAGADAN, J. G. & BONIFACINO, J. S. 2012. Adaptor protein 2-mediated endocytosis of the beta-secretase BACE1 is dispensable for amyloid precursor protein processing. *Molecular Biology of the Cell,* 23**,** 2339-2351.

PRAEFCKE, G. J., FORD, M. G., SCHMID, E. M., OLESEN, L. E., GALLOP, J. L., PEAK-CHEW, S. Y., VALLIS, Y., BABU, M. M., MILLS, I. G. & MCMAHON, H. T. 2004. Evolving nature of the AP2 α-appendage hub during clathrin-coated vesicle endocytosis. *The EMBO journal,* 23**,** 4371-4383.

PROIKAS-CEZANNE, T., RUCKERBAUER, S., STIERHOF, Y.-D., BERG, C. & NORDHEIM, A. 2007. Human WIPI-1 puncta-formation: A novel assay to assess mammalian autophagy. *Febs Letters,* 581**,** 3396-3404.

PUERTOLLANO, R. 2014. mTOR and lysosome regulation. *F1000prime reports,* 6**,** 52-52.

PUIG, O., CASPARY, F., RIGAUT, G., RUTZ, B., BOUVERET, E., BRAGADO-NILSSON, E., WILM, M. & SÉRAPHIN, B. 2001. The tandem affinity purification (TAP) method: a general procedure of protein complex purification. *Methods,* 24**,** 218-229.

RAJENDRAN, L. & ANNAERT, W. 2012. Membrane trafficking pathways in Alzheimer's disease. *Traffic,* 13**,** 759-70.

RAJENDRAN, L., HONSHO, M., ZAHN, T. R., KELLER, P., GEIGER, K. D., VERKADE, P. & SIMONS, K. 2006. Alzheimer's disease beta-amyloid peptides are released in association with exosomes. *Proceedings of the National Academy of Sciences of the United States of America,* 103**,** 11172-11177.

RAMAKER, J. M., SWANSON, T. L. & COPENHAVER, P. F. 2013. Amyloid precursor proteins interact with the heterotrimeric G protein Go in the control of neuronal migration. *The Journal of Neuroscience,* 33**,** 10165-10181.

RAMEH, L. E., TOLIAS, K. F., DUCKWORTH, B. C. & CANTLEY, L. C. 1997. A new pathway for synthesis of phosphatidylinositol-4, 5-bisphosphate. *Nature,* 390**,** 192-196.

REIDER, A., BARKER, S. L., MISHRA, S. K., IM, Y. J., MALDONADO-BÁEZ, L., HURLEY, J. H., TRAUB, L. M. & WENDLAND, B. 2009. Syp1 is a conserved endocytic adaptor that contains domains involved in cargo selection and membrane tubulation. *The EMBO Journal,* 28**,** 3103-3116.

RING, S., WEYER, S. W., KILIAN, S. B., WALDRON, E., PIETRZIK, C. U., FILIPPOV, M. A., HERMS, J., BUCHHOLZ, C., ECKMAN, C. B. & KORTE, M. 2007. The secreted β-amyloid precursor protein ectodomain APPsα is sufficient to rescue the anatomical, behavioral, and electrophysiological abnormalities of APP-deficient mice. *The Journal of neuroscience,* 27**,** 7817-7826.

RIZK, A., PAUL, G., INCARDONA, P., BUGARSKI, M., MANSOURI, M., NIEMANN, A., ZIEGLER, U., BERGER, P. & SBALZARINI, I. F. 2014. Segmentation and quantification of subcellular structures in fluorescence microscopy images using Squassh. *Nat. Protocols,* 9**,** 586-596.

ROBAKIS, N. K., WISNIEWSKI, H. M., JENKINS, E. C., DEVINE-GAGE, E. A., HOUCK, G. E., YAO, X. L., RAMAKRISHNA, N., WOLFE, G., SILVERMAN, W. P. & BROWN, W. T. 1987. Chromosome 21q21 sublocalisation of gene encoding beta-amyloid peptide in cerebral vessels and neuritic (senile) plaques of people with Alzheimer disease and Down syndrome. *Lancet,* 1**,** 384-5.

ROGAEVA, E., MENG, Y., LEE, J. H., GU, Y., KAWARAI, T., ZOU, F., KATAYAMA, T., BALDWIN, C. T., CHENG, R. & HASEGAWA, H. 2007. The neuronal sortilin-related receptor SORL1 is genetically associated with Alzheimer disease. *Nature genetics,* 39**,** 168-177.

ROH, M. H., MAKAROVA, O., LIU, C. J., SHIN, K., LEE, S., LAURINEC, S., GOYAL, M., WIGGINS, R. & MARGOLIS, B. 2002. The Maguk protein, Pals1, functions as an adapter, linking mammalian homologues of Crumbs and Discs Lost. *Journal of Cell Biology,* 157**,** 161-172.

ROSSOR, M. N., IVERSEN, L. L., REYNOLDS, G. P., MOUNTJOY, C. Q. & ROTH, M. 1984. *Neurochemical characteristics of early and late onset types of Alzheimer's disease*.

RUCEVIC, M., HIXSON, D. & JOSIC, D. 2011. Mammalian plasma membrane proteins as potential biomarkers and drug targets. *ELECTROPHORESIS,* 32**,** 1549-1564.

RUDGE, S. A., ANDERSON, D. M. & EMR, S. D. 2004. Vacuole size control: Regulation of PtdIns(3,5)P-2 levels by the vacuole-associated Vac14-Fig4

complex, a PtdIns(3.5)P-2-specific phosphatase. *Molecular Biology of the Cell,* 15**,** 24-36.

RUST, M. J., LAKADAMYALI, M., ZHANG, F. & ZHUANG, X. 2004. Assembly of endocytic machinery around individual influenza viruses during viral entry. *Nature structural & molecular biology,* 11**,** 567-573.

RUSTEN, T. E., VACCARI, T., LINDMO, K., RODAHL, L. M. W., NEZIS, I. P., SEM-JACOBSEN, C., WENDLER, F., VINCENT, J.-P., BRECH, A., BILDER, D. & STENMARK, H. 2007. ESCRTs and Fab1 regulate distinct steps of autophagy. *Current Biology,* 17**,** 1817-1825.

RUTHERFORD, A. C., TRAER, C., WASSMER, T., PATTNI, K., BUJNY, M. V., CARLTON, J. G., STENMARK, H. & CULLEN, P. J. 2006. The mammalian phosphatidylinositol 3-phosphate 5-kinase (PIKfyve) regulates endosome-to-TGN retrograde transport. *Journal of Cell Science,* 119**,** 3944-3957.

SAITO, K., ARAKI, Y., KONTANI, K., NISHINA, H. & KATADA, T. 2005. Novel role of the small GTPase Rheb: Its implication in endocytic pathway independent of the activation of mammalian target of rapamycin. *Journal of Biochemistry,* 137**,** 423-430.

SAMAD, A., SULTANA, Y. & AQIL, M. 2007. Liposomal drug delivery systems: an update review. *Current drug delivery,* 4**,** 297-305.

SAMBAMURTI, K., SHIOI, J., ANDERSON, J., PAPPOLLA, M. & ROBAKIS, N. 1992. Evidence for intracellular cleavage of the Alzheimer's amyloid precursor in PC12 cells. *Journal of neuroscience research,* 33**,** 319-329.

SANCAK, Y., BAR-PELED, L., ZONCU, R., MARKHARD, A. L., NADA, S. & SABATINI, D. M. 2010. Ragulator-Rag Complex Targets mTORC1 to the Lysosomal Surface and Is Necessary for Its Activation by Amino Acids. *Cell,* 141**,** 290-303.

SANCAK, Y., PETERSON, T. R., SHAUL, Y. D., LINDQUIST, R. A., THOREEN, C. C., BAR-PELED, L. & SABATINI, D. M. 2008. The Rag GTPases bind raptor and mediate amino acid signaling to mTORC1. *Science (New York, N.Y.),* 320**,** 1496-1501.

SANNERUD, R., DECLERCK, I., PERIC, A., RAEMAEKERS, T., MENENDEZ, G., ZHOU, L., VEERLE, B., COEN, K., MUNCK, S. & DE STROOPER, B. 2011. ADP ribosylation factor 6 (ARF6) controls amyloid precursor protein (APP) processing by mediating the endosomal sorting of BACE1. *Proceedings of the National Academy of Sciences,* 108**,** E559-E568.

SARBASSOV, D. D., GUERTIN, D. A., ALI, S. M. & SABATINI, D. M. 2005. Phosphorylation and Regulation of Akt/PKB by the Rictor-mTOR Complex. *Science,* 307**,** 1098-1101.

SARKAR, S. 2013. Regulation of autophagy by mTOR-dependent and mTOR-independent pathways: autophagy dysfunction in neurodegenerative diseases and therapeutic application of autophagy enhancers. *Biochemical Society Transactions,* 41**,** 1103-1130.

SBRISSA, D., IKONOMOV, O. C., FENNER, H. & SHISHEVA, A. 2008. ArPIKfyve Homomeric and Heteromeric Interactions Scaffold PIKfyve and Sac3 in a Complex to Promote PIKfyve Activity and Functionality. *Journal of Molecular Biology,* 384**,** 766-779.

SBRISSA, D., IKONOMOV, O. C., FU, Z. Y., IJUIN, T., GRUENBERG, J., TAKENAWA, T. & SHISHEVA, A. 2007. Core protein machinery for mammalian phosphatidylinositol 3,5-bisphosphate synthesis and turnover that regulates the progression of endosomal transport - Novel sac phosphatase joins the arpikfyve-pikfyve complex. *Journal of Biological Chemistry,* 282**,** 23878-23891.

SBRISSA, D., IKONOMOV, O. C., STRAKOVA, J., DONDAPATI, R., MLAK, K., DEEB, R., SILVER, R. & SHISHEVA, A. 2004. A mammalian ortholog of Saccharomyces cerevisiae Vac14 that associates with and up-regulates PIKfyve phosphoinositide 5-kinase activity. *Mol Cell Biol,* 24**,** 10437-10447.

SCHETTINI, G., GOVONI, S., RACCHI, M. & RODRIGUEZ, G. 2010. Phosphorylation of APP-CTF-AICD domains and interaction with adaptor proteins: signal transduction and/or transcriptional role–relevance for Alzheimer pathology. *Journal of neurochemistry,* 115**,** 1299-1308.

SCHLOSSMAN, D. M., SCHMID, S. L., BRAELL, W. A. & ROTHMAN, J. E. 1984. An enzyme that removes clathrin coats: purification of an uncoating ATPase. *The Journal of cell biology,* 99**,** 723-733.

SCHMID, E. M., FORD, M. G. J., BURTEY, A., PRAEFCKE, G. J. K., PEAK-CHEW, S. Y., MILLS, I. G., BENMERAH, A. & MCMAHON, H. T. 2006. Role of the AP2 beta-appendage hub in recruiting partners for clathrin-coated vesicle assembly. *Plos Biology,* 4**,** 1532-1548.

SCHMID, S. L. 1997. CLATHRIN-COATED VESICLE FORMATION AND PROTEIN SORTING:An Integrated Process. *Annual Review of Biochemistry,* 66**,** 511-548.

SCHU, P. V., TAKEGAWA, K., FRY, M. J., STACK, J. H., WATERFIELD, M. D. & EMR, S. D. 1993. Phosphatidylinositol 3-kinase encoded by yeast VPS34 gene essential for protein sorting. *Science,* 260**,** 88-91.

SEAMAN, M. N. 2004. Cargo-selective endosomal sorting for retrieval to the Golgi requires retromer. *J Cell Biol,* 165**,** 111-22.

SEAMAN, M. N. 2005. Recycle your receptors with retromer. *Trends Cell Biol,* 15**,** 68-75.

SHERRINGTON, R., ROGAEV, E. I., LIANG, Y., ROGAEVA, E. A., LEVESQUE, G., IKEDA, M., CHI, H., LIN, C., LI, G., HOLMAN, K., TSUDA, T., MAR, L., FONCIN, J. F., BRUNI, A. C., MONTESI, M. P., SORBI, S., RAINERO, I., PINESSI, L., NEE, L., CHUMAKOV, I., POLLEN, D., BROOKES, A., SANSEAU, P., POLINSKY, R. J., WASCO, W., DASILVA, H. A. R., HAINES, J. L., PERICAKVANCE, M. A., TANZI, R. E., ROSES, A. D., FRASER, P. E., ROMMENS, J. M. & STGEORGEHYSLOP, P. H. 1995. Cloning of a gene bearing missense mutations in early-onset familial Alzheimer's disease. *Nature,* 375**,** 754-760.

SHISHEVA, A. 2008. PIKfyve: Partners, significance, debates and paradoxes. *Cell Biology International,* 32**,** 591-604.

SIMONSEN, A., LIPPE, R., CHRISTOFORIDIS, S., GAULLIER, J.-M., BRECH, A., CALLAGHAN, J., TOH, B.-H., MURPHY, C., ZERIAL, M. & STENMARK, H. 1998. EEA1 links PI (3) K function to Rab5 regulation of endosome fusion. *Nature,* 394**,** 494-498.

SMALL, S. A., KENT, K., PIERCE, A., LEUNG, C., KANG, M. S., OKADA, H., HONIG, L., VONSATTEL, J. P. & KIM, T. W. 2005. Model-guided microarray implicates the retromer complex in Alzheimer's disease. *Annals of neurology,* 58**,** 909-919.

SOBA, P., EGGERT, S., WAGNER, K., ZENTGRAF, H., SIEHL, K., KREGER, S., LÖWER, A., LANGER, A., MERDES, G. & PARO, R. 2005. Homo-and heterodimerization of APP family members promotes intercellular adhesion. *The EMBO journal,* 24**,** 3624-3634.

SOLDANO, A., OKRAY, Z., JANOVSKA, P., TMEJOVA, K., REYNAUD, E., CLAEYS, A., YAN, J., ATAK, Z. K., DE STROOPER, B., DURA, J.-M., BRYJA, V. & HASSAN, B. A. 2013. The Drosophila Homologue of the Amyloid Precursor Protein Is a Conserved Modulator of Wnt PCP Signaling. *Plos Biology,* 11.

SOPJANI, M., KUNERT, A., CZARKOWSKI, K., KLAUS, F., LAUFER, J., FOLLER, M. & LANG, F. 2010. Regulation of the Ca(2+) channel TRPV6 by the kinases SGK1, PKB/Akt, and PIKfyve. *J Membr Biol,* 233**,** 35-41.

STAUFFER, T. P., AHN, S. & MEYER, T. 1998. Receptor-induced transient reduction in plasma membrane PtdIns (4, 5) P 2 concentration monitored in living cells. *Current Biology,* 8**,** 343-346.

SULLIVAN, C. P., JAY, A. G., STACK, E. C., PAKALUK, M., WADLINGER, E., FINE, R. E., WELLS, J. M. & MORIN, P. J. 2011. Retromer disruption promotes amyloidogenic APP processing. *Neurobiology of disease,* 43**,** 338-345.

SUMIOKA, A., NAGAISHI, S., YOSHIDA, T., LIN, A., MIURA, M. & SUZUKI, T. 2005. Role of 14-3-3γ in FE65-dependent gene transactivation mediated by the amyloid β-protein precursor cytoplasmic fragment. *Journal of Biological Chemistry,* 280**,** 42364-42374.

SUNDBORGER, A., SODERBLOM, C., VORONTSOVA, O., EVERGREN, E., HINSHAW, J. E. & SHUPLIAKOV, O. 2011. An endophilin–dynamin complex promotes budding of clathrin-coated vesicles during synaptic vesicle recycling. *Journal of cell science,* 124**,** 133-143.

SZENTPETERY, Z., BALLA, A., KIM, Y. J., LEMMON, M. A. & BALLA, T. 2009. Live cell imaging with protein domains capable of recognizing phosphatidylinositol 4,5-bisphosphate; a comparative study. *Bmc Cell Biology,* 10.

SZUL, T. & SZTUL, E. 2011. COPII and COPI Traffic at the ER-Golgi Interface. *Physiology,* 26**,** 348-364.

TAKEI, N. & NAWA, H. 2014. mTOR signaling and its roles in normal and abnormal brain development. *Frontiers in molecular neuroscience,* 7**,** 28.

TAM, J. H. K., SEAH, C. & PASTERNAK, S. H. 2014. The Amyloid Precursor Protein is rapidly transported from the Golgi apparatus to the lysosome and where it is processed into beta-amyloid. *Molecular Brain,* 7.

TAN, S., TAN, H. T. & CHUNG, M. C. 2008. Membrane proteins and membrane proteomics. *Proteomics,* 8**,** 3924-32.

TANG, Z., BERECZKI, E., ZHANG, H., WANG, S., LI, C., JI, X., BRANCA, R. M., LEHTIÖ, J., GUAN, Z., FILIPCIK, P., XU, S., WINBLAD, B. & PEI, J.-J. 2013. Mammalian Target of Rapamycin (mTor) Mediates Tau Protein Dyshomeostasis: Implication for Alzheimer's disease. *Journal of Biological Chemistry,* 288**,** 15556-15570.

TANZI, R., GUSELLA, J., WATKINS, P., BRUNS, G., ST GEORGE-HYSLOP, P., VAN KEUREN, M., PATTERSON, D., PAGAN, S., KURNIT, D. & NEVE, R. 1987. Amyloid beta protein gene: cDNA, mRNA distribution, and genetic linkage near the Alzheimer locus. *Science,* 235**,** 880-884.

TAYLOR, S. J., CHAE, H. Z., RHEE, S. G. & EXTON, J. H. 1991. Activation of the β1 isozyme of phospholipase C by α subunits of the Gq class of G proteins.

TEBAR, F., SORKINA, T., SORKIN, A., ERICSSON, M. & KIRCHHAUSEN, T. 1996. Eps15 is a component of clathrin-coated pits and vesicles and is located at the rim of coated pits. *Journal of Biological Chemistry,* 271**,** 28727-28730.

TEE, A. R., MANNING, B. D., ROUX, P. P., CANTLEY, L. C. & BLENIS, J. 2003. Tuberous sclerosis complex gene products, tuberin and hamartin, control mTOR signaling by acting as a GTPase-activating protein complex toward Rheb. *Current Biology,* 13**,** 1259-1268.

TEPASS, U., THERES, C. & KNUST, E. 1990. crumbs encodes an EGF-like protein expressed on apical membranes of Drosophila epithelial cells and required for organization of epithelia. *Cell,* 61**,** 787-799.

TER HAAR, E., HARRISON, S. C. & KIRCHHAUSEN, T. 2000. Peptide-in-groove interactions link target proteins to the β-propeller of clathrin. *Proceedings of the National Academy of Sciences,* 97**,** 1096-1100.

THINAKARAN, G. & KOO, E. H. 2008. Amyloid precursor protein trafficking, processing, and function. *J Biol Chem,* 283**,** 29615-9.

TOKAREV, A., ALFONSO, A. & SEGEV, N. 2009. Overview of Intracellular Compartments and Trafficking Pathways. *Trafficking Inside Cells.* Springer New York.

TULI, A., SHARMA, M., CAPEK, H. L., NASLAVSKY, N., CAPLAN, S. & SOLHEIM, J. C. 2009. Mechanism for Amyloid Precursor-like Protein 2 Enhancement of Major Histocompatibility Complex Class I Molecule Degradation. *The Journal of Biological Chemistry,* 284**,** 34296-34307.

UM, S. H., FRIGERIO, F., WATANABE, M., PICARD, F., JOAQUIN, M., STICKER, M., FUMAGALLI, S., ALLEGRINI, P. R., KOZMA, S. C. & AUWERX, J. 2004. Absence of S6K1 protects against age-and diet-induced obesity while enhancing insulin sensitivity. *Nature,* 431**,** 200-205.

UNGEWICKELL, E., UNGEWICKELL, H., HOLSTEIN, S. E., LINDNER, R., PRASAD, K., BAROUCH, W., MARTINI, B., GREENE, L. E. & EISENBERG, E. 1995. Role of auxilin in uncoating clathrin-coated vesicles. *Nature,* 378**,** 632-635.

VAN DEN HURK, J. A., RASHBASS, P., ROEPMAN, R., DAVIS, J., VOESENEK, K. E., ARENDS, M. L., ZONNEVELD-VRIELING, M., VAN ROEKEL, M., CAMERON, K. & ROHRSCHNEIDER, K. 2005. Characterization of the Crumbs homolog 2 (CRB2) gene and analysis of its role in retinitis pigmentosa and Leber congenital amaurosis.

VASSAR, R., BENNETT, B. D., BABU-KHAN, S., KAHN, S., MENDIAZ, E. A., DENIS, P., TEPLOW, D. B., ROSS, S., AMARANTE, P. & LOELOFF, R. 1999. β-Secretase cleavage of Alzheimer's amyloid precursor protein by the transmembrane aspartic protease BACE. *science,* 286**,** 735-741.

VELLAI, T., TAKACS-VELLAI, K., ZHANG, Y., KOVACS, A. L., OROSZ, L. & MÜLLER, F. 2003. Influence of TOR kinase on lifespan in C. elegans. *Nature,* 426**,** 620.

VIEIRA, A. V., LAMAZE, C. & SCHMID, S. L. 1996. Control of EGF receptor signaling by clathrin-mediated endocytosis. *Science,* 274**,** 2086-2089.

VIEIRA, S. I., REBELO, S., ESSELMANN, H., WILTFANG, J., LAH, J., LANE, R., SMALL, S. A., GANDY, S., DA CRUZ, E. S. E. F. & DA CRUZ, E. S. O. A. 2010. Retrieval of the Alzheimer's amyloid precursor protein from the endosome to the TGN is S655 phosphorylation state-dependent and retromer-mediated. *Mol Neurodegener,* 5**,** 40.

VON ROTZ, R. C., KOHLI, B. M., BOSSET, J., MEIER, M., SUZUKI, T., NITSCH, R. M. & KONIETZKO, U. 2004. The APP intracellular domain forms nuclear multiprotein complexes and regulates the transcription of its own precursor. *Journal of cell science,* 117**,** 4435-4448.

WAKELAM, M. J. & CLARK, J. 2011. Methods for analyzing phosphoinositides using mass spectrometry. *Biochim Biophys Acta,* 1811**,** 758-62.

WALDE, P., COSENTINO, K., ENGEL, H. & STANO, P. 2010. Giant vesicles: preparations and applications. *Chembiochem,* 11**,** 848-65.

WALKER, G., HOUTHOOFD, K., VANFLETEREN, J. R. & GEMS, D. 2005. Dietary restriction in C. elegans: From rate-of-living effects to nutrient sensing pathways. *Mechanisms of Ageing and Development,* 126**,** 929-937.

WANG, B., WANG, Z., SUN, L., YANG, L., LI, H., COLE, A. L., RODRIGUEZ-RIVERA, J., LU, H.-C. & ZHENG, H. 2014a. The Amyloid Precursor Protein Controls Adult Hippocampal Neurogenesis through GABAergic Interneurons. *The Journal of neuroscience : the official journal of the Society for Neuroscience,* 34**,** 13314-25.

WANG, B. T., DUCKER, G. S., BARCZAK, A. J., BARBEAU, R., ERLE, D. J. & SHOKAT, K. M. 2011. The mammalian target of rapamycin regulates cholesterol biosynthetic gene expression and exhibits a rapamycin-resistant transcriptional profile. *Proceedings of the National Academy of Sciences,* 108**,** 15201-15206.

WANG, L., RHODES, C. J. & LAWRENCE, J. C., JR. 2006. Activation of mammalian target of rapamycin (mTOR) by insulin is associated with stimulation of 4EBP1 binding to dimeric mTOR complex 1. *Journal of Biological Chemistry,* 281**,** 24293-24303.

WANG, P., YANG, G., MOSIER, D. R., CHANG, P., ZAIDI, T., GONG, Y.-D., ZHAO, N.-M., DOMINGUEZ, B., LEE, K.-F. & GAN, W.-B. 2005. Defective

neuromuscular synapses in mice lacking amyloid precursor protein (APP) and APP-Like protein 2. *The Journal of neuroscience,* 25**,** 1219-1225.

WANG, S., ZHOU, S.-L., MIN, F.-Y., MA, J.-J., SHI, X.-J., BERECZKI, E. & WU, J. 2014b. mTOR-mediated hyperphosphorylation of tau in the hippocampus is involved in cognitive deficits in streptozotocin-induced diabetic mice. *Metabolic Brain Disease,* 29**,** 729-736.

WASCO, W., BUPP, K., MAGENDANTZ, M., GUSELLA, J. F., TANZI, R. E. & SOLOMON, F. 1992. Identification of a mouse brain cDNA that encodes a protein related to the Alzheimer disease-associated amyloid beta protein precursor. *Proceedings of the National Academy of Sciences,* 89**,** 10758-10762.

WASSMER, T., ATTAR, N., BUJNY, M. V., OAKLEY, J., TRAER, C. J. & CULLEN, P. J. 2007. A loss-of-function screen reveals SNX5 and SNX6 as potential components of the mammalian retromer. *Journal of Cell Science,* 120**,** 45-54.

WASSMER, T., ATTAR, N., HARTERINK, M., VAN WEERING, J. R., TRAER, C. J., OAKLEY, J., GOUD, B., STEPHENS, D. J., VERKADE, P., KORSWAGEN, H. C. & CULLEN, P. J. 2009. The retromer coat complex coordinates endosomal sorting and dynein-mediated transport, with carrier recognition by the trans-Golgi network. *Dev Cell,* 17**,** 110-22.

WATANABE, T., HIKICHI, Y., WILLUWEIT, A., SHINTANI, Y. & HORIGUCHI, T. 2012. FBL2 Regulates Amyloid Precursor Protein (APP) Metabolism by Promoting Ubiquitination-Dependent APP Degradation and Inhibition of APP Endocytosis. *Journal of Neuroscience,* 32**,** 3352-3365.

WEN, L., TANG, F.-L., HONG, Y., LUO, S.-W., WANG, C.-L., HE, W., SHEN, C., JUNG, J.-U., XIONG, F. & LEE, D.-H. 2011. VPS35 haploinsufficiency increases Alzheimer's disease neuropathology. *The Journal of cell biology,* 195**,** 765-779.

WEYER, S. W., KLEVANSKI, M., DELEKATE, A., VOIKAR, V., AYDIN, D., HICK, M., FILIPPOV, M., DROST, N., SCHALLER, K. L. & SAAR, M. 2011. APP and APLP2 are essential at PNS and CNS synapses for transmission, spatial learning and LTP. *The EMBO journal,* 30**,** 2266-2280.

WHITEFORD, C., BREARLEY, C. & ULUG, E. 1997. Phosphatidylinositol 3, 5-bisphosphate defines a novel PI 3-kinase pathway in resting mouse fibroblasts. *Biochem. J,* 323**,** 597-601.

WHITLEY, P., REAVES, B. J., HASHIMOTO, M., RILEY, A. M., POTTER, B. V. L. & HOLMAN, G. D. 2003. Identification of mammalian Vps24p as an effector of

phosphatidylinositol 3,5-bisphosphate-dependent endosome compartmentalization. *Journal of Biological Chemistry,* 278**,** 38786-38795.

WIGGE, P., KÖHLER, K., VALLIS, Y., DOYLE, C. A., OWEN, D., HUNT, S. P. & MCMAHON, H. T. 1997. Amphiphysin heterodimers: potential role in clathrin-mediated endocytosis. *Molecular biology of the cell,* 8**,** 2003-2015.

WILBUR, J. D., HWANG, P. K., YBE, J. A., LANE, M., SELLERS, B. D., JACOBSON, M. P., FLETTERICK, R. J. & BRODSKY, F. M. 2010. Conformation Switching of Clathrin Light Chain Regulates Clathrin Lattice Assembly. *Dev Cell,* 18**,** 854-861.

WOLLERT, T. & HURLEY, J. H. 2010. Molecular mechanism of multivesicular body biogenesis by ESCRT complexes. *Nature,* 464**,** 864-9.

WU, F. & YAO, P. J. 2009. Clathrin-mediated endocytosis and Alzheimer's disease: an update. *Ageing Res Rev,* 8**,** 147-9.

XIAO, Z., PATRAKKA, J., NUKUI, M., CHI, L., NIU, D., BETSHOLTZ, C., PIKKARAINEN, T., VAINIO, S. & TRYGGVASON, K. 2011. Deficiency in crumbs homolog 2 (Crb2) affects gastrulation and results in embryonic lethality in mice. *Developmental Dynamics,* 240**,** 2646-2656.

XING, Y., BÖCKING, T., WOLF, M., GRIGORIEFF, N., KIRCHHAUSEN, T. & HARRISON, S. C. 2010. Structure of clathrin coat with bound Hsc70 and auxilin: mechanism of Hsc70-facilitated disassembly. *The EMBO journal,* 29**,** 655-665.

XU, Y., HORTSMAN, H., SEET, L., WONG, S. H. & HONG, W. 2001. SNX3 regulates endosomal function through its PX-domain-mediated interaction with PtdIns (3) P. *Nature cell biology,* 3**,** 658-666.

YANG, A. J., CHANDSWANGBHUVANA, D., MARGOL, L. & GLABE, C. G. 1998. Loss of endosomal/lysosomal membrane impermeability is an early event in amyloid Aβ1-42 pathogenesis. *Journal of neuroscience research,* 52**,** 691-698.

YAO, P. J. 2004. Synaptic frailty and clathrin-mediated synaptic vesicle trafficking in Alzheimer's disease. *Trends in Neurosciences,* 27**,** 24-29.

YATES, S. C., ZAFAR, A., HUBBARD, P., NAGY, S., DURANT, S., BICKNELL, R., WILCOCK, G., CHRISTIE, S., ESIRI, M. M., SMITH, A. D. & NAGY, Z. 2013. Dysfunction of the mTOR pathway is a risk factor for Alzheimer's disease. *Acta neuropathologica communications,* 1**,** 3-3.

YOUNG-PEARSE, T. L., CHEN, A. C., CHANG, R., MARQUEZ, C. & SELKOE, D. J. 2008. Secreted APP regulates the function of full-length APP in neurite outgrowth through interaction with integrin beta1. *Neural Dev,* 3**,** 1749-8104.

ZHANG, C. 2012. Natural compounds that modulate BACE1-processing of amyloid-beta precursor protein in Alzheimer's disease. *Discovery Medicine,* 14**,** 189-97.

ZHANG, H. H., HUANG, J., DÜVEL, K., BOBACK, B., WU, S., SQUILLACE, R. M., WU, C.-L. & MANNING, B. D. 2009. Insulin stimulates adipogenesis through the Akt-TSC2-mTORC1 pathway. *PloS one,* 4**,** e6189.

ZHANG, Y.-W., WANG, R., LIU, Q., ZHANG, H., LIAO, F.-F. & XU, H. 2007a. Presenilin/γ-secretase-dependent processing of β-amyloid precursor protein regulates EGF receptor expression. *Proceedings of the National Academy of Sciences,* 104**,** 10613-10618.

ZHANG, Y., MCCARTNEY, A. J., ZOLOV, S. N., FERGUSON, C. J., MEISLER, M. H., SUTTON, M. A. & WEISMAN, L. S. 2012. Modulation of synaptic function by VAC14, a protein that regulates the phosphoinositides PI(3,5)P2 and PI(5)P. *EMBO J,* 31**,** 3442-3456.

ZHANG, Y., ZOLOV, S. N., CHOW, C. Y., SLUTSKY, S. G., RICHARDSON, S. C., PIPER, R. C., YANG, B., NAU, J. J., WESTRICK, R. J., MORRISON, S. J., MEISLER, M. H. & WEISMAN, L. S. 2007b. Loss of Vac14, a regulator of the signaling lipid phosphatidylinositol 3,5-bisphosphate, results in neurodegeneration in mice. *Proc Natl Acad Sci U S A,* 104**,** 17518-23.

ZHENG, H., JIANG, M., TRUMBAUER, M. E., SIRINATHSINGHJI, D. J., HOPKINS, R., SMITH, D. W., HEAVENS, R. P., DAWSON, G. R., BOYCE, S. & CONNER, M. W. 1995. β-Amyloid precursor protein-deficient mice show reactive gliosis and decreased locomotor activity. *Cell,* 81**,** 525-531.

ZHENG, H. & KOO, E. 2011. Biology and pathophysiology of the amyloid precursor protein. *Molecular Neurodegeneration,* 6**,** 1-16.

ZHENG, P. Z., EASTMAN, J., VANDE POL, S. & PIMPLIKAR, S. W. 1998. PAT1, a microtubule-interacting protein, recognizes the basolateral sorting signal of amyloid precursor protein. *Proceedings of the National Academy of Sciences of the United States of America,* 95**,** 14745-14750.

ZHOU, B., WU, Y. & LIN, X. 2011. Retromer regulates apical-basal polarity through recycling Crumbs. *Dev Biol,* 360**,** 87-95.

ZHU, Y., DRAKE, M. T. & KORNFELD, S. 1999. ADP-ribosylation factor 1 dependent clathrin-coat assembly on synthetic liposomes. *Proceedings of the National Academy of Sciences,* 96**,** 5013-5018.

ZOLOV, S. N., BRIDGES, D., ZHANG, Y., LEE, W. W., RIEHLE, E., VERMA, R., LENK, G. M., CONVERSO-BARAN, K., WEIDE, T., ALBIN, R. L., SALTIEL, A. R., MEISLER, M. H., RUSSELL, M. W. & WEISMAN, L. S. 2012. In vivo,

Pikfyve generates PI(3,5)P2, which serves as both a signaling lipid and the major precursor for PI5P. *Proc Natl Acad Sci U S A,* 109**,** 17472-7.

Appendices

Appendix 1 – Plasmid List

pET28-MBP
pET28-MBP-TEV –AICD
pET28-MBP-TEV –AICD-Tr1
pET28-MBP-TEV –AICD-Tr2
pET28-MBP-TEV –AICD-Tr3
pET28-MBP-TEV –AICD-Tr4
pET28-MBP-TEV-Crb2
pET28-MBP-mTOR kinase domain
pMaIE-TEV
pGEX-6P-1-ATG18
pEGFP-n1
pEGFP-n1-APP
pEGFP-n1-AICD
pEGFP-n1-APP∆YENPTY
pEYFP-n1-APP∆AICD
pEYFP-n1-AICD-Tr4
pEGFP-C3-ML1Nx2
pMCherry-c1-ML1Nx2
pMCitrine-Vac14
pMCherry-c1-Vac14
pRFP-MPR

Appendix 2 – Live cell imaging videos

The videos for the live cell imaging can be found on the attached disk.

Figure 26

Vac14-mCherry with APP-GFP
Vac14-mCherry with GFP

Figure 27

mCherry-ML1Nx2 with APP-GFP
mCherry-ML1Nx2 with GFP